gi-reports@igf

Band 8

Institut für Geoinformatik und Fernerkundung

On the occasion of the 60th birthday of Professor Manfred Ehlers

Geoinformatics paves the Highway to Digital Earth

Editors: Jochen Schiewe & Ulrich Michel

Titel:
Geoinformatics paves the Highway to Digital Earth

Herausgeber:
Prof. Dr. Jochen Schiewe
Dr. Ulrich Michel

Titelgrafik:
Dipl.-Geogr. Christian Plass

Anschrift:
Institut für Geoinformatik und Fernerkundung
Fachbereich Mathematik und Informatik
Seminarstr. 19 a/b
49069 Osnabrück

Telefon: 0541/969-4591
Telefax: 0541/969-4061
Email: sekretariat@igf.uni-osnabrueck.de
Internet: http://www.igf.uni-osnabrueck.de

ISSN 1863-0103

Auflage 1, Osnabrück 2008

Content

Jochen Schiewe
EDITORIAL 05

Jochen Albrecht
FROM VGIS TO STANDARDIZED GEO-SPATIAL PROCESS MODELS 09

Martin Breunig , Andreas Thomsen, Björn Broscheit, Wolfgang Bär, Edgar Butwilowski, P.V. Kuper, Dag Hammerich, Ingo Lünsmann & C. Rolfs (Working Group „Geo-Databases“ at IGF Osnabrueck)
SOME CONTRIBUTIONS TO GEO-DATABASE RESEARCH 15

Ian Dowman
THE CONTRIBUTION OF EARTH OBSERVATION TO DIGITAL EARTH..... 20

Monika Gähler & ZKI-Team
SUPPORT DISASTER MANAGEMENT WITH REMOTE SENSING 24

Thomas K. Gottschalk, M. Bertling, V. Wolters & J. Biermann
A NEW MW ALGORITHM TO SPEED UP LANDSCAPE INDEX CALCULATION OF HIGH RESOLUTION MAPS..... 29

Ansgar Greiwe
ASR - A TOOL FOR THE UNSUPERVISED IMAGE ENDMEMBER DEFINITION 33

Beata Grendus, Thomas Kastler & Jochen Schiewe (Working Group „E-Learning and Post Education“ at IGF Osnabrueck)
SUSTAINABILITY IN E-LEARNING AND POST-EDUCATION AT THE UNIVERSITY OF OSNABRÜCK 37

Michael Heiß
GIS MAKES “CLIMATE CHANGE” VISIBLE 41

Ingrid Jaquemotte
IMPROVING SQUAT INVESTIGATIONS BY VIRTUAL REALITY 44

Wolfgang Kainz
THEORY AND PRACTICE OF FUZZY SETS IN GIS 49

Martina Klärle
SUN-AREA - EIN BEITRAG DER FERNERKUNDUNG GEGEN DEN KLIMAWANDEL 55

Sascha Klonus & Pablo Rosso (Working Group “Remote Sensing” of IGF Osnabrueck)
THE DEVELOPMENT OF THE EHLERS FUSION 60

Gottfried Konecny
WIE WIRD MAN EIN GEOINFORMATIKER? - BEITRAG ZUM 60. GEBURTSTAG VON MANFRED EHLERS 66

André Kopka
THE CAPABILITIES OF MODERATE RESOLUTION SATELLITE DATA 71

Norbert de Lange
NOTES ON MULTISPECTRAL CLASSIFICATION WITH CORRELATED BANDS: EFFECTS ON USING EUCLIDEAN DISTANCE 75

Peter Lohmann, Peter Hofmann & Sönke Müller
UPDATING GIS BY OBJECT-BASED CHANGE DETECTION 81

Marguerite Madden
STEREOCORELAT ION AND IMAGE FUSION: MANFRED EHLERS AT THE UNIVERSITY OF GEORGIA 87

Ulrich Michel, Kai Behncke, Karsten Hoffmann, Christian Plass, Jens Schaefermeyer, Constanze Tschritter & Norbert de Lange (Working Group „GIS“ at IGF Osnabrueck)
GEOINFORMATICS PAVES THE WAY FOR A VIRTUAL 3D CAMPUS 90

Ulrich Michel, Christian Plass & Constanze Tschritter
ZOO OSNABRUECK CHANGES INTO A NEW SUITE - POTENTIAL OF A MODERN PRESENTATION OF ANIMAL AND ENVIRONMENTAL DATA 94

Matthias S. Möller
SUSTAINABLE AND ECOLOGICAL URBAN DEVELOPMENT – CASE STUDY FOR THE BURENKAMP AREA, OSNABRUECK 99

Yan Na, Jie Meng & Hongmin Lu
MULTI-DIRECTIONAL DECOMPOSITION BASED REMOTE SENSING IMAGE FUSION 104

Peter Reinartz
SERIAL IMAGES FROM AIRBORNE DIGITAL FRAME CAMERA SYSTEMS FOR MONITORING OF TRAFFIC DYNAMICS 109

Jochen Schiewe
PAVING THE HIGHWAY TO A DIGITAL EARTH BY INTEGRATING GIS, REMOTE SENSING AND IMAGE PROCESSING 114

Manfred Schroeder
THE RELEVANCE OF SPATIAL RESOLUTION AND STEREO CAPABILITY FOR THE INTERPRETATION OF REMOTE SENSING IMAGERY 119

Ralf W. Schroth
THE CHALLENGE OF PROCESS AND MANAGEMENT OPTIMIZATION FOR PHOTOGRAMMETRIC MAPPING PROJECTS 122

Wenzhong Shi
PROGRESS IN UNCERTAINTY MODELING AND DATA QUALITY CONTROL IN GEOGRAPHIC INFORMATION SCIENCE 127

Josef Strobl
DIGITAL EARTH BRAINWARE. A FRAMEWORK FOR EDUCATION AND QUALIFICATION REQUIREMENTS 134

Katrin Stroemer

NUTZERBASIERTE ADAPTION DES FAHRRADROUTENPLANUNGSPROZESSES IM INTERNET - KONZEPTION VON FUNKTIONALITÄTEN AUF BASIS EINER EMPIRISCHEN UNTERSUCHUNG ……...……139

Lars Tufte

EARTH OBSERVATION AND DISASTER MANAGEMENT IN EUROPE …….. 144

Manfred Weisensee, Hans-Peter Ratzke & Thomas Luhmann

HIGH PRECISION DIGITAL TERRAIN MODELS - INNOVATIVE TOOLS FOR REGIONAL PLANNING ……148

Yeh Fen Yang, Peter Lohmann & Christian Heipke

GENETIC ALGORITHMS FOR MULTI-SPECTRAL IMAGE CLASSIFICATION ……153

Ding Zheng, H. Stoelinga & M. Hartog

SEAFLOOR CHARACTERIZATION DETECTION BY ACOUSTIC BACKSCATTER ……162

Editorial

Jochen Schiewe

*This volume of the "gi_reports" summarizes the contributions that have been submitted within the scope of the Symposium entitled "Geoinformatics paves the Highway to Digital Earth", which was held in Osnabrück (Germany) on June 13th 2008. This event was organized on the occasion of the **60th birthday of Prof. Manfred Ehlers** in order to celebrate this special day and to take some time for a review on the development of Geoinformatics, and the respective contributions of Manfred in particular. This book comprises 32 papers from former PhD and habilitation students along with contributions from many long-term colleagues. Herewith the huge bandwidth of topics is reflected that Manfred was or is still working on or is at least interested in. Because it was impossible to group the contributions according a thematic or any other scheme, it was decided to present them in alphabetical order of authors. The thematic variety is also the reason that this editorial will not give a general overview. Instead of that it will describe Manfred's work and (a little bit…) Manfred himself – of course from a rather subjective perspective.*

SOME FACTS

The above mentioned huge bandwidth of interest is certainly grounded in Manfred's varied academic career. He studied Mathematics in Marburg and Kiel where he graduated with a Diploma in 1975. However, he recognized that the application of Mathematics in professional life is not easy: During an internship he experienced that perpetually re-computing insurance rates is being similar to an infinite loop and by far not a satisfying job. Therefore he stayed with the University of Kiel, but switched over to the discipline of Oceanography. As a Research Associate he made first experiences with remotely sensed data in a project on water pollution in the Baltic Sea. Just by accident he applied at the University of Hannover and "had to accept an offer" (his own words) in 1977. However, he very much enjoyed the following seven years at the Institute for Photogrammetry and Engineering Surveys, the well-known "IPI", directed by Professor Gottfried Konecny. Here he worked in the DFG Collaborative Research Centre 149 on the development of a digital image processing system for remotely sensed data, on radiometric filtering methods and on automatic techniques in digital image processing. Out of this work in 1983 Manfred generated his PhD thesis entitled "Investigations of digital correlation methods for rectifying remotely sensed scenes".

In 1984 a new period of life began – in the United States. What was originally meant for a rather short time, took six years long and certainly shaped his offensive and productive style in professional matters (which, by the way, is sometime too offensive and too productive for some people at German universities…). Manfred worked as Research Associate and later on as Assistant Research Scientist at the University of Georgia at the Laboratory for Remote Sensing and Mapping Science (directed by Professor Roy Welch), and from 1988 on as Associate Professor for Surveying Engineering at the University of Maine. During this time he also acted as Co-Principal Investigator of the National Center for Geographic Information and Analysis (NCGIA). In 1987 he finished his habilitation thesis ("venia legendi") at the University of Hannover, which dealt with the topic of "Integrated processing of digital image data of satellite Photogrammetry and Remote Sensing in the context of Geographical Information Systems".

In 1990 Manfred came back to Europe with a first stop in The Netherlands. At the International Institute for Aerospace Survey and Earth Sciences (ITC) he acted as Full Professor, in addition as Head of the Division of Aerospace Data Acquisition and Photogrammetry and the Department of Geoinformatics, respectively. But this was only an intermediate stop on his way back to Germany: In 1991 he jumped just some kilometers across the border from Enschede to Vechta where he took over a professorship for GIS and Remote Sensing. In 1997 he became the first director of the newly established Institute for Environmental Sciences (IUW), which in 2000 was complemented by the Research Center for Geoinformatics and Remote Sensing (FZG). In Vechta Manfred built up a Master program for Environmental Monitoring and a Diploma Course for Environmental Sciences, both with a strong background in Geoinformatics. Based on political decisions in 2004 his complete group was transferred to the University of Osnabrück where he is now Director of the Institute for Geoinformatics and Remote Sensing (IGF).

REMARKS ON ACHIEVEMENTS AND STYLE

Generally one may group professors into one out of three categories, depending on their preference being in teaching, administration or research. However, to pigeonhole Manfred according to this scheme is nearly impossible.

With respect to his **teaching** duties Manfred started with lectures on GIS, Remote Sensing or Image Processing already in the early 1990s. Beyond that he also promoted several PhD and also two habilitation students (see the list on the following page). Being one of those people I can state that it was pleasant to enjoy the scientific freedom that he gave to us, only asking for some loyalty for the institution and him in return. Certainly we also learned and adopted some things from him: For example, if you find an accumulation of the word "however" in papers written by his students, this is definitively his "fault"…

Promoted theses

Listed are theses with Manfred Ehlers being the first referee, in addition also selected theses as second referee

PhD theses

Wenzshong Shi, 1994. Modelling Positional and Thematic Uncertainties in Integration of Remote Sensing and Geographic Information Systems.

Thomas Christiansen, 1995. Geographical Information Systems for Regional Rural Development Projects in Developing Countries.

Jochen Albrecht, 1995. Universal GIS Operations.

Marion Czeranka, 1996. GIS-basierte Entscheidungsunterstützung in der naturschutzorientierten Raumplanung - dargestellt am Beispiel der Eingriffsregelung in der Flächennutzungsplanung.

Hartmut Brösamle, 1999. Solarthermische Kraftwerke - Standortlokalisation und Potentialabschätzung mit dem Planungsinstrument STEPS.

Gerhard Gröger, 1999. Modellierung raumbezogener Objekte und Datenintegrität in GIS.

Thomas Kolbe, 1999. Identifikation und Rekonstruktion von Gebäuden in Luftbildern mittels unscharfer Constraints.

Ingrid Jaquemotte, 2000. Gebäudegeneralisierung durch parallele Raster- und Vektorverarbeitung.

Martina Klärle, 2000. Prozessorientierung der kommunalen Flächennutzungsplanung mittels GIS-gestützten Informationsmanagement.

Ding Zheng, 2001. Fuzzy Set Theory and Neural Fuzzy Networks for Preservation of Cultivated Land Based on GIS.

Thomas K. Gottschalk, 2002. A Remote Sensing and GIS-Based Model of Avian Species Habitat and its Potential as a Part of an Environmental Monitoring Programme.

Ulrich Michel, 2002. Integration von Geographischen Informationssystemen und Fernerkundung zum automatisierten wissensbasierten Monitoring der Landnutzung.

Matthias Möller, 2002. Untersuchungen an extrem hochauflösenden Flugzeugscannerdaten für urbane Fragestellungen und deren Integration in eine GIS-Umgebung.

Stefan Jung, 2004. HYBRIS: Hybride räumliche Analyse Methoden als Grundlage für ein integriertes GIS.

Lars Tufte, 2006. Fuzzy-Set Veränderungsanalyse für hochauflösende Fernerkundungsdaten.

Karl Gerhards, 2006. Auswirkung des Rauschens und Rauschen vermindernder Verfahren auf ein fernerkundliches Segmentierungsverfahren.

Ansgar Greiwe, 2006. Detektion von Referenzspektren in multisensoralen Bilddaten.

Monika Gähler, 2006. Biotoptypenerfassung auf Basis digitaler höchst auflösender Fernerkundungsdaten.

Katrin Stroemer, 2007. Nutzerbasierte Adaption des Fahrradroutenplanungsprozesses im Internet auf Basis einer empirischen Untersuchung.

(to be continued…)

(continued…)

André Kopka, 2008. Analyse multispektraler Fernerkundungsdaten im Hinblick auf deren Eignung zur Einschätzung des Biomassepotenzials großer Landschaftsräume am Beispiel des Naturparks TERRA.vita.

Habilitation theses

Helmut Lessing, 2001. Zur Konzeption und Entwicklung von Umweltinformationssystemen.

Jochen Schiewe, 2002. Auswertung hoch auflösender und multi-sensoraler Fernerkundungsdaten: Entwicklung von Methoden und Transfer in die Lehre.

By combining his philosophy of playing an active and shaping role with a certain political talent (which he probably inherited from his father, a former member of the State Parliament), Manfred took over a lot of functions in the field of **administration**. The respective amount of efforts can be well illustrated with the large number of logos that are listed below and that stand for those (here only German) organizations Manfred had or still has a considerable impact on and holds leading functions, respectively.

Initiated or strongly influenced organizations

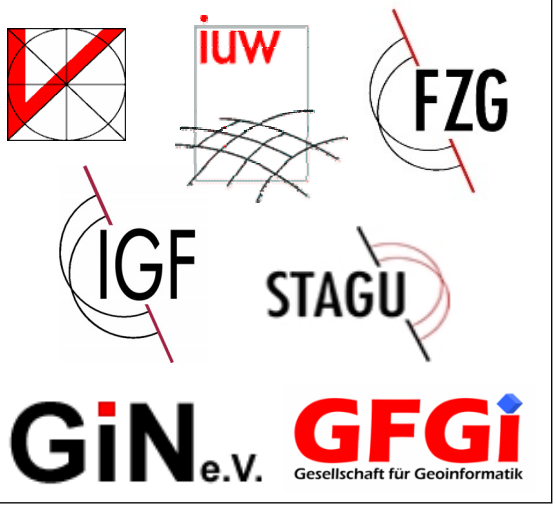

As it has already mentioned before, Manfred acted as first Director of the Institute for Environmental Sciences (IUW) and the Research Center for Geoinformatics and Remote Sensing (FZG), both located at the University of Vechta. The decline of the IUW, in which he had put a lot of ideas, time and power, and which after some years did not work any longer due to some personal disputes, was a bad experience that he probably would like to eliminate from his mind. At the University of Vechta Manfred was also Prorector for Research for a long time. In 2000 he built up a technology transfer center with the (for Germany typically long) name “Steinbeis Transferzentrum für Angewandte Geoinformatik und Umweltforschung (STAGU)“.

ISDE). Furthermore he is founder and President of the association for promoting Geoinformatics in Northern Germany (with the nice German acronym "GiN"). This successful network coordinates activities like technology transfer, consulting, post education as well as research and development. In order to foster the awareness of Geoinformatics as a scientific discipline he also initiated the foundation of the Society for Geoinformatics (GfGI) for the German speaking countries and became its first President in 2006.

Finally, concentrating on **research** issues one may look into this volume for the variety of topics Manfred was and is interested and involved in. Maybe one can identify three general and central themes: Firstly, there is the processing and evaluation of remotely sensed data, presently with the emphasis on thematic interpretation of very high resolution (in Manfred terms "ultra" high resolution) digital air photos. A second favorite topic is concerned with the development of taxonomies for GIS and Remote Sensing operators (which already led to the famous "VGIS"-project, funded by the German Research Foundation (DFG). And finally, there is the integration of all these data and methods, linking Remote Sensing and Digital Image Processing on one hand, and GIS and Remote Sensing on the other hand.

Summarizing these statements on his achievements and his style, one can understand that Manfred's overall philosophy is guided by the origin of the word "professor" (Latin: "profiteri") which means to "avow oneself to something in the public" – consequently, he is a man of direct words. At the same time he has also to be described as being open-minded – consequently, he is not a man of lonely decisions; however, he is definitively a man of decisions. And by looking back I can state that nearly all of his major decisions, which in the beginning not everybody believed in (myself included…), were the right ones. It should also be mentioned that Manfred is not captured in his professional world, but shows also much interest and activities in a lot of "wealthy things" (like politics, music or sports), which makes a communication with him easy and pleasant.

WORDS OF THANKS

Manfred, in the name of all authors I would like to thank you for your assistance and the chance to join you on the highway to Digital Earth (as everybody knows, Germans like to use highways…). Of course, last but not least, we have also to thank your family – first of all, Margret – who supported Manfred for so many years, and with that indirectly supported us. Thank you!

FROM VGIS TO STANDARDIZED GEO-SPATIAL PROCESS MODELS

J. Albrecht

Dept. of Geography, Hunter College, CUNY, 695 Park Ave., New York, NY 10065 USA - jochen@hunter.cuny.edu

KEY WORDS: Computer Supported Cooperative Work, Dynamic GIS, Ontologies, Service architectures, Workflows

ABSTRACT:

We are in the midst of a revolution in GIScience that is up to now hidden from most yet will in the long run affect us all. GIScience has so far mostly dealt with providing the scientific foundation for GISystems and because of this has been mesmerized and captured by the static map paradigm of GISystems. Attempts to move away from the data fetishism of the past have until recently been hampered by both the lack of serious industrial demand and the availability of theoretical foundations and software tools. Neighbouring disciplines, especially often ridiculed AI, are now providing us with examples of process models that invite adoption in the geo-spatial realm. This article covers the ground from process ontologies to standards developments and provides glimpses on first implementations in the geo-spatial arena that promise dramatic changes in the way we use geo-spatial services.

1. INTRODUCTION

The early 1990s were full of promises of a move towards process orientation in GIScience. Looking at Tomlin's (1990) publication of Map Algebra (also Kirby & Pazner, 1990) or vendor-specific implementations in Erdas Imagine (1994) and ESRI ArcView (1995), and Albrecht's (Albrecht & Ehlers 1994) attempt to develop a task-oriented so-called Virtual GIS, the time seemed ripe for a shift from simple GIS data creation to the support of dynamic process models. They all met with a similar fate as Smith *et al*.'s (1995) workflow modelling system – they found no followers.

With the benefit of hindsight, we can now conclude that Smith was too far ahead of the times, Albrecht and Pazner lacked the ontological foundation, and the vendor products were both too limited and not yet standards-based (the OGC was just being founded in those days). In the following sections, we will examine each of those shortcomings and discuss what progress has been made (mostly outside the realm of GIScience) to address the issues.

2. ONTOLOGIES

2.1 From static to process ontologies

At about the same time, ontologies became le dernier cri in GIScience (Paiva *et al*., 1992; Smith, 1995). Once the works of Gruber (1993; 1995) and Guarino (1995; 1997) were discovered, a whole new generation of GIScientists (Kuhn, 2001; Fabrikant, 2001; Fonseca *et al*., 2002) embraced what amounted to a new paradigm, sustaining at least two conference series (COSIT and GIScience). Grenon & Smith (2004) stoked the fire with their SNAP/SPAN formalism, which provided us with kind of a Janus face of event-based spatial reasoning but the development of a true ontology of process is still very much subject to abstract research endeavours (Bittner *et al*., 2008).

The SNAP/SPAN dichotomy is a neat logical device to compartmentalize views of dynamic phenomena but we need a unified view that allows for the application of one methodology rather than the continued parallel use of two. Reitsma (2005) introduces a radical approach, which does not seem to have found too big a following, yet she seems to have been onto something: Line (2004) and Raskin (2004) independently came up with similar notions of 'flux' and 'trajectory' that do away with the idea that we can capture processes in form of discrete automata steps. In information science, the solution to the latter was introduced by Petri (1962). Petri nets, also known as place / transition nets allow for formally complete specifications, are uniquely suited for dynamic phenomena, and could conceivably be linked with network- as well as with Voronoi-based GIS (e.g. Gold since 1987).The International Standards Organization (ISO/IEC JTC1 2005) is about to accept a Petri Net markup language that will go a long way towards public access to what used to be a rather theoretical tool.

2.2 Ontology builders and editors

General purpose ontology builders and editors have matured, at least from an information scientist's perspective (Duineveld *et al.*, 2000; Cardoso & Escorcio, 2007). Within academia and in the open source world, Protégé (2007) has become the tool of choice for close to 100,000 registered users, who (in addition to it being free) appreciate its many extensions for different paradigms (frames vs. OWL), multiple APIs, many export formats, and several different editing tools. Originally developed for the medical community, it is now widely used, even in geo-spatial communities (Souza *et al.*, 2006; Lüscher *et al.*, 2007). However, Protégé has its limitations. As Lüscher *et al*. (2007, p. 9) point out, "Protégé may be too complex for domain experts". They therefore employed a special user interface for creating spatial patterns. Another issue is that while Protégé is well suited for the development of Semantic Web applications, most GIS are still desktop- or heavy server-based, i.e., they require a database schema. Protégé can read database schemas but cannot export to them.

As Noy & Guinness (2001) point out, programmers make design decisions based on the operational properties of a class, whereas an ontology designer makes these decisions based on the structural properties of a class. In consequence, we are still short of ontologies of geographic processes, and ontologies are much easier translated into a database schema than into process models.

Protégé allows for OWL-S output, i.e., the specification of services, which according to the WorldWideWeb Consortium (W3C, 2004) can in turn be modelled as processes. We have, however, yet to see the development of geographic process libraries, notwithstanding the efforts of NASA (Raskin, 2004), a few intrepid companies (GOL 2004), and the odd GIScientist (Reitsma & Albrecht, 2005; Peachavanish & Karimi, 2007), the formal specification of geographic processes is at this point restricted to web services and queries á la Google Maps.

The best we have at this point is UML output based on OWL-S encoded ontologies. As mentioned above, (web) services, the usual target of OWL-S ontologies are a far cry from the complexities of desktop-based spatial decision support systems. The closest so far, seems to be a commercial ontology editor called SemTalk (2008). Originally designed for business workflows, it is an OWL interpreter developed as an extension to MS Visio. Formal consistency is assured with the open source OWL reasoner PELLET (2008). Pre-existing ontologies such as SWEET (Raskin, 2004) can be imported and form the foundation for subsequent user-defined extensions. One of the advantages of this tool is its relationship with MS Visio, a wide-spread software package that is also commonly used to define the data models for various ESRI communities (ESRI, 2008). This allows for using one and the same tool to define both geo-spatial data structures and processes.

It is no coincidence that SemTalk has been designed for and is most widely used for business process models. In the next section, we will revisit the notion of workflows, originally introduced in a GIScience context by Smith *et al*. (1995).

3. PROCESS MODEL SPECIFICATIONS

In GIScience, we distinguish between two different notions of 'process' (Albrecht, 2008). One is the notion of GIS as a sequence of operations with the goal to fulfil a specific set of tasks. The other is the attempt to represent dynamic geo-spatial phenomena. Albrecht (1994) and Smith *et al*. (1995) and may have been the first to combine the two. While the dynamic phenomenon aspect remained on the sidelines, Medeiros (Weske *et al*., 1998) stayed in touch with what is known as plan synthesis (Ghallab et al., 2004; Russel and Norvig, 2003).

Plan synthesis is a mature area in information science, with well-studied algorithms applied to manufacturing processes and emergency management, among others (Munoz-Avila *et al*., 2001; Nau *et al*., 1995). Recent research efforts have investigated the use of plan synthesis to solve the problem of automatic composition of web services (Blythe and Ambite, 2004). This requires to consideration of additional factors such as complex control structures with loops, non-determinism and conditionals (Srivastava and Koehler 2003). None of the plan synthesis methods treats complex objects or objects created dynamically.

In contrast to the primitive analysis of user tasks in a GIS workflow (Albrecht, 1995) we now find solid applications for different user communities (Jayavarapu, 2007), that are based both on a deeper understanding of the communication process (MacEachren *et al*., 2004) and new standards for business applications (Fillies *et al*., 2003). Especially the latter deserve an elucidation.

3.1 Standards for process-oriented systems

In section 2 we saw the establishment of standards for ontologies, albeit usually restricted to static phenomena and with the goal to establish database structures. Outside of GIScience we have a plethora of workflow modelling standards that address the need to use conceptual models as tools for communication across disciplines (Heemskerk *et al*., 2003; Albrecht & Pingel 2004).

Non-withstanding the advent of web and location-based services, much of the GIScience standardisation community is still stuck in the surveying perspective (Albrecht 1999). This contrasts with the development of the Object Management Group's business process modelling notation (BPMN, 2008), which has been widely adopted and could easily be applied to the OGC's Cliff Kottman's (1999) information communities. A direct outflow of that framework is the XML process definition language (Hollingsworth, 2004; WFMC, 2005), which together with the asynchronous service access protocol (Ricker *et al*., 2004) forms the basis of Workflow-XML (Swenson *et al*., 2004).

Using the BPMN framework, XPDL and Wf-XML are now widely accepted standards that are applied in dozens of software packages such as SemTalk, and are used for the formal specification of workflows in neighbouring disciplines such as bioinformatics (Digiampietri *et al*., 2007). Formally, each of these can be proven using Petri Nets (Aalst *et al*., 2000), which are increasingly being supported/implemented in process modelling software packages

On the GIScience side, endeavours such as Jäger *et al*., (2005) and Bambacus *et al*., (2007) are characterised by their reliance on Semantic Web services, which neither incorporate the domain knowledge Pike & Gahegan (2006), nor allow to access functional levels of desktop GIS software.

4. PRACTICAL EXPERIENCES

This section consists of two parts. In the first, we describe and analyze the needs of an agent-based GIS model developed by Groff and described across a range of publications (Groff 2007a, b; 2008). The emphasis in this discussion is on the formal specification of agent behaviour in a geographic context. In the second part, we look at a transportation / land use model developed for a regional planning authority. Together, they illustrate the problems we are currently facing in the formal specification as well as implementation of GIS processes.

4.1 Formal specification of actions in an agent-based GIS

This model has been described in detail in Groff (2007a, b). We will here instead focus on the process of agent specification, which is documented in form of a sample application of AgentAnalyst (2008). The agent-based component is a Repast (North *et al*., 2006) application that links to ArcGIS using a Python interface. Following the logic of Kuhn (2001) Groff develops a formal framework of agent actions within a well-defined context, in this case crime analysis. Theodorakis *et al.* (1999) and subsequently Cai (2007) describe such a process in abstract terms but show no attempt of an implementation. Groff (2008) develops her specifications the way a programmer would: defining in a painstaking iterative process all the variables and actions of the agent based model and arranging them in the complex schedule that operates at four different hierarchical levels.

The total model consists of four types of agents (places, citizens, cops, and activity nodes) that perform 35 defined activities based on the state of 64 variables. It took Groff a good year of her PhD to develop this model. There are no tools that assist in the setup of the model logic, or that would help with the checking for formal consistency of the model. In an agent-based model, the agents are supposed to act depending on context. From a developer's perspective, this context, however, gets fast out of hand because of the combinatorial explosion of possible situations among the many dimensions that Groff's model spans. Ali *et al*. (2007) address this problem with a spatial variant of an online analytical process (OLAP) to keep track of the complexities in the real-time analysis of their multi-agent geosimulation software decision making process. This takes care of some of the implementation issues but leaves the question of ontology-based design tools that this article is about unresolved.

4.2 Formal specification of a land use-based transportation model

The second model is a spatial decision support system (SDSS) developed by this author to investigate existing flow in a multi-modal network and to find optimal locations for transit hub based on existing parcel-level land use. The resulting geodatabase (all vector data) is approximately 2 GBytes in size, and the procedures of the SDSS combine many hundred GIS operations for a single model iteration.

GIS databases are often treated as mere repositories that once created are frozen in time and form a stable basis for subsequent analysis. The efforts of creating a database are hence neglected in academic literature (notwithstanding publications on management (Huxhold & Levinsohn, 1994; Tomlinson, 2003; Watson, 2005; Obermeyer & Pinto, 2007; Yeung & Hall, 2007), metadata (Williamson *et al*., 2003; Nogueras-Iso *et al.*, 2005; Wootton 2007) or spatial decision support (Geertman & Stillwell 2002)).

Similar to the crime model of the previous sub-section although not at the fine-grained individual level of perpetrators and victims, our very model structure is dynamically changing as we run the model. For instance, the choice of a commuter's mode or route is influenced by how many other commuters crowd one's first or second option. Many train riders in Seattle, for example, are familiar with the added number of passengers when flooding closed a highway during exceptional rainstorm in fall of 2007. The same happens on a smaller but cumulatively as effective scale every day in metropolitan areas around the world. From an abstract perspective, the phenomenon is well studied and has become a popular example in complexity theory (Qiu *et al*., 2000; Shen *et al*., 2005; Selçuk, 2007). As a matter of fact, it is one of the hallmarks of complexity theory (Gimblett, 2002) that its object arises from innocent looking simple setups. With the exception of a draft paper by Line (2004), there is no ontology of complex systems and we are left with basic tools such as the Unified Modeling Language (Tsang *et al*., 2005), which in itself is not a formal reasoned and in practice lacks the mechanisms to deal with complex systems.

5. OUTLOOK

Klien & Probst (2005), as well as daSilva *et al*. (2005) call for research on methods and tools that support application ontology engineering, e.g., by automating the process of creating application ontologies. We cannot agree more. We need spatio-temporal schema editors that assist with the development of complex scheduling and update routines in dynamic models. Industrial-strength process modelling tools such as SemTalk (2008) come close with their support of the BPMN. They have, however, yet to be tested to see whether they can cope with the spatio-temporal granularity that is characteristic for real-world GIS applications.

A wide-spread move from static GIS repositories to GIS-based process modelling systems requires the development of reusable libraries of process model specifications, similar to their counterpart in the data model world. The above pages illustrate that we have reached a threshold in the development of tools and standards that for the first time really allows us to bridge domain-specific models and build real-world dynamic GIS (Albrecht 2007). Let's do it!

6. REFERENCES

van der Aalst, W., and A. Ter Hofstede, 2000. Verification of Workflow Task Structures: A Petri-net-based Approach. *Information Systems*, 25 (1): 43-69.

AgentAnalyst, 2008. Agent-based Modeling Extension for ArcGIS Users. http://www.institute.redlands.edu/agentanalyst/, last accessed 29 Jan. 2008.

Albrecht, J. and J. Pingel, 2004. GIS as a Communication Process. *Geographic Information Systems and Crime Analysis*, pp. 2-23. Singapore: Idea Group.

Albrecht, J., 1994. Universal Elementary GIS Tasks: beyond low-level commands. *Proceedings 6th International Symposium on Spatial Data Handling*, pp. 209-222, Edinburgh.

Albrecht, J., 1995. Semantic Net of Universal Elementary GIS Functions. *Proceedings ACSM/ASPRS Annual Convention and Exposition Technical Papers, Vol. 4 (Auto-Carto 12)*, pp. 235-244. Bethesda, MD.

Albrecht, J., 1999. Geospatial information standards a comparative study of approaches in the standardisation of geospatial information. *Computers and Geosciences,* 25(1):9-24.

Albrecht, J., 2007. Dynamic GIS. *The Handbook of Geographic Information Science,* pp. 436-446. London: Blackwell.

Albrecht, J., 2008. Application Planning. *Human Computer Interaction and GIS*. London: Blackwell.

Ali, W., Moulin, B., Bedard, Y. Proulx, M. and S Rivest, 2007. Coupling Multiagent Geosimulation and Spatial OLAP for Better Geosimulation Data Analysis. *URISA Journal*, 19 (2): 23-32.

Bambacus, M., Yang, P., Evans, J., Cole, M., Alameh, N. and S Marley, 2007. An Interoperable Portal Supporting Prototyping Geospatial Applications. *URISA Journal*, 19(2): 33-39.

Bittner, T., Donnelly, M. and B. Smith, 2008. A Spatio-Temporal Ontology for Geographic Information Integration. International Journal for Geographical Information Science.

Blythe, J. and J. Ambite, 2004. *Workshop on Planning and Scheduling for Web and Grid Services*, Whistler, British Columbia, Canada.

BPMN, 2008. Business Process Modeling Notation (BPMN) Information. http://www.bpmn.org/, last accessed 25 Feb. 2008.

Cai, G., 2007. Contextualization of Geospatial Database Semantics for Human-GIS Interaction. *GeoInformatica*, 11(2): 217-237.

Cardoso, J., & A. Escorcio, 2007. Editing tools for ontology construction, in *"Semantic Web Services: Theory, Tools and Applications"*, Idea Group.

Digiampietri, L., de Perez-Alcazar, J., and C. Bauzer Medeiros, 2007. An ontology-based framework for bioinformatics workflows. *International Journal for Bioinformatics Research and Applications*, 268-285.

Duineveld, A., Stoter, R., Weiden, M., Kenepa, B. and V. Benjamins, 2000. Wondertools - a comparative study of ontological engineering tools. *International Journal of Human-Computer Studies*, 52(6):1111-1133.

ESRI, 2008. *ArcGIS Data Models*. Web site at http://support.esri.com/index.cfm?fa=downloads.dataModels.gateway, last accessed 29 Jan. 2008.

Fabrikant, S., 2001. Building Task-Ontologies for GeoVisualization. ICA Commission on Visualization and Virtual Environment Pre-conference Workshop: *Geovisualization on the Web*, Beijing, China, Aug. 3-4, 2001.

Fillies, Ch., Weichhardt, F., and G. Wood-Albrecht, 2003. Semantic Web Service Processes with SemTalk. *Proceedings, 2nd International Semantic Web Conference, ISWC*, Sanibel Island, Florida, October 2003, Lecture Notes in Computer Science 2870, Berlin: Springer.

Fonseca, F., Egenhofer, M., Agouris, P. and G Câmara, 2002. Using Ontologies for Integrated Geographic Information Systems. *Transactions in GIS*, 6(3):231-257.

Geertman, S. and J. Stillwell, 2002. *Planning Support Systems in Practice*. Berlin: Springer.

Ghallab, M., Nau, D. and P. Traverso, 2004. *Automated Planning, Theory and Practice*. London, UK: Elsevier,

Gimblett, R., 2002. *Integrating Geographic Information Systems and Agent-Based Modeling Techniques for Simulating Social and Ecological Processes*. London: Oxford University Press.

GOL, 2004. Georeference Online Ltd. Website at http://www.georeferenceonline.com, last accessed 27 Jan. 2008.

Gold, C. and S. Cormack, 1987. Spatially ordered networks and topographic reconstructions. *International Journal of Geographical Information Systems*, 1:137-148.

Grenon P. and B. Smith 2004. SNAP and SPAN: Towards Dynamic Spatial Ontology. *Spatial Cognition and Computation*, 4 (1): 69–103.

Groff, E., 2007a. 'Situating' Simulation to Model Human Spatio-Temporal Interactions: An Example Using Crime Events. *Transactions in GIS*, 11(4):507-530.

Groff, E., 2007b. "Simulation for Theory Testing and Experimentation: An Example Using Routine Activity Theory and Street Robbery." *Journal of Quantitative Criminology*, 23:75-103.

Groff, E., 2008. Adding the Temporal and Spatial Aspects of Routine Activities: A Further Test of Routine Activity Theory. *Security Journal,* 21(1):95-116.

Gruber, T., 1993. A Translation Approach to Portable Ontology Specifications. *Knowledge Acquisition,* 5(2): 199-220.

Gruber, T., 1995. Toward Principles for the Design of Ontologies Used for Knowledge Sharing. *International Journal Human-Computer Studies*, 43(5-6):907-928.

Guarino, N., 1997. Understanding, building, and using ontologies. A commentary to Using Explicit Ontologies in KBS Development, by van Heijst, Schreiber, and Wielinga. *International Journal of Human and Computer Studies*, 46: 293-310.

Guarino, N., 1995. Formal Ontology, Conceptual Analysis and Knowledge Representation, *International Journal of Human-Computer Studies*, 43(5-6):625–640.

Heemskerk, M., Wilson, K. and M. Pavao-Zuckerman, 2003. Conceptual models as tools for communication across disciplines. *Conservation Ecology*, 7(3): 8. http://www.consecol.org/vol7/iss3/art8/, last accessed 25 Feb. 2008.

Hollingsworth D., 2004. The Workflow Reference Model: 10 Years On. *Workflow Handbook*, pp. 295-313. Lighthouse Point, FL: Future Strategies.

Huxhold, W. and A. Levinsohn, 1994. *Managing Geographic Information Systems*. Oxford University Press.

ISO/IEC JTC1/SC7, 2005. Combined WD Circulation, CD Registration and CD Ballot, WD 15909-2, Software and Systems Engineering, High-level Petri Nets - Part 2: Transfer Format. Montreal, Canada: ISO/IEC JTC1/SC7 Secretariat. http://wwwcs.uni-paderborn.de/cs/kindler/publications/copies /ISO-IEC15909-2-WD0.9.0.Ballot.pdf, last accessed 03 Feb. 2008.

Jäger, E., Altintas, I., Zhang, J., Ludäscher, B., Pennington, D. and W. Michener, 2005. A Scientific Workflow Approach to Distributed Geospatial Data Processing Web Services. *17th International Conference on Scientific and Statistical Database Management (SSDBM'05)*, 27-29 June 2005, Santa Barbara, California, pp. 87-90.

Jayavarapu, A., 2007. Enterprise GIS Projects: challenges and solutions. Paper 1004, *ESRI Federal Users Conference*.

Klien, E. and F. Probst, 2005. Requirements for Geospatial Ontology Engineering. *8th Conference on Geographic Information Science* (AGILE 2005). Estoril, Portugal.

Kottman, C., 1999. The Open GIS Consortium and progress towards interoperability in GIS. *Interoperable Geographic Information Systems*, pp. 39-54. Kluwer Academic.

Kuhn, W. 2001. Ontologies in support of activities in geographical space. *International Journal of Geographical Information Science*, 15:(7): 613-631.

Line, M. 2004. *Proposed Upper Ontology for the semiotics of Complex Systems*. Polymathix white paper. http://www.polymathix.com/papers/socs-upper.html, last accessed 03 Feb. 2008.

Lüsdcher, P., Burghardt, D. and R. Weibel, 2007. Ontology-driven Enrichment of Spatial Databases. *10th ICA Workshop on Generalisation and Multiple Representation*, 2-3 August 2007, Moscow.

MacEachren, A., Gahegan, M. and W. Pike, 2004. Visualization for constructing and sharing geo-scientific concepts. Proceedings of the National Academy of Science. *Proceedings of "Mapping Knowledge Domains*", May 9–11, 2003, Irvine, CA. http://www.pnas.org/cgi/reprint/0307755101v1.pdf, last accessed 25 Feb. 2008.

Munoz-Avila, H., Aha, D.W., Nau, D., Weber, R., Breslow, L. and F. Yaman, 2001. SiN: integrating case-based reasoning with task decomposition. *IJCAI 2001*, pp.999–1004.

Nau, D., Au, T.C., Ilghami, O., Kuter, U., Murdock, W., Wu, D. and F. Yaman, 2003. SHOP2: an HTN planning system. *Journal of Artificial Intelligence Research*, 20:379–404.

Nogueras-Iso, J., Zarazaga-Soria, F., and P. Muro-Medrano, 2005. *Geographic Information Metadata for Spatial Data Infrastructures: resources, interoperability, and information retrieval*. Berlin: Springer.

North, M., Collier, N., and J. Vos, 2006. Experiences creating three implementations of the repast agent modeling toolkit. *ACM Transactions on Modeling and Computer Simulation*, 16:1–25.

Noy, N. and D. McGuinness, 2001. *Ontology Development 101: A Guide to Creating Your First Ontology*. Knowledge Systems Laboratory, March, 2001.

Obermeyer, N. and J. Pinto, 2007. *Managing Geographic Information Systems*. Guilford.

Paiva, J., Egenhofer, M., A. Frank, 1992. Spatial Reasoning about Flow Directions: Towards an Ontology for River Networks. *In Proceedings of International Society for Photogrammetry and Remote Sensing. XVII Congress*, in Washington, D.C., International Archives of Photogrammetry and Remote Sensing, Vol. 24/B3 Commission III, pp: 318-324.

Peachavanish, R. & H. Karimi, 2007. Ontological Engineering for Interpreting Geospatial Queries, *Transactions in GIS*, 11(1): 115-130.

PELLET, 2008. Open source OWL DL reasoner web site at http://pellet.owldl.com/, last accessed 01/29/08.

Peterson, J. 1981. *Petri Net Theory and the Modeling of Systems*. Prentice-Hall.

Petri, C. 1962. *Kommunikation mit Automaten*. PhD thesis, Bonn: Universität Bonn.

Pike, W. and M. Gahegan, 2006. Beyond ontologies: Toward situated representations of scientific knowledge. *International Journal of Human-Computer Studies*, 65(7): 674-688.

Protégé, 2007. Home of the Protégé editor. http://protege.stanford.edu. Last accessed 01/26/08.

Qiu, Q., Wu, Q. and M. Pedram, 2000. Dynamic Power Management of Complex Systems Using Generalized Stochastic Petri Nets. *Proceedings of the 37th ACM Design Automation Conference* (DAC2000), pp 352-56. http://www.sigda.org/Archives/ProceedingArchives/Dac/Dac2000/papers/2000/dac00/pdffiles/21_3.pdf, last accessed 03 Feb. 2008.

Raskin, R., 2004. *Guide to SWEET Ontologies*. Pasadena, CA: NASA / Jet Propulsion Lab.

Reitsma, F. and J. Albrecht, 2005. Implementing a New Data Model for Simulating Process. *International Journal for Geographic Information Science*, 19(10):1073-90.

Ricker, J., Krishnan, M., and K. Swenson, 2004. *Asynchronous Service Access Protocol*. http://www.oasis-open.org/committees/asap/docs/, last accessed 24 Feb. 2008.

Russel, S. and P. Norvig, 2003. *Artificial Intelligence*: A Modern Approach. NJ: Prentice-Hall.

Selçuk, B., 2007. *Dynamic Performance of Hierarchical Planning Systems*. Eindhoven, NL: Technische Universiteit Eindhoven. http://alexandria.tue.nl/extra2/200612552.pdf, last accessed 03 Feb. 2008.

SemTalk, 2008. Business process modeling and ontology editor. Potsdam, Germany: Semtation GmbH. http://www.semtalk.com, last accessed 29 Jan. 2008.

Shen, J., Sun, X., Huag, G., Jiao, W., Sun, Y. and H. Mei, 2005. Towards a unified model for supporting mechanisms of dynamic component update. *ACM SIGSOFT Software Engineering Notes*, 30(5): 80-89.

Smith, B., 1995. On Drawing Lines on a Map. Spatial Information Theory. A Theoretical Basis for GIS. Lecture Notes in Computer Science, 988, pp. 475-484. Berlin: Springer.

Smith, T., Su, J., El Abbadi, A., Agrawal, D., Alonso, G. and A. Saran, 1995. Computational Modeling Systems. *Information Systems*, 20 (2): 127-153.

Souza, D., Salgado, A. and P. Tedesco, 2006. Towards a Context Ontology for Data Integration. *On the Move to Meaningful Internet Systems*, LNCS 4278, pp. 1576-1585, Berlin: Springer.

Srivastava, B. and J. Koehler, 2003. Web service composition – current solutions and open problems, *ICAPS 2003*, pp.28–35.

Swenson, K., Pradhan, S., and M. Gilger, 2004. *Workflow-XML 2.0*. XML Based Protocol for Run-Time Integration of Process Engines. http://www.wfmc.org/, last accessed 25 Feb. 2008.

Theodorakis, M., Analyti, A., Constantopoulos, P., and N. Spyratos, 1999. Contextualization as an Abstraction Mechanism for Conceptual Modeling. *Proceeding of the 18th International Conference on Conceptual Modeling (ER '99)*, Paris, France, pp. 475-489. Lecture Notes in Computer Science 1728, Berlin: Springer.

Tomlinson, R., 2003. *Thinking About GIS: geographic information system planning for management*. Redlands, CA: ESRI Press.

Tsang, H., Lay, C. and Y. Leung, 2004. *Object Oriented Technology: from diagram to code with visual paradigm for UML*. Princeton, NJ: McGraw-Hill.

W3C, 2004. OWL-S: semantic markup for web Verification of Workflow Task Structures services. W3C member submission 22 November 2004. http://www.w3.org/Submission/OWL-S, last accessed 26 Jan 2008.

Watson, R., 2005. *Data management: databases and organizations. Wiley.*

WebODE, 2003. Ontological engineering platform. http://webode.dia.fi.upm.es/WebODEWeb, last accessed 26 Jan. 08.

Weske, M., Vossen, G. Medeiros, C. and F. Pires, 1998. Workflow Management in Geoprocessing Applications. *Proceedings 6th ACM International Symposium on Geographic InformationSystems (ACMGIS)*, pp. 88-93. Washington, DC.

WFMC, 2005. XML Process Definition Language (XPDL) Document Number WFMC-TC-1025, version 1.14, http://www.wfmc.org/standards/docs/TC-1025_xpdl_2_2005-10-03.pdf, last accessed 25 Feb. 2008.

Williamson, I., Rajabifard, A., and M. Feeney, 2003. Developing Spatial Data Infrastructures: from concepts to reality. London: Taylor & Francis.

Wootton, C., 2007. *Developing Quality Metadata: building innovative tools and workflow solutions*. Oxford, UK: Focal Press.

Yeung, A. and B. Hall, 2007. *Spatial Database Systems: design, implementation and project management.* Berlin: Springer.

SOME CONTRIBUTIONS TO GEO-DATABASE RESEARCH

M. Breunig *, A. Thomsen, B. Broscheit, W. Bär, E. Butwilowski, P.V. Kuper, D. Hammerich, I. Lünsmann & C. Rolfs

Institute for Geoinformatics and Remote Sensing (IGF), University of Osnabrück, Kolpingstr. 7, 49069 Osnabrück, mbreunig@uni-osnabrueck.de

KEY WORDS: Geo-databases, mobile information systems, 3D/4D GIS, 3D databases, geo-services, modelling of topology.

ABSTRACT:

Geo-database research may look back to a 25 year old history. The large sets of data used in new applications such as navigation systems for cars and pedestrians, tourist information systems, early warning systems for geological events, and last but not least NASA World Wind or Google Earth strengthen the need for efficient geo-databases. This article summarizes the contributions of the geo-database research group at IGF, University of Osnabrück, to geo-database research. The main activities can be divided into the research fields of 3D geo-database services, database support for mobile information systems, and the modelling and management of 3D topology. Main application fields concern geology, city models, and the early warning of geoscientific events. Concepts, implementation approaches and application examples in some of the mentioned research fields are presented. Finally an outlook is given on future research of the group and activities in teaching concerning geo-databases are shortly described.

1. INTRODUCTION

With the strongly growing amount of data sets needed in many spatial applications, geo-databases come back to the centre of interest in geoinformatics. In application fields such as telecommunication, oil exploitation, and climate modelling the coupling of modelling tools with geo-databases is of central interest. Following the tradition of GeoStore, an information system for geologically defined geometries (Bode et al., 1994), and GeoToolKit, a library of 3D data types inclusive 3D database operations (Balovnev et al. 1997), both developed at the Collaborative Research Centre 350 at Bonn University, the focus of geo-database research at IGF, University of Osnabrück and its predecessor FZG, University of Vechta, is on the development of methods and software components in the fields of 3D geo-database services (Breunig et al., 2007), mobile information systems (Bär, 2002, Bär and Breunig, 2004, Bär and Breunig, 2005, Breunig et al., 2005), and the management of 3D topology (Breunig et al., 2007, Thomsen and Breunig, 2007, Thomsen et al., 2007, Thomsen et al. 2008). This work flowed into the development of DB3D, our service-oriented 3D geo-database kernel (Breunig et al., 2004a, Breunig et al., 2004b, Bär, 2007). Furthermore, work is ongoing concerning the unified modelling and management of 2D and 3D topology in multiple representation databases applied in maps and 3D city models (Breunig et al., 2007, Thomsen et al. 2008). Finally, the management of landslide modelling data and the interaction between geo-databases, mechanical modelling of landslides and spatial data mining algorithms is investigated in the context of early warning systems for geological events (Breunig et al., 2007a). Last but not least, general ideas on geo-database research (Breunig, 2007) and on data structures and operations for 3D geo-databases have been worked out (Breunig 2005, Thomsen 2005, Breunig and Zlatanova, 2006, Breunig 2007).

2. GEO-DATABASE SUPPORT FOR MOBILE INFORMATION SYSTEMS

Mobile and ubiquitous computing is a growing research fields in computer science. Many mobile applications, however, could work more efficiently, if an on-line and off-line access to the data stored at a server database or at other clients connected via an ad-hoc network was provided. In the work of (Bär, 2002) and (Breunig and Bär, 2004) examinations with the geo-database support for mobile route planning data organized in graphs has been executed comparing an XML native database management system with an object-oriented DBMS. As expected the XML-based approach was less efficient, because XML originally was developed for handling texts and other hyper-linked documents, but not for the handling of large sets of geo-objects. XML does not support spatial data types, spatial operations and spatial access methods. In the examinations of (Bär, 2002) it was also confirmed that small devices such as PDAs are not yet efficient enough to run spatial database queries on graph-structured geo-data. However, the same mobile database configuration used on an average laptop showed reasonable database response times.

3. DEVELOPMENT OF 3D GEO-DATABASE SERVICES

In real world application fields such as geology and geophysics, volumetric objects are playing an important role. I.e. attributes may not only be attached to the hull or boundary of the objects, but also to their interiors. Therefore true 3D geo-database services are needed providing a clear interface with 3D functionality, possibly enabling the user to build own user-defined services, e.g. by combining or implementing own 3D geometric and topological database operations.

* Corresponding author.

3.1 Example of a geo-database service

3D geo-database services may contain 3D spatial operations such as distance operations or intersection between volumetric objects. However, some applications such as mobile clients, also need 2D results of spatial operations. They often are not efficient enough to compute complex 3D models. Figure 1 shows schematically the operation chain needed to execute the so called "3D-to-2D service", part of the DB3D database kernel. This geo-database service computes a profile section, specified by the user on a 2D map, from a geological 3D block and projects all boreholes around a given distance.

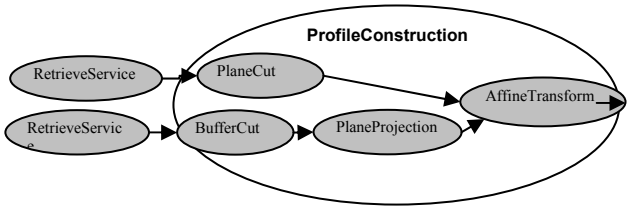

Figure 1. Operation chain needed for the 3D-to-2D service

Note that the 3D geometric operations are directly computed by the DB3D database management system, i.e. spatial data types and spatial access methods may be directly used from DB3D.

The 3D-to-2D service works as follows. First, the location of a vertical profile section is defined on a 2D map. Second, the stored geometries are retrieved from a corresponding window in 3D space. Then the vertical intersection of the section plane with the 3D geometries is computed. Using a 3D buffer surrounding the plane, sample data are retrieved and projected onto the profile plane. Finally, for purposes of visualisation and further analysis, the result can be projected onto a 2D vertical "paper plane" carrying the profile section. Figure 1 describes the chain of operations, which are illustrated in figure 2.

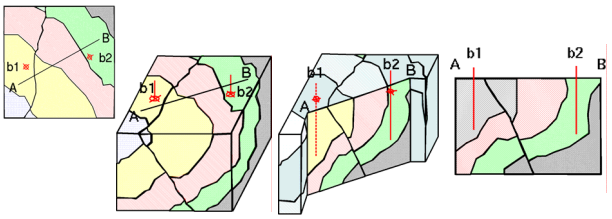

Figure 2. Example of a geo-database service: 3D-to-2D service

The result of this service is a vertical 2D geometry, which can be sent to mobile devices within a mobile client-server database architecture. Another example for DB3D´s services is the "4D-to-3D service" which projects single snapshots from a continuous movement of geometric objects changing with time.

Some first research efforts have been undertaken concerning the interfaces of geo-database services. New interfaces for 3D geo-database services based on augmented reality have been tested in cooperation with the Institute of Photogrammetry and Remote Sensing, University of Karlsruhe (Bär and Breunig, 2005, Breunig et al., 2005). For example, with an augmented-reality flood scenario, buildings recorded by a video camera have been combined with the temporal model of the water level stored in a geo-database. In future this technique may be used for the early warning scenario (Breunig et al., 2007a) to combine the surface of the earth recorded by a video camera with the 3D underground model of this area. Thus the geologist may get new knowledge about the underground geology using this technique.

3.2 DB3D

DB3D (Bär & Breunig 2005, Bär 2007) originated from the experiences gained by the development of GeoToolKit (Balovnev et al., 2004) in the group of Armin B. Cremers and Martin Breunig. However, DB3D has a service-based architecture and is exclusively implemented in the Java programming language, i.e. its interface can be accessed by Java-based services. Presently, Java RMI is used as communication platform. Internally DB3D is based on an object-oriented database management system. In (Bär 2007) also a mobile database client has been realized, that interacts with versioning of 3D geometric objects on the server side. The geometric and topological data model of DB3D is based on simplicial complexes, i.e. on points/nodes, lines/edges, triangle nets/meshes and tetrahedron nets/meshes, respectively. The data model has been extended to simplicial complexes varying with the parameter time. The system architecture of DB3D is presented in figure 3. On the client side, GIS clients or a mobile 3D database may access 3D data managed by the DB3D server. On the server side, DB3D is accessed exclusively by its services, which can be divided into operations and the version management. The most important part of DB3D is its 3D/4D database which is based on a geometry library and spatial access structures (R-tree-based). The whole system is implemented upon an object-oriented database management system (OODBMS).

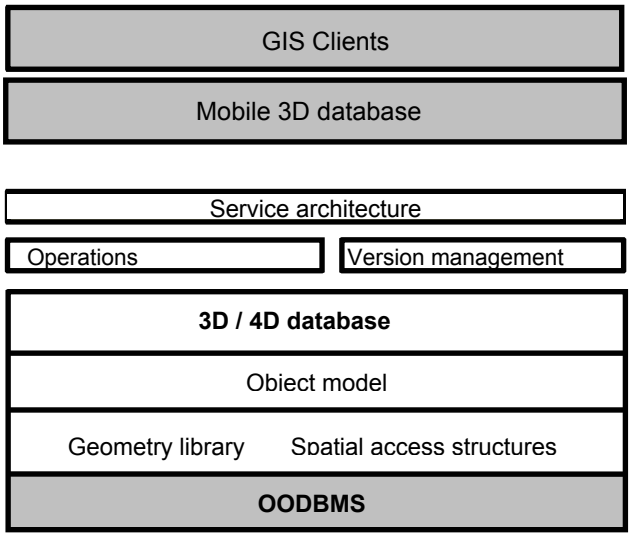

Figure 3. System architecture of DB3D

DB3D may be useful for many 3D database applications or geoscientific applications dealing with 3D objects changing in time. A typical application of DB3D´s version model is shown in figure 4. Here geometries of a landslide movement are changing in time being managed by DB3Ds version model supporting the analysis of geological moving crevasses. Internally this is realized by generating an alternative workspace for each alternative version of an object. Hitherto the management of the versions is only implemented as linear history.

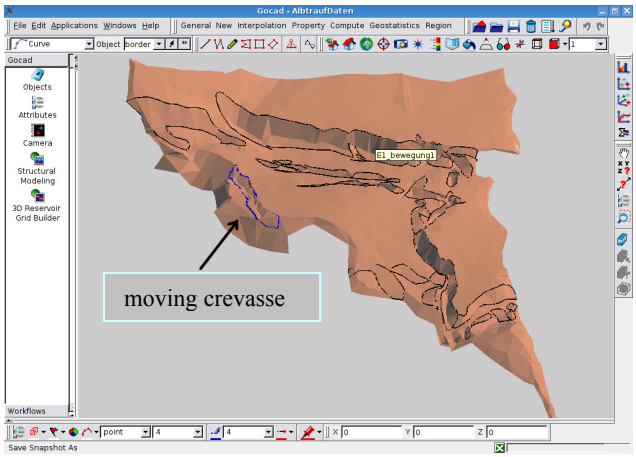

Figure 4. Geological moving crevasses managed by DB3Ds version model (figure from Bär, 2007)

DB3D is planned to be used in the early warning system project (Breunig et al., 2007a) for the management of geometric objects needed for the early warning of landslides.

4. MODELLING AND MANAGEMENT OF 3D TOPOLOGY

Topology plays a central role in many 2D and 3D GIS applications. However, 2D topological data models cannot be easily transferred for 3D purposes. That is why a general approach based on a clear mathematical theory is desirable which provides a unified topological data model for 2D and 3D space. In (Thomsen and Breunig, 2007, Thomsen et al., 2007,

Breunig et al., 2007b) an approach on cellular complexes implemented with d-Generalized Maps (G-Maps) has been examined (Lienhardt, 1988, Lienhardt, 1989, Lienhardt, 1991, Lienhardt, 1994, Brisson, 1989, Brisson, 1993). Topology has also been investigated in the context of multiple representation

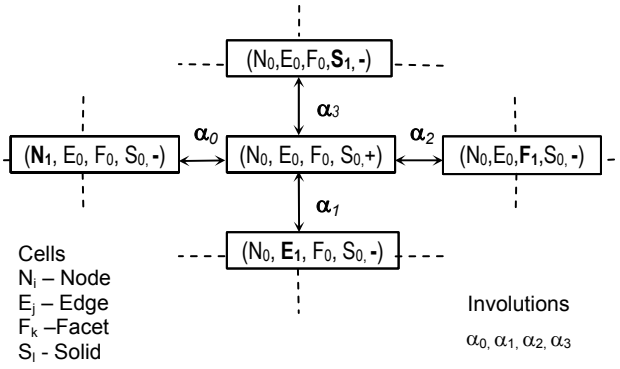

Figure 5: Graph structure of a G-Map

databases (Thomsen et al., 2008). To illustrate the principle of this topological data structure, figure 5 shows 3D-G-Maps represented in a graph structure.

Each cell-tuple (N_i, E_i, F_i, S_i) represents a particular incidence relationship between a node, an edge, a face, and a solid, and references neighbouring relationships by exchanging exactly one component: either a node, or an edge, or a face, or a solid. This Cell-Tuple Structure (Brisson, 1989) or Generalized Map (Lienhardt, 1988) provides a Cellular Complex with the combinatorial structure of an abstract simplicial complex, and completely describes the topological relationships within the Cellular Complex. The graph structure presented above can also be transferred to a relational database structure. To traverse this structure, Orbits are generated using combinations of different types of "involutions" α_0, α_1, α_2, α_3, respectively.
By definition, an orbit $orbit_{i..j..}(ct_0)$ consists of the subset of cell-tuples that can be reached from ct_0 using any combination of $\alpha_{i,...},\alpha_{j,...}$ The components of dimension k where k is not contained in the set of indices i,…,j remain fixed, e.g. if $ct_0=(n,e,f,s)$, then $orbit_{012}(ct_0)$ leaves solid s fixed, and returns all cell-tuples of the form (*,*,*,s).

G-Maps are currently used in the Gocad® 3D modelling and visualization tool (Mallet, 1992, Mallet, 2002) that is particularly used by oil and gas companies. Research on G-Maps and their application in 3D-modelling and visualisation is centered at the Laboratoire SIC of Poitiers University, where the G-Map viewer and editor Moka is available as open source (Moka 2006).

Figure 6 shows a simple example for using G-Maps for the topological representation of a 3D city model. Parts of this model have been implemented in (Butwilowski, 2007). This topological model presents Osnabrück palace, the main building of Osnabrück University, represented by G-Maps.

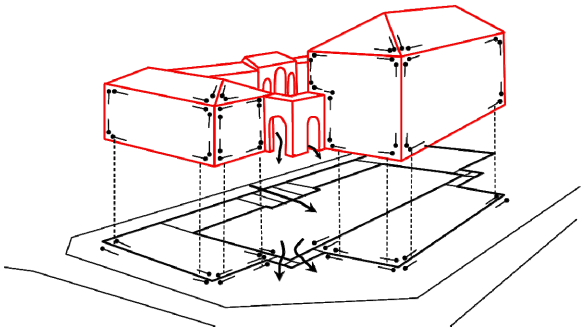

Figure 6: Osnabrück Palace represented by G-Maps

Note that also the archways are represented, i.e. “real 3D” topology may be represented by this approach.

Operations for the processing of cell-tuples may be Euler-operations or non-Euler operations. Let us shortly introduce the following Euler-Operation: the splitting of a solid s by the insertion of a separating face f, into two solids s_1, s_2 (figure 7).

Besides set operations, splitting a 3D-cell requires the use of an $orbit_{012}()$. We start with the definition of a closed connected sequence of nodes and edges that define the contact – the seam – between the circumference of the face and the meshing of the inner surface of the solid. This can be done using a sequence of cell-tuples connected by α_0- α_1-, and α_2-involutions forming a closed loop. This seam location has to be defined by the user or by a client program, and the number of its nodes and edges must coincide with that of the boundary of f. The operation then consists of the following steps:

First, insert face f, and solids s_1 and s_2. Next, for each pair of cell-tuples situated on either side of the seam location, replace

$(n_i,e_j,f_k,s,+)\ \alpha_2\ (n_i,e_j,f,s,-)$

by a sequence

$(n_i,e_j,f_k,s_1,+)\ \alpha_2\ (n_i,e_j,f,s_1,-)\ \alpha_3\ (n_i,e_j,f,s_2,+)\ \alpha_2\ (n_i,ej,f_l,s_2,-)$.

Finally, starting from a cell-tuple $ct_0(n_i,e_j,f,s_1,+)$, use an $orbit_{012}(ct_0)$ to replace s by s_1 on every cell-tuple encountered, and all cell-tuples related by α_3-involutions. By the use of an $orbit_{012}()$, it is assured that all cell-tuples $ct(.,.,.,s)$ selected for update are situated on the boundary of solid s and on one side of face f, independent of the value of the solid component. Next we repeat the same procedure starting with $(n_i,e_j,f,s_2,-)$, replacing s by s_2 on the other side of face f.

Such sequences of operations can be implemented using the insert, delete and update operations of a relational database within a transaction. For the inverse operation "solid merge" to be applicable, a number of consistency checks have to be performed, in order to ensure that no inadmissible "non-manifold" 3D configurations occur. For instance, a "2D-bridge" configuration, i.e. a 2D face incident on both sides with the same solid, can be avoided by ensuring that there is no second contact between s_1 and s_2, and if we remove a cell at the boundary by merging it with the "outside", we have to ensure that there is no second contact with the outside.

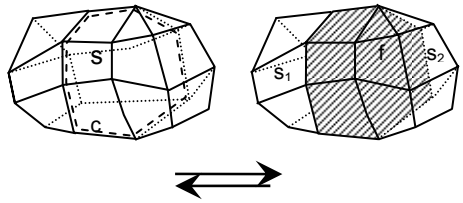

Figure 7. splitting a 3D solid s by the insertion of a 2D face f. The location of the seam is defined by the loop c.

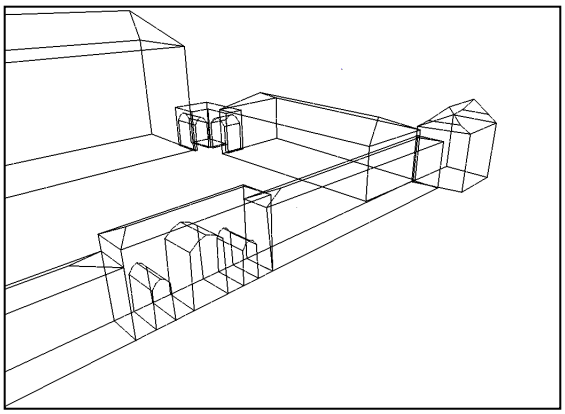

Figure 8: Volumetric model of Osnabrück Palace (visualized by Moka 3D visualization tool, University of Poitiers, France, figure from (Butwilowski, 2007))

The volumetric model of the topology sketched in figure 7 is shown in figures 8 and 9. The Moka 3D visualization tool

(Moka, 2006) allows the visualization of G-Maps in all dimensions, i.e. lines, faces and solids may be drawn in different colours, respectively.

5. OUTLOOK

In the ongoing research the geo-database group at IGF is participating in the GEOTECHNOLOGIEN special research project (Geotechnologien, 2008), working on the development of 3D geo-database for supporting the analysis and warning of landslides. The overall objective of this work is to develop new methods and information system components for the early warning of geological events by combining methods from geodatbases, spatial data mining, simulation and modelling, GIS, and linguistic methods.

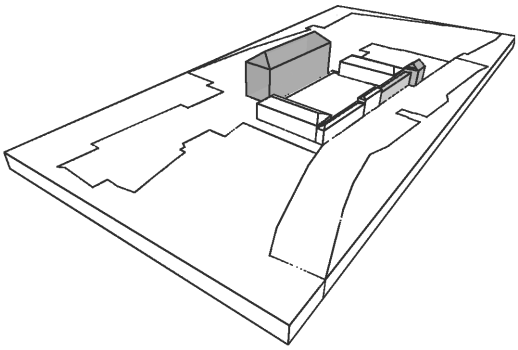

Figure 9: Part of model of Osnabrück palace with passageways, visualised with program Moka (University of Poitiers)

In teaching the geo-database group at IGF is dealing with mobile database management systems, spatial databases, 3D/4D geoinformation systems, algorithms and data structures in geoinformatics, and object-oriented programming for GIS development. Finally in the geoinformatics study project the students are trained in the development of own geo-database software.

6. REFERENCES

Bär, W., 2002. Konzeption und Entwicklung von Software-Komponenten für ein Routenplanungssystem mit mobilen Endgeräten. Diploma thesis, Institute of Environmental Sciences, University of Vechta.

Bär W., 2007. *Verwaltung geowissenschaftlicher 3D Daten in mobilen Datenbanksystemen.* Ph.D. Thesis, University of Osnabrück, 166p.

Bär, W., Breunig, M., 2005. Usage of Mobile Databases for Mobile Geoscientific Applications. Proceedings of the 8th AGILE Conference on Geographic Information Science, Estoril, Portugal, 10p.

Breunig, M., 2005. Räumliche Repräsentationen. In: Coors/Zipf (eds.), *3D-Geoinformationssysteme,* Wichmann Verlag, Heidelberg, pp. 41-55.

Breunig, M., 2007. Geodatenbankforschung: Rückblick und Perspektiven aus Sicht der Informatik. *Datenbank Spektrum,* years issue 7, No. 21, dpunkt Verlag, Heidelberg, pp. 5-14.

Breunig, M, Bär, W., 2004. Database Support for Mobile Route Planning Systems. *Computers, Environment and Urban Systems,* Elsevier Science, Vol. 28, pp. 595-610.

Breunig, M., Bär, W., Thomsen, A., 2004a. Konzeption datenbankgestützter 3D-Geodienste. GeoLeipzig 2004, Leipzig. In: *Schriftenreihe der Deutschen Geologischen* Gesellschaft, No. 34, Hannover, p. 69.

Breunig M., Bär W., Thomsen, A., 2004b. Advancement of Geoservices - Services for Geoscientific Applications based on a 3D-Geodatabase Kernel. *GEOTECHNOLOGIEN Science Report No. 4*, Information Systems in Earth Management, Potsdam, pp. 35-39.

Breunig, M, Bär, W., Thomsen, A. Coelho, A.H. Staub, G. Wursthorn, S., 2005. Ein Blick in die Zukunft: Datenbankunterstützung für mobile AR Systeme. *Proceedings 8. Workshop des GI-Arbeitskreises „Mobile Datenbanken und Informationssysteme",* BTW Karlsruhe, pp. 85-96.

Breunig, M. Reinhardt, W.,Ortlieb, E., Mäs, S. Boley, C., Trauner, F.X.,Wiesel, J., Richter, D., 2007a. Development of suitable information systems for early warning systems. *Geotechnologien Science Report*, Potsdam, pp. 113-123.

Breunig M., Thomsen A., Broscheit B., Butwilowski E., Sander U., 2007b. Representation and analysis of topology in multi-representation databases. *Proceedings of Photogrammetric Image Analysis Conference PIA´07,* Munich, pp. 167-172.

Breunig, M., Zlatanova, S., 2006. Geo-DBM. In: Zlatanova S., Prosperi, D. (Hrsg.), *Large-scale 3D Data Integration – Challenges and Opportunities.* CRCPress, Taylor & Francis group, pp. 88-116.

Brisson E., 1989. Representing Geometric Structures in d Dimensions: Topology and Order. In Symp. Comp. Geom. ACM, pp. 218-227.

Brisson E., 1993. Representing Geometric Structures in d Dimensions: Topology and Order. Discrete and Computational Geometry, 9. pp. 387-426.

Butwilowski, E., 2007. Topologische Fragestellungen bei der Kombination von 3D-Stadtmodellen mit 2D-Karten in einer räumlichen Datenbank, Diplomarbeit, Institut für Geoinformatik und Fernerkundung, Universität Osnabrück, 114p.

Geotechnologien, 2008. Description of the Geotechnologien special research project, www.geotechnologien.de, (accessed february 20th 2008).

Lienhardt P., 1988. Extension of the notion of map and subdivisions of a three-dimensional space. In Proc. 5th Symp. on Theoretical Aspects in Computer Science, Feb. 1988

Lienhardt P., 1989. Subdivision of n-dimensional spaces and n-dimensional generalized maps. 5th annual ACM Symp. on Comp. Geom. Saarbrücken, Germany, pp. 228-236.

Lienhardt P., 1991. Topological models for boundary representation: a comparison with n-dimensional generalized maps. Computer Aided Design 23(1) pp. 59-82.

Lienhardt P., 1994. N-Dimensional Generalized Combinatorial Maps and Cellular Quasi-Manifolds. Journal on Comp. Geom. and App., 4(3): pp. 275-324.

Mallet J.L., 1992. GOCAD: A computer aided design programme for geological applications. Turner, A.K. (Ed.): Three-Dimensional Modelling with Geoscientific Information Systems, proceedings of NATO ASI 354, Kluwer Academic Publishers, Dordrecht, pp. 123-142.

Mallet J.L., 2002. Geomodelling. Oxford University Press, 599 p.

MOKA, 2006. Modeleur de Cartes. http://www.sic.sp2mi.univ-poitiers.fr/moka/ (accessed february 22nd, 2008).

Thomsen, A., 2005. Räumliche Operationen für geowissenschaftliche 3D-Datenbankmanagementsysteme. In: Coors/Zipf (eds.), 3D-Geoinformationssysteme, Wichmann Verlag, Heidelberg, pp. 71-98.

Thomsen, A., Breunig, M., 2007. Some remarks to topological abstraction in multi representation databases. Proceedings of 3rd Internat. Workshop on Information Fusion and Geographical Information Systems IF&GIS-07, St. Petersburg, Lecture Notes in Geoinformation and Cartography, Springer, Heidelberg, pp. 234-251.

Thomsen A., Breunig M., Butwilowski E., Broscheit B., 2007. Modelling and Managing Topology in 3D Geoinformation Systems, Proceedings of 3D Geoinformation 2007, Delft, Lecture Notes in Geoinformation and Cartography, Springer, Heidelberg, pp. 229-246.

Thomsen A., Breunig M., Butwilowski E., 2008. Towards the Unified Modelling and Management of Topology in Multiple Representation Databases. Photogrammetrie – Fernerkundung – Geoinformation, PFG, E. Schweizerbart´sche Verlagsbuchhandlung, Stuttgart, accepted, 8p.

THE CONTRIBUTION OF EARTH OBSERVATION TO DIGITAL EARTH

I. Dowman

Dept. of Civil, Environmental and Geomatic Engineering, University College London, Gower Street, London, WC1E 6BT UK - idowman@ge.ucl.ac.uk

KEY WORDS: Digital Earth, Earth Observation, SDI

ABSTRACT:

The concept of Digital Earth was highlighted by Al Gore in 1998 when he was Vice-President of the USA. His speech has given rise to a number of Digital Earth initiatives, of varying forms. A series of symposia led the way to the formation of The International Society for Digital Earth (ISDE) which has continued the symposia series and set up working groups to study the implementation of Digital Earth. This paper traces the development of Digital Earth and looks at how data from Earth Observation satellites can contribute, and in particular at the organisations which exist to coordinate the activities of Earth observation to deliver data for the benefit of society, and how this relates to Digital Earth and how the concept is being implemented.

1. INTRODUCTION

Digital Earth has many manifestations. The first which comes to mind maybe the concept put forward by Al Gore in 1998 with his vision of a digital Earth to enable a wide range of people to virtually explore the planet. Scientists may think first of global data sets and models of the solid Earth, oceans or the atmosphere. But what is clear is that there is no one Digital Earth and that for the concept to be effective, a single organisation, or recognised consortium or organisations, will be required to strengthen and promote the concept.

People concerned with Earth observation and remote sensing may claim Digital Earth as their own because Earth Observation (EO) has provided the data for many realisations of digital Earth, for example global land cover maps, linking climate, environment with malaria, monitoring deforestation, modelling ocean currents and ozone depletion. Google Earth and similar web based data sets also use EO data and play an important role in democratisation of EO data: in other words making people familiar with the data.

The purpose of this paper is to set out the different views of digital earth and to assess the progress made and the potential of the concept.

2. DIGITAL EARTH

2.1 Definition

The International Society for Digital Earth, (ISDE), founded in China in 2006, defines Digital Earth in the following way (ISDE, 2008):

> "Digital Earth is characterised as a virtual representation of the planet, encompassing all its systems and forms, including human societies, manifested as a multi-dimensional, multi-scale, multi-temporal, and multi-layer information facility.
>
> "The Digital Earth vision incorporates a digitally-formatted Earth, a functionally interfacing metaphor, whereby a corresponding virtual body of knowledge of the real Earth and its digital representation for understanding the Earth and relevant phenomena is accessible to all citizens of the planet via the internet.
>
> "Digital Earth is compromised of a corresponding set of theoretical, technological, scientific, engineering, and applications systems, which are fully integrated as necessary to provide a framework to support national and international cooperation for global sustainable development, and a newly-growing point of economic growth and social well-being."

This is a comprehensive and ambitious definition, and if it is realised will provide a powerful tool for the understanding of the planet.

2.2 Development of Digital Earth

The digital Earth concept can be traced back to Buckminster Fuller in the 1940 with his "Geoscope" envisioned as the first interactive geo-environment, but the real current interest was started by Al Gore in 1998 with his vision to create a "Digital Earth". This has led to a number of realisations of Digital Earth. A Google search results in websites about atlases, catalogues of maps and digital data, blogs as well as sites for the ISDE and the symposium series. It also includes SRI International's DARPA-sponsored Digital Earth project which "incorporates a connected suite of technologies with the vision of enabling a massive, scalable, and open model of the planet where millions of users can interact with vast quantities of geographically referenced (georeferenced) data over the Web" http://www.ai.sri.com/digitalearth/# .

In 1999 China launched the International Digital Earth Symposium series which has been followed up with the foundation of ISDE. Symposia have been held in China, Canada, Czech Republic, Japan and San Francisco and in 2005 The Digital Earth Summit on Sustainable Development was held in Auckland, New Zealand. A further Digital Earth Summit on Geoinformatics: Tools for Global Change Research will be held in Potsdam, Germany in 2008 Whilst these meetings have undoubtedly brought together scientist and users and generated great enthusiasm for the project, the big question is: have these meetings achieved anything to genuinely get us closer to a digital earth as defined by ISDE.

2.3 Progress

In 2005 the Digital Earth Summit on Sustainable Development in Auckland created great interest and the keynote speech was give by the Prime Minister of New Zealand. New Zealand and cities such as Auckland are committed to sustainable development and see a Digital Earth as an important tool to achieve this. There are however many challenges, as set out by Simpson (2006). These include:

- Representation - to find ways to express the infinite complexity of the geographical world in the binary alphabet and limited capacity of a digital computer and dynamism
- Content - to find ways of summarizing, modeling, and visualizing the differences between a digital representation and real phenomena
- Cognition 'Socializing the Pixels' - to achieve smooth transition between cognitive and computational representations and manipulations of geographic information
- Simulation - to create simulations of geographic phenomena in a digital computer that are indistinguishable from their real counterparts
- Assessment to bridge local and global scales and enable meaningful assessment of information pertaining to sustainability of places.

Plans were made to establish Working Groups to tackle these challenges.

3. EARTH OBSERVATION

3.1 Technology

During recent years there have been a number of important technological developments which enable data to be collected more efficiently and delivered to where it is needed. These include the increase in computer power and the maintenance of costs which are affordable, the internet, and the development of Global Navigation Satellite Systems (GNSS), which provide instant positional information, and, when used with inertial navigation systems (INS) allow accurate georeferencing of image data.

The result of these developments has been operational use of high resolution satellites with less than 1 metre pixel size, global observation of the planet with low and medium resolution satellites. Constellations of satellites are being formed to ensure that coordinated, comprehensive data collection is achieved, and that this is linked with in-situ data collection and used to generate products which can be immediately useful to workers in the field. The Committee on Earth Observation Satellites (CEOS) has established the concept of virtual constellations and is developing plans for constellations for precipitation, land surface imaging, ocean surface topography and atmospheric composition. The generation of global data sets showing the terrain in the form of digital elevation models, such as that generated by the Shuttle Topography Radar Mission (SRTM), has been immensely useful, and been used to produce high resolution image maps. Optical missions have been doing the same thing and have produced global map coverage of many types. An increase in processing power has resulted in rapid generation of this data, and the ability to merge data from different satellites.

For Earth Observation (EO) to contribute significantly to the development of a Digital Earth the data needs to be used, not just for observing systems and change, but for modelling it in order to understand the Earth processes. One example of how this might be done is the 7.2 billion Yen Earth Simulator in Japan. This used the world's most powerful computer when it was turned on in 2002. Devoted to mirroring the Earth by holistic simulations of global climate in both the atmosphere and the oceans down to a precision of 10 km. The Earth Simulator's 62 super computers are capable of 35.86 trillion (35,860,000,000,000) floating-point calculations per second, or 35.86 TFLOPS. The Digital Earth Data is stored on 700 terabytes of disk drives.

There is clearly a great potential for use of such technology for modelling Earth processes.

3.2 Applications

There are many documented examples of successful application of Earth Observation data. For example a large set of case studies has been put together by the CEOS Data Utilisation Group under the headings of:

- Land Applications
- Ice Applications
- Atmospheric Applications
- Ocean Applications
- Charters & Conventions

These can be found at: http://www.ceos.org/utilization/

In November 2007 the GEO Ministerial Summit was held in Cape Town and a report on Early Achievements of GEOSS was published, (GEO, 2007). This reports on a number of projects which fit within the Digital Earth concept, including global monitoring of greenhouse gases and collecting information on global runoff from rivers.

When using EO data within Digital Earth the global picture must be considered. A data base for digital Earth must contain a comprehensive set of data which can be accessed to address bother regional and global problems. The data must be collected in an organised manner and an infrastructure for distribution must be in place. The Group on Earth Observation (GEO), see 4.1 below, has a Global Earth Observation System of Systems (GEOSS) in place, which recognises this and is planning around 9 societal benefit areas:

- **Disasters:** Reducing loss of life and property from natural and human induced disasters
- **Health:** Understanding environmental factors affecting human health and well being
- **Energy:** Improving management of energy resources
- **Climate:** Understanding, predicting, mitigating and adapting to climate variability and change
- **Water:** Improving water resource management through better understanding of the water cycle
- **Weather:** Improving weather information, forecasting and warning
- **Ecosystems:** Improving the management and protection of terrestrial, coastal and marine resources
- **Agriculture:** Supporting sustainable agriculture and combating desertification
- **Biodiversity:** Understanding, monitoring and conserving biodiversity

Within each of these the required observation strategy is defined and goals set. For example the following are some of the goals of the 2 year plan:

- Improve the reporting of observations to international data and analysis centres in terms of data volumes, quality and timeliness.
- Establish a strong collaboration mechanism between observational organizations and research communities, and users of climate information, to further refine the analyses and products required.
- Identify the needs and solutions necessary to implement the global observing systems for climate in all regions and countries based on the recommendation of GCOS-92 (GCOS, 2004) and specific regional action plans.
- Initiate an intergovernmental mechanism in the terrestrial domain to prepare and issue regulatory and guidance information on observational procedures and data management.

These emphasise the need to link the data to the requirements of research and monitoring organisations. An example of the way in which EO for climate can be beneficial is quoted in the GEOSS implementation plan:

"Climate Extremes Warning System for Seasonal Forecasts Five years from now, in June, seasonal climate forecasts predict an exceptionally strong El Niño event for the following December to February season in the Central and Eastern Pacific, with heavy impact on regional weather patterns in parts of Latin America. A timely and tailored forecast is broadly disseminated and provides the opportunity to plan adequate mitigation measures in all affected regions and with respect to various societal areas for the coming months: in the agriculture sector, farmers in Northwestern Peru, Southern Ecuador and Uruguay are advised to expect increased likelihood of heavy rainfalls and prepare for reducing possible flood damages, thereby improving national food security; Northeast Brazilian farmers are advised to plant drought-resistant or fast-ripening crops to adapt to forecasts of increased chances of drought conditions; livestock farmers will time their slaughtering, transportation and marketing schedules on information, which includes the likely seasonal rainfall scenarios; countermeasures against possible floods, which can lead to prolonged food shortages by ruining stocks and fertile topsoils, will be taken, saving lives and property in flood-prone areas. For the regional health sector, surveillance by early warning systems within the GEOSS helps to combat diseases, such as malaria, affected by exceptional climatic conditions. The El Niño forecast has been enabled by substantial enhancement since 2005, through the coordinated efforts by GEOSS, of satellite and composite in situ observing networks (e.g., ships, drifting buoys) over previously data-sparse areas. Improved data exchange, capacity building and computer technology in the preceding five years will have improved our understanding of regional atmospheric patterns, and predictability, and the information dissemination to potentially affected countries where specific regional and local response measures are to implemented." (GEO, 2005)

This example illustrates many of the components needed for successful use of EO data: collection of data from many sources, modelling to allow prediction of events which could have an adverse influence on society, distribution of data and its application to areas not normally used to receiving such data. It also covers several areas of societal benefit.

4. INFRASTRUCTURE

4.1 Organisational

The requirements for efficient use of EO data depend on organisation. Data distribution, setting up satellite constellations, interoperability and the establishment of collaborative arrangements is far more than a technical operation.

The World Summit on Sustainable Development (WSSD) in Johannesburg recognized the importance of Earth observation. In the Implementation Plan from WSSD specific mention is made of Earth Observation and GIS to "Promote the development and wider use of earth observation technologies, including satellite remote sensing, global mapping and geographical information systems, to collect quality data on environmental impacts, land use and land-use changes, ….". The plan also calls for support to countries, particularly developing countries, in their national efforts to collect data, use satellite and remote-sensing technologies for data collection and to access, explore and use geographic information. Of major importance in implementing this is the intergovernmental Group on Earth Observations (GEO) established initially by the first Earth Observation Summit in July 2003 which declared the need for "timely, quality, long-term, global information as a basis for sound decision making", and formally recognised at the third Earth Observation Summit in Brussels, February 2005. The 10-Year Implementation Plan for Global Earth Observation System of Systems (GEOSS) was negotiated by the ad hoc GEO and adopted at the summit in Brussels. On-going activities of the United Nations, CEOS and IGOS, (The Integrated Global Observing Strategy) are integrated into GEOSS, and scientific organisation such as ICSU ISPRS, ICA, and FIG are active within GEO.

4.2 Technical

The distribution of data is an essential component of provision and use of data. There are a number of important developments in this field.

GEONETCast is a near real time, global network of satellite-based data dissemination systems designed to distribute space-based, air-borne and in situ data, metadata and products to diverse communities. GEONETCast is a Task in the GEO Work Plan and is led by EUMETSAT, the United States, China, and the World Meteorological Organization (WMO). Many GEO Members and Participating Organizations contribute to this Task. GEONETCast distributes data, such as meteorological data, ocean data and products, landcover data and also varios products from this data.

GEOSS has a major interest in portals and interoperability. GEO (2007) reports on progress with the GEO Web Portal and GEOSS Clearinghouse, as well as the GEOSS Standards and Interoperability Registry and Interoperability Process Pilot Project.

Another example of a portal is the ESA ICEDS (Integrated CEOS European Data Server) with the aims to:

1. use Open Geospatial Consortium (OGC) technologies for map and data serving;
2. serve datasets for Europe and Africa, particularly Landsat TM and Shuttle Radar Topography Mission (SRTM) digital elevation model (DEM) data;
3. provide a website giving access to the served data;

4. provide software scripts, etc., and a document reporting the data processing and software set-up methods developed during the project.

Web based systems such as Google Earth provide access to data through the internet and may be considered to be a small step to democratising geospatial data. However there are many concerns about the quality and accuracy of such data and there is a need to educate people in the proper use of such data.

Spatial data infrastructures (SDI) are a more formal way of distributing data. The Commission on Geosciences, Environment and Resources (CGER, 1993) defines a Spatial Data Infrastructure as the means to assemble geographic information that describes the arrangement and attributes of features and phenomena on the Earth. The infrastructure includes the materials, technology, and people necessary to acquire, process, store, and distribute such information to meet a wide variety of needs.

In practical terms, in the context of imagery, this means providing imagery at low cost, broadband internet connection and the means to process large volumes of data by the receiver. A very basic but essential requirement for tacking the problems is information on where the problem is located, what is there and how to get there. Existing mapping is frequently out of date, especially in less developed areas, but satellite images can provide up to date information.

A key component of a SDI is interoperability and this is now provided by OGC standards. The GEOSS architecture is being built using OGC standards and the portals and catalogues are also OGC compliant.

5. DISCUSSION

We have discussed various components which might contribute to a Digital Earth, but we now need to assess how far along the road we are to a useful system. The task is massive and complex. Technology is available, and data is available, but the organisational task in bringing the components together, ensuring that scientists collaborate and providing the funding is the major challenge. Organisations such as GEO have recognised the need to address problems which benefit society, and these have some political backing. Recent reports from GEO show that some progress in being made and that GEOSS has the potential to deliver systems and data which could be an integral part of Digital Earth.

The Digital Earth Summit on Geoinformatics: Tools for Global Change Research to be held in Potsdam in November 2008, is designed to bring together leading scientists from Geoinformatics and Global Change research and will foster the exchange of ideas, cooperation between so-far disjoint scientific fields and provide time for in-depth discussion. Invited keynote speakers will cover relevant topics in Geoinformatics, Global Change research, Spatial Data Infrastructures, Digital Earth initiatives, and Earth Observation activities as well as the interaction between these fields. Such discussion is valuable but there is a real need for action to co-ordinate research and to work towards a coordinated solution.

6. REFERENCES

CGER 1993. Toward a Coordinated Spatial Data Infrastructure for the Nation. National Academies Press.

GEO, 2005. Global Earth Observation System of Systems

GEOSS, 10-Year Implementation Plan Reference Document. ESA SP-1284. 209 pages.

GEO, 2007. The First 100 Steps to GEOSS. Annex of early Achievements to the Report on Progress 2007. GEO Secretariat. http://www.earthobservations.org/documents/the_first_100_steps_to_geoss.pdf

IGOS, 2004. IGOS Geohazards Theme Report.

ISDE, 2008. http://www.digitalearth-isde.org/ society/bylaws/20.html

Simpson, 2006. http://www.digitalearth06.org.nz/Powerpoint/W_SimpsonForesman.ppt#350

SUPPORT FOR DISASTER MANAGEMENT WITH REMOTE SENSING

Monika Gaehler & ZKI-Team

Center for Satellite based Crisis Information (ZKI) of the German Remote Sensing Data Center (DFD), Oberpfaffenhofen - German Aerospace Center (DLR), Muenchner Str. 20, 82234 Wessling, Germany – monika.gaehler@dlr.de

KEY WORDS: Satellite based Crisis Information, International Charter "Space and Major Disasters", Disaster Response, GMES, Rapid Mapping

ABSTRACT:

During natural or man made disasters generally a fast overview of the extent of the crisis is needed. Therefore satellite data is optimally suited to get an impression of the affected area and the intensity of the devastation. The International Charter "Space and Major Disasters", a consortium of the largest space agencies all over the world, provides satellite data with highest programming and delivery priority in case of natural or man-made disasters. Since the "Charter" formally provides only raw data, service elements like RISK-EOS and RESPOND (part of the GMES 'Global Monitoring for Environment and Security' initiative of EU and ESA) process these data and transform them into user-friendly information products. The Center for satellite based crisis information (ZKI) of the German Aerospace Center (DLR) is providing such rapid mapping services through such GMES projects. It has built up experience in this field over the years in more than 40 rapid mapping activations all over the world.
This article aims to describe the International Charter, the GMES Service Element RISK-EOS and the Center for satellite-based crisis information with respect to the Charter activation for the UK flooding in 2007. Insights will be given to the basic structures and procedures as well as to the results and products provided during this call.

1. INTRODUCTION

The increasing occurrence of natural disasters, humanitarian emergency situations and civil endangerment cause a growing demand for timely information on rapidly evolving events. This includes comprehensive, near-real time earth observation data, which offer independent coverage of wide areas for a broad spectrum of civilian crisis situations. The reasons for this development are manifold and can be seen in the increasing vulnerability of societies and infrastructure and population (Murlidharan, 2003).

Furthermore weather pattern most probably has been shifted to more extreme conditions. Additionally, regional and global cooperation of relief actors has been extended strongly. Satellite imagery can serve as a source of information in emergency, crisis or disaster situation. Having recognized this need, the German Remote Sensing Data Center (DFD) of the German Aerospace Center (DLR) established a service called "Center for Satellite-Based Crisis Information" (ZKI, www.zki.dlr.de). The center links DLR's comprehensive operational remote sensing data handling and analysis capacities with national and international civil protection and humanitarian relief actors as well as with political decision makers. ZKI's function is the rapid acquisition, processing and analysis of satellite data and the provision of satellite based information products on natural and environmental disasters, for humanitarian relief activities, as well as in the context of civil security. The analyses are tailored to meet the specific requirements of national and international political bodies or humanitarian relief organizations. In order to provide up-to-date and relevant satellite based cartographic information and situation analysis, it is necessary to establish efficient and operational data flow lines between satellite operators, receiving stations and distribution networks on the one hand and the decision makers and relief workers on the other hand. Service lines and feedback loops have been established to allow best possible data and information provision as well as optimized decision support.

For emergency situations satellite data has to be available as fast as possible and the information has to be extracted from the raw data. This is actually provided by the International Charter "Space and Major Disaster" (www.disasterscharter.org) that gives rapid access to satellite data to support crisis management. The mandatory processing and analysis, which is not provided through the "Charter" is currently performed, for example, through the GMES (Global Monitoring for Environment and Security) Service elements RISK-EOS (www.risk-eos.com) or RESPOND (www.respond-int.org). The following chapters will explain in depth their roles and functioning.

2. INTERNATIONAL CHARTER "SPACE AND MAJOR DISASTERS": STRUCTURE, OBJECTIVES AND PROCEDURES

The International Charter "Space and Major Disaster" was initiated 1999 by ESA and CNES and started operation in 2000. The Charter represents a network of space agencies worldwide, e.g. ESA, CSA or CNES, sharing the rights and duties, because one single space agency was and is not able to handle the crisis information management alone. The Charter agreed to give access to satellite data fast and free-of-charge in case of natural or man made disasters. After the approval of a Charter request, the Charter suggests a project manager (PM) and a value adder (VA).

After definition of the Charter:
An emergency situation ***in the context of the Charter on Space*** *and Major Disasters is an urgent need for space services associated with a unique and important event, when something unanticipated suddenly occurs and requires prompt action, beyond normal procedures to prevent or limit injury to person or damage to property. Thus, an important aspect of Emergencies is that they are unexpected and, hence, the satellite coverage for them cannot be planned in the usual way.*

Managing emergencies includes preparation for and responding to such impending events as forest fires, tropical storms and the resulting floods, volcanic eruptions and earthquakes.

Industrial hazards of the kind requiring action by Emergency response agencies are caused primarily in the generation and movement of energy-related materials and chemicals. Threats to public safety and security caused by human actions pose infrequent additional hazards (definition from Charter documents).

Based on this definition the Charter defined some acceptance criteria that can be summarized as described in the following list:

1. The request will be received from an Authorized User to be a valid request for which space services can be provided under the provision of the Charter.
2. A disaster event (if natural or man-made) is an emergency situation (see definition above)
3. It is a sudden, uncontrolled or unexpected disaster causing risk to human life, environment or property.

The Charter also defines cases where a request is not identified as Charter relevant:

4. For non-emergency situations, e.g. regular oil spill monitoring or ice monitoring operations
5. If the emergency falls out of the Charter scope. This is present for war or armed conflicts, humanitarian actions or search and rescue actions that are not linked to a specific disaster.
6. Emergencies with doubtful/no benefit from space assets, this means situations like droughts or epidemiological outbreaks.
7. Calls beyond the emergency period. The Charter shall not be activated later than 10 days after the actual crisis started.

In General, a Charter call should be limited to a maximum duration of 15 days after activation. And the request should be rejected if the size of the disaster is not compatible to the resolution of the available satellites.

Concerning the use of the data the Charter defines that the raw data shall only be used for the relevant Charter Call and during the Charter call. It is not foreseen to use the data afterwards for scientific purposes.

The number of data sets for a single Charter activation provided by the Charter is limited due to the volume expected to fully cover the need for analysis. A list of the space resources within the Charter and a description of the Charter can be found on the Charter website (www.disasterscharter.org).

3. ROLES WITHIN THE CHARTER OPERATIONAL LOOP

When a disaster occurs somewhere on the globe, a predefined process is triggered. In the following the roles and the work flow for a fictive Charter activation are described (see Figure 1, International Charter: operational loop):
First a disaster happens and an Authorised User (AU) is involved, either because it happened in his country or a user requested help through the AU to the Charter. The AUs contact the On-Duty Operator (ODO). The ODO checks if the request is coming from an official AU and passes the request Emergency on-Call Officer (ECO). The partner agencies of the Charter take turn on a weekly basis to provide an officer to be on-call. He has the knowledge-base to decide which satellite data are needed for the relevant disaster and starts the requests for image acquisition at the partner space agencies. Simultaneously, the Charter Executive board suggests an organisation to do the project management (PM) during the Call. Aim is to situate the PM as close as possible to the disasters location. However, also other criteria are taken into account like relation of the PM or value adder (VA) to the AU, experience in rapid mapping or expertise relevant to the kind of disaster.
The ECO summarised all the information into a dossier and passes it to the designated PM. At this point the work for the ECO ends and the PM takes over. Both, ODO and ECO are available 24 hours a day, 7 days a week.

The PM has the responsibility to coordinate the value adding. He is the point of contact for the AU and defines in cooperation with the AU or end user the product that should be generated. His task is to receive the data and channel it to the VA or give the AU direct access to the data sets. The raw data remains the property of the supplying Charter partner, however, it may be used for the emergency relief by the AU. Another task of the PM is to perform a quality check of the products before the delivery to the AU and if needed request for modification. The PM is available during normal working hours.

The VA receives the satellite data and extracts the relevant information with respect to the user request. The primary aim is to generate the product as fast as possible and to visualize the important content in a way the user understands. The demand and the form of the needed information depends strongly on the end user, that can be, e.g., an in field team or a Ministry of Environment.

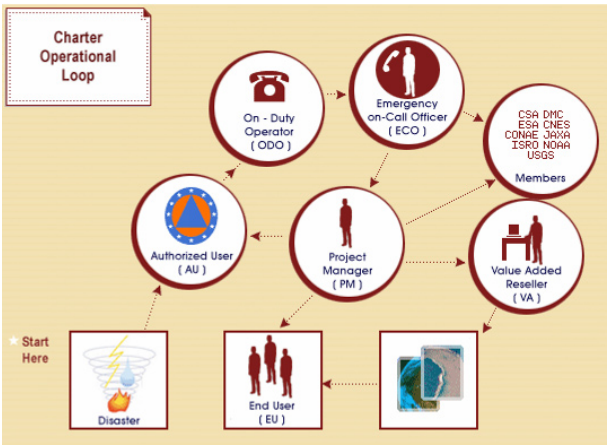

Figure 1. International Charter; operational loop (www.disasterscharter.org).

4. GMES SERVICE ELEMENT RISK-EOS

RISK-EOS is a GMES Service Element that provides several services for all phases of the risk management: prevention – anticipation – crisis – post-crisis (see also www.risk-eos.com). Within RISK-EOS a rapid mapping service is offered for flood, fire and other risks except oil spill monitoring. The rapid mapping is provided by SERTIT and DLR and both partners have gathered a large experience during various mapping activities during the last years for many different kinds of disasters. Some examples in 2007 are the floodings in United Kingdom, Mozambique and Mexico, oil spill in Ukraine/ Russia, the storm over Bangladesh or the forest fires in South Europe.

RISK-EOS performs the value adding for Charter activations that fall within the scope of the project. This overall service is at the moment provided free of charge to the user community. For future scenarios of the GMES Services see Tufte (2008).

5. ZKI – CENTER FOR SATELLITE-BASED CRISIS INFORMATION

The ZKI was created in 2002 and is situated at the German Aerospace Center (DLR) and is an integral part of the German Remote Sensing Data Center (DFD) in Oberpfaffenhofen, Germany. The mission of the ZKI is:

- to bundle existing DLR resources and expertise for effective and coordinated crisis management support,
- to develop and establish methodologies for the generation of customized information products and services,
- to provide advice on establishing crisis information centers,
- and to develop and support the setting-up of distributed European and international networks for satellite-based civil crisis information.

ZKI has the opportunity to revert to all technical and man power resources of the DFD in case of a severe crisis event. This gives ZKI a high flexibility to react on the size of the disaster and merges all the expertise within the DFD, from data acquisition, data processing and archiving to image enhancement, information extraction and map generation. ZKI acts as link between the space technology and the user side. ZKI operates in national and international contexts, closely networking with German public authorities and state levels, non-governmental organizations, satellite operators and space agencies.

All mapping products are tailored to meet the specific requirements of the user. ZKI uses its large experience from intense and long time user contact to generate highly condensed products for the individual use. The resulting satellite based information products are provided for natural and environmental disaster management and humanitarian relief activities and for civil security issues.

DLR has committed itself to support the Charter through, e.g. the project management or the value adding, like it was the case during the UK flooding activation.

6. RAPID MAPPING SERVICE

After the occurrence of a natural or man-made disaster the necessity of fast and reliable spatial information is important not only for situation centers but also for relief organisations and rescue teams. Civil protection authorities have to meet the demand for adequate crisis information in order to ensure an appropriate decision process and an effective crisis management. Therefore all possibilities obtaining spatial crisis information have to be taken into account, particularly earth observation data proved to provide significant information input.

In order to cover these user requests in crisis situations, ZKI set up a rapid mapping work flow (Figure 3) to ensure a fast access to available, reliable and affordable crisis information worldwide.

After the mandatory decision process whether satellite analysis is appropriate for the respective crisis, the area of interest has to be defined and cross checked to avoid false geolocation. Following this iterative process, it has to be assured that all applicable satellites are programmed for data acquisition. This can either be coordinated within the International Charter "Space and Major Disasters" by the responsible project manager or through commercial satellite tasking. Furthermore an enquiry for corresponding archive imagery has to be set up for documentation of the pre-disaster situation and change detection analysis. Beside the procurement of satellite data it is necessary to check and prepare supplementing geo-data like population and infrastructure data, road network, contour lines and administrative boundaries. The experience of several activations and the user feedback shows that additional geo-information increases the satellite data analysis significantly.
This includes place names, critical infrastructure, transportation network or further detailed specifications.

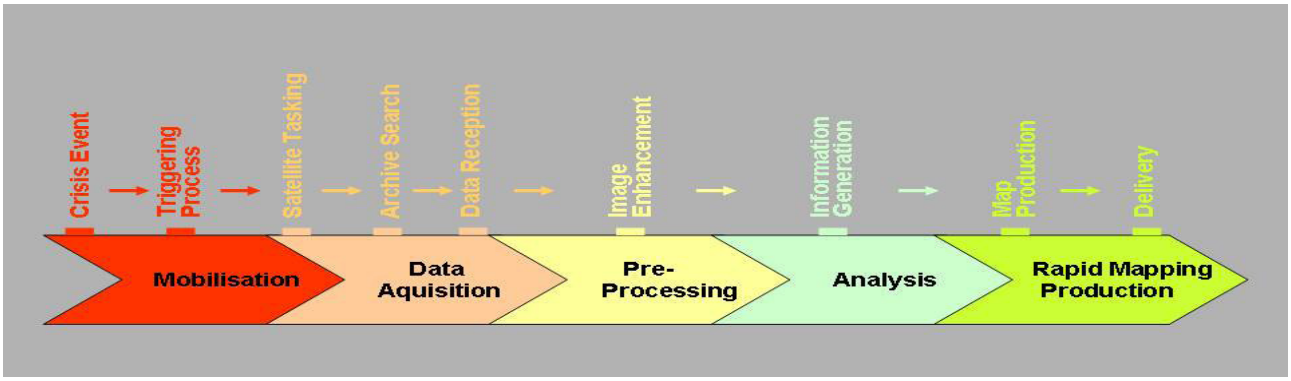

Figure 2, DLR Rapid mapping Service – processing chain

After receiving the archived and recently recorded satellite imagery, essential pre-processing has to be done. This includes geo- and ortho-rectification as well as radiometric corrections and data format conversions. Data re-projection is necessary due to varying demands and standards. In the majority of cases a Universal Transverse Mercator projection (UTM) is used due to global applicability and following international standards. Depending on user needs, crisis type and extent, different analysis process chains have to be applied.

The derivation of water surfaces or general damage assessment is dependent on input data type, scale and possible availability of archived satellite imagery. Before and after image comparison allows the quantification of affected areas. This change detection method can either be applied for optical or radar imagery in order to derive areas where significant change can be stated. Furthermore general image classification and differencing methods allows quantification of flooded areas, fire scars or damaged areas.

In order to translate complex satellite information in readable and coherent crisis information, situation and damage maps are generated. Following this map compilation an adapted map generation process is applied. Before publishing the information products a settled quality control process takes place as after each single product generation step. The delivery is accomplished via internet, intranet, ftp e-mail or satellite communication. Furthermore printed and laminated maps will be sent via express delivery on request.

Besides the quality control during the processing steps, it has proved to be important to insert user feedback from field units. Maps are updated when new and improved data is available or knowledgeable feedback is received even though the maps are published and delivered.

During the past years it has also been shown that training and consulting of decision makers and field workers plays a key role in proper understanding and accepting the space based information products as one information source for decision making or mission planning.

7. CHARTER CALLS 161 & 166 –FLOODINGS IN UK

Heavy rainstorms caused by an extraordinary weather situation led to major floodings in parts of the UK. During June 2007 a large low-pressure area coming from the Atlantic Ocean was trapped over Wales and England. The highest precipitation rates measured over the last decade were recorded at a number of meteorological stations in Yorkshire, Lincolnshire and the Midlands. Recently, those areas were mainly affected by floods which led to breakdowns in power supply and the evacuation of residents such as in the city of Sheffield. The threat of reservoir dam breaks further exacerbated relief activities of the local authorities.

Following these severe flooding that had affected the central and northern parts of England in the end of June and the beginning of July, the South-west of England and Wales have been hit by severe weather again in the end of July, with flooding affecting thousands of homes and leaving many without water and electricity. The areas worst affected include the counties of Gloucestershire, Oxfordshire and Berkshire, Hereford and Worcestershire.

The Charter Calls 161 & 166 – Flooding in UK - was triggered on June 28th 2007 and on July 24th 2007 by the Cabinet Office of the UK, initiated by the Environment Agency UK. ESA resp. CONAE acted as the Emergency On-Call Officer (ECO) and the Environment Agency as the Project Manager of the activations; they were supported by DLR-ZKI. The value adding was also performed by ZKI through the GMES Service RISK-EOS.

The ECOs prepared for each Charter Call an archive and acquisition plan for several different satellite data (optical and radar). The portfolio of products that was provided during the Charter Call was based on the analysis of several different satellite data sets, like archived optical SPOT 5 and Landsat ETM+ scenes, ALOS AVNIR and PRISM images as well as on radar imagery from RADARSAT and ENVISAT ASAR (see Table 1).

In addition to the Charter satellite fleet, DLR tasked the TerraSar-X satellite, launched two weeks before on June 15th 2007, to provide high resolution radar imagery, although the satellite was still in the commissioning phase at this time.

Satellite/ Sensor	Data format	Number of Scenes	Date of Acquisition	new	archived
ALOS AVNIR		1	30-06-2007	1	
ALOS PRISM		1	01-06-2007		1
ALOS PRISM		1	30-06-2007	1	
ENVISAT ASAR	APP	1	02-08-2007	1	
	APP	1	02-08-2007	1	
	IMP	1	26-07-2007	1	
	IMP	1	26-07-2007	1	
	IMM	1	09-07-2007		1
	WSM	1	15-06-2007		1
	WSM	1	23-07-2007		1
LANDSAT		2	12-05-2001		2
		1	11-09-2001		1
		1	04-04-2002		1
		1	11-09-2002		1
RADARSAT	SGF	1	30-06-2007	1	
	SGF	1	03-07-2007	1	
	SGF	1	06-07-1998		1
SPOT		1	03-11-2006		1
TerraSAR-X	StripMap	1	03-07-2007	1	
TerraSAR-X	StripMap	1	25-07-2007	1	

Table 1. Detailed list of all satellite scenes used for Calls 161 & 166

In this activation the user requested the extent of the current flooding situation as shapefiles for including them into there own GIS system. Therefore, DLR concentrated on delivering this product and generated map product afterwards.

None of the data sets showed the ability to cover the region of interest alone in space and time, therefore a variety of sensors have been used. Additionally, each type of data showed specific advantages and short comings in the mapping of the flooding. For instance the new acquired optical ALOS PRISM and AVNIR data, that are dependent on cloud coverage, made it impossible to extract the extent of the flooding. But also the radar data analysis, which is the “classical” approach for such a scenario, has disadvantages e.g. in visualization purposes. Therefore, a combination of all sensors was used to get the best impression of the flooding extent and to fill the coverage gaps between the scenes.

During the calls different products were generated to fulfill the user needs. On July 4th 2007 the first products were delivered to the Environmental Agency. It was a vector-shape file and a kml-file with the flood extend detected in the RADARSAT scene that was taken just one day before on July 3rd, approximately one week after the start of charter activation. The flood mask was derived by ZKI in a semi-automatic processing and cross checked with pre-disaster RADARSAT imagery from July 6th, 1998. The flood mask covered a region of approximately 1750 sqkm south of York and was illustrated superimposed onto Landsat ETM+ images.

Figure 3 First Flood Mapping using TerraSAR-X stripmap mode (DLR-ZKI; www.zki.dlr.de)

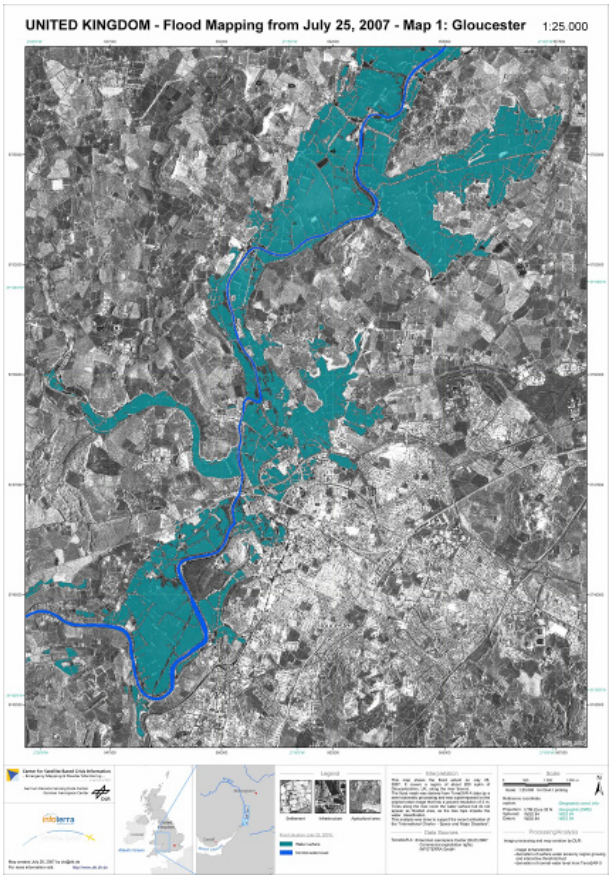

Figure 4 Flood Mapping using TerraSAR-X stripmap mode (DLR-ZKI; www.zki.dlr.de)

The extent of the flood situation was also mapped on July 3rd 2007 by the German TerraSAR-X satellite. Approximately two weeks after the launch of the satellite and during the commissioning phase first scenes supported the rapid mapping activation. One day after the acquisition the flood mask was derived from the TerraSAR-X radar image at 3m pixel spacing (Stripmap Mode) in a semi-automatic processing and cross-checked by seasoned interpreters with the imagery from RADARSAT. This flood mask covered a region of approximately 950 sqkm south of York, Yorkshire. A map was created on the next day (see Figure 3) showing the flood extent and major roads. For visualisation purposes these information were superimposed onto Landsat ETM+ images dating from 2001 or 2002.

For the second call 166 TerraSAR-X stripmap data were recorded one day after the Charter was triggered. After the orbit parameters were delivered the data could be analyzed and mapped at the same day. The normal water level was derived from pre-disaster RADARSAT data. These layers were superimposed on the original radar image (see Figure 4). Moreover the different ASAR data were processed and analyzed and the derived flood mask was also mapped in different scales a few days later.

8. CONCLUSIONS AND OUTLOOK

Over the years the Charter demonstrated in an impressive way the possibilities to support relief efforts with up-to-date satellite based information. Nevertheless, the Charter can only be successful if the satellite data is transformed into user-friendly information products. In the case of the flooding in the UK the Charter showed that it is able to respond to crisis situations.

In addition to the Charter satellite fleet, DLR tasked the TerraSar-X satellite to provide high resolution radar imagery, although the satellite was still in the commissioning phase. The Environmental Agency included the maps and especially the vector-shape-files in their analysis of this disaster. Therefore Satellite based crisis information is optimally suited to fulfil this request covering large areas and having the ability to react in due time on disasters occurring all over the globe. Therefore future financial and operational scenarios of the GMES Services are essential (see Tufte 2008).

9. REFERENCES

Murlidharan, T.L., 2003. Economic consequences of catastrophes triggered by natural hazards, John A. Blume Earthquake Engineering Center, Report No. 143.

Riedlinger, T., Voigt, S., Kemper, T and H. Mehl, 2005. Working towards an improved Monitoring Infrastructure to support Disaster Management, Humanitarian Relief and Civil Security", Proc. of Int. Symp. on Remote Sensing of Environment.

Schneiderhan, T., Kemper, T. and S. Voigt, 2007. The International Charter "space and major disasters", RISK-EOS and ZKI: Their roles during the Lebanon Oil Spill Activation, Proc. of 7th meeting of the European Group of Experts on satellite Monitoring of sea-based oil Pollution, Ispra, Italy.

Tufte, L., 2008. Earth Observation and Disaster Management. Festschrift Ehlers.

A NEW MW ALGORITHM TO SPEED UP LANDSCAPE INDEX CALCULATION OF HIGH RESOLUTION MAPS

T.K. Gottschalk [a], M. Bertling [b], V. Wolters [a] & J. Biermann [b]

[a] Justus-Liebig-University-Giessen, Department of Animal Ecology, Heinrich-Buff-Ring 26-32, 35398 Giessen, Germany. thomasgottschalk@surfeu.de

[b] Fachhochschule Osnabrück, Fakultät Ingenieurwissenschaften und Informatik, Albrechtstr. 30, 49076 Osnabrück. marcusbertling@googlemail.com

KEY WORDS: Slicer, Moving Window, landscape analysis

ABSTRACT:

The use of high spatial resolution data dramatically prolongs computer processing time when analysing large areas. For example, the duration of Moving Window analysis, a method that is widely used for calculating landscape metrics, not only increases with window size but also with the amount of underlying data. An algorithm was developed to alleviate this problem. It was implemented in the new program SLICER 1.0. The algorithm utilizes a maximum of information from previous computing operations and therefore reduces processing time by a factor of more than 1E+06. The current version of SLICER is confined to quadratic windows and allows for calculating three landscape metrics. Here we compare the results of two landscape metrics (Shannon diversity index, Interspersion and Juxtaposition index) calculated by means of SLICER 1.0 with those gained by applying a conventional algorithm. The computational results are very similar, but SLICER 1.0 proved to have a much shorter processing time. The algorithm will be further refined to include additional landscape metrics and to be applicable to octagonal windows.

1. INTRODUCTION

Moving Window (MW) analyses have been widely used in landscape ecology to calculate metrics for each cell of a map (Brownstein *et al.,* 2005, Graf *et al.,* 2005, Gottschalk *et al.*, 2007, Reunanen *et al.,* 2004). The window moves cell-wise over the digital map, calculates a metric within a particular window, and then returns the respective result to the centre cell (McGarigal & Cushman, 2002). The resulting metric maps provide information e.g. on landscape diversity or percentage cover of land-use types for each cell and are an essential prerequisite for quantifying landscape patterns. Typically, the Fragstats program (McGarigal & Marks 1995) is used for achieving this aim. One critical problem is that the time consumed for generating such maps is strongly related to the amount of cells of the window as well as to both extend and grain size of the map. The amount of cells of circle shaped windows is approximately given by (cs denotes the size of one cell)

$$\text{Amount of cells} \approx \frac{r^2 * Pi}{cs}$$

This means that a window of a 1000m radius (r) has a four times bigger amount of cells than a window of a 500m radius. However, execution time does not increase at the same rate, as it mainly depends on the algorithm used.

Recent advances in high resolution (1–5 m) remote sensing are very useful for landscape analysis, spatial planning and modelling purposes (Surazakov *et al.,* 2007, Johansen & Phinn, 2006, Goetz *et al.,* 2007). However, the use of high spatial resolution data dramatically prolongs computer processing time when analysing data from large areas. For example, moving window analyses on fine scaled maps with more than 1,000,000 cells for a 2000m-window size can last several weeks or even years using the MW algorithms that are currently available.

We have developed an algorithm to alleviate this problem. It was implemented in the new program SLICER 1.0 (Bertling *et al.,* 2007).

2. THE SLICER ALGORITHM

Conventional algorithms separately calculate landscape metrics for each individual window. Since, however, information from one cell to the neighbouring cell often does not change much, it is not necessary to entirely redo the calculation of the landscape metrics for each window. Based on this idea, we have developed an algorithm, which uses a maximum of information from the previous window (Fig. 1).

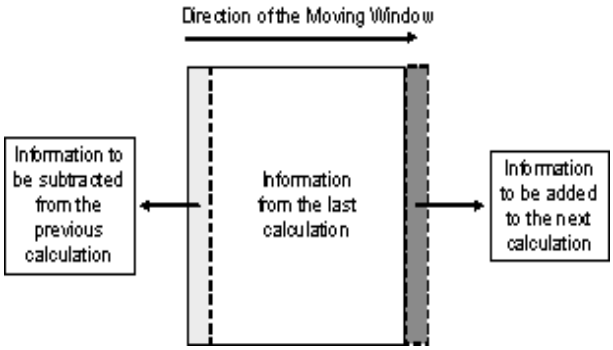

Figure 1. The "slice-method" is based on reusing a maximum of information from previous windows. Information in the inner part of the window is reused from the last step. Only the last and the first row have to be calculated by discarding or adding data.

Since the first column of each squared window is discarded and a new column of identical size is added with each step, the information of every column can be reused by subsequent window analyses. Landscape metrics of cells in subsequent rows of a map can be calculated much quicker as more and more information can be reused (Fig. 2).

Figure 2. After the landscape metric of the first row of a map has been calculated in the following rows only single cells has to be added or subtracted from the previous calculation.

The reduction of processing time is mainly due to the fact that the information of only one new column / cell has to be added and the cell information of the previous column / cell has to be discarded from the last calculation. However, reusability of information from previous cells strongly depends on the landscape-metric to be calculated. Thus, the algorithm had to be adjusted to each metric. Already implemented algorithms were encapsulated in the strategy pattern to implement additional landscape metric without difficulty (Gamma *et al.,* 2004).

The program SLICER 1.0 was programmed in C++. The prototype is able to calculate three landscape metrics: Shannon diversity, fragmentation (using the Interspersion and Juxtaposition Index, IJI) and percent cover of land-use. These metrics have often been used for landscape analyses and species distribution modelling. Since SLICER 1.0, in contrast to other MW programs, reads landscape data by using only one instead of four byte(s) per cell, it has a comparatively low memory demand.

3. COMPARISON OF EXECUTING TIME

The most remarkable achievement of the "Slice-method" is that it reduces processing time by a factor of more than 1E+06 (Fig. 3). However, the time actually needed to calculate a MW map depends on various factors: computer system, size of the window, landscape metric, and the total cell number of the map, respectively. The Shannon diversity index (SHDI) as well as the Interspersion and Juxtaposition Index (IJI, i.e. the degree to which similar patch types are uniformly distributed and mixed across a landscape) are widely used in landscape analyses. We thus evaluated the properties of the new algorithm for these two indices. For small windows, less time is needed to calculate a SHDI map than to calculate an IJI map and relative calculation time of the SHDI decreases with increasing window size (Fig. 4).

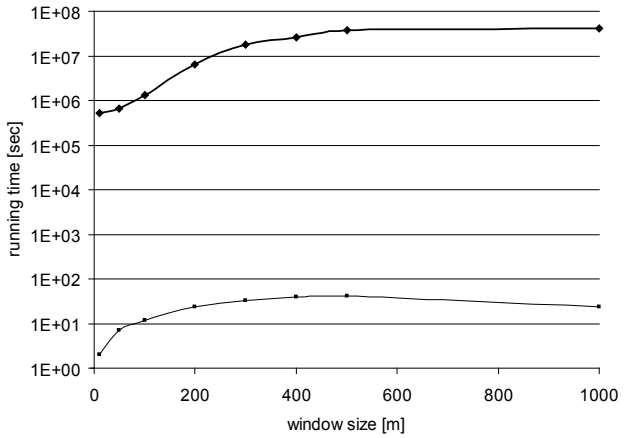

Figure 3. Processing time and quadratic window size of different algorithm used to calculate the Interspersion and Juxtaposition Index using Moving Windows (upper curve: Fragstats, lower curve: SLICER). The landscape contained 9,000,000 cells.

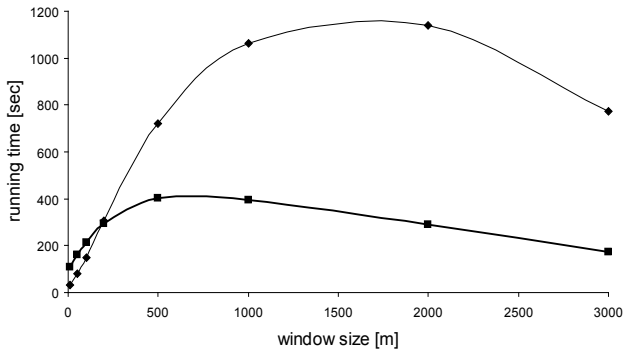

Figure 4. Time consumed to calculate Moving Windows of different landscape metrics in response of the radius used (quadratic dots: Shannon diversity index, rhombic dots: Interspersion and Juxtaposition Index). The landscape contained 100,000,000 cells.

This is because SHDI only processes the number of classes and the area of each class, while the information processed by IJI is more complex. At least three patch types are needed to calculate an IJI value within a window. It divides the edge type of two different patches by the length of the total landscape edge and thus involves the observed interspersion over the maximum possible interspersion for the given number of patch types. Therefore, the IJI cannot be calculated for homogenous landscapes that contain only one or two land-use types. As such conditions often occur in small windows, the processing time on these radii is low.

4. COMPARISON OF THE MAP OUTPUT

Currently, SLICER 1.0 is only applicable to quadratic windows, since this shape provides the highest amount of reusable cells. Although for many ecological applications a circular window might be preferable, the difference between these map types seems to be negligible for the SHDI maps (Fig. 5) and low - though obvious - for the IJI maps (Fig. 6). Executing time, however, was extremely different.

5. CONCLUSIONS

The increasing availability of remote sensing data of high spatial resolution requires programs able to process such data in a quick and comfortable manner. With the help of the newly developed slicer-method, it is possible to perform MW analysis of large squared windows within a few seconds or minutes that would otherwise require several weeks or years. SLICER 1.0 currently allows for calculating three different landscape metrics from quadratic windows. The forthcoming SLICER 2.0 shall include additional landscape metrics and should be applicable to octagon windows, which are very similar to circle shaped windows.

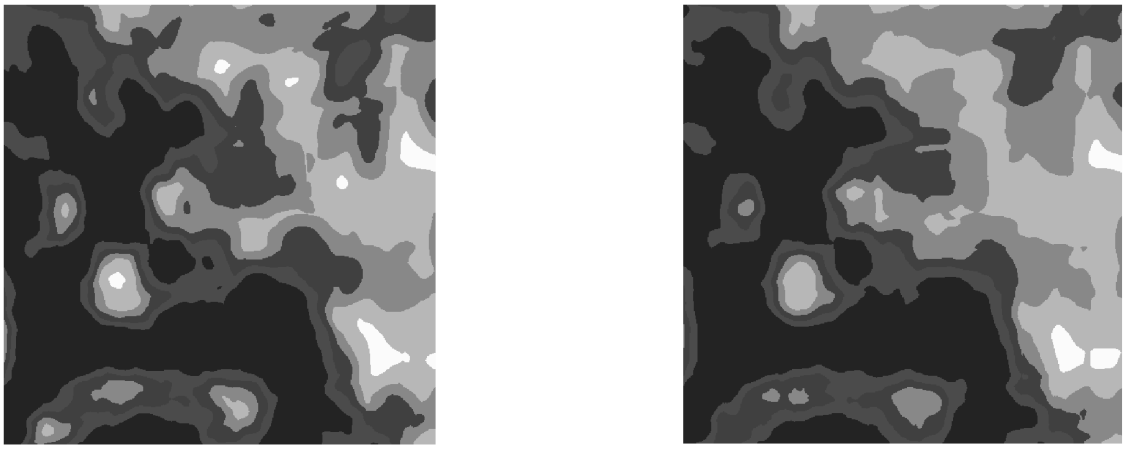

Figure 6. Interspersion and Juxtaposition index. The left map was generated using a circular window (200m radius) and the program Fragstats (processing time: 77 days and 10 hours) and the right map was generated using a quadratic window (400m edge distance) and the program SLICER 1.0 (processing time: 24 seconds). The landscape contained 9,000,000 cells. Calculation was done using an Intel Pentium 1.6 GHz processor and 512 MB RAM.

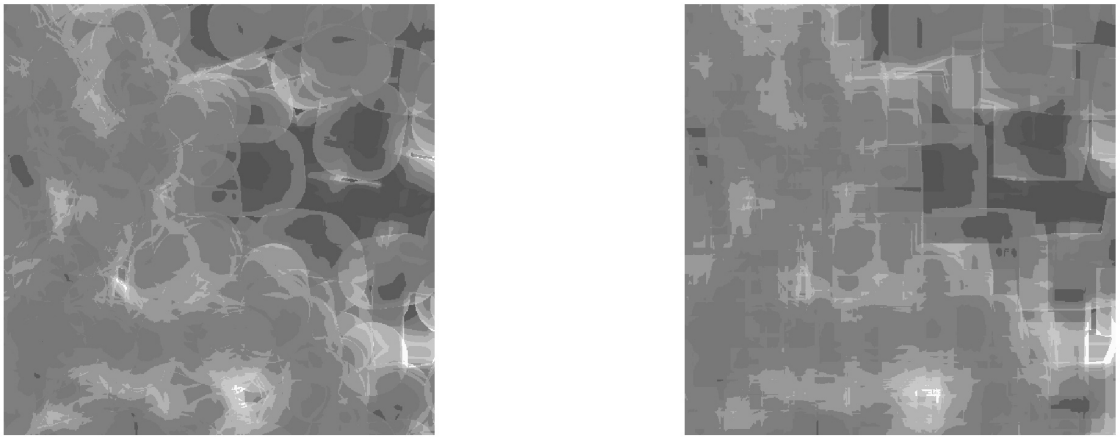

Figure 5. Shannon diversity index. The left map was generated using a circular window (200m radius) and the program Fragstats (processing time: 75 days and 2.7 hours) and the right map was generated using a quadratic window (400m edge distance) and the program SLICER 1.0 (processing time: 15 seconds). The landscape contained 9,000,000 cells. Calculation was done using an Intel Pentium 1.6 GHz processor and 512 MB RAM.

6. REFERENCES

Bertling, M., Gottschalk, T. K. & Biermann, J., 2007. SLICER 1.0 - ein Programm zur beschleunigten Berechnung von Landschaftsindizes. Justus-Liebig-University Giessen und Fachhochschule Osnabrück - Fakultät Ingenieurwissenschaften und Informatik. http://home.edvsz.fh-osnabrueck.de/~std9124/Diplom/ (accessed 15 Mar. 2008).

Brownstein, J. S., Skelly, D. K., Holford, T. R. & Fish, D., 2005. Forest fragmentation predicts local scale heterogeneity of Lyme disease risk. Oecologia 146, pp. 469-475.

Gamma, E., Helm R. & Johnson R. E., 2004. Entwurfsmuster. Elemente wiederverwendbarer objektorientierter Software, Addison-Wesley, München.

Goetz, S., Steinberg, D., Dubayah, R. & Blair, B., 2007. Laser remote sensing of canopy habitat heterogeneity as a predictor of bird species richness in an eastern temperate forest, USA. Remote Sens. Environ. 108, pp. 254-263.

Gottschalk, T.K., Ekschmitt, K., Kuhlmann, F., Weinmann, B., Purtauf, T., Dauber, J., Diekötter, T. & Wolters, V., 2007. Impact of agricultural subsidies on biodiversity at the landscape level. Landscape Ecol. 22, pp. 643-656.

Graf, R. F., Bollmann, K., Suter, W. & Bugmann, H., 2005. The importance of spatial scale in habitat models: capercaillie in the Swiss. Landscape Ecol. 20, pp. 703-717.

Johansen, K. & Phinn, S., 2006. Mapping structural parameters and species composition of riparian vegetation using IKONOS and landsat ETM plus data in Australian tropical savannahs. Photogrammetric Engineering & Remote Sensing 72, pp. 71-80.

McGarigal, K. & Cushman, S. A., 2002. The Gradient Concept of Landscape Structure. Landscape Ecol. 8, pp. 201-211.

McGarigal, K. & Marks, B. J., 1995. FRAGSTATS: spatial pattern analysis program for quantifying landscape structure. Version 3.3, Portland, OR: USDA Forest Service, Pacific Northwest Research Station.

Reunanen, P., Mönkkönen, M., Nikula, A., Hurme, E. & Nivala, V., 2004. Assessing landscape thresholds for the Siberian flying squirrel. Ecol. Bull. 51, pp. 277-286.

Surazakov, A. B., Aizen, V. B., Aizen, E. M. & Nikitin, S. A., 2007. Glacier changes in the Siberian Altai Mountains, Ob river basin, (1952-2006) estimated with high resolution imagery. Environ. Res. Lett. 2, pp. 1-7.

ASR - A TOOL FOR THE UNSUPERVISED IMAGE ENDMEMEBER DEFINITION

A. Greiwe

Nordkirchen, Germany,
ansgar.greiwe@altaweb.de

KEY WORDS: imaging spectroscopy, image endmember, reference spectra, urban monitoring

ABSTRACT:

Hyperspectral image data contains a large number of narrow bands that form a high dimensional “image data cube”. To process this large amount of data, special classification algorithms for spectral unmixing or for material detection have been developed. Material detection algorithms like the Spectral Angle Mapper (SAM) calculate a deterministic value to express the spectral similarity of a pixel to a given reference. Unmixing approaches like the Mixture Tuned Matched Filtering (MTMF) determine for a measured spectrum the abundance fraction of a given reference spectrum. In both cases, the term “endmember” is used for the spectral reference definition. For unmixing approaches, several manual or unsupervised endmember selection methods such as the Manual Endmember Selection Tool (MEST) (Bateson and Curtis 1998), the Pixel Purity Index (PPI), implemented in ENVI (Boardman et al. 1995), or the NFINDR (Winter 1999), have been developed.

Algorithms for material detection purposes, like SAM, determine the spectral similarity between a pixel’s spectra and a given endmember. In contrast to endmembers for spectral unmixing, which often represent ’spectral extreme’ features, algorithms like SAM require endmember containing the ‘mean spectrum’ of a material class in order to produce the best possible results between classes with a similar spectral behaviour. If this reference spectrum for a material class is selected from the image data instead of a in situ field survey, these definitions are so called ‘image endmembers’. These image endmembers are often selected manually by the user. The result of this non objective endmember selection is a user dependent spectral library which leads to sub optimal classification results. As an alternative, the author developed an unsupervised image endmember definition approach. In this paper, some details of the described methodology will be described as well as the ASR-Tool, which was developed to support the user within the unsupervised process.

1. INTRODUCTION

For the detection of a material within hyperspectral image data, there should be at least one image pixel, whose reflectance represents the spectral signature of the material. By merging the spectral properties of one or more similar pixel, a reference spectrum for a material, a so called *image endmembercan* be created.

In most cases, there are more than one image pixel, that defines the spectral signature of a certain material. However, it is not a must, that all suitable pixels in an image are used to define the spectral signature of a material. In most cases, only a few pixels are used to define the material’s spectral signature and the rest of a pixel set are discarded by the user.

In the approach, the set of hyperspectral image pixels which can be used to define one image endmember are selected in an user independend, repeatable process (Greiwe2006a, Greiwe 2006b).

The set of hyperspectral image pixels, suitable for a spectral characterization of a certain material are called *endmember candidates,* due to the fact, that members of such a set of pixels could be a *candidate* for the definition of an *image endmember*.

The approach of an unsupervised, segment based image endmember selection can be characterized by three steps:

1. Selection of endmember candidates within the hyperspectral image data by use of image segments from co-registered orthophotos.
2. Transformation of candidate spectra from step one into a correlation feature space.
3. Grouping of spectral similar candidates by a density based clustering algorithm.
4.

To support the user within the workflow of the three above described steps, a software tool for the automated segment based reference spectra selection (ASR-Tool) was developed (see figure 1).

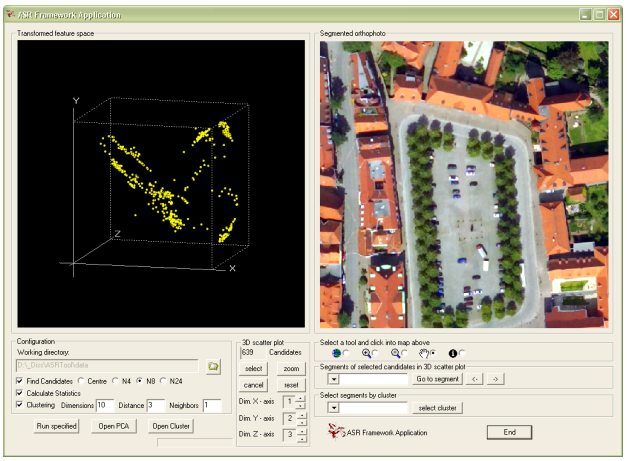

Figure 1: ASR Tool with endmember candidates in correlation feature space (left) and the segmented orthophoto (right). The user is able to change parameters of the process with some GUI controls (bottom).

2. METHODOLOGY

2.1 Determination of endmember candidates

In this approach, we assume, that an endmember candidate is a hyperspectral image pixel that lies within a spectral homogenous area (like a rooftop or paved parking lot). To collect all possible endmember candidates, the user has to select manually all the hyperspectral image pixel in such image areas.
In a multisensor environment, orthophotos can be used to determine the endmember candidates instead of a manual selection of endmember candidates. The spatial high resolution image data could be segmented in order to retrieve the homogenous areas as polygons (Baatz and Schäpe 1999, eCognition software).
All image pixel within the Hyperspectral image data, that are within a homogenous area, can be viewed as candidates for the spectral definition of the area's material. By superimposing the image segments of the orthophoto on the hyperspectral image, pixels of the hyperspectral image data, that are completely (within N4 or N8 neighborhood, see figure. 1) included in these segments were chosen as candidates for an endmember definition.

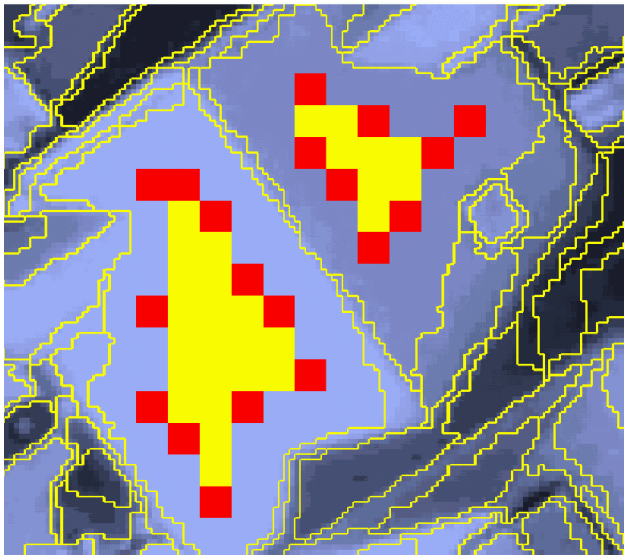

Figure 2: Segments (yellow lines) of an orthophoto (shown as blue background) are used to determine candidate pixel in the hyperspectral image data. N8-filtered candidates are shown in yellow, N4-filtered, in red.

At first sight, errors within the orthophoto image segmentation would lead to "material mixed" endmember candidates. But this step only selects set of hyperspectral image pixels as endmember candidates. No geometric information (link between candidate and segment) are stored within the endmember candidates. Hence, the image segment information is not used to group endmember candidates to an image endmember. As a consequence, invalid image segments containing different material spectra have no influence on the following processes.

2.2 Measuring spectral similarity

The set of endmember candidates is not yet divided into groups for the several materials within the hyperspectral image. This step is done by clustering the endmember candidates by their spectral similarity. The chosen clustering approach is a density based approach.

For this, a feature space to determine the proximity matrix between all objects to be clustered was developed (Greiwe 2006a).
The spectral similarity between two given spectra is estimated by the correlation coefficient. The correlation coefficient allows a more precise differentiation of spectrally similar materials (Carvalho et al., 2000). This technique is also used in classification approaches like the Cross Correlogram Spectral Matching (CCSM, van der Meer and Bakker, 1997) and pattern recognition in hyperspectral image data (Ingram et al., 2004).

The calculation of the correlation coefficient between a given number (n) of candidates results in a n×n correlation matrix. In a second step, a Principal Component Analysis (PCA) is carried out within the complete correlation matrix data. The result is a PCA-transformed correlation matrix with rows sorted by the eigenvalues of the PCA. The rows of this transformed matrix can also be used as definition for the coordinate axes of an n-dimension feature space (see Figure 3).

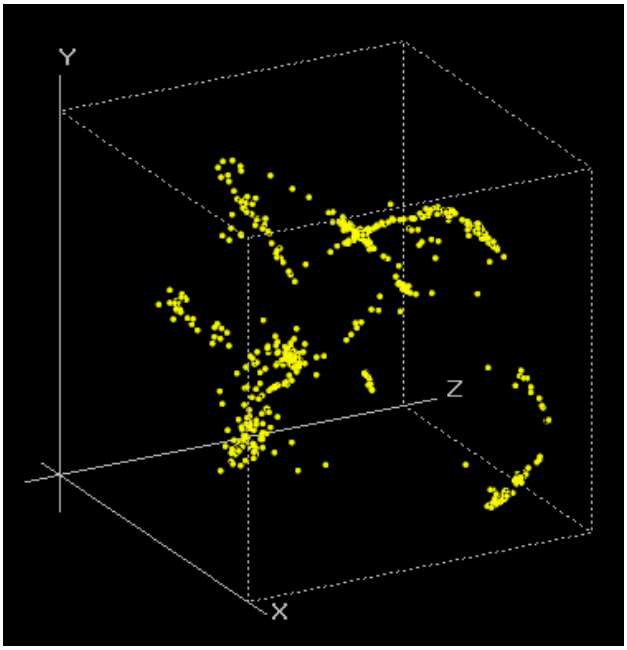

Figure 3: The first three rows of a PCA transformed correlation matrix define a feature space. The first row defines the x-axis, the second the y-axis and the third row the z-axis.

2.3 Clustering of similar spectra

Candidates in the PCA-transformed feature space build linear point clouds (see figure 3). Clustering algorithms such as k-means or ISODATA offer no solution to separate distinct clusters from an aggregated cloud of points like the one shown in figure 3.
Therefore, the density based clustering algorithm (also known as DBSCAN) was used here to cluster the candidates.

A radius representing the neighborhood of a point is predefined by the user. This neighborhood has to contain a minimum number of points in order to build a cluster. The radius and the number of points in the given neighborhood are the two threshold values defining the 'density' of a cluster (see figure 4).

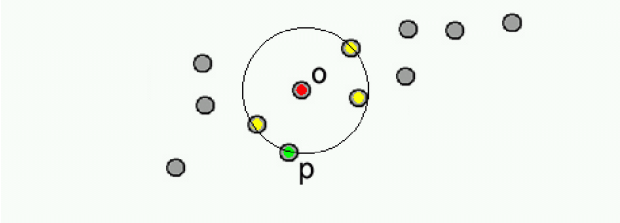

Figure 4: For a given radius and a minimum numbers of reachable neighbor points, point O is a core object of a new cluster including neighbor points like P.

In further iterations, reachable neighbors are gradually included into the cluster. Based on this strategy, point clouds with drawn-out shapes could be clustered (see figure 5).

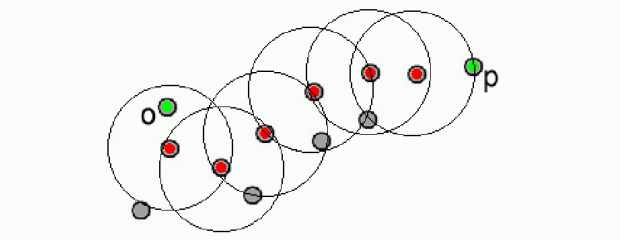

Figure 5: The points O and P belong to the same cluster, connected through the core objects (displayed in red).

Within the ASR-Tool, the user is able to control the clustering process through the parameters “Dimensions”, “Distance” and “Neighbors”. The parameter “Dimensions” defines the number of rows from the PCA-transformed correlation matrix that are used to calculate the distance matrix for the clustering algorithm. The parameter “Distance” controls the radius described in figure 4. It is a multiplier for the mean minimum distance to the next neighbor over all endmember candidates in the dataset. The number of neighbors is defined by the parameter “Neighbors”.

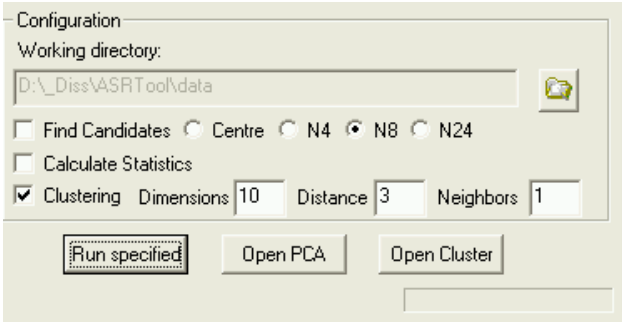

Figure 6: ASR-Tool: Parameters for the estimation of endmember candidates and the Clustering.

2.4 Building the spectral library

DBSCAN provides a Cluster-ID for each candidate. If a candidate belongs to a specific cluster, he retrieves the ID of the assigned cluster. A negative ID (-1) indicates those candidates, who are not assigned to any cluster. As a result of the clustering process, a mask image with the same extent as the hyperspectral image data contains these cluster IDs at the geometric location of each candidate.

Pixels with the same ID (member of a cluster) could be joined into one group (using a region of interest, ROI, ENVI).

Averaging the corresponding spectra of such a group in the hyperspectral dataset leads to a reference spectra (see figure 7).

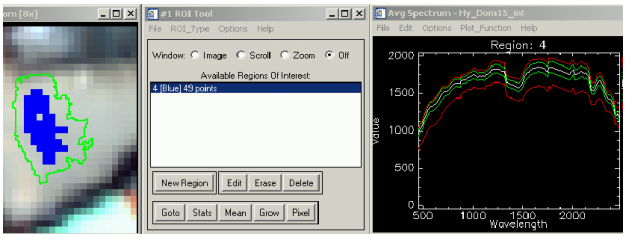

Figure 7: Image pixel, grouped by their cluster ID on the left lead to a group of 49 pixel (middle) with an average spectrum (right).

3. ASR TOOL

The ASR-Tool was developed to assist the user within the above described workflow. After an assessment of the user requirements, several commercially available image processing applications were evaluated. After a few prototypes implemented in 4GL languages within systems like ERDAS or ENVI and ArcGIS, the ASR-Tool was realised as a standalone application due to performance reasons. Additionally, no commercially available system was able a offer the DBSCAN algorithm for clustering.

3.1 Class library

As a consequence of the decision for a stand alone application, an own class library for the processing of raster and vector data was implemented in c++ (see figure 8)

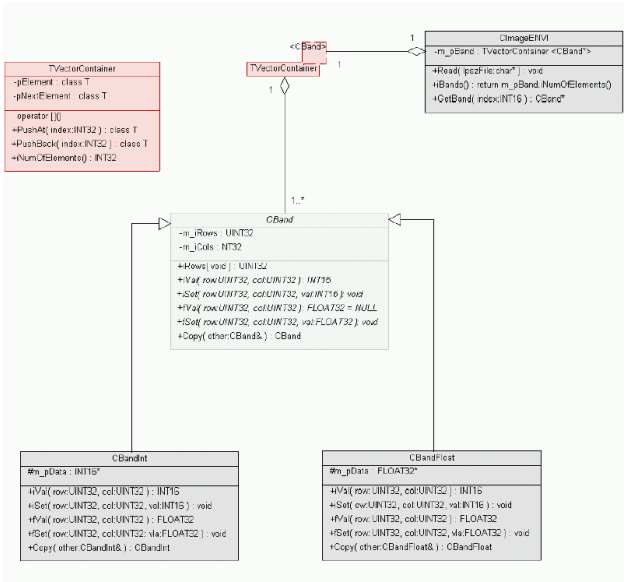

Figure 8: Subset of the image processing classes in UML.

For the estimation of endmember candidates image segments of the orthophoto are a pre-condition. This image segmentation is not implemented in the ASR-Tool. Instead of an own image segmentation, ASR is able to handle every segment definition (e.g. Definiens eCognition) as polygon data in the ESRI compatible shape format. Additionally, the hyperspectral image data must be binary raw data with header information in ENVI format.

3.2 Switching between cluster and material

After the clustering of the image endmembers, the tool is able to link between a pixel's position an the corresponding image segment in the orthophoto. This functionality helps the user to define the material, which is represented by a certain cluster.

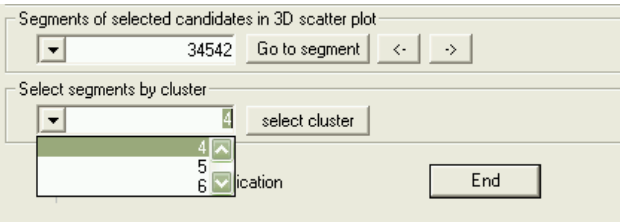

Figure 9: The ASR-Tool allows the user to select a specific cluster.

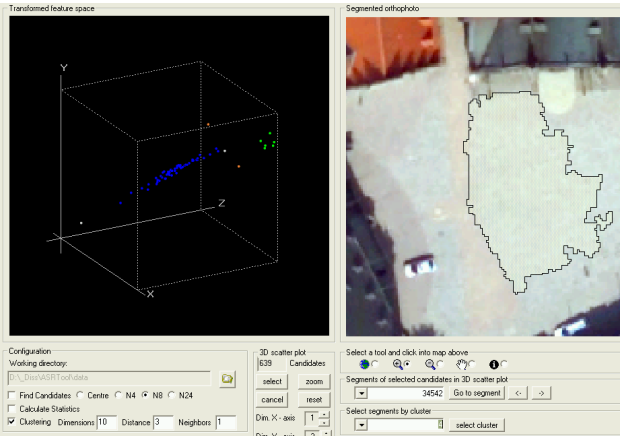

Figure 10: After the selection of a cluster, the ASR-Tool shows the cluster in the correlation feature space and the corresponding image segment.

4. CONCLUSION

All steps of the workflow described in this paper can be done within the ASR TOOL. In this paper, the author showed the user interface and the benefits such an application which assists the user for quality assessment and a visual control on the clustering process.

5. REFERENCES

Baatz, M. und Schäpe, A., 1999: Object-oriented and multiscale image analysis in semantic networks. In: Proc. of the 2nd International Symposium on Operationalization of Remote Sensing, Enschede, ITC.

Bateson and Curtiss, 1996: A Method for manual endmember Selection and Spectral Unmixing, Remote Sensing and Environment (55), pp. 229-243.

de Carvalho Jr, O. A., de Carvalho, A. P. Ferreira und Meneses, P. R., 2000: Sequential mini-mum noise fraction use: An approach to noise elimination. In: Summaries of the Ninth Annual JPL Airborne Earth Science Workshop. JPL Pub 00-18.

J. W. Boardman, F. A. Kruse, and R. O. Green 1995: Mapping target signatures via partial unmixing of aviris data. In: Summaries, Fifth JPL Airborne Earth Science Workshop, JPL Publication 95-1 (1), pp. 23-26.

A. Greiwe and M. Ehlers, 2005: Combined analysis of hyperspectral and high resolution image data in an object oriented classification approach, in Proceedings of 3rd International Symposium on Remote Sensing and Data Fusion over Urban Areas 13-15 March 2005, Phoenix(Arizona), USA, 2005

A. Greiwe, 2006a: An Unsupervised Image Endmember Definition Approach, in Proceedings of "1st EARSeL Workshop on Urban Remote Sensing", 2-3 March 2006, Berlin, Germany.

A. Greiwe, 2006b: Unsupervised image endmember definition in multisensor image data, in Proceedings of ISPRS Symposium "Remote Sensing: From Pixels to Processes" 8-11 May 2006, Enschede, the Netherlands, pp.130-136.

Ingram, R. N., Lewis, A. S. und Tutweiler, R. L., 2004: An automatic nonliear correlation approach for processing of hyperspectral images. International Journal of Remote Sensing, Vol 25(20): pp. 4981-4998.

F. van der Meer and W. Bakker, 1997. CCSM: Cross Correlogram spectral matching. International Journal of Remote Sensing 18, pp. 1197-1201.

M. E. Winter, 1999: Fast autonomous spectral endmember determination in hyperspectral data, in Proceedings of the Thirteenth International Conference on Applied Geologic Remote Sensing, pp. 337 - 344, Volume II, Vancouver B.C., Canada, 1999

SUSTAINABILITY IN E-LEARNING AND POST-EDUCATION AT THE UNIVERSITY OF OSNABRÜCK

B. Grendus[1], T. Kastler[1] & J. Schiewe[2]
Working Group „E-Learning and Post Education“

[1]University of Osnabrück, Seminarstraße 19a/b, 49069 Osnabrück, Germany
{bgrendus, tkastler}@igf.uni-osnabrueck.de
[2]HafenCity University Hamburg, Hebebrandstraße 1, 22297 Hamburg, Germany
jochen.schiewe@hcu-hamburg.de

KEY WORDS: E-Learning, post-education, multimedia

1. INTRODUCTION

Obviously, a Working Group on „E-Learning and Post-Education“ is a quite unusual element in the structure of a institute like the one for Geoinformatics and Remote Sensing (IGF) at the University of Osnabrück (Germany). However, the respective development was a logical – and finally successful – process, which led the key actors not only through all experiences that are associated with advanced methods and tools for teaching and learning, but certainly also led to some improvements in teaching quality as such. In the meantime this has been documented by approving IGF as a certified educational organization and eligible course provider, respectively.

The efforts in E-Learning started as early as 1999, when the institute was still located in Vechta and it took the order to establish a multimedia lab for teaching and learning purposes. With that a top-down approach for implementing E-Learning at a rather small university started and gave insight not only into technical, but even more into organizational issues related to E-Learning (see section 2).

Parallel to that development members of the institutes were also involved in the conceptualization, implementation, usage and evaluation of advanced learning materials and programs, leading to two long-term funded projects: “Fernstudienmaterialen Geoinformatik (FerGI)” (Distance learning materials for Geoinformatics) and “UNIGIS eXpress”. The respective concepts and successful outcome of these projects are described in sections 3 and 4.

All activities have in common, that the overall goal – to improve the quality of teaching and learning – demands not only for the development of good content and the use of suitable, modern hardware, but equally important, for the consideration of a variety of didactical, organizational and economical factors. All these factors together are linked together and form an *E-Learning network* (see figure 1), which obviously makes an interdisciplinary (and by the way very interesting!) co-operation beyond the borders of Geoinformatics necessary. This field of activity is even more exciting and important due to the overall structural developments (like the introduction of Bachelor and Master programs) that currently take place in German universities (Schiewe, 2005).

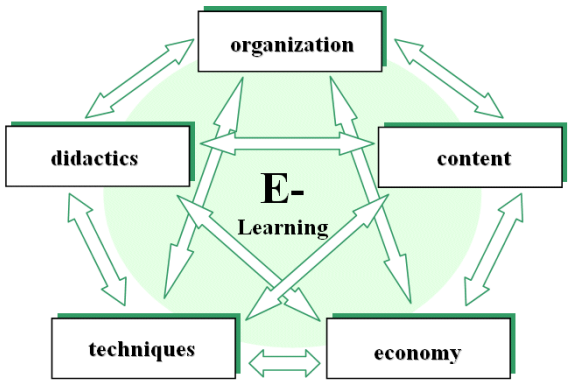

Figure 1. E-Learning network: Factors responsible for a successful implementation of E-Learning materials and programs

2. MULTIMEDIA LAB

In 1999 the Rector of the University of Vechta charged the Geoinformatics Group (led by Prof. Manfred Ehlers) to lead an interdisciplinary steering group to implement an advanced multimedia infrastructure. With funding from the State of Lower Saxony a multimedia lab and a multimedia lecture room were established (see figure 2). The lab consisting of 8 workstations was dedicated to the generation of multimedia based course materials and to the use for special purpose courses. The lecture room offered possibilities for multimedia-based presentations, for an audio-visual recording of lectures, and for video conferences.

The technical equipment was definitively appropriate with respect to the number of potential users. Nevertheless, the capacity of the Computing Center (consisting of only three people) has not been grown in a parallel manner to the advent of new multimedia components so that a necessary sustainable administration could not be guaranteed.

Very quickly it became clear that the technical installations had to go along with several actions concerning the motivation and education for both lecturers and students. Experiences showed that especially the goal of increasing the sensibility for the use of new media is very important, but also rather difficult to achieve (Schiewe, 2002). Core of the motivation measures was a series of open lectures (called “CyberRing-Lecture”) which covered a variety of E-Learning related topics (like general introduction in common software packages, web design, etc.).

Figure 2. View into the multimedia lab at University of Vechta

The organizational structure with a centralized steering group has been proofed an effective solution for such a small university which is not affected by long distances and complicated communication channels. On the other hand, the emphasis of political funding at that time was laid upon technical equipment rather than on application projects or on technical personal. With that a sustainable development of the E-Learning activities was not possible and the multimedia lab was not adequately used for many years.

3. FERNSTUDIENMATERIALIEN GEOINFORMATIK (FERGI)

When the project FerGI started in 2003, E-Learning was already on the agenda of various other German and international institutes, also in the field of Geoinformatics. Several experiences had already been made, for example within projects funded by the "New Media in education I"-initiative of the German government. A lot of these experiences – for example, concerning missing sustainability of developed modules after project financing has stopped – led to the overall concept of FerGI, which nowadays is certainly the largest project of its kind for the discipline of Geoinformatics.

For more than three years FerGI was funded by the Ministry for Science and Culture of the State of Lower Saxony and the Federal Ministry for Education and Research. Under the leadership of the IGF in Osnabrück (Prof. Ehlers, Prof. Schiewe, Prof. de Lange) 24 E-Learning modules covering new and highly demanded topics of Geoinformatics were developed, implemented used and evaluated. This work was done in a joint venture with partners at the University of Applied Sciences in Oldenburg (Prof. Brinkhoff), the University of Hannover (Prof. Sester, Prof. Heipke), and the University of Hildesheim (Prof. Wagner).

Since May 2007 the project continues under the title "FerGI+" with additional funding by the State of Lower Saxony. The IGF in Osnabrück and institutes of the University of Applied Sciences in Oldenburg (Prof. Brinkhoff) and the University of Applied Sciences in Osnabrück (Prof. Anlauf) deliver the module content. The Center for Information Management and Virtual Teaching (virtUOS) at the University of Osnabrück (Dr. Knaden) provides the know-how for media didactics and learning platforms.

Within FerGI+ 10 additional modules will be created in order to expand the portfolio (see figure 3) and to fill thematic gaps identified by users. As already pointed out, the modules do not cover a complete curriculum but build smaller units covering specific topics, each with a workload of 0.3 to 1 credit points according to the European Credit Transfer System (ECTS). Worth mentionable is the fact that the modules will be developed in German and/or in English language depending on the subject and target group.

Figure 3. Overview of FerGI modules

The overall project goal is the flexible use of modules in terms of different target groups, different learning scenarios and different hardware and software environments. Therefore, the E-Learning materials are implemented independently of any learning platform on a standard technical basis (HTML, Flash, JavaScript; see figure 4). Simple tools for communication (forum) and quizzes are also integrated into this stand-alone version. On the other hand many educational organizations already use learning platforms for additional course management functions (like enrolment, keeping exam results, etc.). It is possible to embed the stand-alone versions of the FerGI modules into these platforms without any problems. Successful implementation tests have already been performed with the systems *Moodle*, *LearningSpace* and *ILIAS* in combination with *Stud.IP*, with the latter being the most used platform at universities in the German State of Lower Saxony.

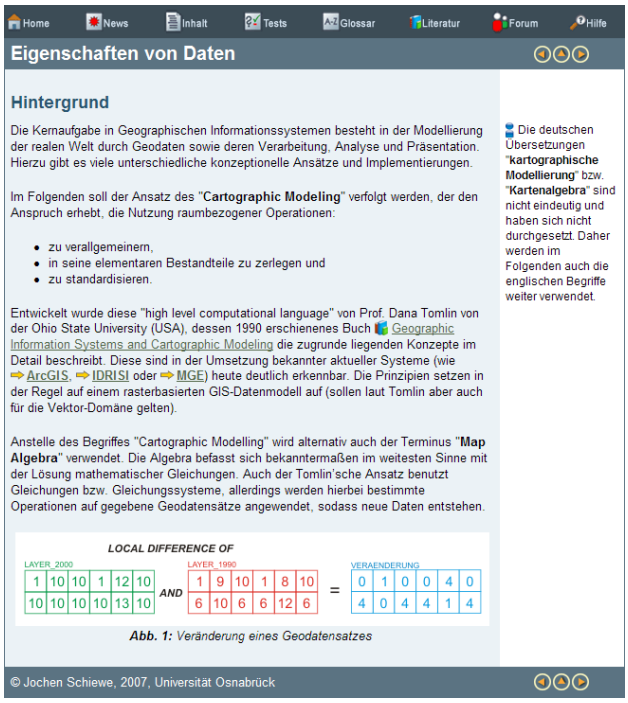

Figure 4. Example for a typical FerGI content page, taken from the module *Map Algebra*

Due to the fact, that modules are tailored to smaller units, they are meant for supplementing or replacing some sessions of regular university lectures or seminars. Their (free) usage is not limited to the project partners.

In addition the materials can also be used – at no costs and for a limited period of time (in this case without tutoring) – for self training purposes. Currently more than 1,000 participants, most of them from outside the universities, are registered in the FerGI user database. Regular evaluations show a good user satisfaction (with an average value of better than 2 on a scale ranging from 1 – very good – to 5 – very disappointing).

Furthermore FerGI modules can also be used within professional training programmes. First experiences with embedding FerGI materials into respective courses have already been made with the *GIS-KombiPLUS* course offered at IGF in Osnabrück and a seminar on Geodatabases (in Oldenburg). Based on these experiences, in 2008 a follow-up project called FerGI@KMU will start with funding from the European Union. FerGI@KMU is a six-month professional training programme for self-employed people and employees of small and medium-sized enterprises (SME, German abbreviation: "KMU"). This training is characterized by alternating presence and online phases (so called *blended learning*). The successful participation will be documented with a certificate.

It can be concluded that the flexible concept of FerGI as well as several promotion activities have led to a huge acceptance and a large number of satisfied users. For the future, additional funding from the Network for the Promotion of Geoinformatics in Northern Germany (GiN e.V., www.gin-online.de) guarantees for a long term support and update of materials, and with that for the desired sustainable E-Learning solution.

Up-to-date information about the project can be obtained from the website www.fergi-online.de.

4. UNIGIS EXPRESS

UNIGIS is the world's leading distance education network offering programs in Geoinformatics. Since 1990 a worldwide network of universities is co-operating in the design and release of distance learning material. Since 2001 UNIGIS eXpress at the IGF in Osnabrück is affiliated with UNIGIS Salzburg which is part of the UNIGIS network (Kastler, 2005).

We offer an add-on qualification for jobless post academic professionals, such as geographers, geologists, biologists, ecologists, landscape architects, land surveyors, and urban planners. The adapted full-time courses provide basic theoretical knowledge as well as practical application-oriented skills in GIS within an up-to-date working environment. Each year UNIGIS eXpress enrolls up to 40 students so that it has about 240 UNIGIS eXpress alumni so far. More than 70% of our former students have gained new positions in a broad range of organizations, including federal and regional government, utilities, consultancy, GI business, system vendors, and research as well as in education.

Modul No.	Core Modules	Days
1	Introduction/GIS-Basics	15
2	Geodata (Models, Structures)	15
3	Geodata (Acquisition, Sources)	15
4	Attribute Tables, Databases	15
5	Cartography & Visualization	15
6	Application Development /Programming	15
7	Spatial Analysis	15
8	Applied Geoinformatics	45

Figure 5. UNIGIS core modules

UNIGIS eXpress courses are internet based flexible study modules. The core content offers a complete basic curriculum in GIS; in addition optional modules give the opportunity to adapt an individual study plan to meet the special requirements and interests of the students. Moreover, thematic oriented workshops and summer schools give the opportunity to acquire in-depth knowledge and special skills in applied Geoinformatics sciences (Kastler, 2007a).

IGF Osnabrück gives administrative support and provides access to the online course material which is maintained by a team of experienced tutors. Thomas Kastler is the local study coordinator for UNIGIS eXpress and also author of an optional module (entitled "Environmental Monitoring"; Kastler, 2007b). Tutoring and student's assessment is conducted by E-Mail, online chat, mail, and phone, or by using the E-Learning platform. The UNIGIS website also supports the learning process.

Students use the digital study materials including annotations, guided readings, and practical exercises using GIS software which is available to the students at low or even no costs. There are no exams – the assessment is based on the submitted assignments and study papers.

Students are encouraged to use their personal work experience in the course to apply knowledge and skills which are essential for their future work situations.

Figure 6. Students at the UNIGIS Introduction Workshop

The German Federal Employment Office supports students with financial aid according to the national employment promotion program.

The admission for the IGF as an eligible course provider has been determined by a certification which comprised an assessment of the organization's academic qualifications, work experience, conformance to requirements of the GIS job market and commitment to the field of higher education. The assessment has been carried out by a certification agency that makes the final decision on the admission.

Future development of the UNIGIS courses at Osnabrück will focus on the objective of a standardized and internationalized add-on qualification for professionals active in the field of GIS: this extends to further efforts in European co-operation, the exchange of data sets, standards and issues as well as trans-national and multi-lingual projects.

Up-to-date information about the course can be obtained from the website www.unigis.uni-osnabrueck.de.

5. REFERENCES

Schiewe, J., 2002. Potential and Problems of Small Universities Implementing eLearning Concepts - The Case Study University of Vechta. Proceedings of 2nd Research Workshop of EDEN "Research and Policy in Open and Distance Learning": 60-62.

Schiewe, J., 2005. Quo vadis photogrammetry education? The contribution of E-Learning. In: Fritsch, D. (Ed.): Photogrammetric Week ´05, Wichmann-Verlag: 295-302.

Kastler, T., 2005. UNIGIS eXpress - Konzeption und Realisierung. Geo-Informationssysteme GIS, (6): 33-39.

Kastler, T. 2007a. Neues von UNIGIS_eXpress. UNIGIS_offline 01/07: 4.
Kastler, T. 2007b. Umweltmonitoring in Neuauflage. UNIGIS_offline 02/07: 6.

GIS makes “Climate Change” visible

Dr. Michael Heiß

LAND+SYSTEM GmbH, Mary-Somervillestr. 1, D-28359 Bremen

1. Global Challenge

Today „Climate Change“ is one of the most prominent key words in politics and civil society. “Climate Change”, that means the current effects of unusual wheather events just as long-term changes, we have to expect as a result of global warming. Mainly responsible for this is the vast use of fossil fuel, that brings us to an increase of CO^2 emissions in the atmosphere. This increase causes the “greenhouse effect” and means global changes of temperature. Many regions in the world for example warm up quicker and more intensive (while other regions will become cooler) and the global changes of temperature will influence the intensity and distribution of precipitation worldwide.

These climate parameters have a big influence on the living conditions of flora and fauna and with it on the ecology of the worlds habitats. This is very important for man, if you consider, that already in the past climate changes have had catastrophic effects on agriculture. Unfortunately we have to take into account, that areas, where man settles and works will be threatened by storm tide, high tide or drought. Owing to these gloomy predictions we have to answer in what way man can respond to the callenge. Of course this answers are different and they correspond with the variety of interests. Nevertheless the world society now is in agreement that it is necessary to reduce the global warming. It is undeniable that our deal with the world’s natural heritage and our available resources must be sustainable and careful.

Sustainable development is our promising option, because

“Planet Earth is the only planet that can sustain human life. Human life would never have been possible and man cannot survive without its resources and that which is provided for by its ecosphere” [Stiftung Forum für Verantwortung, ASKO EUROPA Stiftung & Europäische Akademie Otzenhausen, 2007. Encouraging Sustainability. Twelve Books about the Future of the Earth. Brochure].

2. What GIS can do

„Climate Change“ is a global problem and therefore you need global solutions to solve it. Especially the world’s civil society has the right to get extensive information. Global warming does not stop at the national border and more often than not reason and effect of environmental changes are thousands of miles wide apart. Therefore Geographic Information Systems (GIS) can make a contribution, because GIS is spatial related, scalable and suitable to bring together different geodata layer. The use of GIS techniques offers scientists, researchers, educators, and planners the possibility to bring together scenarios of global climate change with data of different subject areas; a precondition of interdisciplinary work.

Changes in climate involve a complex interplay of physical, chemical, and biological processes of the earth. The difficult job of a Climate System Model is to calculate the principal components of the climate system and their interactions. The National Center for Atmospheric Research (NCAR) is publishing climate change model output data in a GIS format. The climate change model output data is produced by the Community Climate System Model (CCSM). CCSM is one of the world’s leading general circulation climate models, a communitywide effort led by NCAR. Now, outputs produced as a result of the model simulations are available to anyone interested in viewing and analyzing them in a more interdisciplinary way through GIS [compare NCAR (National Centre for Atmospheric Research) - GIS Initiative http://www.gisclimatechange.org].

3. Demonstration

Sponsors and organizers of the educational program and initiative “ Encouraging Sustainability” — namely the “Stiftung Forum für Verantwortung”, the “ASKO EUROPA- STIFTUNG”, and the “Europäische Akademie Otzenhausen” — have made it their goal to intensify the public discourse with civil society and to give politics an opportunity to create a new framework to set the course for sustainable development. In 2007 this educational initiative published twelve books about the topic “Sustainability” in which renowned scientists present the current state of research and possible courses for action in understandable language are a first step to provide the public with basic information. However, in order to progress from knowledge to action several “Didactical Modules” has been developed based on the twelve books [compare www.mut-zur-nachhaltigkeit.de].

Because a large part of data collected in the context of the “Didactical Modules” is related to space the authors job was to verify whether geoinformation is available, that is closely related to the content of the books and whether such data is available in a global extent. Therefore a data catalog was build up at first, where nearly 300 sources are described in detail. A lot of sources offer suitable information, unfortunately the data processing means a lot of work, because the data formats and exchange file are not up to standard.

The figures 1 to 3 show the global distribution of air temperature in july 2005, the predicted air temperature 2050 compared to air temperature 2000 (representation of difference, referred to degree below / above zero) and the predicted air temperature 2095 again compared to air temperature 2000. The figures 4 to 6 show the global distribution of precipitation in july (amount / day), the predicted precipitation in 2050 compared to 2000 and the predicted precipitation 2095.

4. Note of thanks

Dedicated to Manfred Ehlers. Thank you very much for help and advice.

Figure 1
Air temperature July 2005, IPCC 4th assessment report, Community Climate System Model (CCSM), A1B scenario (data management & layout by courtesy of ASKO EUROPA Foundation, Saarbrücken)

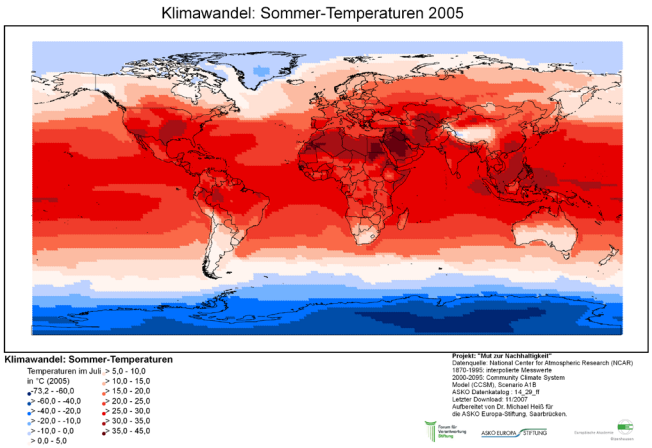

Figure 2
Air temperature 2050 compared to air temperature 2000, representation of difference, referred to degree below / above zero (IPCC 4th assessment report, Community Climate System Model (CCSM), A1B scenario (data management & layout by courtesy of ASKO EUROPA Foundation, Saarbrücken)

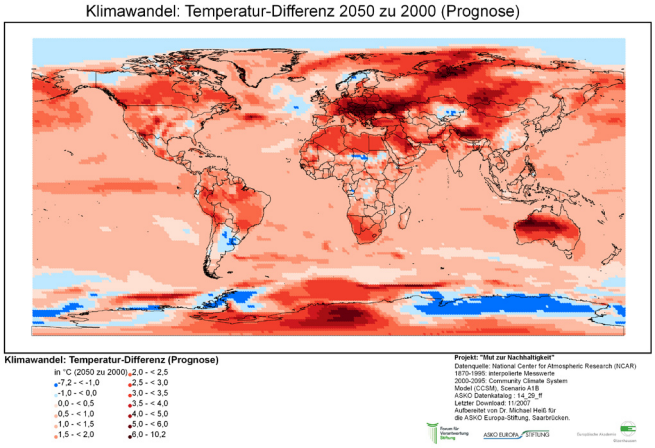

Figure 3
Air temperature 2095 compared to air temperature 2000, representation of difference, referred to degree below / above zero (IPCC 4th assessment report, Community Climate System Model (CCSM), A1B scenario (data management & layout by courtesy of ASKO EUROPA Foundtion, Saarbrücken)

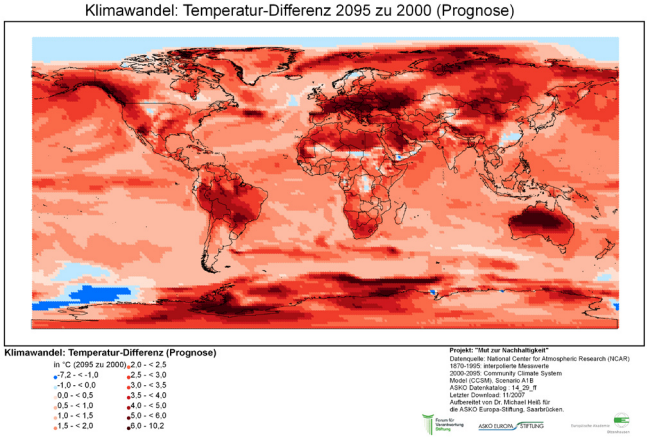

The representation do not claim completeness

Figure 4
Precipitation in July (amount / day) IPCC 4th assessment report, Community Climate System Model (CCSM), A1B scenario (data management & layout by courtesy of ASKO EUROPA Foundation, Saarbrücken)

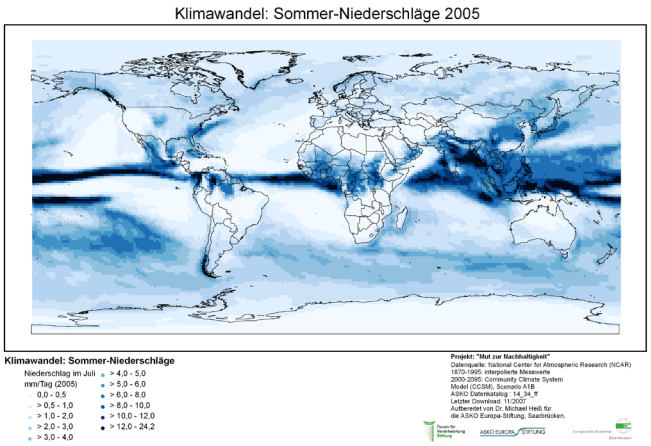

Figure 5
Increase / decrease of Precipitation 2050 compared to 2000, (prediction) (IPCC 4th assessment report, Community Climate System Model (CCSM), A1B scenario (data management & layout by courtesy of ASKO EUROPA Foundation, Saarbrücken)

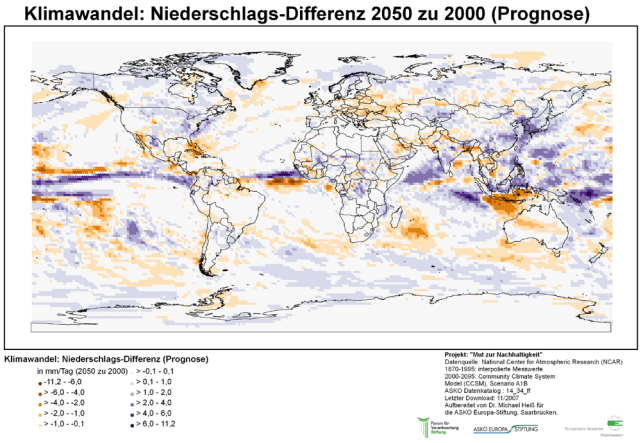

Figure 6
Increase / decrease of Precipitation 2095 compared to 2000, (prediction) (IPCC 4th assessment report, Community Climate System Model (CCSM), A1B scenario (data management & layout by courtesy of ASKO EUROPA Foundation, Saarbrücken)

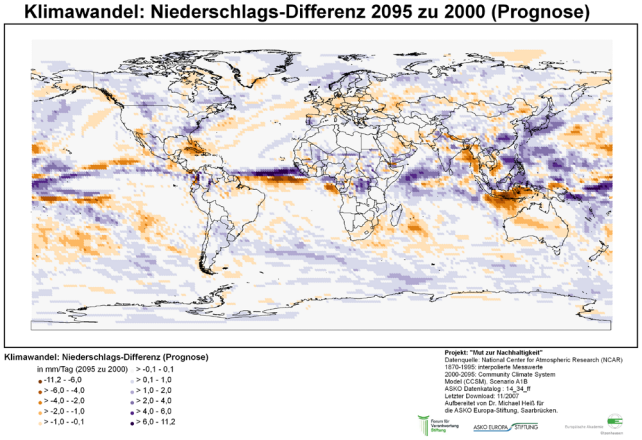

IMPROVING SQUAT INVESTIGATIONS BY VIRTUAL REALITY

I. Jaquemotte

University of Applied Sciences Oldenburg/Ostfriesland/Wilhelmshaven, Institute for Applied Photogrammetry and Geoinformatics, 26121 Oldenburg, Germany – jaquemotte@fh-oow.de

KEY WORDS: Ship Squat, Virtual Reality, Visualisation, 3D Modelling

ABSTRACT:

Since 1997 the University of Applied Sciences Oldenburg/Ostfriesland/Wilhelmshaven is actively involved in squat research. Last year a research project on ship dynamics was initiated by the Department of Geo Information and the Department of Maritime Studies. Objectives of the project are to obtain profound knowledge about ship motion and its influencing factors, and to apply this knowledge for improving prediction of ship behaviour. In consequence, techniques are developed in order to ensure ship navigation safety and economic efficiency.
As part of the project, an application is developed to support analysis of precise measuring data about proceeding vessels in a virtual environment. Processing those dynamic 3D data makes high demands on data management and visualisation. Existing Spatial Information Systems focus on management and analysis of a large amount of data, but they are limited in processing 3D geometry and time. In contrast, computer graphics provide a multitude of applications for visualising 3D data. In this context, graphical presentation is of essential interest, whereas analysis is usually not intended. With the benefits of both techniques in mind, methods of spatial information science and 3D computer graphics are applied in parallel. The focus lies on modelling full scale measurements of ship motion, visualising the moving ship within a virtual environment and providing analysis features that can be used interactively in a dynamical scene.

1. INTRODUCTION

1.1 The problem

When a ship proceeds through water, it changes sinking and trim. This phenomenon is called ship squat and results in increased draught (Fig. 1). Since ship sizes have steadily grown in the last 40 years, and ship speed has increased gradually, squat can nowadays reach the order of 1.50 m to 1.75 m (Barras, 2004). The resulting decrease of underkeel clearance in restricted waterways must be taken into account to ensure safety in navigation. Several groundings in recent years demonstrate the danger of excessive squat. This is the main reason why research groups are examining factors that influence ship squat.

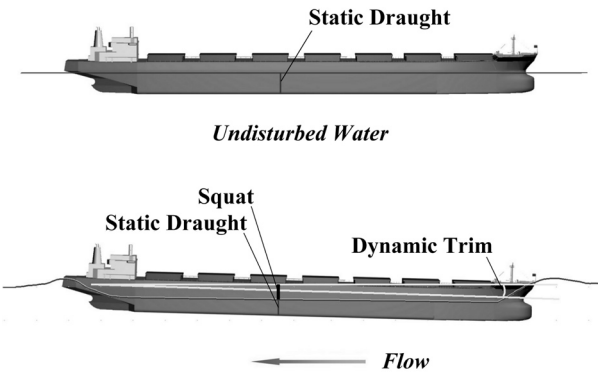

Figure 1: Squat

Speed is recognized as a main factor: If speed is doubled, squat increases approximately with the speed squared. This relation can be observed in open water conditions as well as in restricted waterways. Another factor is underkeel clearance. If the ratio of water depth to ship draught is near 1, underkeel clearance is small and squat increases. To give an example for the influence of water depth, take a bulk carrier at a breadth of 32 m and a static draught of 11 m. In this case, a water depth less then 60 m already increases ship squat. Lateral restrictions also affect squat. In our example, a channel breadth below 270 m results in increasing squat (Barras, 2004). Based on such results of investigation, two types of approach were developed for squat prediction, the empirical and the theoretical:

- Empirical formulae result from analysis of model tests and full scale measurements for different types of vessels.
- Numerical models consider the physics of the phenomenon. In those models, sinkage is derived from hydrodynamic forces and buoyancy distribution of a ship (Debaillon, 2004).

Both types of models use average or even fixed values for water depth and breadth of waterway and do not consider the accurate bathymetry of a riverbed. Underkeel clearance is usually measured and/or calculated at few point of a ship, mainly at the LCF (Longitudinal Centre of Floatation) and/or at the Bow/Stern. Regarding the size of ships and the variation of a river bed, it is not sufficient to deal with few selective points.

Measurement data of ship motions permit detailed analysis using all three dimensions. In the past 10 years methods for monitoring location, orientation and vertical motion of proceeding ships based on Differential Global Positioning Systems (DGPS) were established. At the University of Applied Sciences Oldenburg/Ostfriesland/Wilhelmshaven, for example, a new method called SHIPS has been developed to determine squat (Reinking, Härting, 2004).

It relies on DGPS, using a boat as moving reference station going along with the vessel under investigation. These measurements result in precise information (3-4 cm accuracy) about ship motion, separated in translation, rotation about the three axes of a vessel and squat.

1.2 Objectives

For analysing impacts of riverbed variations on squat, full scale measurements must be investigated together with the precise surface of a riverbed. In this context, the following questions arise:

- What is the minimum underkeel clearance referring to the entire hull of a vessel and where exactly does it occur?
- What is the water volume around the ship and how does that volume influence squat?
- How do different shapes of a riverbed surface influence squat behaviour?

All those questions demand a 3D approach, first for analysis, but also for visualisation. With precise data about ship motions and detailed information about riverbed surface a dynamical 3D computer scene can be generated. This scene, embedded in a virtual environment, enables the user to observe and analyse ship behaviour interactively. Thus, the user is capable to gain knowledge about squat behaviour, to review empirical as well as numerical methods of squat prediction, and to refine those methods.

First the paper describes the data sets available for squat investigation and different types of applications for modelling and visualising them. Further on some aspects of data management are discussed, followed by methods of 3D analysis meeting the requirements. In conclusion the status of development and further steps are presented.

2. MODELING AND VISUALISATION

The data available for analysis of squat contain a large amount of unprocessed information. To apply this information to the full extent, precise models must be generated.

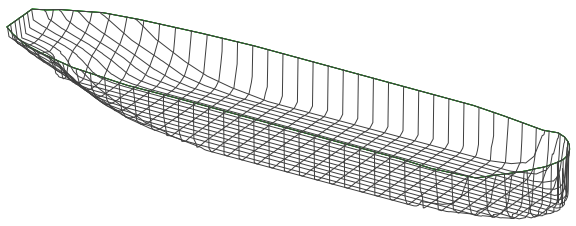

Figure 2: Hull of a tanker ship

2.1 Available data

Geometry of a ship is well known, since ship owners have detailed drawings or even digital 3D models at their disposal. With drawings, the hull can be designed accurately in a CAD system for further processing (Fig. 2).

Water and Shipping Authorities continuously collect data of waterway surfaces and provide them in form of digital elevation models (DEM) with a grid cell size of 2 to 3 m (Fig. 3). It is their sovereign task to maintain river beds for navigation by surveying and dredging in regular intervals. Since dredging is expensive, they are interested in accurate squat prediction, with a more optimal use of channels in mind.

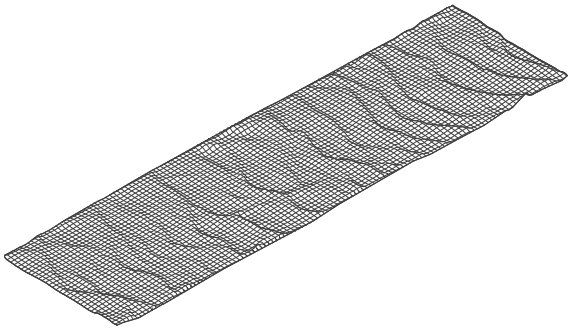

Figure 3: Riverbed (fairway)

The amount of data for modelling a riverbed for a whole expedition is considerable. For a fairway at an average breadth of 300m, a model consists of 75 000 Points per km. With an expedition way of 20 km that makes 1.5 million elevation points for the riverbed surface.

As a part of the project ship motion data in restricted waterways are continuously collected using DGPS. Thus, a large amount of precise motion data will arise. To give an example, measuring position and orientation of a ship every second over 20 km produces about 6000 measurements per expedition way.

2.2 Applications for 3D modelling

Computer graphics provide a lot of different options for modelling spatial 3D data. With a so called 3D modeller the user is able to create sophisticated 3D models for various real-world or artificial entities. Dedicated programs offer several features for composing whole computer scenes, texturing and lightning and creating animations. They focus on interactive modelling and modification and on realistic high quality presentation of artificial models rather then on precise drawing. 3D models generated like that are used in a wide variety of fields, particularly in the movie and the video game industry.

CAD tools are suitable for designing precise 3D models and presenting them on the monitor in a more or less realistic manner. They offer drafting aids in order to comfortably generate precision coordinates. These systems are able to export many 3D graphics formats, VRML and X3D amongst others.

Terrain modelling applications create surface models using different data sources such as lists of x, y, z coordinates or graphical data. Differences in elevation and volumes between two surfaces can be calculated accurately. Querying elevations

of user-defined points or dropping lines on surfaces are other useful features. Some of these applications are integrated in a CAD system, so that all CAD features are applicable. In addition application programming interfaces (APIs) are provided, which can be embedded in user applications.

Spatial information systems are capable to manage a large amount of spatial data and to analyse them. These systems focus on 2D data, but recently they also provide features to visualise and analyse 2.5D data like terrain models and even to visualize true 3D-Data. Nevertheless 3D functionality is limited to presentation and does not support 3D analysis (Tiede, Blaschke, 2005).

Since none of the products meet the requirements of the project in full extent, only modelling functionality will be considered. Surface models of the waterway are created by terrain modelling applications, embedded into the program. 3D models of a ship have to be accurately drawn for further analysis and are therefore generated in a CAD.

2.3 Options of visualisation

Up to now 2D diagrams are used to present and analyse correlations between squat and underkeel clearance. Squat is usually derived for few point of the ship, typically for the longitudinal centre of floatation (LCF) and the forward perpendicular (FP). Underkeel clearance is also calculated in those points by quantifying elevations in a riverbed model. The diagram below (Fig. 4) shows clearly, that squat increases with decreasing underkeel clearance. However particular river bed structures effecting squat behaviour can not be taken into account.

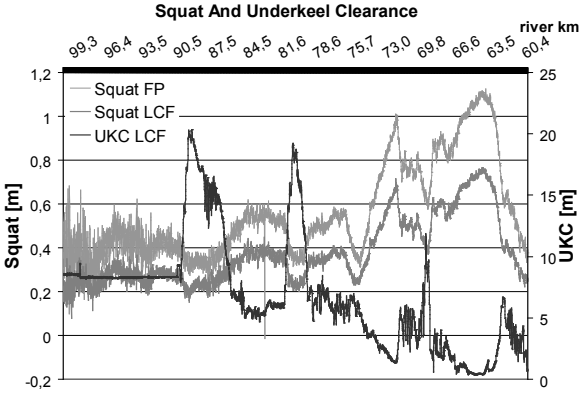

Figure 4: Correlation between squat and underkeel clearance

Animations are a good way to visualize processes, but viewpoints and perspectives must be pre-planed and pre-processed. The observer is able to start and stop such an animation, but he has no possibility to interact with the model.

In contrast, virtual reality allows the user to interact with a virtual environment using three-dimensional real time graphics. The user is able to walk or fly through a virtual world, to examine it or to activate new processes. Animating objects is optional. With virtual reality a computer model can reach a point of near realism by using textures and lightning. Virtual Reality Modelling Language (VRML) is one format amongst others to create such a virtual environment.

VRML is a file format, which was primarily designed for three-dimensional interactive vector graphics presented in the World Wide Web. In 1997 the latest version, VRML97, has been accepted by International Organization for Standardization (ISO) as an international standard. Because of its open specifications VRML is widely used in the fields of education and research and for exchange of 3D models between different graphical applications.

Although graphical hardware and software were fast-paced in recent years, VRML was not enhanced any more. That is the reason why the Web3D Consortium started working on a successor for VRML called X3D (Extensible 3D), a royalty free, meanwhile ISO-ratified format. X3D provides an XML encoding, that enables users to read or write 3D content using standard XML. A number of extra features for VRML, for example a geospatial component, is now fully integrated in X3D. Latest advances in graphics hardware capability, file compression and data security are considered as well. In addition X3D provides program scripting in order to support extensions and new language functionality defined by authors.

For viewing X3D files, a browser has to be used. X3D browsers are software applications that are capable to parse an X3D scene and to render it, to animate objects and to enable the user to interact with single objects or a whole scene. Often they are implemented as plug-in, but they are also available as standalone or embedded applications. Meantime browser developers are providing software development kids embedding an X3D browser in an external application. A virtual environment can be controlled by the application and the user is capable to control the program by interacting with the browser.

In this project X3D as an international standard manages visualisation and analysis, since it perfectly meets the requirements. The riverbed surface can be presented together with an animated model of the ship, and in addition the user is able to navigate through the 3D scene and to start analysis features interactively.

3. DATA MANAGEMENT

The large amount of time-sensitive spatial 3D data in this project requires efficient techniques for storage, management and retrieval. Over the past years Spatial database management systems (SDBMS) provide techniques for processing 2D data and recently even the third dimension entered SDBMS. Handling different 3D geometry types as well as querying data within a cuboid or generating a TIN are available features (Brinkhoff, 2008). Although time can be stored, temporal queries are usually not intended.

3.1 Time

Information about ship motions are time and location dependent, there are measurements of position and orientation of a vessel every second. In this context time is an important parameter to determine speed over ground or to move a ship in a virtual environment in proportion to its real speed. For analysing the ship hull together with the riverbed it is adequate to know the date of measurement. Water and Shipping Authorities are surveying river beds completely once a year and only critical sections of the river more frequently.

With the date it is possible to select the surface model for a river bed, collected the closest to the measurements on a ship.

3.2 Geometry

For managing geometry, existing data sets must be considered together with geometry types applicable for presentation and analysis.

With X3D surface models can be managed either as Elevation Grid or as Indexed Faceset. An Elevation Grid is a rectangular array of evenly spaced points. Since riverbed is not rectangular, those models are not is not applicable in this context. Indexed Facesets in contrast consist of polygons that are defined through their vertex indices. Those indices are enclosed within a list of point coordinates. Thus a vertex with its x, y, z coordinates needs to be listed only once although it is used for many polygons. This geometry type is well suited for the riverbed, even more, since surface models are frequently managed in the form of Triangulated Irregular Networks (TIN), which are surfaces composed of triangles.

Elevation data for the riverbed are delivered as digital elevation models, consisting of a grid of x,y,z numerical coordinates. There are different methods available to generate a TIN out of that data. The first is to use a terrain modelling application and triangulate points. For further processing the entire TIN file can be stored in the spatial database management system in all, together with information about river section and acquisition time. In this case entire surface models of the riverbed can be accessed for a user-defined time and place. As a second option TINs are generated by the SDBMS. Both options will be compared in the project.

A model of the ship hull has to be applicable for numerical squat models and surface analysis as well. For the latter a TIN shall be generated. For realistic presentation in a virtual environment a detailed model of the whole vessel should be drawn in a CAD system. Since this model is used exclusively for visualisation, any geometry type available in X3D can be applied. It still remains to decide, which data types are appropriate to store the ship models in the SDBMS.

Information about ship motion (time, position, orientation, squat) is managed in tables, where they can be accessed for further processing. These data are suitable to govern an animation within a virtual environment, and they are although used to examine correlation between squat and underkeel clearance or riverbed surface.

4. ANALYSIS

For analysing squat effects caused by the riverbed surface, methods derived from terrain modelling are appropriate. Up to now underkeel clearance is observed in few points of a vessel. With a 3D-model it can be calculated for the whole underwater area of a ship by subtracting one model from the other and generating an isopach surface (Fig. 4). Thus, bathymetry of a river and its influence on squat can be examined in detail.

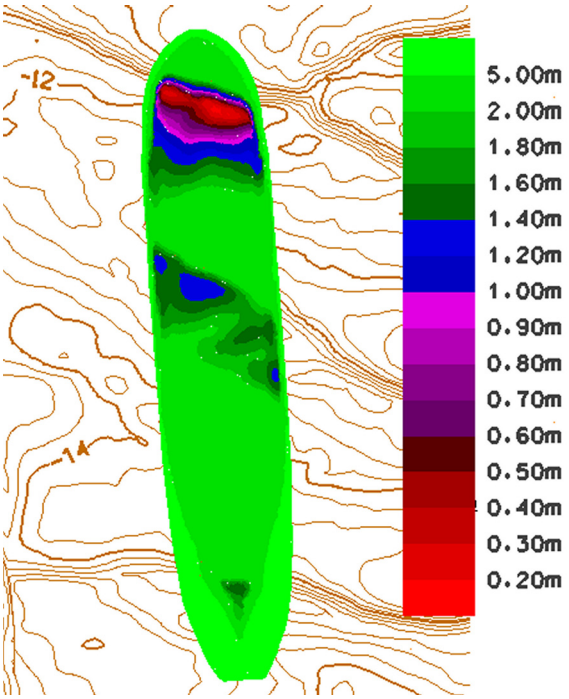

Figure 4: Underkeel clearance (isopach surface)

Water volume around the ship hull can also be used to examine river bed structures that influence squat behaviour. Since restricted breadth of a waterway as well as shallow water affect squat (Barras, 2004), water volume should be calculated within the whole breadth of influence (Fig. 5). Thus, both influence factors together can be taken into consideration.

Profiles and cross sections along the ship's longitudinal axis are also suitable to study squat behaviour in restricted water ways.

5. CONCLUSION

Challenge of the project is to develop an application enabling the user to examine nature measurements of squat in a virtual environment. Up to now a frame application is implemented permitting real time animation of a ship within an X3D browser. Information about ship motion is stored and managed in a SDBMS for further processing. An application programming interface uses that information to control the ship motion within the virtual environment. Surface models of the waterway, segmented in manageable parts, can be loaded und unloaded dynamically depending on the actual position of a vessel. Precise information about actual position, heading, rolling and heaving, as well as about squat and time can be surveyed by the user during the whole animation. Besides squat and speed are presented time-dependant in a diagram as an additional tool, enabling the user to overview a whole time period.

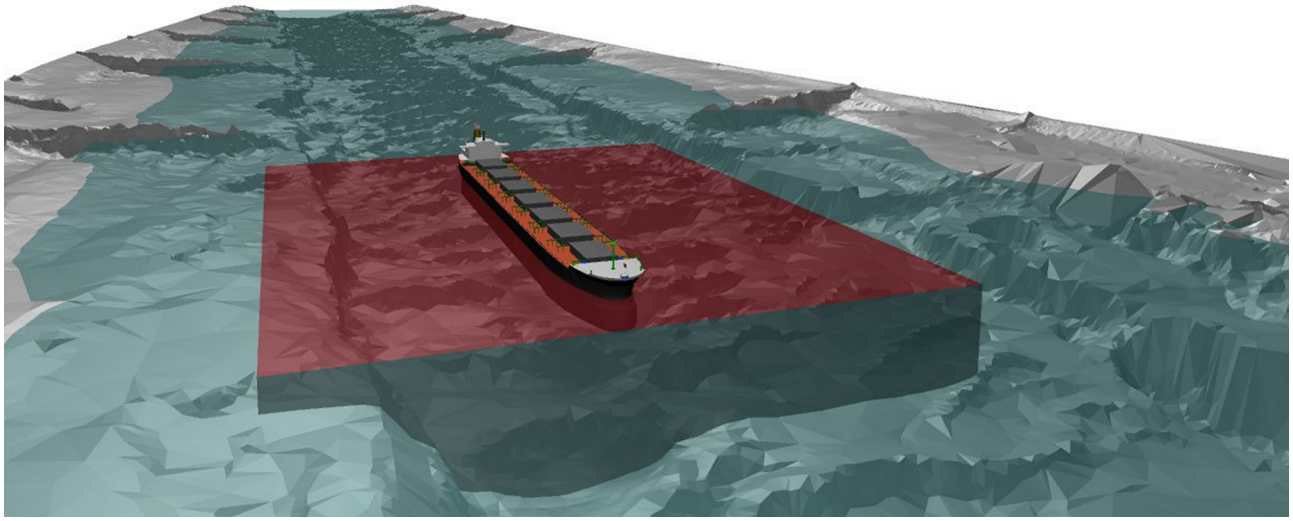

Figure 5: Water volume around the ship within breadth of influence in restricted waterway

Several tests in handling different 3D geometry types in a database management system have to be realised to determine an appropriate database design. While analysis features of a terrain modelling application, embedded in the user application, are available and tested, comparable features of a SDBM remain to be examined. These analysis tools shall be available within a virtual environment enabling the user to activate them on demand. In this context, the presentation of analysis results in a comprehensible way should not be neglected. As a further requirement numerical squat models shall be visualised in order to compare them with field measurements.

A future application, installed on a ship, could analyse and visualise the actual position and trim of the vessel in a restricted waterway in order to avoid groundings. For that purpose an efficient spatial data infrastructure (Ehlers, 2006), allowing to retrieve actual surface data of the water way, would be essential.

6. REFERENCES

Barras, C.B., 2004. *Thirty-two years of Research into Ship Squat.* 2. Squat Workshop 2004, *Aspects of Underkeel Clearance in Analyses and Application,* Elsflether Schriften zur Seeverkehrs- und Hafenwirtschaft, Band 3

Brinkhoff, T., 2008. *Geodatenbanksysteme in Theorie und Praxis*. Herbert Wichmann Verlag, Heidelberg

Debaillon, P. Lefrancois, E., Sergent, P., Dhatt, G., 2004. *Numerical Modelling of Ship Squat in Shallow Restricted Water.* 2. Squat Workshop 2004, *Aspects of Underkeel Clearance in Analyses and Application,* Elsflether Schriften zur Seeverkehrs- und Hafenwirtschaft, Band 3

Ehlers, M., 2006. Geodateninfrastrukturen (GDI) In: *GIS im Küstenzonenmanagement.* Herbert Wichmann Verlag, Heidelberg, pp.138-149

Jaquemotte, I., 2006. *Visualisierung und Analyse dynamischer Geodaten am Beispiel von Schiffsbewegungen in begrenzten Fahrwasssern.* PFG Heft 5

Reinking, J., Härting,A., 2007. *Geodetic Contributions to Ship Dynamics*. PositionIT online Nov/Dec, EE Publishers, Muldersdrift, South Africa, pp 18-23

Tiede, D., Blaschke, Th. 2005. Visualisierung und Analyse in 2,5D und 3D-GIS – von loser Koppelung zu voller Integration? Beispiele anhand kommerzieller Produkte. In: *3D-Geoinformationssysteme.* Herbert Wichmann Verlag, Heidelberg

7. ACKNOWLEDGEMENTS

The research project is funded by AGIP (Arbeitsgruppe Innovative Projekte der angewandten Hochschulforschung beim Ministerium für Wissenschaft und Kultur des Landes Niedersachsen). Furthermore our thanks go to the Wasser- und Schifffahrtsamt Bremerhaven for supporting the project.

THEORY AND PRACTICE OF FUZZY SETS IN GIS

W. Kainz

Department of Geography and Regional Research, University of Vienna
Universitätsstraße 7, 1010 Vienna, Austria
wolfgang.kainz@univie.ac.at

KEY WORDS: Fuzzy logic, membership functions, fuzzy reasoning, GIS

ABSTRACT:

Many phenomena show a degree of vagueness or uncertainty that cannot be properly expressed with crisp class boundaries. Spatial features often do not have clearly defined boundaries or a classification according to clearly defined classes cannot be made. Concepts frequently used in spatial analysis like "flat slope", "close to", or "suitable for" can better be expressed with degrees of membership to a fuzzy set than with a binary yes/no classification. This paper introduces the basic principles of fuzzy logic and its application to spatial data handling. It discusses the mathematics of membership functions, fuzzy reasoning, and how vague spatial data can be represented and processed in a GIS.

1. INTRODUCTION

In human thinking and language we often use uncertain or vague concepts. Our thinking and language is not binary, i.e., black or white, zero or one, yes or no. In real life we add much more variation to our judgments and classifications. These vague or uncertain concepts are said to be fuzzy. We encounter fuzziness almost everywhere in our everyday lives.

For instance, when we talk about high elevation, the concept of "high" will be depending on the context. In a country like the Netherlands where the highest elevation reaches only 300 meters, high elevation will be considered differently from a region like Tibet. In land cover analysis we are not able to draw crisp boundaries of, for instance, forest areas or grassland. Where does the grassland end and the forest start? The boundaries will be vague or fuzzy.

In real life applications we might look for a suitable site to build a house. The criteria for the site that we are looking for could be formulated that it must

- have flat slope
- have favorable aspect
- have moderate elevation
- be close to a lake
- be not near a major road

All these conditions are vague concepts, but correspond to the way we express these things in our natural languages and thinking. Using the conventional approach the above mentioned conditions would be translated into crisp classes, such as

- slope less than 10 degrees
- aspect between 135 degrees and 225 degrees, or the terrain is flat
- elevation between 1,500 meters and 2,000 meters
- within 1 kilometer from a lake
- not within 300 meters from a major road

If a location falls within the given criteria we would accept it, otherwise (even if it would be very close to the threshold) it would be excluded from our analysis. If, however, we allow degrees of membership to the defined classes, we can accommodate also those locations that just miss a criterion by a few meters. They will just get a low degree of membership, but will be included in the analysis. Usually, we assign a degree of membership to a class as a value between zero and one, where zero indicates no membership and one represents full membership. Any value in between can be a possible degree of membership.

Degrees of membership as values ranging between zero and one look very similar to probabilities, which are computed as a value between zero and one. We might be tempted to assume that fuzziness and probability are basically the same. There is, however, a subtle, yet important, difference. *Probability* gives us an indication with which likelihood an event will occur. Whether it is going to happen, however, is not sure. *Fuzziness* is an indication to what degree something belongs to a class (or phenomenon). We know that the phenomenon exists. What we do not know, however, is its extent, i.e., to which degree members of a given universe belong to the class. In the following sections we will establish the mathematical basis to deal with vague and fuzzy concepts as well as perform analysis with fuzzy spatial data.

2. FUZZY SETS

In general set theory an element is either a member of a given set or not. We can express this fact with the characteristic function for the elements of a given universe to belong to a certain subset of this universe. We call such a set a crisp set.

2.1.1 Characteristic function: Let A be a subset of a universe X. The *characteristic function* χ_A of A is defined as $\chi_A : X \rightarrow \{0,1\}$ with

$$\chi_A(x) = \begin{cases} 1 & \text{iff} \quad x \in A \\ 0 & \text{iff} \quad x \notin A \end{cases} \tag{1}$$

In this way we always can clearly indicate whether an element belongs to a set or not. If, however, we allow some degree of uncertainty as to whether an element belongs to a set, we can express the membership of an element to a set by its

membership function. This leads us to the definition of fuzzy sets.

2.1.2 Fuzzy set: A *fuzzy set* A of a universe X is defined by a *membership function* μ_A such that $\mu_A : X \to [0,1]$ where $\mu_A(x)$ is the *membership value* of x in A.

If the universe is a finite set $X = \{x_1, x_2, \ldots, x_n\}$, then a fuzzy set A on X is denoted as

$$A = \mu_A(x_1)/x_1 + \cdots + \mu_A(x_n)/x_n = \sum_{i=1}^{n} \mu_A(x_i)/x_i \qquad (2)$$

The term $\mu_A(x_i)/x_i$ indicates the membership value to fuzzy set A for x_i. The symbol "/" is called *separator*, "Σ" and "+" serve as *aggregation* and *connection* of terms. They should not be confused with the usual symbols for division, sum and addition.

If the universe is an infinite set $X = \{x_1, x_2, \ldots\}$, then a fuzzy set A on X is expressed as $A = \int_X \mu_A(x)/x$. The symbols "$\int$"and "/" function as aggregation and separator, respectively. They should not be confused with the integral and division.

The *empty fuzzy set* $\varnothing$ is defined as $\forall x \in X, \mu_{\varnothing}(x) = 0$. For every element of the universe X we trivially have $\forall x \in X, \mu_X(x) = 1$, i.e., the universe is always crisp.

A membership function assigns to every element of the universe a degree of membership (or membership value) to a fuzzy set. This membership value must be between 0 (no membership) and 1 (definite membership). All other values between 0 and 1 indicate to which degree an element belongs to the fuzzy set. It is important to note that the membership degree of 1 does not necessarily need to be obtained for members of a fuzzy set.

2.2 Membership Functions

The selection of a suitable membership function for a fuzzy set is one of the most important activities in fuzzy logic. It is the responsibility of the user to select a function that is a best representation for the fuzzy concept to be modeled. The following criteria are valid for all membership functions:

- The membership function must be a real valued function whose values are between 0 and 1.
- The membership values should be 1 at the center of the set, i.e., for those members that definitely belong to the set.
- The membership function should fall off in an appropriate way from the center through the boundary.
- The points with membership value 0.5 (*crossover point*) should be at the boundary of the crisp set, i.e., if we would apply a crisp classification, the class boundary should be represented by the crossover points.

We know two types of membership functions: (i) linear membership functions and (ii) sinusoidal membership functions. Figure 1 shows the general form of a linear membership function.

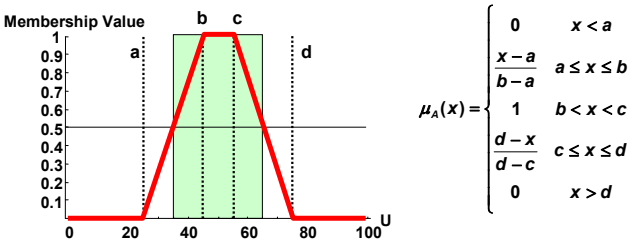

Figure 1. Linear membership function

This function has four parameters that determine the shape of the function. By choosing proper values for a, b, c, and d we can create S-shaped, trapezoidal, triangular, and L-shaped membership functions (Figure 2).

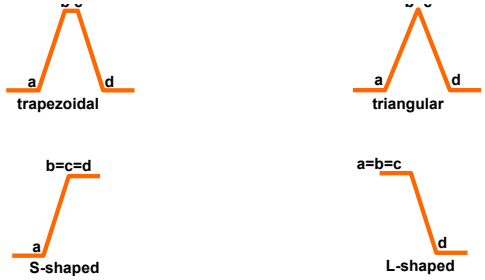

Figure 2. Shapes of membership functions

If a rounded shape of the membership function is more appropriate for our purpose we should choose a sinusoidal membership function (Figure 3). As with linear membership functions we can achieve S-shaped, bell-shaped, and L-shaped membership functions by proper selection of the four parameters.

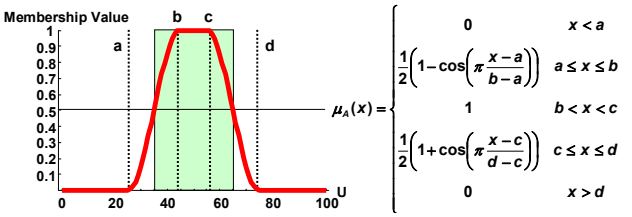

Figure 3. Sinusoidal membership function

A special case of bell-shaped membership functions is the Gaussian function derived from the probability density function of the normal distribution with two parameters c (mean) and σ (standard deviation) as illustrated in Figure 4.

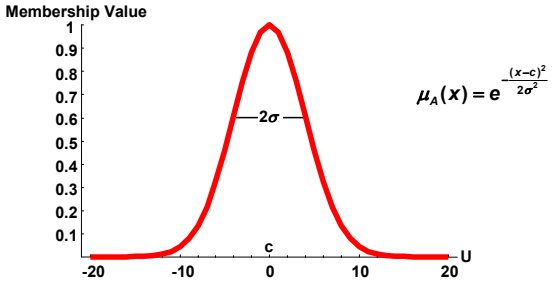

Figure 4. Gaussian membership function

2.3 Operations on Fuzzy Sets

Operations on fuzzy sets are defined in a similar way as for crisp sets. However, not all rules for crisp set operations are also valid for fuzzy sets. Like for crisp sets we have subset, union, intersection, and complement. In addition, there are support, height, and alternate operations for union and intersection of fuzzy sets.

2.3.1 Support: All elements of the universe X that have a membership value greater than zero for a fuzzy set A are called the support of A, or $\text{supp}(A) = \{x \in X \mid \mu_A(x) > 0\}$.

2.3.2 Height: The height of a fuzzy set A is the largest membership value in A, written as $\text{hgt}(A)$. If $\text{hgt}(A) = 1$ then the set is called *normal*. We can always normalize a fuzzy set by dividing all its membership values by the height of the set.

2.3.3 Equality: Two fuzzy sets A and B are *equal* (written as $A = B$) if for all members of the universe X their membership values are equal, i.e., $\forall x \in X, \mu_A(x) = \mu_B(x)$.

2.3.4 Inclusion: A fuzzy set A is included in a fuzzy set B (written as $A \subseteq B$) if for every element of the universe the membership values for A are less than or equal to those of B, i.e., $\forall x \in X, \mu_A(x) \le \mu_B(x)$. Looking at the graph of membership functions, a fuzzy set A will be included in fuzzy set B when the graph of A is completely covered by the graph of B.

2.3.5 Union: The union of two fuzzy sets A and B can be computed for all elements of the universe X by one of the three operators:

$$\mu_{A\cup B}(x) = \max(\mu_A(x), \mu_B(x)) \quad (3)$$

$$\mu_{A\cup B}(x) = \mu_A(x) + \mu_B(x) - \mu_A(x) \cdot \mu_B(x) \quad (4)$$

$$\mu_{A\cup B}(x) = \min(1, \mu_A(x) + \mu_B(x)) \quad (5)$$

The max-operator is a *non-interactive* operator in the sense that the membership values of both sets do not interact with each other. In fact, one set could be completely ignored in a union operation when it is included in the other. The two other operators are called *interactive*, because the membership value of the union is determined by the membership values of both sets.

2.3.6 Intersection: The intersection of two fuzzy sets A and B can be computed for all elements of the universe X by one of the three operators:

$$\mu_{A\cap B}(x) = \min(\mu_A(x), \mu_B(x)) \quad (6)$$

$$\mu_{A\cap B}(x) = \mu_A(x) \cdot \mu_B(x) \quad (7)$$

$$\mu_{A\cap B}(x) = \max(0, \mu_A(x) + \mu_B(x) - 1) \quad (8)$$

The min-operator is a non-interactive, the two others are interactive operators as explained above. The multiplication operator is sometimes called "soft intersection."

2.3.7 Complement: The complement $\overline{A}$ of a fuzzy set A in the universe X is defined as $\forall x \in X, \mu_{\overline{A}}(x) = 1 - \mu_A(x)$.

Many rules for set operations are valid for both crisp and fuzzy sets. However, the well known laws in classic logic of the excluded middle and the law of contradiction are not valid for fuzzy sets.

2.4 α -Cuts

If we wish to know all those elements of the universe that belong to a fuzzy set and have at least a certain degree of membership, we can use α-level sets. With α-level sets we can identify those members of the universe that typically belong to a fuzzy set.

2.4.1 α -Cut: A (*weak*) α-cut (or α-level set) A_α with $0 < \alpha \le 1$ is the set of all elements of the universe such that $A_\alpha = \{x \in X \mid \mu_A(x) \ge \alpha\}$. A *strong* α-cut $A_{\overline{\alpha}}$ is defined as $A_{\overline{\alpha}} = \{x \in X \mid \mu_A(x) > \alpha\}$.

3. LINGUISTIC VARIABLES AND HEDGES

In mathematics variables usually assume numbers as values. A *linguistic variable* is a variable that assumes linguistic values which are words (linguistic terms). If, for example, we have the linguistic variable "slope", the linguistic values for slope could be "flat", "moderate", and "steep". These linguistic values possess a certain degree of uncertainty or vagueness that can be expressed by a membership function for every term. Often, we modify a linguistic term by adding words like "very", "somewhat", "slightly", or "more or less" and arrive at expressions such as "very steep", "not flat", or "somewhat moderate".

Such modifiers are called *hedges*. They can be expressed with operators applied to the fuzzy sets representing linguistic terms (see Table 1).

Operator	Expression
Normalization	$\mu_{\text{norm}(A)}(x) = \dfrac{\mu_A(x)}{\text{hgt}(\mu_A)}$
Concentration	$\mu_{\text{con}(A)}(x) = \mu_A^2(x)$
Dilation	$\mu_{\text{dil}(A)}(x) = \sqrt{\mu_A(x)}$
Negation	$\mu_{\text{not}(A)}(x) = \mu_{\overline{A}}(x) = 1 - \mu_A(x)$
Contrast intensification	$\mu_{\text{int}(A)}(x) = \begin{cases} 2\mu_A^2(x) & \mu_A(x) \in [0, 0.5] \\ 1 - 2(1-\mu_A(x))^2 & \text{otherwise} \end{cases}$

Table 1. Operators for hedges

Table 2 shows the models being used to represent hedges for linguistic terms.

Hedge	Operator
very A	con(A)
more or less A (fairly A)	dil(A)
plus A	$A^{1.25}$
not A	not(A)
slightly A	int(norm(plus $A \cap$ not(very A)))

Table 2. Hedges and their models

4. FUZZY INFERENCE

In binary logic we have only two possible values for a logical variable, *true* or *false*, 1 or 0. As we have seen, many phenomena can be better represented by fuzzy sets than by crisp classes. Fuzzy sets can also be applied to reasoning when vague concepts are involved. In binary logic reasoning is based on either deduction (*modus ponens*) or induction (*modus tollens*). In fuzzy reasoning we use a generalized modus ponens which reads as

Premise$_1$:	If x is A then y is B
Premise$_2$:	x is A'
Conclusion:	y is B'

Here, A, B, A', and B' are fuzzy sets where A' and B' are not exactly the same as A and B. As an example consider the generalized modus ponens for risk assessment:

Premise$_1$:	If the slope is steep then the risk is high
Premise$_2$:	Slope is very steep
Conclusion:	Risk is very high

With logic inference the number of rules can be rather large. Here we discuss two methods for fuzzy reasoning.

4.1 Mamdani's Direct Method

This method is based on a generalized modus ponens:

$$p \Rightarrow q: \begin{cases} \text{If } x \text{ is } A_1 \text{ and } y \text{ is } B_1 \text{ then } z \text{ is } C_1 \\ \text{If } x \text{ is } A_2 \text{ and } y \text{ is } B_2 \text{ then } z \text{ is } C_2 \\ \vdots \\ \text{If } x \text{ is } A_n \text{ and } y \text{ is } B_n \text{ then z is } C_n \end{cases}$$

$$\frac{p_1: \quad x \text{ is } A', \text{ y is } B'}{q_1: \quad z \text{ is } C'}$$

Premise$_1$ becomes a set of if-then rules. A, B, and C are fuzzy sets; x and y are *premise variables*, z is the *consequence variable*. The reasoning process is then straightforward according to the following procedure. Let x_0 and y_0 be the input for the premise variables.

Step 1: Apply the input values to the premise variables for every rule and compute min of $\mu_{A_i}(x_0)$ and $\mu_{B_i}(y_0)$:

$$\begin{aligned} \text{Rule}_1: &\quad m_1 = \min(\mu_{A_1}(x_0), \mu_{B_1}(y_0)) \\ \text{Rule}_2: &\quad m_2 = \min(\mu_{A_2}(x_0), \mu_{B_2}(y_0)) \\ &\vdots \\ \text{Rule}_n: &\quad m_n = \min(\mu_{A_n}(x_0), \mu_{B_n}(y_0)) \end{aligned}$$

Step 2: Compute the conclusion per rule by cutting the membership function of the consequence $\mu_{C_i}(z)$ at m_i:

$$\begin{aligned} \text{Rule}_1: &\quad \mu_{C_1'}(z) = \min(m_1, \mu_{C_1}(z)) \quad \forall z \in C_1 \\ \text{Rule}_2: &\quad \mu_{C_2'}(z) = \min(m_2, \mu_{C_2}(z)) \quad \forall z \in C_2 \\ &\vdots \\ \text{Rule}_n: &\quad \mu_{C_n'}(z) = \min(m_n, \mu_{C_n}(z)) \quad \forall z \in C_n \end{aligned}$$

Step 3: Compute the final conclusion by determining the union of all individual conclusions from step 2:

$$\mu_C(z) = \max(\mu_{C_1'}(z), \mu_{C_2'}(z), \ldots, \mu_{C_n'}(z))$$

The result of the final conclusion is a fuzzy set. For practical reasons we need a crisp value for the consequence variable. The process to determine this value is called *defuzzification*. There are several methods to defuzzify a given fuzzy set. One of the most common is the center of gravity (or center of area) method. For a discrete fuzzy set the center of area is computed as:

$$z_0 = \frac{\sum \mu_C(z) \cdot z}{\sum \mu_C(z)} \tag{9}$$

For a continuous fuzzy set this becomes

$$z_0 = \frac{\int \mu_C(z) \cdot z dz}{\int \mu_C(z) dz} \tag{10}$$

4.2 Simplified Method

Often, the defuzzification process is too time-consuming and complicated. An alternative approach is the simplified method where the conclusion is a real value c instead of a fuzzy set. It is based on a generalized modus ponens of the form:

$$p \Rightarrow q: \begin{cases} \text{If } x \text{ is } A_1 \text{ and } y \text{ is } B_1 \text{ then } z \text{ is } c_1 \\ \text{If } x \text{ is } A_2 \text{ and } y \text{ is } B_2 \text{ then } z \text{ is } c_2 \\ \vdots \\ \text{If } x \text{ is } A_n \text{ and } y \text{ is } B_n \text{ then z is } c_n \end{cases}$$

$$\frac{p_1: \quad x \text{ is } A', \text{ y is } B'}{q_1: \quad z \text{ is } c'}$$

Premise$_1$ becomes a set of if-then rules. The premise variables are fuzzy sets; the conclusion is a real number (fuzzy singleton). The reasoning process is then straightforward in analogy to the previous method with the difference that the result is not a fuzzy set that needs to be defuzzified but we can compute the final result directly after step 2 in the algorithm.

The algorithm works as outlined in the following procedure. Let x_0 and y_0 be the input for the premise variables.

Step 1: Apply the input values to the premise variables for every rule and compute min of $\mu_{A_i}(x_0)$ and $\mu_{B_i}(y_0)$:

$$\begin{aligned} \text{Rule}_1: &\quad m_1 = \min(\mu_{A_1}(x_0), \mu_{B_1}(y_0)) \\ \text{Rule}_2: &\quad m_2 = \min(\mu_{A_2}(x_0), \mu_{B_2}(y_0)) \\ &\vdots \\ \text{Rule}_n: &\quad m_n = \min(\mu_{A_n}(x_0), \mu_{B_n}(y_0)) \end{aligned}$$

Step 2: Compute the conclusion value per rule as:

$$\begin{aligned} \text{Rule}_1: &\quad c_1' = m_1 \cdot c_1 \\ \text{Rule}_2: &\quad c_2' = m_2 \cdot c_2 \\ &\vdots \\ \text{Rule}_n: &\quad c_n' = m_n \cdot c_n \end{aligned}$$

Step 3: Compute the final conclusion as:

$$c' = \frac{\sum_{i=1}^{n} c_i'}{\sum_{i=1}^{n} m_i}$$

5. APPLICATIONS OF FUZZY LOGIC IN GIS

Many spatial phenomena are inherently fuzzy or vague or possess indeterminate boundaries. Fuzzy logic has been applied for many areas in GIS such as fuzzy spatial analysis, fuzzy reasoning, and the representation of fuzzy boundaries. The following example illustrates how a fuzzy set can be computed from a given grid data set.

The objective of this example is to determine high elevation in the area covered by the 1 : 24,000 USGS topographic map sheet of Boulder, Colorado.

Elevation is considered high when it is above 1,700 meters. We represent the features meeting the criterion as a fuzzy set with a sinusoidal membership function defined as

$$\mu_{\text{high elevation}}(x) = \begin{cases} 0 & x \le 1700 \\ \frac{1}{2}\left(1 - \cos\left(\pi \frac{x - 1700}{300}\right)\right) & 1700 < x \le 2000 \\ 1 & x > 2000 \end{cases} \quad (11)$$

The graph of the membership function is displayed in Figure 6.

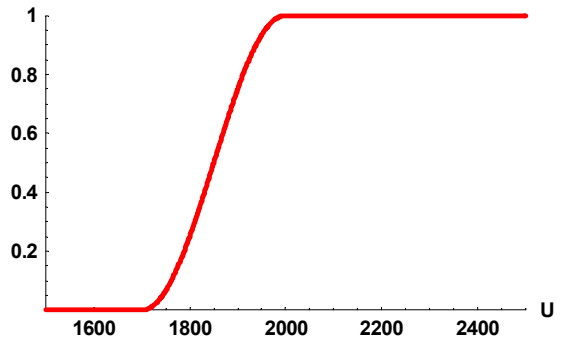

Figure 6. Membership function for "high elevation"

The 1 : 24K DEM was downloaded from the USGS web site and imported into ArcGIS as a grid. In principle, there are several ways to solve the problem in ArcInfo. We can use Workstation ArcInfo GRID, ArcMap Spatial Analyst, or ArcView 3.x Spatial Analyst. We can even create our own fuzzy logic tool using the scripting environment of the geoprocessor in ArcGIS 9. The grid involved is called elevation. The fuzzy set will be a grid felevation whose cell values are between zero and one.

5.1 Workstation ArcInfo GRID

To compute the fuzzy set we use an AML script that is run from ArcInfo GRID applying the CON command:

```
felevation = con(elevation le 1700, 0, elevation gt 1700 & elevation ~
le 2000, 0.5 * (1 - COS(3.14159 * (elevation - 1700) / 300)), 1)
```

5.2 ArcMap Spatial Analyst

To solve the problem we use the raster calculator of the Spatial Analyst. The following screen dump shows the command to produce the required fuzzy set.

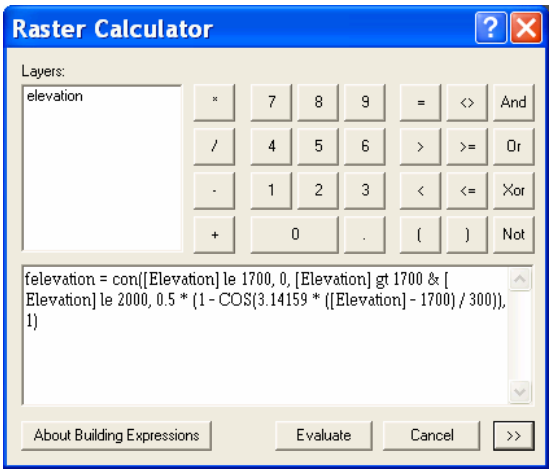

5.3 ArcView 3.x

The same results can be achieved by using requests in the ArcView GIS Spatial Analyst map calculator. The following screen dump shows how to use the Avenue Con request for computing the fuzzy set for high elevation.

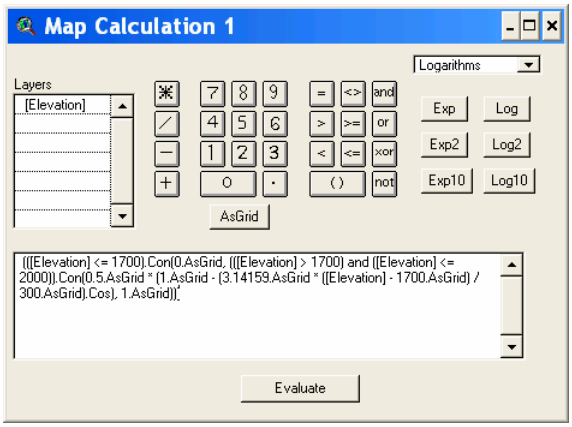

5.4 ArcGIS 9 Script

We have written a Python script that generates a fuzzy raster data set from a given input raster data set. This script is used here as a tool in the ArcToolbox.

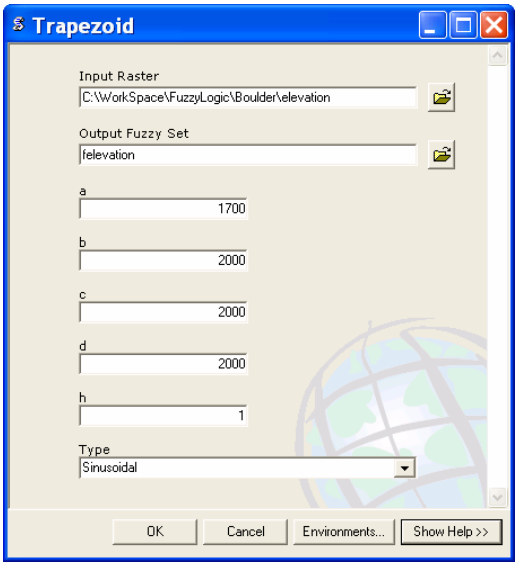

5.5 Results

Figure 7 shows the result of the analysis with a fuzzy logic approach (right) and a crisp approach (left) with a threshold of 1,850 meters.

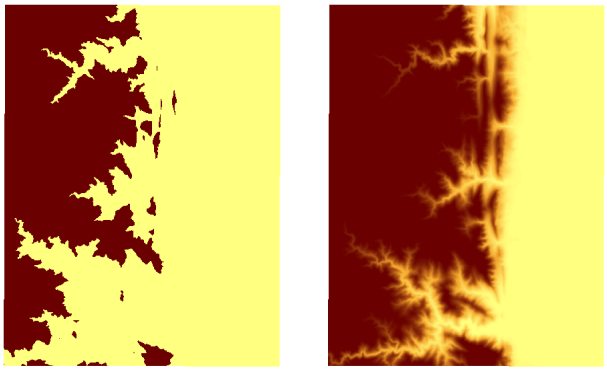

Crisp set Fuzzy set

Figure 7. High elevation computed with a fuzzy logic approach (right) and a crisp approach (left)

Figure 8 shows the result of the site analysis mentioned in the introduction using a traditional crisp approach and fuzzy sets. From the pink color tones in the right picture we can see that the fuzzy approach gives us more possibilities to express grades of membership to the desired result than just one single color tone for crisp sets.

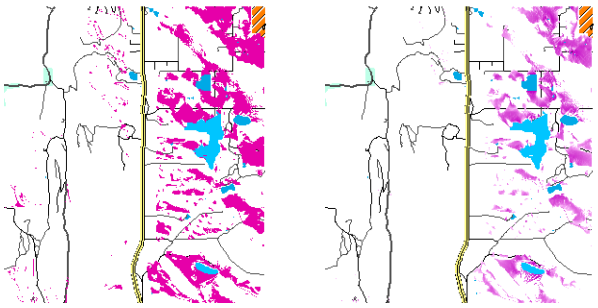

Crisp analysis Fuzzy analysis

Figure 8. Crisp (left) and fuzzy (right) approach

The following bibliography gives a selection of relevant literature about fuzzy logic and applications in GIS.

6. BIBLIOGRAPHY

Aliev R.A., Aliev R.R., 2001. *Soft Computing and Its Applications*. World Scientific Publishing Co. Pte. Ltd., Singapore, London.

Bonham-Carter G.F., 1994. *Geographic Information Systems for Geoscientists: Modelling with GIS*. Pergamon, Elsevier Science, Kidlington, U.K.

Burrough P.A., McDonnell R.A., 1998. *Principles of Geographical Information Systems*. Oxford University Press.

Burrough P.A., Frank A.U., 1996. *Geographic Objects with Indeterminate Boundaries*. GISDATA II, Taylor & Francis, London.

Demicco R.V., Klir G.J., 2004. *Fuzzy Logic in Geology*. Elsevier Science (USA).

Dubois D., Prade H., 2000. *Fundamentals of Fuzzy Sets*. Kluwer Academic Publishers, Boston, London, Dordrecht.

Hootsmans R., 1996. Fuzzy Sets and Series Analysis for Visual Decision Support in Spatial Data Exploration. PhD thesis, University Utrecht, The Netherlands. ISBN 90 6266 134 3.

Jiang B., 1996. Fuzzy Overlay Analysis and Visualization in Geographic Information Systems. PhD Thesis, University Utrecht and ITC, The Netherlands. ISBN 90 6266 128 9.

Leung Y., 1997. *Intelligent Spatial Decision Support Systems*. Springer-Verlag, Berlin, Heidelberg.

Petry F.E., Robinson V.B., Cobb M.A. (Eds.), 2005. *Fuzzy Modeling with Spatial Information for Geographic Problems*. Springer-Verlag, Berlin, Heidelberg

Tanaka K., 1997. *An Introduction to Fuzzy Logic for Practical Applications*. Springer-Verlag, New York.

Tang X.M., Kainz W., 2004. Formation of fuzzy land cover objects from TM images. In: Li Z., Zhou Q., Kainz W. (eds.) (2004), *Advances in Spatial Analysis and Decision Making*. ISPRS Book Series, Swets & Zeitlinger B.V., Lisse, The Netherlands, pp. 73-87.

Tang X.M., 2004. Spatial Object Modelling in Fuzzy Topological Spaces with Applications to Land Cover Change. PhD thesis, University of Twente, Enschede, The Netherlands, ITC dissertation number 108.

Tang X.M., Kainz W., Fang Y., 2005. Reasoning about changes of land covers with fuzzy settings. In: *International Journal of Remote Sensing*, Vol. 26, No. 14, pp.3025-3046.

Tang X.M., Fang Y., Kainz W., 2006. Fuzzy Topological Relations between Fuzzy Spatial Objects. In: Wang, L.; Jiao, L.; Shi, G.; Lu, X.; Liu, J. (eds.), *Proceedings, 3rd International Conference on Fuzzy Systems and Knowledge Discovery*. Lecture Notes in Artificial Intelligence 4223, Springer-Verlag Berlin Heidelberg, pp. 324-333.

Zadeh L.A., 1965. Fuzzy Sets. *Information and Control*, Vol. 8, pp. 338 – 353.

Zheng D., Kainz W., Ehlers M., 1999. Fuzzy Rule Acquisition and Assessment in Spatial Decision Exploration. In: Chen J., Zhan Q., Li Z., Jiang J. (eds.), Proceedings Dynamic and Multi-Dimensional GIS, *International Archives of Photogrammetry and Remote Sensing*, Vol. 32, Part 4W12, pp. 51-58.

Zheng D., 2001. A Neuro-Fuzzy Approach to Linguistic Knowledge Acquisition and Assessment in Spatial Decision Making. PhD thesis, University Vechta and ITC, Enschede.

Zimmermann H.J., 1987. *Fuzzy Sets, Decision Making, and Expert Systems*. Kluwer Academic Publishers, Dordrecht, The Netherlands.

Zimmermann H.J., 2001. *Fuzzy Set Theory and Its Applications*, Fourth Edition. Kluwer Academic Publishers, Boston, Dordrecht, London.

SUN-AREA
EIN BEITRAG DER FERNERKUNDUNG GEGEN DEN KLIMAWANDEL

M. Klärle

Fachhochschule Osnabrück, Fakultät Agrarwissenschaften und Landschaftsarchitektur D-49090 Osnabrück,
Fachhochschule Frankfurt, Geoinformation und Kommunaltechnik, D-60318 Frankfurt,
martina.klaerle@fb1.fh-frankfurt.de

KEY WORDS: Stanortanalyse, Fotovoltaik, Laserscanner, Web-GIS, Solarenergie, Fernerkundung, GIS, Geoinformatik

ZUSAMMENFASSUNG

Das vom Land Niedersachsen (AGIP) gefördertes Forschungsprojekt SUN-AREA verfolgt das Ziel mit vorhandenen hochgenauen Laserscannerdaten optimale Standorte für Photovoltaik-Anlagen zu finden. Das daraus resultierende Energiepotential jeder Stadt verlässlich zu berechnen und über eine WEB-GIS-Anwendung jede geeignete Dachfläche darzustellen. Möglich wird dies durch die Entwicklung einer vollautomatischen Algorithmenkette aus Raster- und Vektor-GIS-Funktionen die die Form, Neigung, Ausrichtung und Verschattung jeder Dachfläche ermittelt.

1. DANKE

Das Forschungsprojekt SUN-AREA, `Standortanalyse für Fotovoltaikanlagen mittels hochauflösender flugzeuggetragener Laserscannerdaten. Ist das erste Forschungsprojekt der Fachhochschule Osnabrück im Umfeld der Fernerkundung und Geoinformatik.

Prof. Dr. Manfred Ehlers unterstützte den Antrag als Kooperationspartner. Die Kooperation der anwendungsorientierten Fachhochschule und dem forschungsorientierten Institut für Geoinformatik und Fernerkundung öffnete der Fachhochschule die Tür in die Forschungslandschaft.

Auf diesem Wege möchte ich mich bei Manfred Ehlers für seine Unterstützung und Kooperationsbereitschaft über die Hochschul-, Alters-, Sprach- und Geschlechtsgrenzen hinweg herzlich bedanken.

2. KOOPERATIONSPARTNER

Das Labor für Geoinformatik an der Fakultät Agrarwissenschaften & Landschaftsarchitektur führt in Zusammenarbeit mit dem Wirtschaftsunternehmen TopScan, Gesellschaft zur Erfassung topographischer Informationen, Rheine vertreten durch Herrn Dr. Lindenberger, und der Universität Osnabrück, Forschungszentrum für Geoinformatik und Fernerkundung vertreten durch Herrn Prof. Dr. Ehlers ein Forschungsprojekt im Bereich Fernerkundung und Geoinformatik durch (Januar 2006 – März 2008).

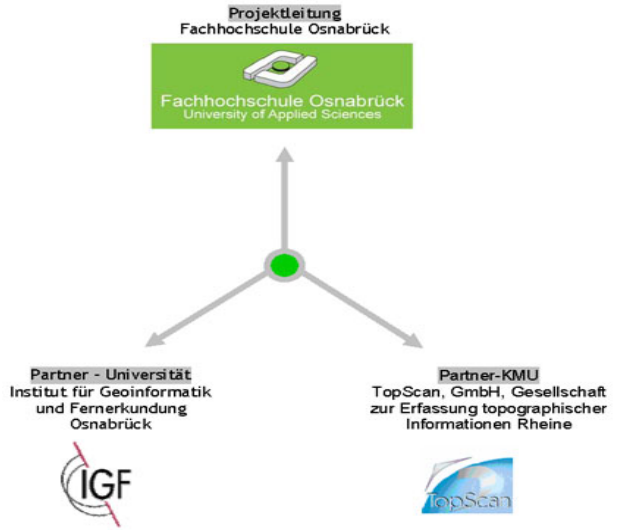

Prof. Dr. M. Ehlers, Prof. Dr. M. Klärle, Dr. J. Lindenberger

3. DAS ZIEL

Das Projekt befasst sich mit der Einsatzoptimierung der Sonnenenergie durch computergestützte Analyse und Verknüpfung von Laserscandaten.

Ziel des Vorhabens ist es, auf der Basis von Flugzeugscannerdaten Standorte zu finden, die für die Gewinnung von Solarenergie optimal geeignet sind. Dabei geht es insbesondere um die Interpretation von kleingliedrigen Landschaftsaufnahmen, die durch die neuen Sensoren der Laserscannerverfahren möglich werden.

Für eine Reihe von Bundesländern z.B. Baden-Württemberg liegen die hochgenauen, dreidimensionalen Flugzeug-scannerdaten bereits flächendeckend vor . In absehbarer Zeit werden sie für das gesamte Bundesgebiet vorliegen. Die Punktedichte liegt durchschnittlich bei ca. 4 Punkte pro m² mit einer Höhengenauigkeit von 0,1 m. Mehrfachreflexionen der Lichtimpulse („first pulse“ und „last pulse“) lassen eine Klassifizierung der Punktwolke in Bodenpunkte sowie Hö-henpunkte (Vegetation und Gebäude) zu. Diese Laserscandaten erlauben erstmals kleinräumige Analysen (z.B. Bestimmung der Dachneigung) über große Untersuchungsbereiche.

Das anwendungsorientierte Projekt SUN-AREA zeichnet sich durch die Nutzung ausschließlich vorhandene Daten (Höhe = Laserscandaten, Lage = Automatisierte Liegenschaftskarte) aus und stellt damit ein Glied der Wertschöpfungskette zur wirtschaftlichen Nutzung vorhandener Fernerkundungsdaten dar.

4. DIE METHODE

4.1 Datengrundlage

Ausgangsdaten zur Berechnung des Solarenergiepotentials sind die mit einem x, y und z Wert versehenen Daten des Digitalen Oberflächenmodells (im Folgenden DOM genannt) für das Stadtgebiet Osnabrück.

Die Gebäudegrundrissflächen aus der ALK dienen als Auswahl-polygone (siehe Abb. 3). Die Selektion der DOM-Daten innerhalb des Gebäudegrundrisses führt zu einer erheblichen Reduzierung der Datenmenge.

Abbildung 2 DOM-Laserscandaten innerhalb der Gebäudegrundrisse

4.2 Datenqualität

Der Hersteller der Laserscannerdaten gibt die technischen Daten des Airborne Laser Scanning Verfahrens wie folgt an:

- RIEGL LMS-Q560
- Befliegung 12. und13.Juli 2005
- auf 120 km² 630 Mio. Rohpunkte
- ca. 4 - 5 Punkte pro m²
- Höhengenauigkeit: 5 – 7 cm
- Lagegenauigkeit: 2 – 15 cm

Die Messpunktmenge pro Quadratmeter von 4 Punkten reicht aus um die Dachneigung und Dachausrichtung verlässlich zu berechnen. Bei den 70.000 Dächern der Modellstadt Osnabrück ergab sich jedoch bei 6% der Dächer eine deutlich geringere Messpunktdichte, von unter 0,75 Messpunkte pro Quadratmeter, die nicht genügen um die Standortfaktoren ausreichend genau zu berechnen.

Das extremste Beispiel ist in nachfolgender Grafik abgedruckt. Bei einem Dach von 200m² wurden nur 9 Messpunkte registriert.

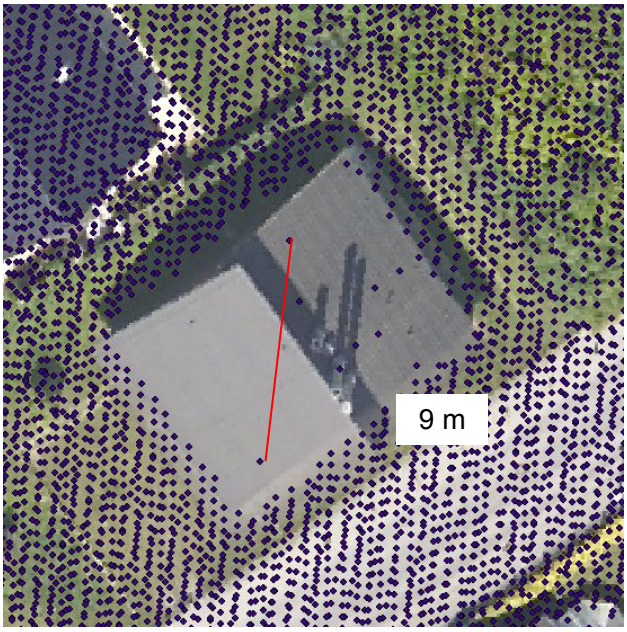

Abbildung 3Laserscandaten mit großen Datenlücken

Die Gleichmäßigkeit der Messpunkte über dem Gelände und dem Nachbargebäude weisen die volle Funktionsfähigkeit des Lasers nach.

Nach einer Klassifizierung der betroffenen Gebäude und demVergleich mit den Luftbildern wurde deutlich, dass der Grund für die fehlende Laserreflexion in einer ungünstigen Verkettung von Dachfarbe, Dachmaterial und dem Winkel zwischen Dachneigung und Flugrichtung zu suchen ist.

4.3 Das Regelwertk

SUN-AREA erarbeitet ein Regelwerk zur Beurteilung der Dachform, –neigung, -ausrichtung, -größe und -verschattung und leitet daraus einerseits das Solarenergiepotential einer großen Region ab und stellt andererseits ganz konkret dar, welche Fläche eines Gebäudes sich für die effiziente Nutzung der Sonnenenergie eignen. Dies geschiet durch die Implementierung vorhandener Algorithmen, die Integration von Standard-GIS-Funktionen und die damit einhergehende Verschneidung der Laserscannerdaten mit Grundrissdaten.

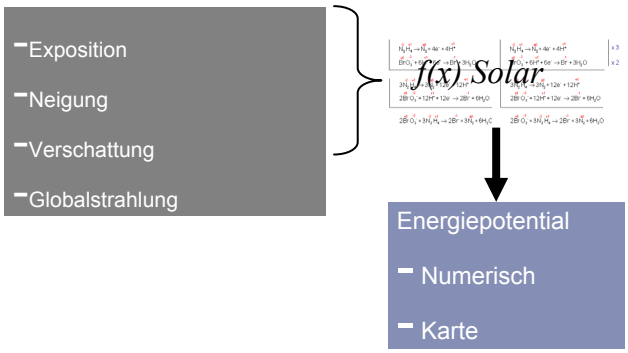

Die Ermittlung des Solarenergiepotentials über die modellierung der Algorithmenkette eird ausschließlich über ein Rastermodell erreicht.

Bewusst wird auf eine Flächenmodellierung über die Laserscandaten verzichtet. Verfahren zur 3D-Gebäudemodellierung aus hochauflösenden Laserscandaten wurden bisher nur halbautomatisch und sehr rechenintensiv umgesetzt. Diese sind für vollautomatische Berechnungen mit großen Datenmengen nicht einsetzbar (z.B. Schwalbe et al 2005, Steinle 2005, Hofmann 2005).

Exposition
Die Nutzung der Globalstrahlung ist abhängig von der Exposition. Optimal ist eine Ausrichtung nach Süden. Eine Dachfläche nach Osten oder Westen kann die Energie zu ca. 80% nutzen.

Die Exposition wird errechnet über die steilste Neigungsrichtung jeder Zelle gegenüber den Nachbarzellen. Abbildung 6 zeigt die Klassifizierung der Rohdaten des DOM hinsichtlich der Exposition in acht Klassen. Zur weiteren Berechnung des relativen Anteils an der Solarstrahlung wurde allerdings eine Reklassifizierung der Expositionswerte in 20 Klassen vorgenommen.

Neigung
Das Optimum der Dachneigung liegt bei ca. 30° – 45°. Eine Abweichung bis hin zu einem Flachdach oder zu einem 70° bewirkt eine Ertragsminimierung von bis zu 20 %

Die Neigung wird für jede Zelle des DOM-Rasters bestimmt und berechnet. sich aus der maximalen Höhenänderungsrate in jeder Zelle im Vergleich zu ihren acht benachbarten Zellen.
Die Abbildung zeigt die Klassifizierung der Rohdaten des DOM hinsichtlich ihrer Neigung in sieben Klassen.

Ausrichtungs und Neigungsmatrix
Die Standortnachteile aus Neigung und Ausrichtung münden in einen Faktor. Dieser ist aus der nachfolgenden Grafik ablesbar und zeigt den prozentualen Abschlag aufgrund der Standortbedingungen:

				West		Süd-west		Süd		Süd-ost		Ost		
			>90	70-90	50-70	30-50	10-30	-10-10	10-30	30-50	50-70	70-90	90 - 110	>110
		1	12	11	10	9	8	7	6	5	4	3	2	1
				210	195	180	165	150	135	120	105	90		
Neigung	Neigungs-wert	280 - 360	270 - 280	250 - 270	230 - 250	210 - 230	190 - 210	170 – 190	170 - 150	150 - 130	130 - 110	110 - 90	90 - 70	<70
0-10	0°	85	85	85	85	85	85	85	85	85	85	85	85	85
10-20	10		80	85	85	90	95	95	95	90	85	85	80	
20 - 30	20°		75	80	85	95	95	100	95	95	85	80	75	
30 - 40	30°		75	80	85	95	100	100	100	95	85	80	75	
40 - 50	40°			75	85	95	100	100	100	95	85	75		
50 - 60	50°				80	90	95	95	95	90	80			
60 - 70	60°				75	85	90	90	90	85	75			
70 - 80	70					75	80	80	80	75				
80 - 90	80							75						

Abbildung 4 Matrix der Standortfaktoren

Verschattungsanalyse
Zur Ermittlung der jährlichen Strahlungsbilanz in den definierten Zeitintervallen wird jede Dachteilfläche auf ihre direkte Sonneneinstrahlung hin analysieren, dabei fließen ebenfalls metrologische Parameter ein. Für die Berechnung lassen sich Verfahren aus dem Bereich der 3D-Grafik verwenden. Die direkte Sonneneinstrahlung wird aus der Winkeldifferenz zwischen einfallendem Licht und dem Polygonnormal der Dachteil- oder Geländefläche errechnet. Zur Ermittlung der diffusen, schattigen Bereiche wird die Polygonfläche gerastert. Für jede Zelle wird dann geprüft, ob ein Strahl zur Sonne das DOM (Digitales Oberflächenmodell) oder das DGM (Digitales Geländemodell) schneidet
(siehe Abb. 5)

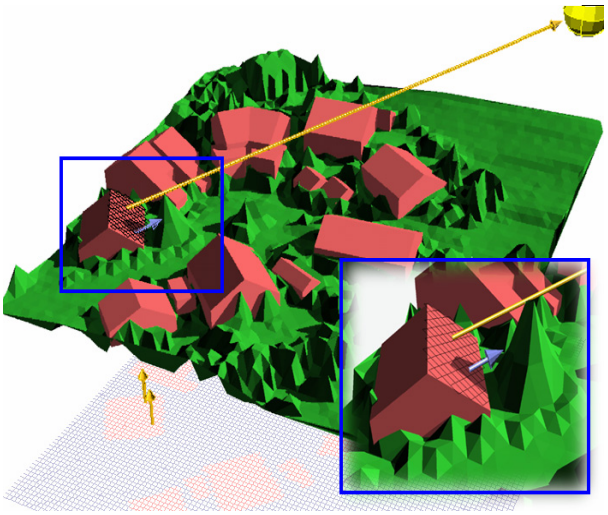

Abbildung 5 Modellierung der Verschattung mit Laserscandaten

4.4 Berechnung des Solarenergiepotentials

Zur Berechnung des mittleren jährlichen Solarenergiepotentials in kWh/a wird folgende Formel zugrunde gelegt:

$$Y = \eta \cdot F \cdot H \cdot f$$

η = Anlagenwirkungsgrad
F = Fläche der Anlage in [m²]
H = lokaler Globalstrahlungsenergie/a
F = Korrekturfaktor Neigung/Ausrichtung

5. DAS ERGEBNIS

Die SUN-AREA Methode würde für gesamt Osnabrück angewandt. Das Untersuchungsgebiet ist 120km² groß und umfasst ca. 70.000 Dächer.

Bei einer anfänglichen Mindestgröße von 10m² liefert die Flächenstatistik für Osnabrück ein Potential von geeigneten Flächen von 224ha. Die nachfolgende Tabelle zeigt, wie groß diese im einzelnen sind und wie gut diese geeignet sind.

	Unter 100m²	100-500m²	über 500 m²
Geeignet	12 ha	0,8 ha	-
Gut geeignet	82 ha	40 ha	36 ha
Sehr gut geeignet	48 ha	5 ha	0,16 ha

Die nachfolgende Grafik zeigt das Potential im Vergleich zum Bedarf. Sie zeigt, dass 118% des privaten Strombedarfs aus PV gewonnen werden könnten. 2006 lag Osnabrück bei 0,3%.

	Ertrag	**Bedarf 06** Privathaushalte (233.000 MWh/a)	**Bedarf 06** Gesamtstrom (1.188.000 MWh/a)
Solarstrom Potential	277.000 MWh/a	**118%**	**23%**
Solarstrom Bestand 06	746 MWh/a	**0,3%**	**0,06%**

6. DIE DARSTELLUNG

In Osnabrück kann frei zugänglich, basierend auf der ArcIMS-Technologie, das Solarenergiepotenzial für jede Dachfläche vom Web-Server über einen Standard-Web-Browser auf den Online-Seiten der Stadt Osnabrück unter http://geodaten.osnabrueck.de/website/SunArea/viewer.htm in Form einer digitalen Karte abgerufenen werden. Über den Web-Server per HTTP-Protokoll kommunizieren der clientseitige Browser und der Map Server miteinander. Technisch handelt es sich hier um den Internet Information Server (IIS) mit Apache Tomcat Servlet. Der Internetnutzer stellt eine Anfrage über den Browser an den Karten-Server. Dieser liefert die entsprechende Antwort, d.h. den angeforderten Kartenausschnitt zurück.

Über die Web-Site der Stadt Osnabrück kann der Internet-Nutzer verschiedene Anfragen an das System richten. Basierend auf Active Server Pages (ASP) können Nutzer durch die interaktive Adresssuche direkt Gebäudeanfragen an den ArcIMS senden. In dem dynamisch generierten Kartenausschnitt wird die gesuchte Adresse zentral dargestellt. Parallel werden die entsprechenden Ergebnisse zur Solareignung angezeigt. Die ASP-Scripte greifen auf eine zentrale Adress-Datenbank zu, welche mit der SUN-AREA-Datenbank verknüpft ist. Die entsprechenden Ergebnisse der Solarpotenzialanlayse kann somit in Abhängigkeit der Adresseingabe angezeigt werden.

Der HTML-Browser bietet hier eine sehr gute Performance und Skalierbarkeit. Die Geodatengrundlage liefert das kommunale Rauminformationsystem (RIS) der Stadt Osnabrück. Es handelt sich hier, um einen zentralen Datenserver, basierend auf der ESRI ArcSDE, der für die Bereitstellung der Geodateninfrastruktur zuständig ist.

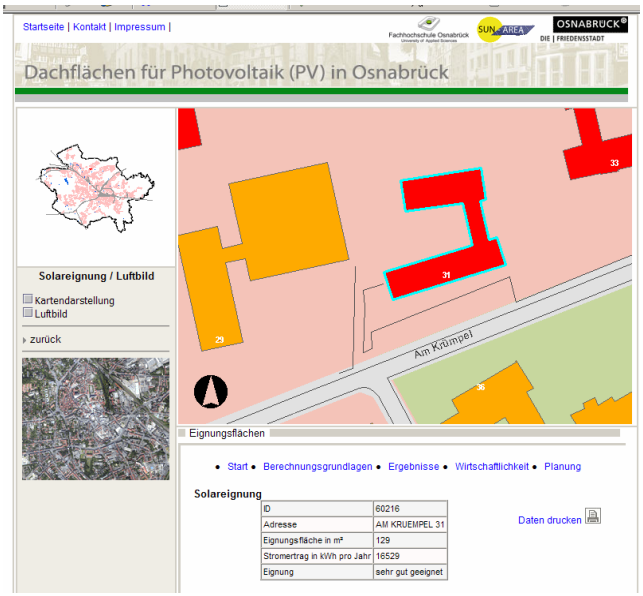

7. AUSBLICK

Mit hohem, finanziellem Aufwand werden Laserscandaten für große Bereiche der Bundesrepublik aufgenommen. Eine Nutzung der Daten in der hohen Aufnahmegenauigkeit findet bisher kaum statt. Gerade für flächendeckende Umweltsimulationen großer Gebiete liefern hochauflösende Laserscandaten eine viel versprechende Basis. Die bisher über SUN-AREA ermittelten Ergebnisse liefern den Beweis.
Die „einfache“ Analyse der bisher untersuchten Standortparameter über ein Rastermodell liefert sehr genaue und vor allem vollautomatische Ergebnisse.

Weitere mögliche Einsatzbereiche sind z.B.

- Modellierung der großflächigen Kaltluftabflussströmung
- Modellierung von Schallausbreitungsmodellen
- Überflutungsmodellierung
- Sichtanalysen
- Modellierung von Neigungsverhältnissen
- Landschaftsmonitoring
- Monitoring von großflächigen Setzungen und Landschaftsveränderungen
- Selektion von Dächern mit Dachlawinengefahr
- Nutzen für Baugenehmigungsbehörden
- Darstellen nicht genehmigter Gebäudeteile

Der volkswirtschaftliche Nutzen der Laserscandaten ist enorm
Die Geoinformatik liefert uns das Werkzeug.
Wir müssen lediglich die Bewertungsmodelle generieren

8. LITERATUR

Schwalbe, E., Maas, H.-G., Seidel, F. (2005): 3D Building Models Generation From Airborne Laser Scanner Data Using 2D GIS Data and Orthogonal Point Claud Projections, Tchnische Universität Dresden

Steinle, E. (2005): Gebäudemodellierung und änderungserkennung aus multitemporalen Laserscanningdaten Dissertation, DRK Reihe C, 594.

Klärle, M., Ludwig, D. (2005) Einsatz von Flugzeugscanner-Daten für die Standortoptimierung erneuerbaren Energien, AGIT-Fachtagung Salzburg, Wichmann Verlag

Hofmann, A. D. (2005): An Approach To 3D Building Model Reconstruction from Airborne Laser Scanner Data Using Parameter Space Analysis and Fusion of Primitives. Dissertation, Technische Universität Dresden, Fakultät Forst-GEO- Und Hydrowissneschaften, Institut für Photogrammetrie und Fernerkundung

Schuster, H-F., Weidner Uwe, (2003) A nes Aproach Towards Quantitative Quality Evalutation of 3D Building Models

Klärle M., Ludwig D. (2006) Standortanalyse für Photovoltaik-Anlagen durch hochauflösende Sensoren in der Fernerkundung – Forschungsprojekt an der Fachhochschule Osnabrück – AK Fernerkundung IGF Osnabrück

THE DEVELOPMENT OF THE EHLERS FUSION

S. Klonus & P. Rosso

Institute for Geoinformatics and Remote Sensing (IGF), Universität Osnabrück, 49069 Osnabrück, Germany – (sklonus, prosso)@igf.uni-osnabrueck.de

KEY WORDS: Ehlers Fusion, TerraSAR-X, Color Preservation, Evaluation, Pansharpening

ABSTRACT:

Image fusion is a technique that combines the spatial structure of a high resolution panchromatic image with the spectral information of a low resolution multispectral image to produce a high resolution multispectral image. Image fusion can be classified into three levels: pixel level (iconic), feature level (symbolic) and knowledge or decision level (Pohl and van Genderen, 1998). The Ehlers fusion is an iconic image fusion technique and was developed in 2004. The Ehlers fusion is a spectral characteristic preserving fusion method. In this paper the development and the performance of the Ehlers fusion is shown using image data of a radar satellite to improve a multispectral Quickbird image. The results demonstrate that it is possible to use the Ehlers fusion to enhance optical multispectral data with TerraSAR-X data.

1. INTRODUCTION

Several definitions for data fusion can be found in the literature. Data fusion exists in different forms in different scientific disciplines. The remote sensing community defines data fusion as "… a formal framework in which are expressed means and tools for the alliance of data originating from different sources. It aims at obtaining information of greater quality; the exact definition of greater quality will depend upon the application" (Wald 1999). Image fusion forms a subgroup within this definition, with the objective to generate a single image from multiple image data for the extraction of information of higher quality (Pohl 1999). Image fusion can be classified into three levels: pixel level (iconic), feature level (symbolic) and knowledge or decision level (Pohl and van Genderen, 1998). The Ehlers fusion is an iconic image fusion technique, hence the focus are on these methods.

Iconic image fusion is a technique that combines the spatial structure of a high resolution panchromatic image with the spectral information of a low resolution multispectral image to produce a high resolution multispectral image.

The Ehlers fusion is named after Prof. Dr.-Ing Manfred Ehlers. Ehlers received his diploma in mathematics and physics (as minor field) of study in 1970. In 1983 he completed his doctoral thesis in remote sensing with the issue "Research in digital correlation algorithms to rectify remote sensing data" (Ehlers 1983). He obtained his postdoctoral lecture qualification in digital image processing and remote sensing (Ehlers 1987) in Hannover, year 1987.

Research on image fusion techniques is a central topic of many projects of Prof. Ehlers. Already in 1987, the first paper on merging SPOT panchromatic and Landsat TM multispectral data was published during Ehlers' stay at the University of Georgia, USA (Welch & Ehlers 1987). Further studies included merging of multispectral scanner and radar data as well as the analysis of fused data sets for cartographic feature extraction and visual interpretation (Welch & Ehlers 1988, Ehlers 1991). Other research included error modeling of merged remote sensing datasets (Shi & Ehlers 1996) and fusion of hyperspectral and panchromatic/ multispectral scanner data (Greiwe et al. 2004).

2. STUDY AREA AND DATASETS

The study area is located in Egypt and shows the area around the pyramids of Gizeh. The TerraSAR-X image (fig. 1) of this area was provided by the DLR (German Aerospace Centre). TerraSAR-X is the first non-military RADAR satellite which provides data with a ground resolution of 1 m. The image is recorded in high resolution spot mode (1 m ground resolution), on the 29th November 2007. The multispectral Quickbird image (fig. 2) is recorded on the 2nd February 2002, available with a ground resolution of 2,40 m. To demonstrate the effects of spatial improvement in the fused image, the Quickbird multispectral image is degraded by a factor of 3, from a ground resolution of 2,40 m to 7,20 m. The degraded Quickbird image is resampled to the spatial resolution of the TerraSAR-X image.

Before the fusion is performed the speckle from the TerraSAR-X image is removed through the use of different despeckle filters implemented in standard image processing software. After some statistical and visual assessment, a median filter with a window size of 7x7 was used for despeckling.

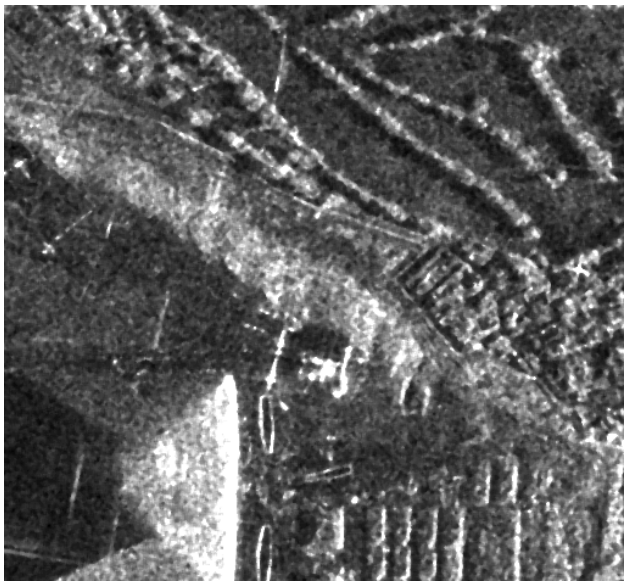

Figure 1: TerraSAR-X image of Gizeh recorded in high resolution spot mode. Recording date: 29th November 2007 ©DLR (2007)

Figure 2: Multispectral Quickbird image recorded on the 2nd February 2002, degraded to 7.20 m, the displayed band is the near infrared.

3. EHLERS FUSION

During his DFG funded sabbatical year at the University of Georgia/USA, Prof. Ehlers conducted research on data fusion issues within his project "Integrated Analysis of GIS and remote sensing data for the management of coastal areas". First results of the Ehlers fusion were published at the ISPRS congress in Istanbul (Ehlers et al. 2004b), the SPIE "Conference on Remote Sensing for Environmental Monitoring, GIS Applications and Geology IV" (Ehlers 2004b), the "10th Annual Conference on Control with Remote Sensing of Area-based Subsidies" (Ehlers 2004a) and the Remote Sensing and GIS conference at the University of Göttingen (Ehlers et al. 2004a).

The main idea behind a spectral characteristic preserving image fusion is that the high resolution image has to sharpen the multispectral image without adding new gray level information to its spectral components. An ideal fusion algorithm should enhance high frequency changes such as edges and gray level changes in an image without altering the multispectral components in homogeneous regions. To achieve these requirements, color and spatial information need to be separated.
The Ehlers fusion was presented first in Ehlers and Klonus (2004). For optimal color separation, an IHS transform is carried out. This technique is extended to include more than 3 bands by using multiple IHS transforms until the number of bands is exhausted. Klonus (2005) showed that there is only a slight dependency on the selection or order of bands for the IHS transform. A subsequent Fourier transform of the intensity component and the panchromatic image allows an adaptive filter design in the frequency domain. The power spectrum of the Fourier transform provides the information about the distribution of image content along the spatial frequency axes, thus allowing the design of filters that are adapted to the image contents (see Figures 5 and 6). Using Fourier transform techniques, the spatial components to be enhanced or suppressed can be directly accessed (Ehlers et al. 1984). An overview flowchart of the method is given in Fig. 3.

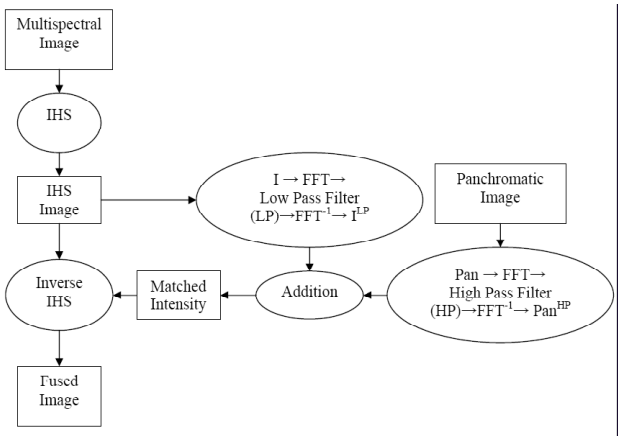

Figure 3: Overview flowchart of the Ehlers Fusion

The first step is the transformation of the multispectral image into an Intensity-Hue-Saturation (IHS) image, which works with three bands at each step. To demonstrate the procedure a Quickbird image (fig. 2) is used. Fig. 4 shows the intensity component of the transformed bands. The image is resampled to the ground sampling distance of the TerraSAR-X image (fig. 1), which is used for the fusion process. As resampling algorithm, a cubic convolution interpolation is used because it approximates the theoretically best interpolation function in the spatial domain (Richards and Jia 1999).

The next step is to fit the gray value range of the high resolution image to the intensity component of the IHS image. The intensity component is usually measured in values ranging from 0 to 1, whereas the gray values for the high resolution image vary normally between 0 and 65536, depending of the radiometric resolution of the sensor. Therefore, the panchromatic image is normalized by fitting it to the range from 0 to 1. To achieve this normalization several methods are applied. In the past the high resolution image was simply divided by the maximum in the image (Ehlers & Klonus 2004).

Currently there are two other methods for the normalization. The first is a histogram match of the high resolution image to the intensity image of the IHS image. To apply the second method the mean value of the image is subtracted from the maximum value and the result is divided by two. After this, the mean value is added again to the result. To create the normalized image the high resolution image is divided by the result of this calculation. This method was chosen to eliminate gray value outliers that can appear in the image.

Figure 3: Intensity component of the IHS image

After this, the high resolution image and the intensity component are transformed into the spectral domain using a two-dimensional Fast Fourier Transform (FFT). For the design of the appropriate low pass filter for the intensity component and the corresponding high pass filter for the panchromatic image the power spectra of both images (fig. 5 and fig. 6) are used (Gonzalez and Woods 2002).

The ratio of spatial resolution between the TerraSAR-X image and the degraded multispectral Quickbird image is 1:7.2. Based on this ratio and an image size of 1132 x 1117 pixel, it can be calculated that for the intensity component all information in the frequency spectrum above a frequency of 157 (1132 / 7.2) for the Quickbird intensity can be regarded as artificial. The higher frequencies represent artifacts that are caused by the resampling process of the multispectral image to the pixel size of the panchromatic image. Consequently, a low pass filter at a cutoff frequency above 157 would not change the image information content. In addition, the filter design depends on the spatial strength of the image content and the size of the geo objects to be enhanced. Ideally, the low pass filter for the intensity component of the resampled multispectral image should be inverse to the high pass filter for the enhancement of edges in the panchromatic image. During the test phase of our algorithm, however, it proved to be advantageous to define the cutoff frequencies independent from each other (Ehlers and Klonus 2004).

The final filter design is adapted to the image content and the desired application. For example, a homogeneous image (e.g. rural structure) requires a cutoff frequency shifted to the higher values, i.e. a stronger high pass filter. Otherwise, small differences within homogeneous areas will be enhanced and that might introduce a change in the spectral characteristics. For a heterogeneous region (e.g. urban structure) the color changes are suppressed by a strong power signal in the high-frequency domain. Here, an enhancement of the urban structure might be desired, which makes it necessary to move the cutoff frequency to the left, e.g. the lower frequency part of the spectrum. Although the size of buildings and streets are usually known and can be used to define the cutoff frequency, some interaction for optimum filter design is usually required. Generally, the cutoff frequency is calculated from the resolution ratio between the multispectral and the panchromatic image. (Klonus 2005). This fusion method and the automated calculation of the respective filters are implemented in the Erdas Imagine Version 9.1 and in Matlab.

To avoid the Gibb's effect (gray value oscillations) in the spatial domain after an inverse FFT typical filter masks such as a Hanning or Gaussian window to smooth the filter functions are used. Filtering with an ideal filter, however, has the disadvantage that it creates artifacts. Practical tests with varying filter widths and masks show best results with a low pass Hanning window filter and a cut-off frequency of $\omega n = 157$. Ideally the filters should be complementary, so that the frequency bands which are kept by the low pass filter should be the ones that are suppressed by the high pass filter. However, in practice an overlap is accepted, because of the smoothing effects of the filter masks. Therefore the high resolution image was filtered with a high pass Hanning window filter and a cut-off frequency $\omega n = 157$ to avoid the inclusion of too much information from the panchromatic image. The filtered power spectra are presented in fig. 7 and fig. 8. A Hanning window function is used to avoid oscillations in the spatial domain.

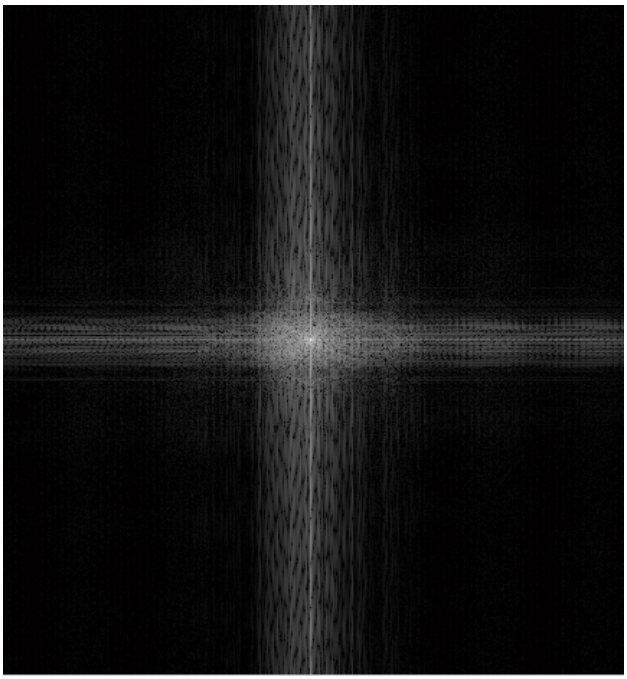

Figure 5: Intensity spectrum. The zero frequency which corresponds to the mean gray value is in the center of the image

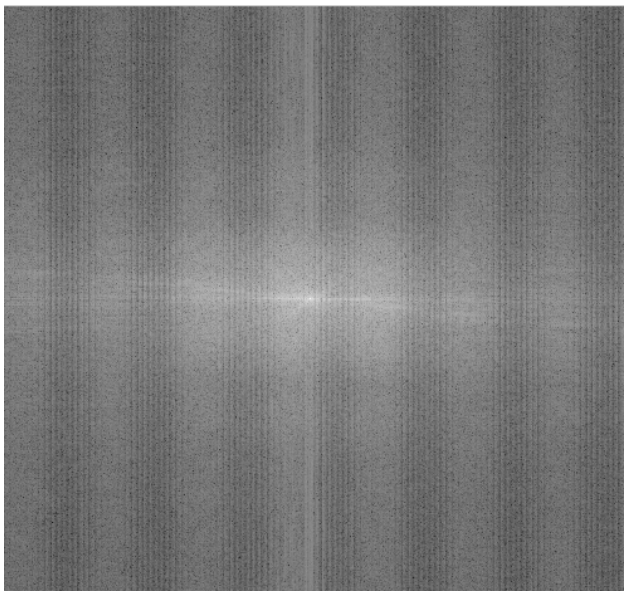

Figure 6: Intensity spectrum of the TerraSAR-X image

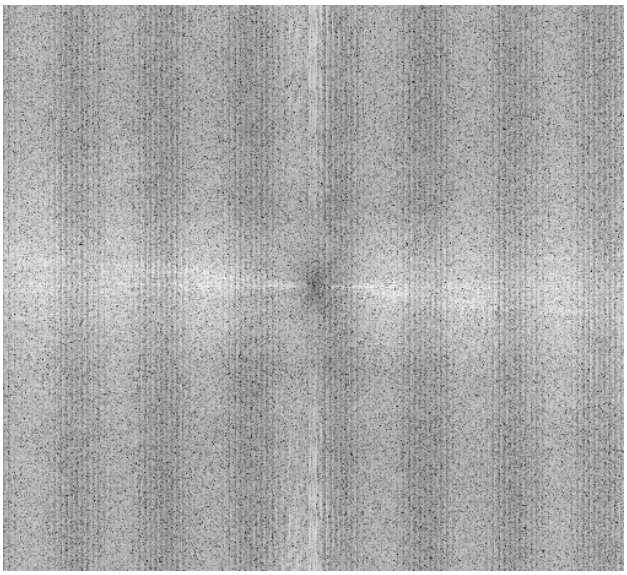

Figure 8: TerraSAR-X spectrum after high pass filtering in the frequency domain (Hanning filter with a cut-off frequency ωn = 157)

After filtering, the images are transformed back into the spatial domain with an inverse FFT where the effects of the filtering are clearly visible (Fig. 9 and 10). The actual low pass filtering of the intensity component showed very little difference with the original (Fig. 3) which confirms the statement that most of the high frequency information is related to artifacts of the resampling process. It has to be noted that the high pass filtered high resolution image has been contrast stretched for display purposes.

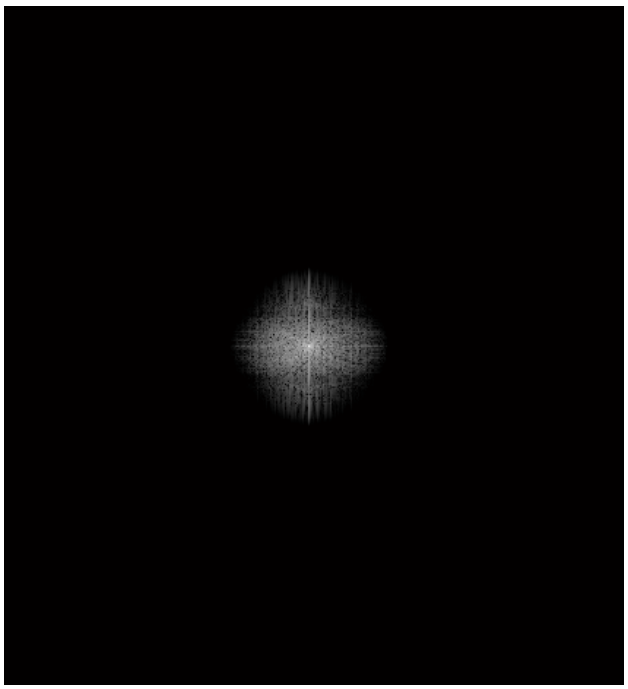

Figure 7: Quickbird intensity spectrum after low pass filtering in the frequency domain (Hanning filter with a cut-off frequency $\omega_n = 130$)

The two images are added together to form a fused intensity component with the low frequency information from the low resolution multispectral image and the high frequency information from the high resolution image. To control for the impact of the high resolution image, additional weights on this image could be applied for improved results. The fused image is histogram matched to the original intensity component to map the fused image into the spectral range of the original image. This new intensity component and the original hue and saturation components of the multispectral image form a new IHS image.

Figure 9: High pass filtered TerraSAR-X image after an inverse FFT

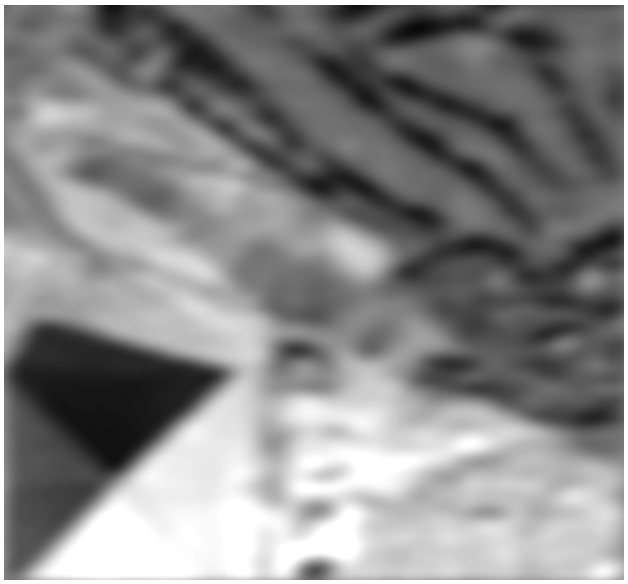

Figure 10: Low pass filtered intensity component of the Quickbird image after an inverse FFT

An inverse IHS transformation was finally performed to produce a fused RGB image (fig. 11) that contains the spatial resolution of the panchromatic image and the spectral characteristics of the multispectral image. These steps can be repeated with successive 3-band selections until all bands are fused with the panchromatic image. The order of bands and the inclusion of spectral bands for more than one IHS transform is not critical because of the color preservation of the procedure. The multispectral layers are registered to form one multispectral image, which contains the same number of bands as the original image (Klonus & Ehlers 2007).

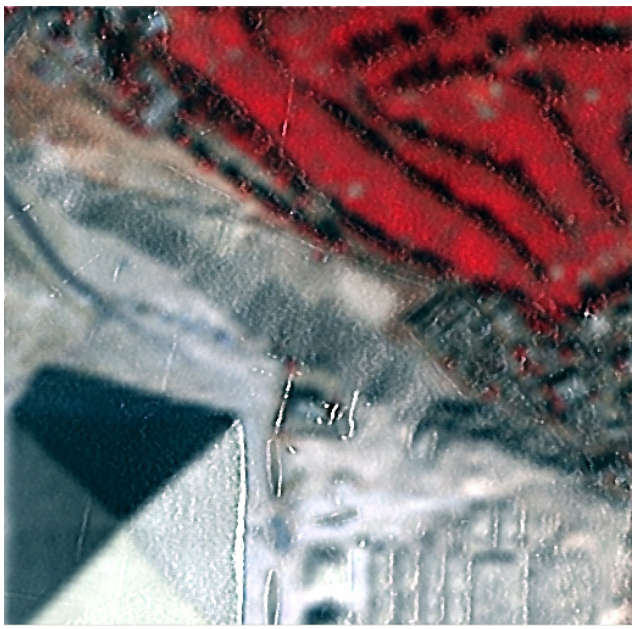

Figure 11: Fused Quickbird image in the near infrared band

Many publications have focused on how to fuse high resolution panchromatic images with lower resolution multispectral data to obtain high resolution multispectral imagery while retaining the spectral characteristics of the multispectral data (see, for example Welche & Ehlers 1987, Ehlers 1991, Klonus 2005). It was evident that the methods employed seem to work well for many applications, especially for single-sensor single-date fusion. Most methods, however, showed significant color distortions for multitemporal and multisensoral case studies (Klonus 2006). The Ehlers fusion technique was designed to overcome these problems and has already proven its superiority over the standard pan sharpening techniques such as IHS, PC, Brovey and multiplicative fusion methods (Klonus 2006), and more advanced methods (Klonus & Ehlers 2007), such as color normalized spectral sharpening, the Gram Schmidt spectral sharpening, UNB fusion and the modified IHS. The combination of IHS and wavelet transforms is somewhat similar to the Ehlers fusion with the wavelet transform replacing the Fourier filter analysis. It is, however, limited with respect to the flexibility of the filter design, which is the real advantage of the employed algorithm. Results from a predecessor of the Ehlers fusion (with less flexibility) indicate a slight superiority over the combination of IHS and wavelet transforms for image fusion (Ling et al. 2006). Wavelet based fusion (without IHS) shows serious deficiencies with respect to the spatial improvement (Klonus 2006) and thus, was not included in our analyses.

In addition, the Ehlers fusion could improve Computer aided photo interpretation (Klonus et al. 2006)It is already used by the European Union for the monitoring of agriculture with remote sensing.

4. CONCLUSIONS

The results demonstrate that it is possible to use the Ehlers fusion to enhance optical multispectral data with TerraSAR-X data. Future work will consider the impact of fusion on a classification of the fused images in comparison with the original image. Especially the impact of the differences in the per-pixel deviation has to be investigated. Also to be considered in future work is a combined method for a quantitative assessment of spatial improvement and spectral preservation, because otherwise the best color preservation is observed if no pansharpening is performed, which makes the fusion obsolete.

5. ACKNOWLEDGEMENTS

The TerraSAR-X project is supported by the German BMWI through the DLR with the contract number 50EE0704.

6. REFERENCES

Ehlers, M., 1983. Untersuchung von digitalen Korrelationsverfahren zur Entzerrung von Fernerkundungsaufnahmen. *Wissenschaftliche Arbeiten der Fachrichtung Vermessungswesen der Universität Hannover*, Nr. 121, Dissertation, 248 pp.

Ehlers, M., 1987. Integrative Auswertung von digitalen Bilddaten aus der Satellitenphotogrammetrie und -Fernerkundung im Rahmen von Geographischen Informationssystemen. *Wissenschaftliche Arbeiten der Fachrichtung Vermessungswesen der Universität Hannover*, Nr. 149, Habilitation, 139 pp.

Ehlers, M., 1991. Multisensor image fusion techniques in remote sensing. *ISPRS Journal of Photogrammetry and Remote Sensing* 46(1), pp. 19–30.

Ehlers, M., 2004a. Image Fusion without changes in spectral characteristics: FFT based filtering and IHS transform. P*roceedings of the 10th Annual Conference on Control with Remote Sensing of Area-based Subsidies*, Budapest, Hungary, pp. 279-291.

Ehlers, M., 2004b. Spectral characteristics preserving image fusion based on Fourier domain filtering. In: Ehlers, M., F. Posa, H.J. Kaufmann, U. Michel and G. De Carolis (Eds.) Remote Sensing for Environmental Monitoring, GIS Applications, and Geology IV, *Proceedings of SPIE* Vol. 5574, Bellingham, WA, pp 1-13.

Ehlers, M. and S. Klonus, 2004. Erhalt der spektralen Charakteristika bei der Bildfusion durch FFT basierte Filterung, *Photogrammetrie-Fernerkundung-Geoinformation* (PFG) 6/2004, pp. 495-506.

Ehlers, M., E. Dennert-Möller, D. Kolouch, and P. Lohmann, 1984. Non-recursive filter techniques in digital processing of remote sensing data. *Proceedings of the XVth international Congress of ISPRS*, Rio de Janeiro, Brazil, IAPRS XXV/A7, 163 – 175.

Ehlers, M., S. Klonus, C. Aden, H. Bast, T. Buchholz, T. Kreutzer and L. Loesewitz, 2004a. IHS Transform revisited: spectral characteristics preserving data fusion based on Fourier Domain Filtering. *Proceedings, 1st Göttingen GIS and Remote Sensing Days 'Environmental Studies'*, Göttingen (accepted for publication)

Ehlers, M., R.Welch and Y. Lin, 2004b. GIS and Context Based Image Enhancement. *Proceedings of the XXth International Congress of ISPRS*, Istanbul, Turkey, IAPRS XXXV/B4, pp. 397-402.

Gonzalez, R.C. and R.E. Woods, 2002. *Digital image processing*, 2nd Edition, Prentice-Hall, Upper saddle River, NJ, USA.

Greiwe, A., M. Bochow and M. Ehlers, 2004. Fusion of multisensor remote sensing data for urban land cover classification. In: Ehlers, M. (Ed.) Remote Sensing for Environmental Monitoring, GIS Applications, and Geology III, *Proceedings of SPIE* Vol. 5239, Bellingham, WA, pp. 306-313.

Klonus, S., 2005. *Untersuchungen zu Datenfusionsverfahren in der Fernerkundung Diplomarbeit*. Hochschule Vechta (Universität) (unpublished).

Klonus, S., 2006. *Technical report – Image fusion techniques*. European Commission, Joint Research Center, Ispra, Institute for the Protection and the Security of the Citizen, Agriculture and Fisheries Unit.

Klonus, S., F. G. Ibáñez and P. J. Åstrand, 2006. Improving CAPI through spectral characteristics preserving image fusion. *Presentation on the Geographical Information in Support of the CAP Toulouse* (France) 27th - 29th November 2006.

Klonus, S. and M. Ehlers, 2007. Image fusion using the Ehlers spectral characteristics preserving algorithm. *GIScience and Remote Sensing*, 44, No. 2, pp. 93–116.

Pohl C, 1999. Tools and methods for fusion of images of different spatial resolution. *International Archives of Photogrammetry and Remote Sensing*, Vol. 32, Part 7-4-3 W6, Valladolid, Spain.

Pohl C & J L van Genderen, 1998. Multisensor image fusion in remote sensing: concepts, methods and applications. *International Journal of Remote Sensing*, vol. 19, 823–854.

Ling, Y., Ehlers M., Usery L. and M. Madden, 2006. FFT-Enhance IHS transform method for fusing high-resolution Satellite Images. *ISPRS Journal of Photogrammetry and Remote Sensing* Inc. Vol. 61, issue 6, p. 381-392.

Richards, J.A. and X. Jia, 1999. *Remote sensing digital image analysis*. 3rd edition, Springer Verlag Berlin Heidelberg New York, 363 pp.

Shi, W. and M. Ehlers, 1996. Determining uncertainties and their propagation in classified remotely-sensed image-based dynamic change detection. *International Journal of Remote Sensing* , Vol. 17, No. 14, 2729-2741.

Wald L, 1999. Some terms of reference in data fusion. *IEEE Transactions on Geoscience and Remote Sensing*, 37, 1190–1193.

Welch, R. and M. Ehlers, 1987. Merging multiresolution SPOT HRV and Landsat TM data. *Photogrammetric Engineering and Remote Sensing*, 53, pp. 301–303.

Welch, R. and M. Ehlers, 1988. Cartographic feature extraction from integrated SIR-B and Landsat TM images. *International Journal of Remote Sensing*, 9, 873-889.

Wie wird man ein Geoinformatiker?
Beitrag zum 60. Geburtstag von Manfred Ehlers

Gottfried Konecny

1. Einleitung

Es mag zwar vermessen sein, wenn ein knapp 78-Jähriger einen 60-Jährigen einen fachlichen Geburtstagsbeitrag liefert. Aber das Vermessen(sein) ist ja Sache eines Geodäten, der sich mit Geoinformatik und Geoinformation befasst.

Manfred Ehlers ist als Mathematiker den anderen Weg in diese Disziplin gegangen. Wir brauchen beide Mathematik bei der Anwendung der Geoinformation. Wir sind beide in einer günstigen Zeit für die Entwicklung des Geoinformationswesens geboren, der eine früher, der andere etwas später:

Konrad Zuse hat den ersten funktionsfähigen Elektronenrechner, die Z3, im Jahre 1941 in Deutschland fertiggestellt und Howard Hathaway Aiken hat unabhängig davon im Jahre 2944 die Mark I in den USA zum Laufen gebracht.

Schon 1956 durfte ich an der Ohio State University auf der IBM 650 das Programmieren in Maschinensprache lernen und später in München auf der Zuse Z23 und noch später an der University of New Brunswick auf der Royal MacBee LGP30 die ersten photogrammetrischen Anwendungen machen. Aber die Leistungsfähigkeit von Computern begriff ich erst während meines Sabbaticals auf den Univacs der NASA. Kein Wunder also, dass ich mich in New Brunswick und ab 18971 in Hannover für den ersten photogrammetrischen Analytischen Plotter interessierte.
Bei einem Besuch von MIT im Jahre 1963 beeindruckte mich Miller mit seinen COGO- und DGM-Programmen und 1970 führte mir Tomlinson in Ottawa sein Canada Land Inventory System vor, das als erstes GIS bezeichnet wird.

Ich weiß´nicht, wie und wann Manfred Ehlers seine ersten Computererfahrungen machte, aber er kam als diplomierter Mathematiker im Jahre 1977 als Mitarbeiter des SFB 149 an unser Institut in Hannover. Zunächst arbeitete er mit Bernhard Wrobel zusammen, doch als dieser in Darmstadt einen Ruf annahm, promovierte und habilitierte sich Manfred Ehlers unter meiner Mitwirkung. Natürlich war es die digitale Bildverarbeitung in Fernerkundung und Photogrammetrie, die ihn besonders reizte. Durch unsere häufigen ISPRS-Kontakte mit den USA erhielt er bald ein Angebot dorthin, so dass er auch noch die Bezeichnung, erhielt, wie man damals sagte, Dr. i.A.g. (in Amerika gewesen). Er blieb 4 Jahre an der University of Georgia und weitere zwei Jahre an der University of Maine, das dem amerikanischen Förderprogramm des NCGIA angehörte. Diese sechs Jahre waren für ihn prägend, und sie verhalfen ihm zum Schritt zurück nach Europa, erst zwei Jahre beim ITC in Holland und dann an der Universität Osnabrück.

Im vermessungstechnisch orientierten Geoinformationswesen Deutschlands ist er dabei anerkennenswerte unkonventionelle Wege gegangen, in der Lehre und auch in der Gründung von GIN, welches die GIS-Anwendung in Deutschland nachhaltig gefördert hat.
Wie er es geschafft hat, mit den neuen fachlichen Entwicklungen in Lehre und Forschung fertig zu werden, das können seine Mitarbeiter besser beurteilen als ich. Hier darf ich nur den Zeitplan der markanten Entwicklungen aufführen:
Manfred Ehlers kam im Jahre 1990 nach Europa zurück, damals wurde gerade das Internet erfunden. 1991 gab es den ersten Webserver und das erste Mobilfunknet in Finnland. 1993 gab es den ersten PDA. 1995 wurde Java als Programmiersprache eingeführt und 1998 XML, sowie die Entwicklung von Web-Portalen. Schließlich folgte im Jahre 2005 Google Earth. Das Geoinformationswesen hat von all diesen Entwicklungen enorm profitiert.

Wenn man die 60 an Lebensjahren überschreitet oder wenn man gar das Ruhestandsalter von 65 oder 68 erreicht hat, dann will man keine Doktorarbeiten mehr schreiben, die einem eine Position verschaffen, oder Forschungsberichte, die einem einen guten Start bei Forschungsanträgen versprechen. Man möchte einen Beitrag dazu leisten ein Problem unserer Gesellschaft aus der Welt zu schaffen, mit all den Werkzeugen, mit denen man gelernt hat, umzugehen.

2. Das Tirana-Projekt

Ich hatte in den Jahren 2005 und 2006 Gelegenheit zur beratenden Tägigkeit eines kleinen von der Weltbank finanzierten Projekts in Albanien. Es ging um die rasche und kostengünstige Erstellung von Planungsunterlagen für die Stadt Tirana.

Was war das Problem? 1990 wurde in den Balkanstaaten offiziell der Sozialismus abgeschafft. Albanien hatte zwar ein türkisches Katastersystem aus der Zeit vor dem 1. Weltkrieg, welches bis 1945 unter italienischem Einfluss nachgeführt wurde. Ab 1945 wurden alle Ländereien verstaatlicht. Die Vermessung von Flurstücken und Gebäuden bekam eine untergeordnete Bedeutung. Die Datenbestände waren deshalb mit großen Fehlern behaftet, aber es waren wenigstens analoge Pläne vorhanden.

Im Jahre 1990 brach das System vollends zusammen, als die Katasterbehörde kurzfristig geschlossen wurde. Im Jahre 1992 erfolgte, unterstützt durch US Aid die Digitalisierung der alten Pläne. Mit Autocad konnten bei der Stadtverwaltung wenigstens die wichtigsten Veränderungen von Straßen nachgeführt werden. Allerdings war das keine Möglichkeit, die wilde Bebauung von bis zu 15stöckigen Wohnhäusern quer über die Katastergrenzen hinweg zu stoppen. Um die Stadtplanung wenigstens notdürftig zu ermöglichen, war die Erfassung der urbanen Infrastruktur vonnöten.

Im Jahre 1990 hatte Tirana etwa 300 000 Einwohner. Mit der Einführung der neuen demokratischen Freizügigkeit war ein sprunghaftes Anwachsen der Bevölkerungszahl verbunden. Im Jahre 2005 betrug die Einwohnerzahl von Tirana 600 000.

Wie bekommt eine solche Stadt rasch Planungsunterlagen? Zunächst wurde beschlossen, ein geographisches Informationssystem auf der Basis von ArcGIS einzurichten. Als Grundlage zur Datenerfassung diente ein nahezu senkrechtes Quickbird Satellitenbild vom Oktober 2004. Das Bild, welches 273 km^2 erfasste,

deckte das 60 km² große Stadtgebiet vollständig ab. Das Bild wurde als Orthoready-Produkt für etwa 5000 $ bei Eurosense gekauft.

Zur Geokodierung wurde zunächst ein städtisches GPS-Netz eingerichtet. Nachdem das militärgeographische Institut, welches über ein offizielles GPS für Albanien verfügte, keine Koordinaten bereitstellen wollte, wurden auf vier eigenen Stationen Langzeitbeobachtungen gemacht. Somit konnte mit Hilfe von WGS-Stationen ein eigenes ITRF referenziertes Netz eingerichtet werden. Ferner wurde das Netz der vier Stationen mit RTK auf etwa 60 Stationen verdichtet. Sie stehen der Stadtverwaltung jetzt mit einer Genauigkeit von etwa ± 2 cm zur Verfügung.

Abb.1 Gebäudedigitalisierung im Quickbirdbild in 2D

Das Satellitenbild musste vorerst orthorektifiziert werden. Dazu war ein digitales Höhenmodell nötig. Es waren zwar topographische Karten 1:50 000 mit Schichtlinien vorhanden, doch der Kontraktor für das Projekt IntoSpaceturk aus Ankara war gleichzeitig Betreiber einer Ikonos-Satellitenempfangsstation. Es war IntoSpaceturk ein Leichtes, eine Stereoaufnahme mit 1 m GSD von Tirana aufzunehmen, die Bilder zu geokodieren und das DGM über digitale Bildkorrelation abzuleiten. Mit diesem DGM wurde das Quickbird-Bild mit 0,6 m GSD orthorektifiziert. Natürlich war es nicht möglich, die fehlenden oder nicht nachgeführten Katastergrenzen zu rekonstruieren, obwohl es bereits seit dem Jahre 2000 Versuche gegeben hat, dies mit US und europäischen Mitteln zu tun. Für die 25 Katasterdistrikte von Tirana wurden insgesamt 10 M $ für diesen Zweck ausgegeben. Allerdings wurden nur drei der 25 Distrikte fertig. Das Projekt ist deshalb eingestellt worden, und das albanische Kataster muss auf bessere Zeiten warten.

Allerdings sind im Satellitenbild alle existierenden Gebäude klar erkennbar. Es genügt also, diese Gebäude in ihren Umrissen am Bildschirm als Shapefiles zu erfassen. Das ist eine unkomplizierte Routineaufgabe. Allerdings ist bei den erfassten Umrissen nicht eindeutig, ob es sich um ein Gebäude oder mehrere zusammenhängende Gebäude handelt. Die Klärung dieser Frage ist aber während einer Feldbegehung möglich.

Die Feldbegehung wurde für alle Häuser der Stadt durch zwei Teams innerhalb eines Monats durchgeführt. Jedes Team hatte einen Tablet-PC und einen Code-GPS-Empfänger mit durch kommerzielle Satelliten übertragenen Positionskorrekturen die es erlaubten, die Hauseingänge auf etwa 2 m genau zu bestimmen.

Für jeden Hauseingang wurde eine Reihe von Attributen erfasst und in den PC eingegeben, also:

- Hausnutzung (Wohnhaus, Behörde, religiöse Einrichtung, Schule, Krankenhaus, Name des Gebäudes, kommerzielle Nutzung, Zustand, Material)
- Anzahl der Geschosse
- erfragte oder geschätzte Anzahl der Bewohner

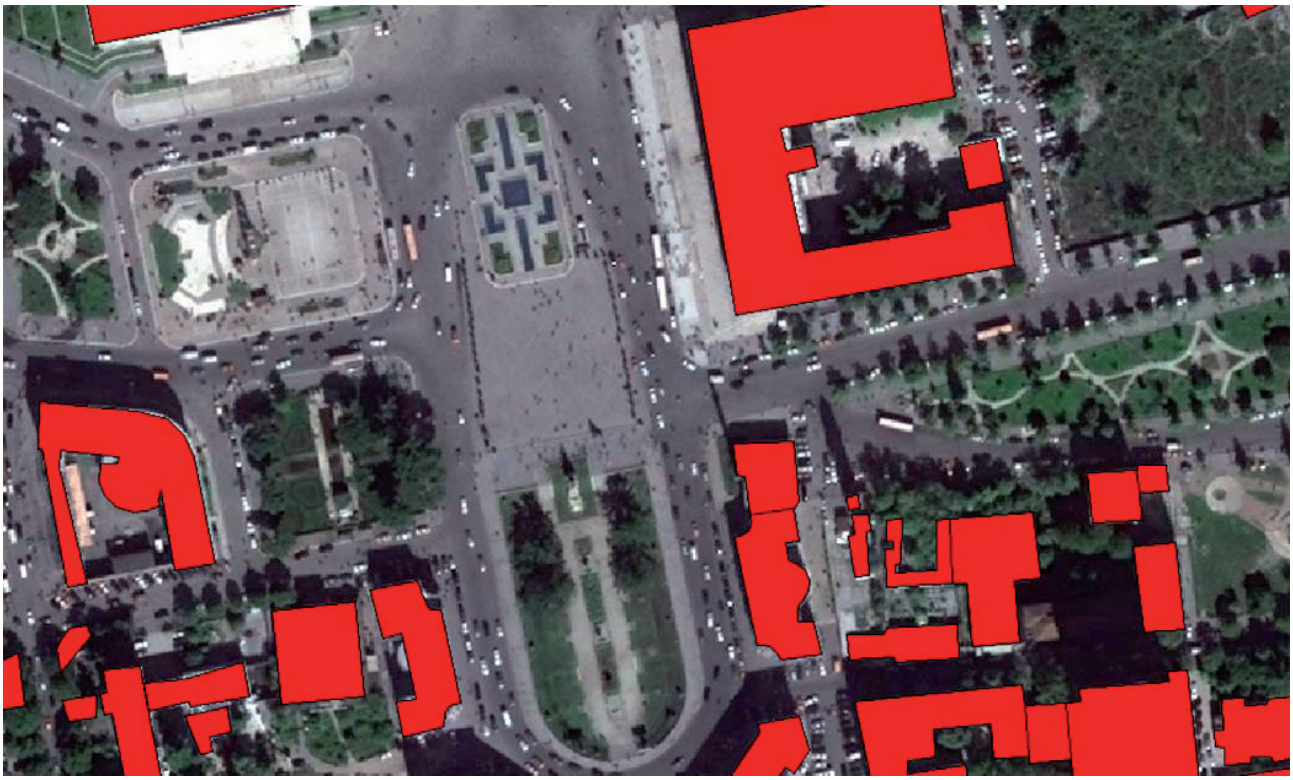

Abb.2 Digitalisierte Gebäude mit ArcGIS Attributen

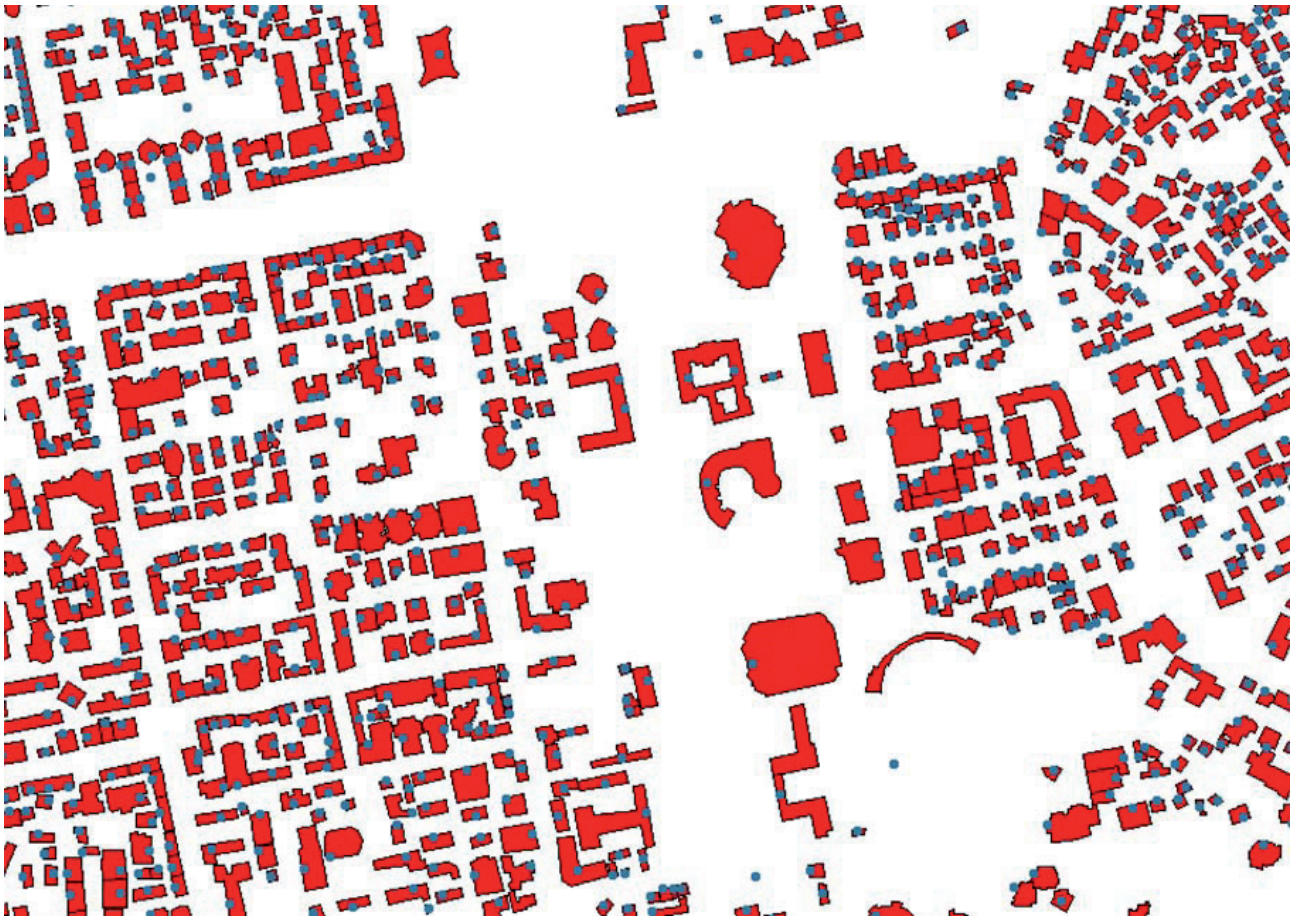

Abb.3 GPS vermessene Hauseingänge

Die Nutzung und die Analyse dieser Daten wurde durch die „Personal Database“ über ArcEditor oder ArcView ermöglicht.
Außer den Gebäuden waren die Straßendaten von Interesse:

- Name der Straße
- Parkplätze
- Müllcontainer
- Bushaltestationen und Busrouten
- Straßenmaterial
- Straßenzustand
- Anzahl der Fahrbahnen
- Gehsteige und ihr Zustand.

Daneben waren natürlich auch die Daten der Infrastruktur von Interesse. Für diese gab es zwar schematische Pläne, doch bislang war ohne GIS keine Zusammenschau möglich. Mit Hilfe der Pläne und der Bilder zur Einsparung der Informationen wurde die Erfassung der folgenden Infrastruktur ermöglicht:

- Elektrizitätsleitungen (Überland oder unterirdisch) und die zugehörigen Objekte (Masten, Schachtdeckel)
- Wasserleitungen und Abwasserkanäle (Durchmesser, Fließrichtung)
- Unterirdische Telefonleitungen.

Abb.4 Infrastrukturleitungen

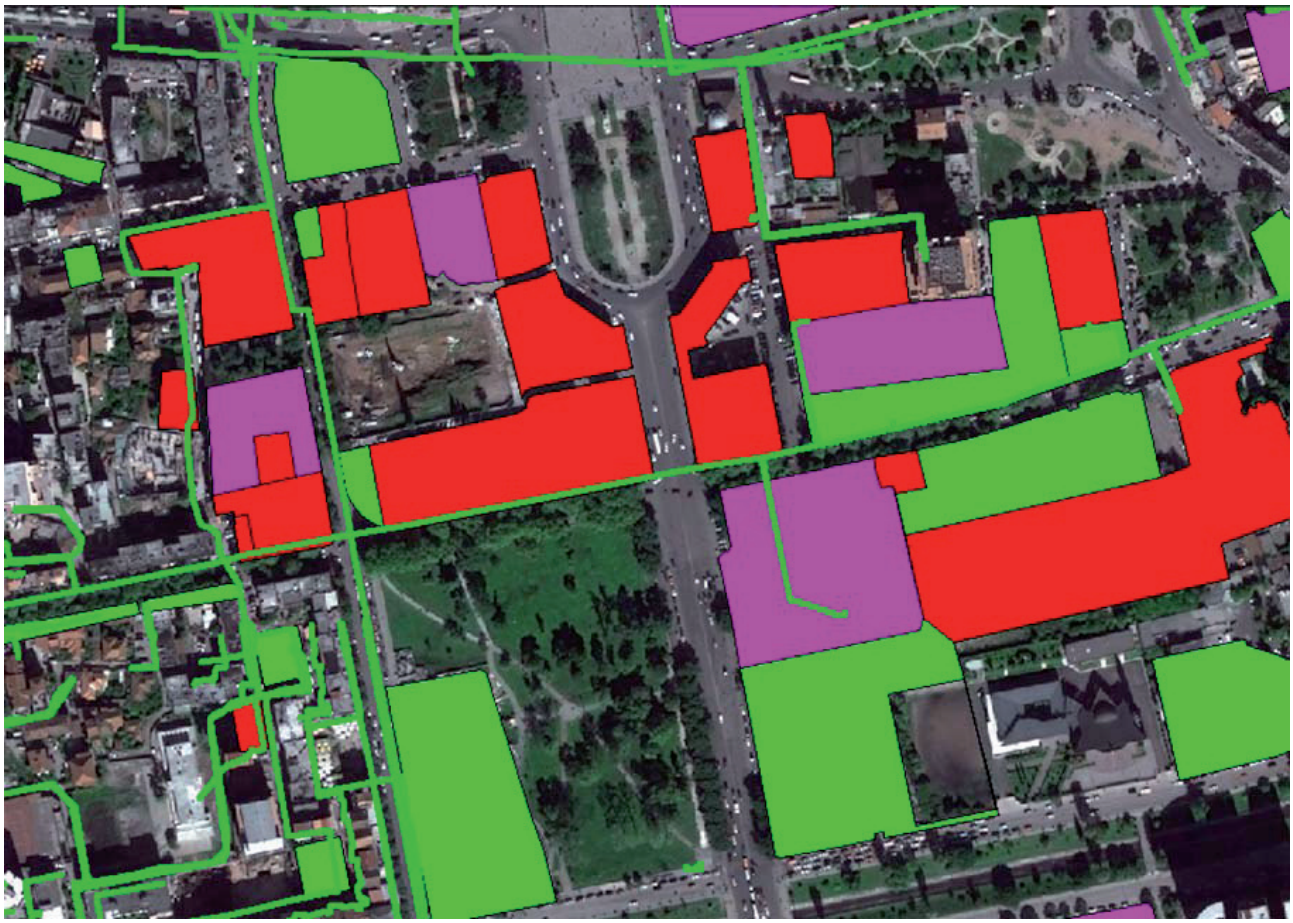

Abb.5 Institutionelle, kulturelle und kommerzielle Gebäude mit Elektrizitätsleitungen

Die Stadtverwaltung von Tirana hat auf diese Weise innerhalb eines Jahres planungsrelevante Daten erhalten. Die Gesamtkosten des Projektes (Satellitenbilder, GPS-Netzvermessungen, die Anschaffung von 8 ArcView- und 2 ArcEditor-Lizenzen einschließlich der PCs, die Gebäudedigitalisierung, die Felddatenerfassung, der Entwurf der Datenbank und die Lieferung des Gesamtsystems mit allen Daten) beliefen sich auf insgesamt 200 000 US $.

Die Nachführung der Daten ist jährlich durch ein neues Satellitenbild, eine neue Felddatenerfassung mit dem Tablet-PC für Kosten weit unter 100 000 $ vorgesehen.

3. Schlussfolgerung

Ich glaube, Manfred Ehlers wird mir recht geben: Ein Geoinformatiker wird man, indem man sich mit den IT-Werkzeugen im Hinblick auf die Ziele unserer Gesellschaft zu helfen weiß.

THE CAPABILITIES OF MODERATE RESOLUTION SATELLITE DATA

A. Kopka

University of Münster, International Institute for Forest Ecosystem Management and Timber Utilization North-Rhine/ Westphalia, Robert-Koch-Str. 26, 48149 Münster, Germany, andre.kopka@wald-zentrum.de

KEY WORDS: Climate Change, Forestry, Remote Sensing, Vegetation Model, MODIS, ASTER, LANDSAT, CORINE

ABSTRACT:

What are the benefits of moderate resolution data and which parameters could the user recveive from these data? The following text tries to give some answers to this question.

In an examination, the satellite images from the sensors MODIS (Moderate Resolution Imaging Spectroradiometer), ASTER (Advanced Space borne Thermal Emission and Reflection Radiometer) and LANDSAT are compared to show which parameters for vegetation models, e.g. the Leaf Area Index (LAI), the Normalized Differenced Vegetation Index (NDVI) or the Photo Synthetically Active Radiation (APAR) can be estimated. The adapted model is the Global Production Efficiency Model (GLOPEM) invented by Goetz et al. (1996).

All parameters were compared with a classification of the standard Maximum Likelihood (ML) and Minimum Distance to mean (MD) methods. The accuracy of the ASTER data in comparison with CORINE Land Cover 2000 lies around 80 percent and declares the best results. But also the results of the MODIS and LANDSAT images were beneath the marks of ASTER.

1. INTRODUCTION

In 2008 the Kyoto Protocol to the United Nations framework convention on climate change has been started in which the leading industrial nations obligate themselves to reduce greenhouse gases from 2008 to 2012 by 5.2 percent. The European Union will play thereby a central role with their voluntary agreement about twenty percent up to the year 2020. Flexible mechanisms of compensation (such as the 'Clean Development Mechanism' and 'Joint Implementation') could help the carbon dioxide producing industries to implement their high aims. Based on these mechanisms tradable emission rights arise which advance - among other things - the regional measures and policies on the fixation of carbon in the form of biomass, e.g. by afforestation.

The trade with the emission rights contains a lot of opportunities: With the publishing of the carbon dioxide balances, emissions from the industry obtain a real market value, particularly in dependence of the costs for avoiding of the emissions. As a result of this development the companies are interested in reducing atmospheric greenhouse gases in the future. But these environmental measures should be audited by an independent institution or system; conventional methods are not suitable for the controlling and monitoring. Large-scale and contemporary data products derived from moderate resolution satellite systems, such as MODIS (Moderate Resolution Imaging Spectroradiometer) can help to assist these monitoring systems.

2. METHODOLOGY

In this paper - as a part of the dissertation - the benefit of remote sensing based vegetation models is analysed: In this case the Global Production Efficiency Model (GLOPEM) (fig.1) invented by Goetz et al. (1996) is adapted.

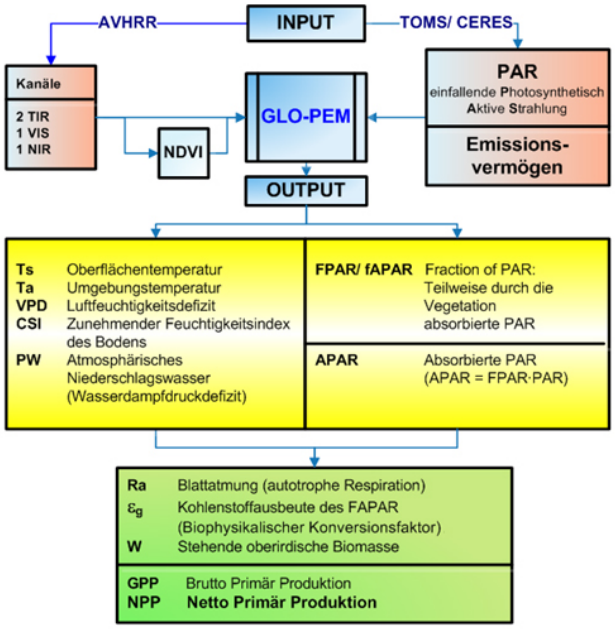

Figure 1. Global Production Efficiency Model (GLOPEM) by Goetz et al. (1996)

Instead of TOMS/CERES and AVHRR the satellite images from the sensors MODIS, ASTER (Advanced Space borne Thermal Emission and Reflection Radiometer) and LANDSAT are compared to show which parameters for vegetation models, e.g. the Leaf Area Index (LAI), the Normalized Differenced Vegetation Index (NDVI) or the Photo Synthetically Active Radiation (APAR) can be estimated. All parameters were calculated by the specifications of the model GLOPEM, except for the LAI, which was estimated with special software and validated by forest research data.

Further important parameters of this vegetation model are the Fraction of Absorbed Photo Synthetically Active Radiation (FAPAR), the biophysical conversion factor (ε) and the autotrophic respiration (Ra). All parameters are important to determine the Net Primary Productivity (NPP), which balances the fraction of the photosynthesis and respiration in a forest stand. These indices are analysed and compared with the classification results of the three satellite images and also with the land cover information of CORINE (Coordinated Information on the European Environment) and terrestrial information (DLR 2006).

All parameters as well as the radiation specific parameters are calculated based on remote sensing data and further products, e.g. CORINE Land cover data. Also special geo-information data, such as climate indices, a digital terrain model and forest inventory data are used for the examination. All images and geo data were integrated and analysed in a Geographic Information System (GIS).

The research area of about 400 square kilometres is located in the European Geoparc TERRA.vita in Northern Germany in the forest district of Minden (s. fig.2). The TERRA.vita Geoparc with a size of 1250 square kilometres with its special vegetation, forest and agricultural sites in a hilly terrain represents a typical northern region of Germany (Europarc & IUCN 2000). Special investigations are made in the forest stands, with the species oak, spruce and beech. Therefore additional forest inventory data was collected.

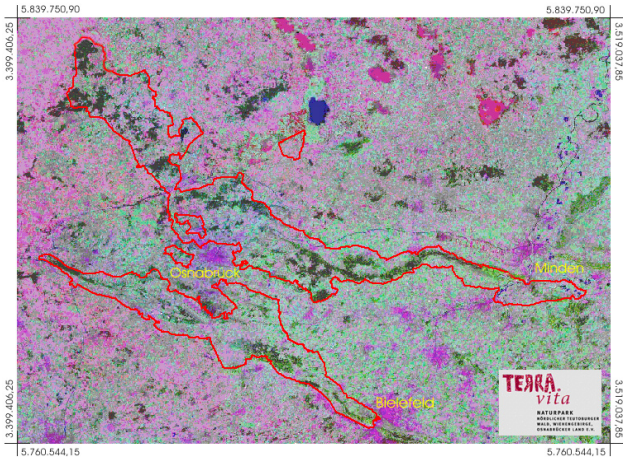

Figure 2. The Geoparc TERRA.vita in Northern Germany, a view of LANDSAT data

The remote sensing satellite images from MODIS have a spatial resolution from 250 meters up to 500 meters. At least 21 scenes of MODIS were examined, investigated and estimated for a time series in 2003. In this case also change detection was calculated for the MODIS data. The LANDSAT images, as a well known and long-term satellite image data, with a spatial resolution of about 30 meters, were used in the present research.

ASTER has the best spatial resolution of the investigated satellite images with 15 meters. All used satellite image data contain multi-spectral sensor information. Especially the spectral range of the visible light and the near infrared radiations were used for the examination.

3. RESULTS

The Leaf Area Index (LAI) in combination with the Normalized Differenced Vegetation Index (NDVI) can very well be calculated from remote sensing data; especially the results from the ASTER images are significant (s. fig. 3).

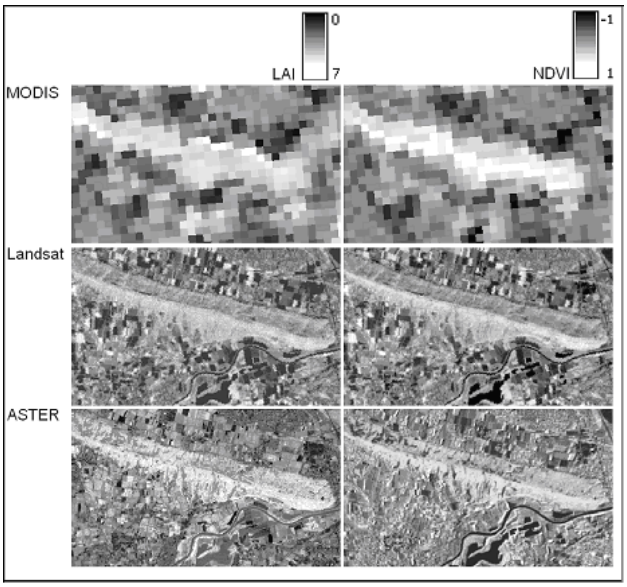

Figure 3. Comparison of LAI and NDVI for the three different satellite images

In addition all satellite images were classified with the standard Maximum Likelihood (ML) and Minimum Distance to mean (MD) methods.

The present examination shows that the Maximum Likelihood classification of the ASTER images, but also the LANDSAT images, with accordance about over 80 percent with the ground truth, are best suited to calculate these parameters. The good results of the MODIS satellite data with the Minimum Distance to mean classification were comparable with the results of the two satellite images ASTER and LANDSAT.

It explains on the one hand which parameters of the developed model can determined using remote sensing satellite images and, on the other hand, which parameters must be measured in the field to complete the statistics. The high chronology and availability of data with a moderate resolution compensates sometimes the disturbances and problems with the data evaluation and analysis. “Low- cost-data” could be used in large-scaled areas, especially for environmental research. But the primal condition for the use of satellite data - especially in vegetation models with multispectral data - is (and remains) the infrared channel.

Summarized, the research shows the quality and robustness of the calculated parameters for the different satellite images MODIS, LANDSAT and ASTER in combination with CORINE and in the comparison with the terrestrial measurements. New improvements on these remote sensing based vegetation models are imaginable. At least moderate resolution satellite data can have a useful impact on forest monitoring systems.

4. REFERENCES

Blaschke, R. & Felbermeier, B. (2003): Satellitendaten für die Forstwirtschaft, Nutzungsanforderungen der forstlichen Praxis und Potential der optischen Satellitenfernerkundung, Forstliche Forschungsberichte München, Nr. 196, München.

BMELV, Bundesministerium für Ernährung, Landwirtschaft und Verbraucherschutz (2005): Die zweite Bundeswaldinventur-BWI². Der Inventurbericht. Zu den Bundeswaldinventur-Erhebungen 2001 bis 2002 und 1986 bis 1988.

Böswald, K. (1996): Zur Bedeutung des Waldes und der Forstwirtschaft im Kohlenstoffhaushalt, eine Analyse am Beispiel des Bundeslandes Bayern. Forstliche Forschungsberichte München, Nr. 159, München (S. 4, 5 und 7).

Böswald, K., Martini, S. & Schröder, M. (2001): Das Bonn Agreement und die Rolle der Wälder. Erschienen in AFZ-Der Wald v. 56(23) S. 1246-1248.

Dawson, T.P., North, P., Plummer, S. E. & Curran, P.J. (2003): Forest ecosystem chlorophyll content: implications for remotely sensed estimates of net primary productivity, Taylor & Francis Ltd., Journal of Remote Sensing, Ausgabe 24, Nr. 3 (S. 612 f).

Di Bella, C.M., Paruelo, J.M., Becerra, J.E., Bacour, C., Baret, F. (2004): Effect of senescent leaves on NDVI- based estimates of fAPAR: experimental and modelling evidences, Taylor & Francis Ltd., International Journal of Remote Sensing, Ausgabe 35, Nr. 23, 2004 (S. 5425).

DLR, Deutsches Zentrum für Luft- und Raumfahrt (2006): Corine Landcover 2000 - Bodenbedeckungsdaten für Deutschland, http://www.corine.dfd.dlr.de/ intro_de.html (letzer Zugriff: 11.01.2006).

Ehlers, M. (2002): Fernerkundung für GIS- Anwender – Sensoren und Methoden zwischen Anspruch und Wirklichkeit, in: Blaschke, T. (Hrsg.), Fernerkundung und GIS: Neue Sensoren – innovative Methoden, Herbert Wichmann Verlag, Heidelberg (S. 18).

Europarc & IUCN (2000): Richtlinien für Managementkategorien von Schutzgebieten - Interpretation und Anwendung der Managemenkategorien in Europa. Europarc und WCPA Grafenau, Deutschland.

Goetz, S.J. & Prince, S.D. (1996): Remote sensing of net primary production in boreal forest stands, Departement of Geography, University of Maryland, Elsevier Science B.V., Agricultural and Forest Meteorology, Nr. 78, 1996 (S. 152, 159).
Goetz, S.J., Prince, S.D., Goward, S.N., Thawley, M.M. & Small, J. (1999): Satellite remote sensing of primary production: an improved production efficiency modelling approach, Elsevier Science B.V., Ecological Modelling, Nr. 122 (S. 239 – 247).

Gangkofner, U. (1996): Methodische Untersuchung zur Vor- und Nachbereitung der Maximum Likelihood Klassifizierung optischer Fernerkundungsdaten. Dissertation, Fakultät für Geowissenschaften der Ludwig-Maximilians- Universität, München (S. 15, 115, 136, 138).

Gower, S.T., Kucharik, C.J. & Norman, J.M. (1999): Direct and Indirect Estimation of Leaf Area Index, fAPAR, and Net Primary Production of Terrestrial Ecosystems, Elsevier Science Inc., Remote Sensing of the Environment, Nr. 70, 1999 (S. 30).

IPCC, Intergovernmental Panel on Climate Change (2007): http://www.ipcc.ch (letzter Zugriff: 10.05.2007).

Janssens, J. (2002): Risk Management of investments in Joint implementation and clean development mechanism projects. Dissertation der Universität St. Gallen.

Kurz, F. (2003): Schätzung von Vegetationsparametern aus multispektralen Fernerkundungsdaten, Dissertation, Deutsche Geodätische Kommission, München (S. 16, 19).

Kopka, A. (2003): TERRA.vita - Ein Naturpark als Kohlenstoffspeicher ? Möglichkeiten der Umsetzung des Kyoto Protokolls in einem ausgewählten Landschaftsraum in Niedersachsen, http://www.naturpark-terravita.de (letzter Zugriff: 23.09.2003).

Kopka, A. (2005): MODIS-Zeitreihenanalyse für das Jahr 2003 in verschiedenen Landschaftsräumen Norddeutschlands. Forschungsbericht der Fakultät Ressourcenmanagement, Göttingen (n. veröffentlicht).

Kopka, A.: (2008): Analyse multispektraler Fernerkundungsdaten im Hinblick auf deren Eignung zur Einschätzung des Biomassepotenzials großer Landschaftsräume am Beispiel des Naturparks TERRA.vita (Dissertation). Veröffentlicht im Electronic Library (ELib) System der Universitätsbibliothek Osnabrück am 28.01.2008.

Müller-Using, B. (2002): Wegmarken und Unzulänglichkeiten in der CO_2-Minderungspolitik und die Rolle der Forstwirtschaft in diesem Prozess – von Kyoto bis Marrakesch. AFZ-Der Wald, 57 Jahrgang/Nr.13/14, 15.Juli 2002.
Richters, J. (2005): Entwicklung eines fernerkundungsgestützten Modells zur Erfassung von pflanzlicher Biomasse in NW-Namibia, Dissertation, Mathematisch-Naturwissenschaftliche Fakultät der Rheinischen Friedrich- Wilhelm-Universität, Bonn (S. 41 f, 47 – 50, 57 f, 65 f).

Sander, H.H. (2004): Biomassenutzung in Niedersachsen, Chancen für die Region, Rede von Umweltminister Hans-Heinrich Sander anlässlich der 65. Informationsgespräche des ANS e.V. am 6.12.2004 in Braunschweig.

Schulte, A. (2000): Proceedings: Forstwirtschaft nach Kyoto: Holz als Kohlenstoffspeicher und regenerativer Energieträger. Internationaler und Interdisziplinärer Kongress in Paderborn, vom 20.-22.11.2000.

Schulze, E.D. (2000): Carbon and Nitrogen Cycling in European Forest Ecosystems. Ecological Studies 142. Erschienen im Springer Verlag.2000.

Strahler, A. et. al (1999): MODIS Land Cover Product, Algorithm Theoretical Basis Document Version 5.0, Boston MA: Center for Remote Sensing, Department of Geography Boston University.

UNFCCC, United Nations Framework Convention on Climate Change (1997): Kyoto Protocol to the United Nations framework convention on climate change. COP 3 in Kyoto, Japan, on 11 December 1997.

Veroustraete F, Sabbe H. (1999): C-FIX, a satellite based carbon budgeting tool applied at the European scale for NPP and NEP upscaling in the LTEEF project. Mol, Belgium: VITO, TAP, technical note. 8 p.

NOTES ON MULTISPECTRAL CLASSIFICATION WITH CORRELATED BANDS: EFFECTS ON USING EUCLIDEAN DISTANCE.

N. de Lange

Dept. of Geoinformatics and Remote Sensing, University of Osnabrueck, Seminarstrasse 19ab, D-49069 Osnabrueck
ndelange@igf.uni-osnabrueck.de

KEY WORDS: Multispectral classification, correlated bands, Euclidean- and Mahalanobis-distance, principal component analysis

ABSTRACT:

This article discusses the problem of computing Euclidian distance as a measure of dissimilarity or similarity of pixels by classifying remotely-sensed images. Within multispectral classification it has to be pointed out that the bands are often not uncorrelated and do not build an Euclidean space with orthogonal axes. Therefore the computing of Euclidean distance is not allowed in a strict mathematical meaning. Two main approaches are discussed which may meet but do not solve this problem: computing Mahalanobis distance and using (uncorrelated) principal components instead of the original data. Finally the core sentence is performed: Computing Euclidean distance using the original (correlated) data leads to the same result as computing Euclidean distance using principal components which are weighted with the square roots of their corresponding eigenvalues.

1. INTRODUCTION

Classification procedures form a central part when analysing remotely-sensed images. All techniques are derived from the graphic process to group points in a two-dimensional scatter-diagram. A Cartesian coordinate system is given whose axes are built of the variables. It is also assumed that the variables are uncorrelated so that the axes are orthogonal. But in reality this assumption is correct very rarely.

Workbooks on cluster analysis mention this problem in passing. At the end they advise their readers to use the original (and probably correlated) variables in order not to destroy the internal structure or internal weighting (Backhaus u.a. 2006 p. 550, Bortz 2005 p. 569, Vogel 1975 p. 60 and 91). They argue that it can be necessary as well as desirable to use correlated variables if obvious arguments exist with respect to the aims of the classification. They recommend users to examine carefully whether to exclude (only) high correlated variables. But the analysis of remotely-sensed images has nearly no chance to exclude correlated bands. Furthermore literature on image classification offers no discussion about what happens if correlated variables are used within classification. Scanning literature on cluster analysis Vogel (1975 p. 84) is the only one who quotes an article of Harris (1955) which is supposed to show that using correlated variables is similar to using principal components weighted with their corresponding eigenvalues. But the discussion by Harris (1955) is confusing and wrong.

This article provides a new approach to use correlated variables (especially with respect to remote sensing) in classification procedures. First selected mathematical concepts of multivariate statistics are compiled based on Bock (1974). Then the central sentence will be shown: “Computing Euclidean distance using the original (correlated) data leads to the same result as computing Euclidean distance using principal components which are weighted with the square roots of their corresponding eigenvalues.”

2. CLASSIFICATION OF REMOTELY-SENSED IMAGES

2.1 The central idea of image classification

Remotely-sensed images consist of a set of pixels which represent a small part of the land surface (for details look at the numerous papers of remote sensing, e.g. Mather 1999 and Lillesand et al 2003). A single pixel is characterized by a vector of p values, p is the number of spectral bands, the values are the so-called grey-scale values. A set of grey-scale values is known as a pattern. In the case of Landsat TM a pixel is marked by seven spectral bands and eight bit grey-scale values (integers from 0 to 255). The spectral bands are called features. On the one hand a single pixel is a print of one land surface category for example woodland, water or grassland. On the other hand classification of these pixels should work out these categories. “The classification process may therefore be considered as a form of pattern recognition, that is, the identification of the pattern associated with each pixel position in an image in terms of the characteristics of the objects or materials that are present at the corresponding point on the Earth”s surface.” (Mather 1999 p. 167).

2.2 Geometric concept of classification

In processing remotely-sensed images two categories of pixel orientated classification techniques exist: unsupervised and supervised classification procedures. The so called isodata-algorithm (iterative self-organizing data analysis technique) is the most commonly used procedure in the first category as the parallelepiped or box classifier and the centroid (k-means) classifier belong to the second category. All of these algorithms are based on the fundamental “shortest-distance-to-centre-decision-rule” which means that a pixel is assigned to the nearest cluster centre. In all cases the grey-scale values of the pixel to be classified determine the location in the feature space and the allocation to landcover categories (see fig. 1).

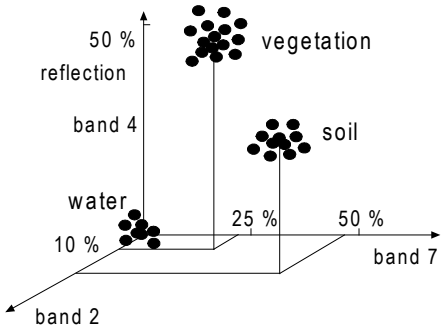

Figure 1. Geometric concept of classification

It has to be said that the maximum likelihood classifier which is most commonly used within supervised classification is not based on distances but on computing probabilities that a pixel belongs to a cluster (see end of chapter 3.3).

2.3 Measuring similarity

Figure 1 and 2 show the fundamental concepts of classification:

- Each pixel is represented in a Euclidean space (the feature space) whose axes define the features, particularly as the axes are orthogonal.
- Distance is being used as a measure of dissimilarity and proximity as a measure of similarity.
- The smaller the distance between two points (the closer the points in the feature space), the more similar the points are. Or: The greater the inter-point distance is the less the similarity is.

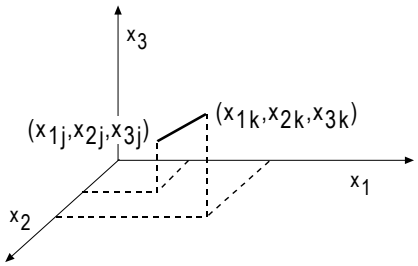

Figure 2. Distance and similarity in Euclidean Space

Dissimilarity or similarity is measured by the Euclidean distance between x_j and x_k, whose square is computed by:

$$\|x_i - x_k\|_2^2 = (x_j - x_k)^t * (x_j - x_k) \quad (1)$$

or in a three-dimensional space as in figure 2:

$$x_j = \begin{pmatrix} x_{1j} \\ x_{2j} \\ x_{3j} \end{pmatrix} \quad x_k = \begin{pmatrix} x_{1k} \\ x_{2k} \\ x_{3k} \end{pmatrix} \quad and \quad (x_j - x_k) = \begin{pmatrix} x_{1j} - x_{1k} \\ x_{2j} - x_{2k} \\ x_{3j} - x_{3k} \end{pmatrix} \quad (2)$$

$$\|x_i - x_k\|_2^2 = (x_{1j} - x_{1k})^2 + (x_{2j} - x_{2k})^2 + (x_{3j} - x_{3k})^2 \quad (3)$$

3. STRATEGIES IN USING CORRELATED BANDS

3.1 The starting position

The algorithms and techniques mentioned in chapter 2 are based on the fundamental assumption that the features (the spectral bands) represent a Cartesian coordinate system, that means:

- the axes are orthogonal or:
- the features (bands) are uncorrelated or:
- correlation between all features equals zero (not: the feature correlation within one group).

These assumptions cause some problems within the processing of remotely-sensed images. Adjacent bands in a multispectral remotely-sensed image are generally correlated (see Mather p. 126). For example: A multispectral image of areas with vital vegetation will show a negative correlation between the near infrared and visible red bands. As the greenness of the vegetation increases, the red reflectance diminishes and the near-infrared reflectance increases. Cluster analysis techniques provide two different approaches to meet this situation:

- performing principal component analysis (also known as the Karhunen-Loève transformation)
- calculating Mahalanobis distance.

3.2 Principal component analysis

Principal component analysis of p variables or features calculates p new or hypothetical variables (the principal components) which are always uncorrelated. Principal components explain different proportions of the total variance (as a measure of information content). The proportions of the total variance decrease from the first to the p^{th} principal component. Generally much of the variance of the original data is concentrated in the first components (e.g. in the first two or three principal components using a multiband spectral set).

When examine remotely-sensed images principal component analysis is used mainly for three reasons:

- feature-selection technique before image classification
- reducing redundancy or data compression by using only high-order principal components
- generating a new set of images based on (only few) principal components to improve the differentiation of various clusters.

Therefore principal component analysis is not used primarily to determine an orthogonal reference system in order to calculate Euclidean distances. This effect is used as well, but is definitely not the main aim.

It has to be pointed out that spectral distinction may decrease for some groups as well as computing costs may increase. Principal component analyses do not always produce the same components when using image data sets of different locations and different time. The use of principal components means that all components have the same weight or importance, which sometimes may not reflect reality. Finally the interpretation of the calculated classes at the end of the classification process can be more complex or difficult due to the use of abstract and hypothetical components instead of the original data.

A short description of the principal component analysis is necessary as the following discussion needs this theoretical background. The basic equation of principal component analysis in algebraic notation is:

$$ {}_pZ_n = {}_pA_p * {}_pF_n \tag{4} $$

where ${}_pZ_n$ matrix of standardized input data, n columns (number of pixels or objects), p rows (number of features or bands), mean=0 and variance = 1 for all features or bands
${}_pA_p$ matrix of factor loadings
${}_pF_n$ matrix of principal components

Equation (4) means that the observed data (here: the grey-scale values of the bands) are linear combinations of hypothetical, not observed and not observable factors, the principal components.

Steps to compute the two unknown matrices *A* and *F*:

$$ {}_pR_p = \frac{1}{n} * {}_pZ_n * {}_nZ_p^t \tag{5} $$

where ${}_pR_p$ matrix of correlation coefficients of the p features or bands, symmetric

By inserting equation (4) in equation (5):

$$ R = \frac{1}{n} * {}_pA_p * {}_pF_n * ({}_pA_p * {}_pF_n)^t \tag{6} $$

$$ R = \frac{1}{n} * {}_pA_p * {}_pF_n * {}_nF_p^t * {}_pA_p^t \tag{7} $$

Then similar to equation (5) the matrix $\frac{1}{n} * {}_pF_n * {}_nF_p^t$ is a correlation matrix which contains the correlations between the principal components. As it is postulated that these principal components are uncorrelated this matrix is the identity matrix. Then equation (7) turns to equation (8)

$$ R = \frac{1}{n} * {}_pA_p * {}_pA_p^t \tag{8} $$

As R is symmetric with real numbers the equation (8) leads to the so called eigenvalue problem of a real symmetric matrix. All eigenvalues of R are real numbers, the corresponding eigenvectors are orthogonal. Then the matrix *A* is determined:

$$ {}_pA_p = {}_pV_p * {}_p\Lambda_p^{\frac{1}{2}} \tag{9} $$

or

$$ {}_pR_p = \frac{1}{n} * ({}_pV_p * {}_p\Lambda_p^{\frac{1}{2}}) * ({}_pV_p * {}_p\Lambda_p^{\frac{1}{2}})^t = \frac{1}{n} * {}_pV_p * {}_p\Lambda_p * {}_pV_p^t \tag{10} $$

where: ${}_pV_p$ matrix of orthonormal eigenvecto $(v_1, v_2, ..., v_p)$ of matrix R, ${}_pV_p^{-1} = {}_pV_p^t$

${}_p\Lambda_p$ diagonal matrix with $\Lambda_{ii} = \sqrt{\lambda_i}$ and λ_i the corresponding eigenvalue to ${}_pV_p$ with $\lambda_1 \geq \lambda_2 \geq \lambda_p > 0$

The eigenvectors scaled by the square roots of the corresponding eigenvalues are called factor loadings, which can be interpreted as correlations between the principal components and the observed variables (here: the different bands of the multispectral image).

Then by inserting equation (9) in equation (4)

$$ {}_pZ_n = {}_pV_p * {}_p\Lambda_p^{\frac{1}{2}} * {}_pF_n \tag{11} $$

and finally:

$$ {}_pF_n = {}_p\Lambda_p^{-\frac{1}{2}} * {}_pV_p^t * {}_pZ_n \tag{12} $$

A mentioned in chapter 3.2 principal component analysis is used to reduce redundancy of the p bands and to analyse q principal components with q < p. Then the Matrix A of factor loadings is still not quadratic and equation (9) turns to:

$$ {}_pA_q = {}_pV_q * {}_q\Lambda_q^{\frac{1}{2}} \quad q < p \tag{9*} $$

Then equation (12) turns to:

$$ {}_qF_n = {}_q\Lambda_q^{-\frac{1}{2}} * {}_qV_p^t * {}_pZ_n \tag{12*} $$

Within multivariate statistic the broader factor analysis approach cancels the postulation of uncorrelated factors which leads to so called oblique rotated factors.

It is also possible to assume non-standardized features which have means unequal 0 und standard deviations unequal 1. Then the correlation matrix R turns to the covariance matrix S, which is the non-standardized analogue of the correlation matrix.

3.3 Mahalanobis distance

The square of the Mahalanobis distance between two points in feature space or between the vectors x_j and x_k is defined as (see Bock p. 237):

$$ \|x_i - x_k\|_M^2 = (x_j - x_k)^t * {}_pS_p^{-1} * (x_j - x_k) \tag{13} $$

with ${}_pS_p^{-1}$ the inverse of the covariance matrix ${}_pS_p$ with the coefficients (covariance of variable i and j):

$$ s_{ij} = \frac{1}{n} \sum_{k=1}^{n} (x_{ik} - \bar{x}_i) * (x_{jk} - \bar{x}_j) \tag{14} $$

where: x_j column j of matrix x (input data, n columns, number of pixels or objects), p rows (number of features or bands)
$\bar{x}_i$ mean of variable i

Formula (1) and (13) show that Euclidean distance is a special case of Mahalanobis distance as for uncorrelated features the matrix S equals the identity matrix.

From the formulas (14) and (15) it is evident that Mahalanobis distance depends on all n pixels (using S). In contrast to the Euclidean distance, which depends only on the values of the two feature vectors, the Mahalanobis distance considers the global structure of the data set.

In this context of classification with correlated bands another property is much more important: Mahalanobis distance eliminates the correlation of the feature, or: the correlation of the features has no influence on computing the Mahalanobis distance.

Similar to equation (10) the decomposition of the symmetric covariance matrix S with $\det S \neq 0$ leads to (except factor 1/n):

$$ {}_pS_p = {}_pV_p * {}_p\Lambda_p * {}_pV_p^t \tag{15} $$

Suppose the transformation for the vector x_k, which turns to y_k:

$$ y_k = \Lambda^{-\frac{1}{2}} * {}_pV_p^t * (x_k - \bar{x}) \tag{16} $$

Then (see Bock 1974 p. 41f.) :

$$ (y_k - \bar{y}) = \left[(\Lambda^{-\frac{1}{2}} * V^t * (x_k - \bar{x}) - \frac{1}{n} * \sum \Lambda^{-\frac{1}{2}} * V^t * (x_k - \bar{x}) \right] \tag{17} $$

$$ = \left[(\Lambda^{-\frac{1}{2}} * V^t * (x_k - \bar{x}) - \Lambda^{-\frac{1}{2}} * V^t * \frac{1}{n} * \sum (x_k - \bar{x}) \right] \tag{18} $$

$$ = \left[(\Lambda^{-\frac{1}{2}} * V^t * (x_k - \bar{x}) - \Lambda^{-\frac{1}{2}} * V^t * (0) \right] \tag{19} $$

$$ = (\Lambda^{-\frac{1}{2}} * V^t * (x_k - \bar{x}) \tag{20} $$

Then the covariance matrix S_y of the transformed data is:

$$ S_y = \frac{1}{n} * (y_i - \bar{y}) * (y_i - \bar{y})^t \tag{21} $$

In equation (21) the term $(y_i - \bar{y})$ describes the whole matrix which columns i are built of the elements $(y_{ik} - \bar{y}_k)$ with $1 \le k \le p$.

$$ S_y = \frac{1}{n} * \left[\Lambda^{-\frac{1}{2}} * V^t * (x_i - \bar{x}) \right] * \left[\Lambda^{-\frac{1}{2}} * V^t * (x_i - \bar{x}) \right]^t \tag{22} $$

$$ = \Lambda^{-\frac{1}{2}} * V^t * \frac{1}{n} * (x_i - \bar{x}) * (x_i - \bar{x})^t * V * \Lambda^{-\frac{1}{2}} \tag{23} $$

$$ = \Lambda^{-\frac{1}{2}} * V^t * S_x * V * \Lambda^{-\frac{1}{2}} \tag{24} $$

$$ = \Lambda^{-\frac{1}{2}} * V^t * V * \Lambda * V^t * V * \Lambda^{-\frac{1}{2}} \tag{25} $$

$$ = \Lambda^{-\frac{1}{2}} * \mathrm{I} * \Lambda * \mathrm{I} * \Lambda^{-\frac{1}{2}} \tag{26} $$

$$ = \mathrm{I} \tag{27} $$

This means that the covariance matrix S_y of the transformed data equals the identity matrix, therefore the new variables are uncorrelated. Then it is allowed to compute the Euclidean distance between the two vectors y_k and y_j in Euclidean space:

$$ \| y_k - y_j \|_2^2 = (y_k - y_j)^t * (y_k - y_j) \tag{28} $$

$$ = \left[(\Lambda^{-\frac{1}{2}} * {}_pV_p^t * (x_k - \bar{x}) - (\Lambda^{-\frac{1}{2}} * {}_pV_p^t * (x_j - \bar{x}) \right]^t * [..] \tag{29} $$

$$ = \left[\Lambda^{-\frac{1}{2}} * {}_pV_p^t * (x_k - x_j) \right]^t * [..] \tag{30} $$

$$ = \left[{}_pV_p * \Lambda^{-\frac{1}{2}} * (x_k - x_j)^t \right] * \left[\Lambda^{-\frac{1}{2}} * {}_pV_p^t * (x_k - x_j) \right] \tag{31} $$

$$ = (x_k - x_j)^t * {}_pV_p * \Lambda^{-\frac{1}{2}} * \Lambda^{-\frac{1}{2}} * {}_pV_p^t * (x_k - x_j) \tag{32} $$

$$ = (x_k - x_j)^t * {}_pV_p * \Lambda^{-1} * {}_pV_p^t * (x_k - x_j) \tag{33} $$

$$ = (x_k - x_j)^t * S^{-1} * (x_k - x_j) \tag{34} $$

This is the Mahalanobis distance of the untransformed and correlated feature vectors x_k and x_j.

These computings show:

Mahalanobis distance between two correlated feature vectors x_k and x_j equals the Euclidean distance between two uncorrelated feature vectors y_k and y_j. This result can be interpreted as:

Mahalanobis distance eliminates the correlation of features. Or: The correlation of features has no influence on computing the Mahalanobis distance.

The use of Mahalanobis distance implies that mean, variance and covariance (of the whole data set) can adequately describe the structure of the data. But just this idea violates the general assumption of classification approaches: the existence of different clusters with different means, variances and covariance. Therefore cluster analyses as well as classification within processing of remotely-sensed images do not use Mahalanobis distance to determine a similarity between different objects or pixels.

But the processing of remotely-sensed images uses Mahalanobis distance to compute probabilities P(x) that a pixel vector x (of p features) is a member of Cluster k (see the maximum likelihood classifier as a supervised classification procedure):

$$ P(x) = 2 * \mathrm{p}^{-\frac{1}{2}p} * \det(S_i)^{-\frac{1}{2}} * e^M $$

where:

$$ M = -0.5 * y^t * S_i^{-1} * y \quad and \quad y = (x - \bar{x}_i) \quad \bar{x}_i \quad mean\ of\ cluster\ i $$

While S_i is the covariance matrix of class i, M is the Mahalanobis distance from pixel vector x to the centre of cluster i (see Mather 1999 p. 182).

Therefore the maximum likelihood classifier is not touched by the problem of correlated features. But this method is faced with other problems. One assumption is that all clusters are equally likely. But it is far more important that this technique assumes that the frequency distribution of the class membership can be approximated by the multivariate normal probability distribution.

4. USING EUCLIDEAN DISTANCE WITH CORRELATES BANDS: THE EFFECT

Commonly multispectral classifications use untransformed and then (naturally) correlated features (grey-scale values of multispectral band image). Normally multispectral classifications do not use principal classification analyses nor Mahalanobis distances to meet the problem of correlated features. Thus the crucial question is:

What happens when using correlated bands in the classification procedures based on Euclidean distances as a measure of dissimilarity or similarity?

As shown above in equation (12)

$$ {}_pF_n = {}_p\Lambda_p^{-\frac{1}{2}} * {}_pV_p^t * {}_pZ_n \tag{35} $$

where:
- ${}_pZ_n$ matrix of standardized observed data
- ${}_pV_p$ matrix of p orthonormalized eigenvectors of matrix R
- ${}_p\Lambda_p$ diagonal matrix with $\Lambda_{ii} = \sqrt{\lambda_i}$ and λ_i corresponding eigenvalue to ${}_pV_p$ with $\lambda_1 \geq \lambda_2 \geq \ldots \geq \lambda_p \geq 0$
- ${}_pF_n$ matrix of (uncorrelated) principal components

Then two pixels are represented as two vectors in the original feature space or as two columns z_j and z_k of the matrix Z and as two vectors in Euclidean space of principal components or as two columns f_j and f_k of the matrix F with

$$ f_j = {}_p\Lambda_p^{-\frac{1}{2}} * {}_pV_p^t * z_j \text{ and } z_j = {}_pV_p * {}_p\Lambda_p^{\frac{1}{2}} * f_j \tag{36} $$

Then the square of the Euclidean distance between z_j and z_k is:

$$ \|z_i - z_k\|_2^2 = (z_j - z_k)^t * (z_j - z_k) \tag{37} $$

$$ = ({}_p\Lambda_p^{\frac{1}{2}} * {}_pV_p * f_j - {}_p\Lambda_p^{\frac{1}{2}} * {}_pV_p * f_k)^t * ({}_p\Lambda_p^{\frac{1}{2}} * {}_pV_p * f_j - {}_p\Lambda_p^{\frac{1}{2}} * {}_pV_p * f_k) $$

$$ = ({}_p\Lambda_p^{\frac{1}{2}} * {}_pV_p * (f_j - f_k)^t * ({}_p\Lambda_p^{\frac{1}{2}} * {}_pV_p * (f_j - f_k) \tag{39} $$

$$ = (f_j - f_k)^t * ({}_p\Lambda_p^{\frac{1}{2}} * {}_pV_p^t) * ({}_pV_p * {}_p\Lambda_q^{\frac{1}{2}} * (f_j - f_k) \tag{40} $$

and as ${}_pV_p^t * {}_pV_p = I$, because the matrix V is orthonormal, the equation (40) turns to:

$$ \|z_i - z_k\|_2^2 = (f_j - f_k)^t * {}_p\Lambda_p^{\frac{1}{2}} * {}_p\Lambda_p^{\frac{1}{2}} * (f_j - f_k) \tag{41} $$

$$ = (f_j^t * {}_p\Lambda_p^{\frac{1}{2}} - f_k^t * {}_p\Lambda_p^{\frac{1}{2}}) * ({}_p\Lambda_p^{\frac{1}{2}} * f_j - {}_p\Lambda_p^{\frac{1}{2}} * f_k) \tag{42} $$

$$ = ({}_p\Lambda_p^{\frac{1}{2}} * f_j - {}_p\Lambda_p^{\frac{1}{2}} * f_k)^t * ({}_p\Lambda_p^{\frac{1}{2}} * f_j - {}_p\Lambda_p^{\frac{1}{2}} * f_k) \tag{43} $$

$$ = \| \tilde{f}_j - \tilde{f}_k \|_2^2 \tag{44} $$

where: $$ \tilde{f}_j = {}_p\Lambda_q^{\frac{1}{2}} * f_j \tag{45} $$

or detailed with all coefficients of $\tilde{f}_j$ (as f_j a column)

$$ \tilde{f}_j = (f_{1j} * \sqrt{\lambda_1}, f_{2j} * \sqrt{\lambda_2}, f_{3j} * \sqrt{\lambda_3}, \ldots, f_{pj} * \sqrt{\lambda_p}) \tag{46} $$

Equation (46) describes the pixel j by the values of principal components, which are weighted with the square roots of their corresponding eigenvalues.

5. CONCLUSION

This article has started with the question if it is allowed (in a strict mathematical sense) to compute Euclidean distances if the features are correlated and therefore do not build a Euclidean space.

The discussion shows that computing Euclidean distance using the original (correlated) data leads to the same result as computing Euclidean distance using (orthogonal) principal components which are weighted with the square roots of their corresponding eigenvalues.

Or by illustrating it in a graphical way: When computing Euclidean distance using the original (correlated) data then classification takes place in a Euclidean space built of principal components expanded (or contracted) by the square roots of their corresponding eigenvalues.

Thus the above mentioned question does no longer exist as now the effects are evident if applying Euclidean distance formula to correlated features. If using original data the internal structure will not be changed.

7. REFERENCES

Backhaus, K. et al, 2006. Multivariate Analysemethoden. Eine anwendungsorientierte Einführung. Berlin, Springer. 11th ed.

Bock, H.H.,1974. Automatische Klassifikation. Theoretische und praktische Methoden zur Gruppierung und Strukturierung von Daten. Göttingen, Vandenhoeck & Ruprecht.

Bortz, J., 2005. Statistik für Human- und Sozialwissenschaftler. Berlin, Springer.

Harris, C.W., 1955. Characteristics of two measures of profile similarity. Psychometrika 20, p. 289-297.

Lange, N. de, 1981. Zum Problem interkorrelierter Variablen bei clusteranalytischen Verfahren. In. Klagenfurter Geographische Schriften 2, S. 167- 184.

Lillesand, T. M., Kiefer, R.W. a. J. Chipman, 2003. Remote Sensing and Image Interpretation. New York. John Wiley & Sons Inc. 5th ed.

Mather, P.M., 1999. Computer processing of remotely-sensed images. An introduction. Chichester, John Wiley & Sons. 2nd ed.

Überla, K., 1971. Faktorenanalyse. Eine systematische Einführung für Psychologen, Mediziner, Wirtschafts- und Sozialwissenschaftler. Berlin, Springer. 2nd ed.

Vogel, F., 1975. Probleme und Verfahren der numerischen Klassifikation. Göttingen, Vandenhoeck & Ruprecht.

UPDATING GIS BY OBJECT-BASED CHANGE DETECTION

P. Lohmann, P. Hofmann & S. Müller

Institute of Photogrammetry and GeoInformation (IPI), Leibniz Universität Hannover (LUH),
Nienburger Str. 1, 30167 Hannover, Germany, mailto:lohmann@ipi.uni-hannover.de

KEY WORDS: Change detection, change indications, update landuse, landcover

ABSTRACT:

Today with the situation of rapidly emerging of high resolution earth observation data by optical and microwave sensors there is a growing need for efficient methods to derive, maintain and revise land cover data at various scales by regional, national and European authorities. Main drivers are recent and upcoming European directives and initiatives, which contain increasingly spatially differentiated monitoring and reporting obligations in agriculture, environmental protection and planning, water management and soil protection. This paper focusses on part of a current research project named DeCOVER, namely the change detection which is used to identify candidates of change in land-use (LU) or land-cover (LC). Within this project a consortium of eleven partners with co-funding from the Federal Ministry of Economics and Technology via the German Aerospace Center (DLR) an attempt is being made to develop and demonstrate an innovative and cost-efficient geo-information service aiming in the establishment of a national landcover data base to serve different monitoring and reporting obligations of official users to the EC in the fields of agriculture, environment protection, water management, soil protection or spatial planning. This data base is intended to serve with its structure as a GIS source for ontology-based semantic interoperable methods and data to meet also the requirements of other national data bases like ATKIS, CORINE CLC and BNTK.

The planned implementation of DeCOVER includes a concept for an object-based change detection attempt to efficiently update existing geo-spatial data which is described in this paper. The change information needed is derived from recent satellite images using automatic image processing and analysis. The conceptual idea includes both, manual (applying visual interpretation) and automatic image analysis steps resulting in a change layer, which highlights those areas or objects which are suspect for change and gives an indication of the direction of change.

This investigation uses multitemporal remote sensing satellite data of a spatial resolution of approximate 5 m to be comparable to the planned German RapidEye system and the existing TerraSAR-X data. Different pre-processing steps have been implemented in order to avoid seasonal effects or changes due to different imaging conditions, such as atmospheric conditions, different sun angles, etc.. However not always ideal imaging conditions can be found which result in change indications, like shadows which becomes more dominant with increasing image resolution. Further pre-processing includes an automatic haze reduction and a shade correction using an appropriate DTM. Image co-registration and automatic cloud and shade-of-clouds detection is performed. Additionally, a priori knowledge of potential change for the object classes used in the GIS of concern is used as input to control the subsequent image processing.

The concept of the change detection starts by setting up a focusing step to selectively initiate the following steps only for those objects which are considered as *changed*. Thereafter all changed objects are classified either visually (manually) or by an automatic procedure depending on the type of change detected. The decision which classification procedure is used depends on a transition-probability-matrix which indicates for each class the degree of likelihood of possible and impossible class-transitions respectively in combination with a table of available classification operators which can be applied to validate the predicted change. The transition-probability-matrix is generated manually and contains assumed possible changes from one class to another. If an automatic classification is indicated, the procedure then consists of two parts: First it is evaluated if the object's geometry is changed or if the object is changed as a whole. If a change in geometry is detected, the object of concern has to be re-segmented and re-classified. If not, the object has to be re-classified only. If a manual classification is indicated, changes will be mapped respectively. At the end the results of the visual/manual classification and the automatic classification are joined into one change layer, which holds for each changed object besides its change indication information, the objects' historical classification and its new classification. This layer can then be directly used as input for updating existing GIS databases.

This paper concentrates on the first part of the process chain, namely the focusing module. The focusing module has two tasks: First, objects have to be found in the GIS data which are affected by change. Second, the focusing module has to decide, whether the changed objects subsequently can be processed automatically or must be processed manually.

Different change indicators are implemented based on a comparison of the input satellite data of two different dates. These indicators in combination with a transition-probability-matrix are used to limit the new possible classes and control the subsequent re-cursive processing and use of operators to verify the indicated changes according to the sorted probabilities of change. The obtained results of the proposed object-based change detection process chain are compared to change-detection results obtained by completely visual interpretation. Finally all results are assembled to a resultant change indication map.

1. DECOVER BACKGROUND AND CONTEXT

In the context of GMES (Global Monitoring for Environment and Security), a joint initiative of European Commission and European Space Agency, several services are developed to provide spatial information in support of the monitoring and reporting obligations of European directives (Overview at www.gmes.info, Example Water Framework Directive Dworak et al 2005). These implementations take place with strong participation of German authorities, researchers and service providers. Current developments at the European level support a new European-wide land cover data set (Core Service Land Monitoring). This data set must be seen as a European consensus and will solely contain thematic land cover data information supporting European reporting obligations. Its geometric and thematic resolution will only partly support national and regional needs. DeCOVER (Büscher, et al., 2007) will complement and extend these developments at the national and regional level for German users.

A set of geo-information services has been designed to support national and regional users in their monitoring and reporting obligations. The DeCOVER service concept is divided into core and additional services. The DeCOVER core service has two main focal points. First, the provision of national harmonized land cover data supports the German spatial data infrastructure (GDI-DE) in providing selected and validated geo-information and second, the development and application of change detection and interoperability methods to sustain existing data bases (namely ATKIS, CLC and BNTK). The project is co-funded by the Federal Ministry of Economics and Technology (BMWI) via the German Aerospace Center (DLR) and implemented by a consortium of 11 partners (see Table 1) each using its own expertise and specialized skills.

Partner	Expertise
EFTAS GmbH	Coordination, Agriculture
GAF AG	Validation, Forestry
DELPHI IMM GmbH	Interoperability, Link to INSPIRE
IPI, LUH	Innovation, Quality Control
Infoterra GmbH	Spec. Core Service, Economics, Link GMES
RapidEye AG	Implement. Process. Chain
GDS GmbH	Change Detection, SAR-Appl., Urban Areas
Definiens AG	SW support,Object oriented Segmentation. & Classific. of Water Areas
RSS RemoteSensing Solutions GmbH	Nature Landscape conservation
Jena.Optronik GmbH	SAR-Optical Co-Registration
DLR Assoc. Partner	Support. Urban, SAR-Proc.

Table 1: Consortial Partners, Expertises and Skills

The overall structure of the project is shown in Fig. 1. In a coordinated attempt the processing (segmentation & classification of the satellite data is being done according to rules and directives as demanded by European and National directives and policies. Much effort has been put into the consideration of user requirements, which directly influence the service definition and design of the DeCOVER database and its production chain which has a strong feedback to user demands. Methods

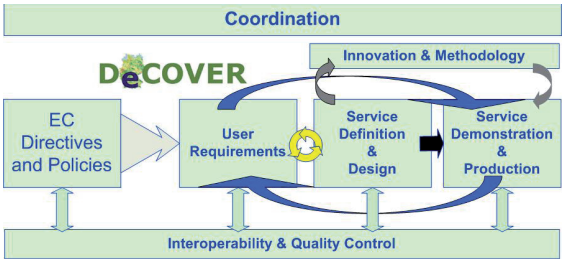

Figure 1: DeCOVER Organisation

developed and strategies used are being implemented for the creation of the core service and have direct impact to the processing chain, quality control and data revision, considering at each stage the specification and standards as demanded by the interoperability task. An initial user requirement analysis has shown real synergies between (thematically) different user needs. Parallel to the user requirement analysis, interoperability potential between the identified land cover classes has been analyzed, to optimize synergies between existing data sets and newly collected information. The currently tested core-service object catalogue includes 39 land cover (LC)/land use (LU) classes arranged in hierarchical order. The detailed object catalogue and mapping guide can be found in the user portal of the DeCover homepage (http://www.decover.info/).

There are three major areas of innovative research and development in the project, where methodologies are developed, namely

- the area of semantic interoperability
- change detection
- data fusion of optical and SAR images

In the following this paper will focus only to the second part, the change detection.

2. CONCEPT OF DECOVER CHANGE DETECTION

2.1 General

Change detection (CD) algorithms can be classified either into the comparison of classes following an interpretation at different dates (post-classification) or to image differencing (Singh, 1989). The former focuses on the comparative analyses of independently produced interpretations from different times, the latter comprises simultaneous analysis of multitemporal data. Because a second classification of the whole area results in costs, that are far too expensive for most of the users another procedure is envisaged here. CD in this case is regarded not as a change mapping but rather as a "notification/indication" of change with a possibility to indicate geometric and attributive change occurrences (i.e. class transition). It relates to objects as part of an existing database but compares two images at different dates on pixel level, giving a pixel-based indication of LU/LC change. Methods for the comparison of images from different dates may be grouped into those which use univariate image differencing alone (Singh, 1989, Fung, 1990), methods to compare vegetation properties like NDVI or Tasseled Cap Tranformations (Richards, 1993), or change vector analysis (Lambin, 1994, Bruzzone et al, 2002). A comprehensive overview of existing pixel based techniques, their advantages, disadvantages and resulting accuracies is given by Lu et al, 2004. Relating these pixel-based indications to objects means, that an approach for integration and validation of the indications is needed. There are several ways to implement such

a procedure as has been shown by different authors (Schöpfer, 2005, Busch et al., 2005 and Gerke et al., 2004). Because users of DeCOVER prefer some type of a "change notification", which might also be useful for their specific application, like updating of user operated databases (i.e. ATKIS) by proprietary techniques the following attempt has been made to set up a framework for CD.

2.2 The Concept of Change Detection Workflow

2.2.1 The Focusing Module

A focusing module has been designed in close cooperation between the company GeoData Solutions (GDS) and the Institute of Photogrammetry, University of Hannover (IPI). It is a central part of the total CD-concept (see Section 2.2.2) and applies image differencing. Steps of pre-processing, necessary to render the two images comparable in both the spatial and spectral domains are included. Fig. 2 shows an outline of the focusing module.

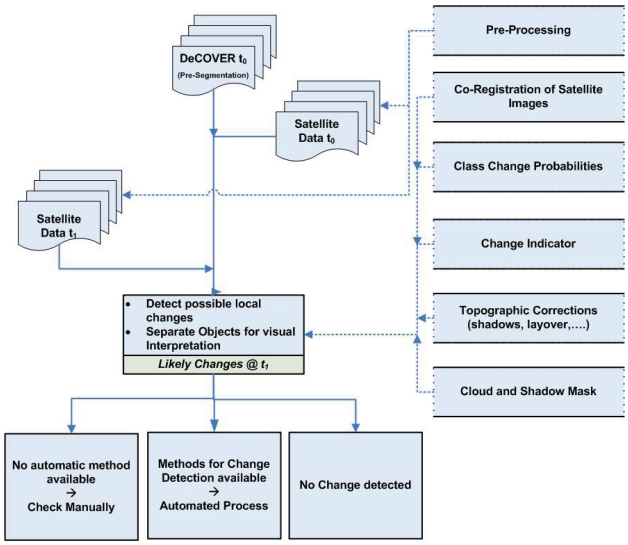

Fgure 2: The Focusing module

Concerning the spatial domain the images have to be co-registered, which is critical, considering the combined use of optical and SAR-data or using high resolution optical satellites with different viewing angles. A "registration noise" is obvious in looking at the indicator images as of section 3, where even though advanced techniques for co-registration had been used, differences from different looking directions become visible. Changes in light and atmospheric conditions between both observations may be a potential further source of error. Although atmospheric corrections as well as image normalization is performed and cloud and shadow masks are generated in the processing chain, still the appearance of shadows at buildings in the high resolution data (IKONOS, Quickbird, SPOT5) is apparent.
The focusing module computes the pixel-based CD indicators and compares on the given initial object level if a class change is observed or not. As the difference image is assumed to be normal distributed, all pixel belonging to the +/- 0.1 quantile are considered to be change pixel. Because a crisp threshold is very often not satisfactory a new fuzzy approach is proposed (see 2.2.2). At the moment spectral differences, PCA, Texture and IHS-differences (see Fig. 3) are investigated but many more may be applied.

The data used in this work consists of two IKONOS multispectral images of May 28th, 2005 and April 16th, 2007 resampled to 5m resolution. Concerning the image dates it is obvious, that many changes with respect to phenology can be expected.
It turned out that using IHS-Difference indicator between both dates overestimates apparent changes to a certain extent. This is especially true for

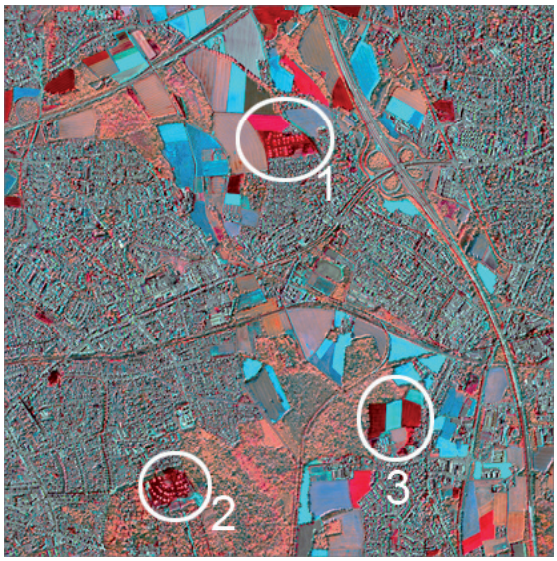

Figure 3: IHS-differences reflecting vegetation changes

vegetated areas, but color (1 to 3 in Fig. 3) can be used as an indication of change from/to vegetation cover, i.e. vivid red indicates a change from vegetation cover to bare soil, vivid blue from bare soil to vegetation cover. In addition by looking to the settlement areas it can be seen that shadow (because of different sun angles and different look angles at image acquisition) plays an important role. It can be noticed too, that a light pink tone accounts for the different image acquisition dates. For built up areas the texture information (Gimel'Farb, 1997) proved to give the best results. However the results shown in section 3 do yet not include the IHS tests.

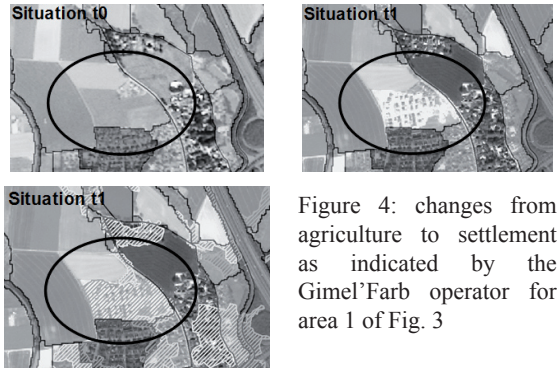

Figure 4: changes from agriculture to settlement as indicated by the Gimel'Farb operator for area 1 of Fig. 3

2.2.2 From Pixel to Object Change Indications

Once the change indicators have been computed, they are spatially combined before they are compared to the t_0 reference map (i.e. the existing database). One way of combining is the modification of a procedure which has been used by Earth Satellite Corporation, named Cross-Correlation -Analysis (Koeln et al., 2000). In this method class boundaries from the older thematic

map separate image pixels into distinct class zones. Within these boundaries the pixels as of a new unsupervised classification are validated using a multivariate z-statistic. This idea has been adopted within this project using the old database as reference and computing within the object boundaries the Z-Value from a stacked (multiband) indicator image:

$$Z_i = \sum_{i=1}^{n} \left(\frac{r - \mu}{\sigma_i} \right)^2$$

with:
n = Number of features (indicators) used
r_i = feature value of band i
μ = mean of band i for the segment from period $(t-1)$
σ_i = stand. dev. of band i for the segment from period $(t-1)$

According to Fig. 5 this value then is thresholded to indicate a change for the object selected. An á priori class transition probability matrice ($\mathbf{T}_P$), which has been set up beforehand and which reflects the probabilities of

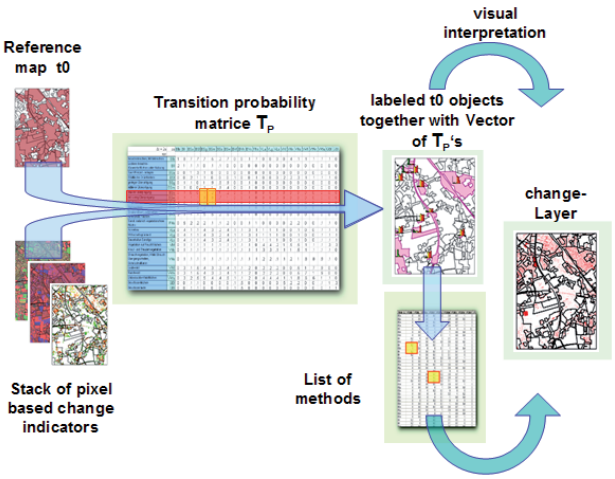

Figure 5: Use of Transition Probability Matrice

changes from one class to another is used to compute for the t_0 - objects a change vector consisting of a list of new possible classes sorted by the probability of change to that class.

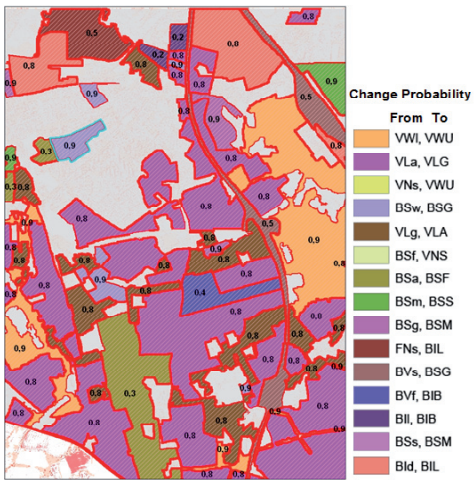

Figure 6: Change Probabilities and Target Classes as of $\mathbf{T}_P$

The focusing module then controls the way of further checking. If for the most probable class change an automated validation (re-classifier) exists it is applied. If no automatic method exists the object is labeled for further visual interpretation. If the first (most probable) change cannot be verified the next class out of the $\mathbf{T}_P$-vector is tested, until a change can be validated or the object remains labelled as unchanged. It should be noted, that the $\mathbf{T}_P$-matrice is a living document which is set-up by the experience of the DeCOVER partners first and then updated by the statistics of changes over time.

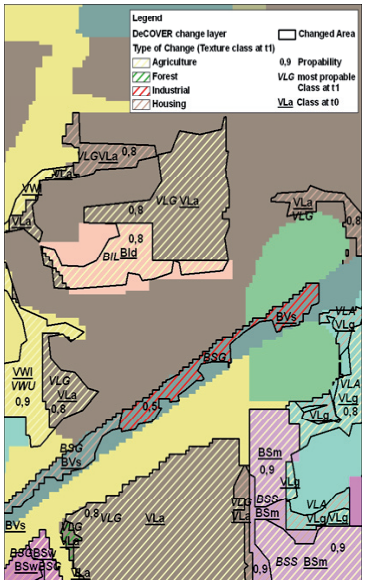

Figure 7: Change layer as output according to Fig. 5

As most of the operations are implemented in the Definiens Developer Software another way of combining the indicator images is planned, avoiding crisp thresholds for specific indicators. Thresholds are difficult to set and using more flexible fuzzy membership functions is desirable.

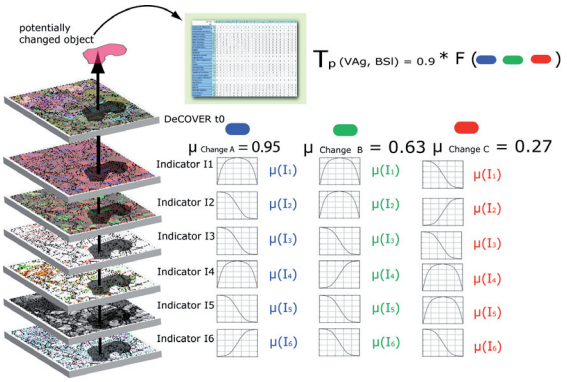

Figure 8: Using fuzzy membership functions and the $\mathbf{T}_p$ matrix

For a given object $\mathbf{T}_p$ contains the probability change vector which is combined with the membership functions $\boldsymbol{\mu}$ of possible transitions in a rule based manner to give the result as shown in Fig. 7.
The design of the total CD workflow is shown in Fig. 9.
Following the decision being made by the focusing module and the selection of automatic or manual (visual) interpretation methods the results are combined within the CD layer (Fig. 7). For all labelled objects, for which a change could be validated the presumed target class and the degree of probability is stored.

If no exact change indication is possible, which for instance can happen in the case of very specific LU classes that only can be verified or classified by additional expert information, a flag is set. This flag serves as an indication for the experts in the processing chain, that this object is to be handled specially. Then the change layer is used in the processing chain for updating the changed objects.

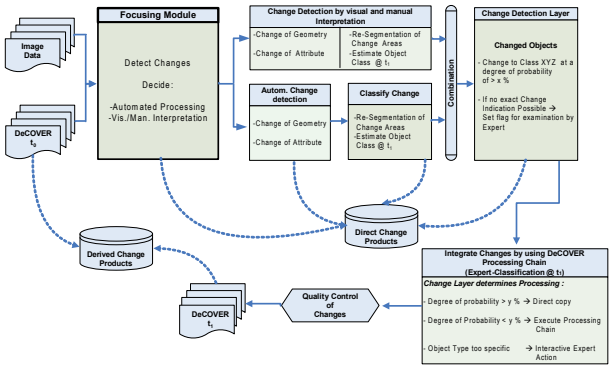

Figure 9: Design of the complete CD workflow

The intermediate results like those of the indicators can be stored as "Direct Change" products, for further use by the end-user. The current DeCOVER processing chain applies a sequential processing in the sequence of the main categories "Urban", Water", "Forest", "Agriculture" and "Sub-natural open areas". The identified new object type together with its change probability now is used to enter the sequence of classification operations at the appropriate position. This is followed by a quality control, which follows a procedure described by Hofmann et al., 2007.

2.3 Prelimnary Assessment of Indicators used

As reported above the focusing module computes pixel based indicators. Out of the variety of possible indicators (Lu et al., 2004) a selection is shown based on principal components (PCA), image differencing using the Pan channel and a 10% quantile (DP, see 2.2.1), texture like the Gimel'Farb-operator (GF), and the Haralik operators (variance H2 and dissimilarity H5).
The reference used for this investigation is based on a visual interpretation of the changes for DeCOVER objects out of Fig. 3 originating from 2005. A total of 877 objects belonging to the main object categories "Urban", "Vegetation" (mixture of "Forest", "Agriculture" and "Sub-natural open areas") have been checked by using the 2005 object boundaries the visual change interpretation and the pixel-based indicators. A rating has been set up using the classification as shown in Table 2.

Change in	Reference true	Reference false
Indicator true	True positive (TP)	False positive (FP)
Indicator false	False negative (FN)	—

Table 2: Rating nomenclature used

Indicator	Object	TP	FP	FN	DP	BF
H5	U	3	56	10	23	95
	V	0	26	4	0	100
H2	U	20	45	11	65	69
	V	4	16	4	50	80
GF	U	5	61	2	71	92
	V	1	29	0	100	97
DP	U	7	64	0	100	90
	V	1	28	0	100	97
PCA	U	7	66	0	100	90
	V	2	24	0	100	92

Table3: Differences Vis. Interpr. to Indicators [%]

Calculating the results according to Table 2 allows to rate the indicators by using measures which have been described by Lin, 1998 and Müller, 2007. They use the Detection Percentage (DP) and the Branching Factor (BF)

$$DP = \frac{TP}{TP+FN} \quad ; \quad BF = \frac{FP}{TP+FP}$$

DP [%] reflects the amount of automatically indicated object changes, while BF [%] gives the percentage of found objects not belonging to the indicated type. The goal is to maximize DP while minimizing BF.
A problem with this assessment is that the reference which is used here is not a pixel-based one. So the results (Table 3) reflect more or less trends, than exact measures. There is a clear indication, that most differences belong to "False positive". This is due to false detections at the pixel level because of shadows and look angles, as can be seen by looking to Fig. 10, which shows the difference of the indicator image and a simple morphological opening. These false indications can be avoided by integration using a threshold distance between detections or at object level taking into account a minimum object relevance area of for instance 0.4 ha.

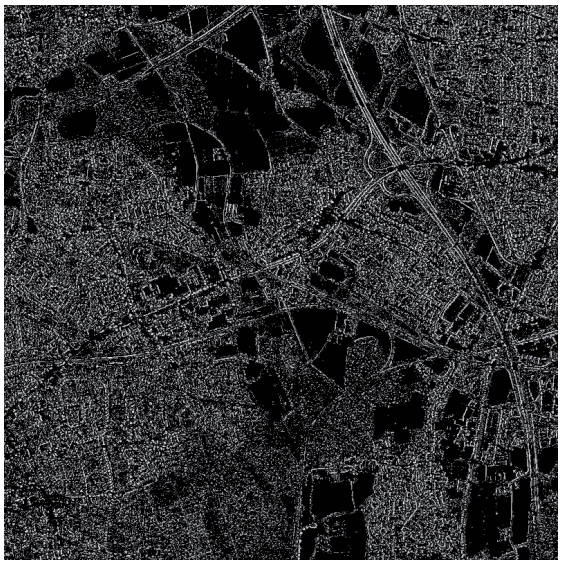

Figure 10: Difference of indicator image and its opening

In any cases the procedure as described allows a quick rating of the indicators, which presently for one indicator alone is very poor, but their combination or integration as described above may be comprising and is tested at the moment.

3. CONCLUSIONS

The paper pointed out some possibilities in using indicator images for highlighting areas of change. The results however show that no matter what single pixel based indicator is used, further integration to object or segment boundaries has to be done. Furthermore a combination of different operators possibly improves the results. Presently many other operators (especially the IHS and derivates thereof) are tested and the procedures for integrating their results to object level in combination with the class-transition probability matrice is developed and will be presented in future.

4. REFERENCES

Bruzzone, L.; Cossu, R., 2002 : Analysis of Multitemporal Remote-Sensing Images for CD: Bayesian Thresholding Approaches, University of Trento, Technical Report No: DIT-02-0031

Büscher,O.; Buck,O., 2007: DeCover- Geoinformation Services to Update and Supplement Land Cover Data for German Decision Makers, ISPRS Hannover Workshop: High Resolution Earth Imaging for Geospatial Information , IntArchPhRS XXXVI. Band 1/W51. Hannover, CD .

Busch, A.; Gerke, M.; Grünreich, D.; Heipke, C. ; Liedtke, C.; Müller, S., 2005: Automatisierte Verifikation topographischer Geoinformation unter Nutzung optischer Fernerkundungsdaten. In: PFG (2005), Nr. 2, S. 111- 122

Schöpfer, E. 2005: Change Detection in Multitemporal Remote sensing Images Utilizing Object-Based Image Analysis, Doctoral Thesis, University of Salzburg

Fung, T., 1990: An assessment of TM imagery for Land-cover Change detection, IEEE Transactions on Geoscience and remote sensing, 28, 12, 681-684

Gerke, M.; Heipke, C.; Willrich, F., 2004: Automatisierte Qualitätskontrolle von Geobasisdaten auf der Grundlage digitaler Luftbilder : Proceedings Arbeitsgruppe Automation in der Kartographie. In: Mitteilungen des BKG (Hrsg.). Band 31. Frankfurt a. Main, S. 55-58 .

Gimel'Farb, G.L., 1997 : Gibbs fields with multiple pairwise pixel interactions for texture simulation and segmentation. – Rapport de Recherche RR-3202, INRIA, Sophia Antipolis, France

Hofmann, P.; Lohmann, P., 2007: A Strategy for Quality Assurance of Land-Cover/Land-Use Interpretation Results with Faulty or Obsolete Reference Data : IntArchPhRS XXXVI. Band 1/W51. Hannover, 6S., CD .

Koeln, G.; Bissonnette J., 2000: Cross-Correlation Analysis: Mapping LandCover Changes with a Historic LandCover DataBase and a Recent, Single-date, Multispectral Image, Proc. 2000 ASPRS Annual Convention, Washington, DC http://glc.org/wetlands/flora-fauna.html (last visited February 2008)

Lambin, E. F.; Strahler, A. H., 1994: Change-vector analysis in multitemporal space: a tool to detect and categorize land-cover change processes using high temporal resolution satellite data, Remote Sensing of Environment. 48, 231–244.

Lin, C.; Nevatia, R., 1998: Building Detection and Description from a Single Intensity Image. Computer vision and Image Understanding, Bd. 72(2):101–121

Lu D.; Mausel P.; Brondisio E.; Moran E., 2004: Change detection Techniques, Int. J. Remote Sensing, 2004, Vol. 25, no. 12, 2365-2407

Müller, S., 2007 : Extraktion baulich geprägter Flächen aus Fernerkundungsdaten zur Qualitätssicherung flächenhafter Geobasisdaten, Dissertation, Wissensbasierte Bildauswertung-Schriftenreihe des Instituts für Informationsverarbeitung der Leibniz Universität Hannover, Band 9

Singh, A., 1989: Digital change detection techniques using remotely-sensed data. International Journal of Remote Sensing. 10, 989-1003.

STEREOCORRELATION AND IMAGE FUSION: MANFRED EHLERS AT THE UNIVERSITY OF GEORGIA

M. Madden

Center for Remote Sensing and Mapping Science, Department of Geography,
University of Georgia, Athens, GA 30602, USA, mmadden@uga.edu

KEY WORDS: Manfred Ehlers, University of Georgia, stereocorrelation, image fusion

ABSTRACT:

One of the early stages of Prof. Dr.-Ing. Manfred Ehlers's career was conducted at the Laboratory of Remote Sensing and Mapping Science (LRMS) where he was a Research Scientist from 1984 to 1988. Working with Roy Welch, and Tommy Jordan, his research included evaluation of the geodetic accuracy and cartographic potential of SIR-B and Landsat-4 and -5 Thematic Mapper (TM) image data, digital image stereocorrelation and multimodal image fusion. He also developed methods for merging multi-sensor, multi-resolution and multi-temporal imagery that nearly 20 years later led to his return to UGA and development of the Ehlers Fusion method. His work furthered the integration of remote sensing and geographic information systems (GIS) and foreshadowed the advent of virtual globes and Digital Earth initiatives.

1. ISPRS LED MANFRED TO UGA-LRMS

1.1 ISPRS Commission VII Symposium, Toulouse, France

In September of 1982, two tall men met at the banquet of the International Society for Photogrammetry and Remote Sensing (ISPRS) Commission VII Symposium in Toulouse, France. Roy Welch from the University of Georgia and Manfred Ehlers, a Research Associate at the Institute for Photogrammetry and Engineering Surveys, University of Hannover, Germany found themselves at the Symposium social being held out of doors on a beautiful late summer night. Amid southern French cuisine and wine, and at least one drinking game that involved Fred Doyle standing on his head, a lasting friendship and professional relationship was formed. Two years later, Manfred, his wife Margret and their young daughter, Franziska, moved from Germany to Athens, Georgia so Manfred could join the University of Georgia's Laboratory for Remote Sensing and Mapping Science (LRMS), a laboratory newly formed by Roy Welch within the Department of Geography.

1.2 Merging Multi-sensor Image Data

When Manfred Ehlers arrived at UGA in 1984, his knowledge of mathematics and computer programming provided him with the background he needed to perform rigorous testing and manipulation of satellite images. His initial research at LRMS followed Roy Welch's assessments of image quality and cartographic potential. He joined Thomas Jordan and Welch in a comparative evaluation of the geodetic accuracy and cartographic potential of the relatively recently launched Landsat-4 and Landsat-5 Thematic Mapper (TM) imagery (Welch et al., 1985; Ehlers and Welch, 1988a and 1988b).

While other scientists at this time were interpreting features on hardcopy "pictures" and false color displays of landscapes acquired from space, Manfred and Roy understood them as simply digital files of numbers arranged in rows and columns. As such, these data could be subjected to any number of mathematical transformations and there was no reason images from one satellite could not be merged with those of another sensor. Manfred's subsequent research involved the merging of multiresolution images such as SPOT HRV and Landsat TM (Welch and Ehlers, 1987). They also explored the blending of imagery from optical and radar sensors. In 1988, they integrated Shuttle Imaging Radar-B (SIR-B) with Landsat TM and concluded the merged products were suitable for planimetric mapping at scales of 1:100,000 or smaller (Welch and Ehlers, 1988).

1.3 Automated Stereocorrelation

The across-track pointable sensors on-board SPOT satellite platforms provided, for the first time, options for stereo image data. Welch, Ehlers and Jordan next explored a new realm of digital image processing, automated stereocorrelation to produce digital elevation models. Operating on the PDP 1126 mini-computer, Manfred wrote programs that resulted in elevations at the rate of 12 minutes per pixel with over 50,000 arithmetic operations required per pixel.

Stereo scenes acquired by across-track sensors suffered from temporal delays between adjacent data acquisitions and increased chances of cloud cover. Making the most use of available imagery, the LRMS team also experimented with Landsat TM side lap areas and multi-sensor imagery covering the same geographic area (Ehlers and Welch, 1987 and 1988).

1.4 Early Days of Desktop Mapping System

In the mid 1980s there was a rapid improvement in the computing performance of personal computers (PCs). As costs decreased and capability increased, university laboratories such as LRMS opted to transfer their research platforms from expensive, large and resource demanding mini-computers to desktop PCs. The algorithms and digital image processing procedures Welch, Ehlers and Jordan had previously developed were compiled into a single mapping package to create the Desktop Mapping System (DMS). A small company, R-WEL, Inc. was formed and UGA created the first official agreement with a company to allocate the resources from sales of the program. In 1987, the DMS was ready to demonstrate in the Exhibit Hall of the American Society for Photogrammetry and Remote Sensing (ASPRS) Annual

Conference held in Baltimore, Maryland. Figure 1 shows the LRMS team eager and ready to demonstrate DMS capabilities to the ASPRS Conference participants.

Figure 1. The UGA-LRMS team exhibiting DMS at the 1987 ASPRS Annual conference. Left to right are Thomas Jordan, Devlin Fung, Manfred Ehlers, Demitrios Papacharalampos, Marguerite Madden and Roy Welch.

Improvements in computer processing resulted in increased speed of autostereocorrelation and before long results were being measured in DEM points per minute instead of minutes per point. The DMS also provided users with 2.5D terrain perspectives and the option to wear anaglyph glasses for early true 3D displays (Figure 2).

1.5 Integration of Remote Sensing and GIS

Along with advancements in remote sensing and digital processing, the late 1980s also saw a natural progression towards the integration of remote sensing with geographic information systems (GIS). Roy Welch published a landmark paper in Photogrammetric Record that documented the integration of photogrammetric remote sensing and database technologies for mapping applications (Welch, 1987) and this was followed by a joint paper by Welch and Ehlers (1988) on LIS/GIS products and issues. The integration of remote sensing and GIS would be a research topic Welch and Ehlers would share for many years to come, each in their own direction, but originating from their joint research at UGA in the 1980s.

2. POST UGA-LRMS

2.1 Manfred Ehlers Returned to UGA-CRMS

Manfred and Margret left Athens, Georgia in 1988 and decided to brave the cold winters at the University of Maine. They adapted well to life in the north and following the birth of their second child, Niklas, found their way back to their homeland, Germany, by way of The Netherlands. In 20 years time, Manfred found himself in need of a break from the pressures of administrative duties which did not allow him enough time to devote to his research interests. Following the retirement of Roy Welch in December of 2003, Manfred was able to take a sabbatical leave and return to UGA. He filled in as a Visiting Instructor and taught Remote Sensing of Environment to upper level undergraduate and graduate students in the Department of Geography. He and Roy Welch's Ph.D. student, Yangrong Ling, also worked on image fusion techniques examining the effects of spatial resolution ratio of images of different pixel size on image fusion quality and Fast Fourier Transform (FFT)-enhanced Intensity-Hue-Saturation (HIS) image fusion techniques for preserving spectral and spatial information (Ling et al., 2007 and 2008). This research led to the famous Ehlers Fusion method sited by many as an improved method of image fusion for maintaining color fidelity.

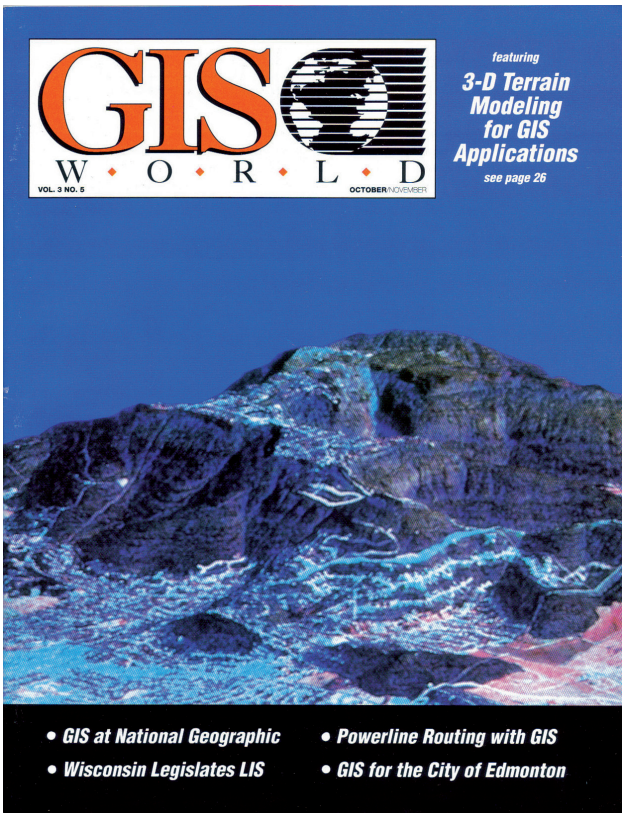

Figure 2. A merged panchromatic SPOT HRV and multispectral Landsat TM image draped on a 2.5D perspective view of the terrain in DMS and shown on the cover of a 1990 issue of GIS WORLD.

3. CONCLUSIONS

The four years Manfred Ehlers spent at UGA fostered a lifetime of friendship and collaboration. Individual strengths and talents can be augmented when colleagues join together to take advantage of advancements in technology and opportunities to evaluate new imagery and analysis capabilities. We look forward to many more years of collaborative research grounded in true friendship.

4. REFERENCES

Ehlers, M. and R. Welch, 1987. Stereocorrelation of Landsat TM images. *Photogrammetric Engineering and Remote Sensing*, 53(9), pp. 1231-1237.

Ehlers, M. and R. Welch, 1988a. Kartographische Leistungsfähigkeit von Landsat TM-Aufnahmen (Teil I). BuL Photogrammetrie und Fernerkundung, 56(4), pp. 138-148.

Ehlers, M. and R. Welch, 1988b**.** Kartographische Leistungsfähigkeit von Landsat TM-Aufnahmen (Teil II). BuL Photogrammetrie und Fernerkundung, 56(5), pp. 157-166.

Ehlers, M. and R. Welch, 1988. Comments on "Stereocorrelation of Landsat TM images", A Response. *Photogrammetric Engineering and Remote Sensing*, 54(4), p. 474.

Ling, Y., M. Ehlers, E.L. Usery and M. Madden, 2008. Effects of spatial resolution ratio in image fusion, *International Journal of Remote Sensing*, 29(7): 2157–2167.

Ling, Y., M. Ehlers, E.L. Usery and M. Madden, 2007. FFT-Enhanced IHS transform method for fusing high-resolution satellite images, *ISPRS Journal of Photogrammetry and Remote Sensing*, 61(6): 381-392.

Welch, R. and M. Ehlers, 1988. LIS/GIS products and issues: A manufacturers' forum. *Photogrammetric Engineering and Remote Sensing,* 54(2), pp. 207-210.

Welch, R. and M. Ehlers, 1988. Cartographic feature extraction from integrated SIR-B and Landsat TM images. *International Journal of Remote Sensing*, 9(5), pp. 873-889**.**

Welch, R. and M. Ehlers, 1987. Merging multiresolution SPOT HRV and Landsat TM data. *Photogrammetric Engineering and Remote Sensing*, 53(3), pp. 301-303.

Welch, R., T.R. Jordan and M. Ehlers, 1985. Comparative evaluations of the geodetic accuracy and cartographic potential of Landsat-4/-5 TM image data. *Photogrammetric Engineering and Remote Sensing,* 51(9), pp. 1249-1262. Erratum in *Photogrammetric Engineering and Remote Sensing*, 51(11), pp. 1799-1812.

GEOINFORMATICS PAVES THE WAY FOR A VIRTUAL 3D-CAMPUS

Ulrich Michel, Kai Behncke, Karsten Hoffmann, Christian Plass, Jens Schaefermeyer, Constanze Tschritter & Norbert de Lange

Institute for Geoinformatics and Remote Sensing (IGF), University of Osnabrueck, Seminarstrasse 19a/b, D-49069 Osnabrueck
umichel@igf.uni-osnabrueck.de

KEYWORDS: Pocket PC, GIS, Content Management System, UMPC, Open Source, GPS

ABSTRACT:

Various 2D & 3D applications have been developed at the Institute for Geoinformatics and Remote Sensing (IGF) at the University of Osnabrueck. In addition to an art and culture guide, an area information system and an interactive map application for the University of Osnabrueck have been developed, based on the so-called MapServer technology. Furthermore, a VRML scene showing three-dimensional models of several buildings of the university and the City of Osnabrueck has been created. The purpose of those applications, among other uses, is to provide navigational aid. For the administration of associated attribute data a complex management system was designed and built. These applications are based on Open Source software and therefore can be used in combination with other software products.
This paper describes how these applications can be used in mobile devices and to what extent mobile devices are deployable for the acquisition of necessary base data. In addition to common mobile devices a new group, the so-called Ultra Mobile PCs (UMPC), was recently developed. These devices offer many useful properties, which can be utilized in our projects.

1. INTRODUCTION

Currently a web-based system for visualization and georeferencing of university buildings as well as for the management of additional building data is being developed at the IGF (Michel et al, 2007a). This application is especially interesting due to its ability to display buildings two- and three-dimensionally, the generation of associated attribute data through a database and its provision of a mobile component.
Besides students, lecturers and university staff the potential users of the future system could be any internet user, who wants to obtain an insight into, and overview of, or require current information about buildings, rooms and people.
The prototype of a 2D system (fig. 1), which represents a synthesis of Content Management System (CMS) and mapping application, and is based on Open Source Software, has already been introduced at the CeBIT in Hannover, the world's largest trade fair. A 3D version (VRML linked to a CMS, fig. 2) has been presented at the conference „Gi-Tage-Nord" in 2007.
In addition to software development, another emphasis is on the use of modern hardware like Pocket PCs (PDA) and Ultra Mobile PCs (UMPC) in connection with WLAN and GPS.

2. AREA INFORMATION SYSTEM GEOPLP

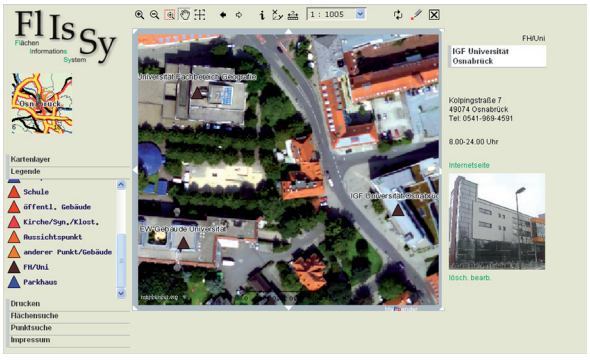

Figure 1: 2D Web GIS Application

"GeoPLP" is an application based on MapServer, Mapbender and PostgreSQL/PostGIS. It was originally developed as a system for the management of area objects and was later complemented by additional programming (Michel et al, 2007b). In general it is capable of realizing many different tasks especially due to its boundless expandability. For example, point objects (car-parks, bus stops, shopping malls etc.) are also integrated at the moment. Within the emerging system the user of the Web GIS can localize objects quickly and comfortably, and is able to query the associated information.
The geodata is visualized by the UMN MapServer. Mapbender is used as a Web GIS client. The entire point data and their attributes are stored in the database PostgreSQL/PostGIS, which also allows the data administration. A user-friendly search function was integrated in the Web GIS client. The user can search for street names and buildings, as well as measure distances and zoom to different scales on the map.
The individual layers can also be switched on or off interactively. Additional information is being accessed by clicking on a building. For example, it is planned to illustrate, the location of the departments in their corresponding buildings or, for example, to inform on special events taking place at the selected facility. A Point object can be digitized within the Web GIS client. In this connection not the usual in Mapbender known course of action via a transactional Web Feature Service (WFS) with the help of the software „Geoserver" is taken, but objects are entered into the database via JavaScript and PHP in the „Well Known Text (WKT) format". Additionally, attribute values which can be assigned to the objects by the user by means of manageable select lists are directly administrable. That way a straightforward generation of new objects is guaranteed.
The integration of a WFS along with the parsing of the data via PHP and JavaScript allows for example highlighting within the client. When moving the cursor over an object additional information is displayed. Therefore geometrical information is being integrated and visualized within Mapbender via WMS and WFS, respectively.

being integrated and visualized within Mapbender via WMS and WFS, respectively.
A special feature of the application is the Content Management System (CMS), which assures a quick and easy way to manipulate all kinds of attribute data. The CMS can manage new digitized objects at once and it allows the creation of new data or the deletion of existing attribute data. Additionally, advanced user management capabilities have been integrated.
Administrators can enter new geodata in a simple way. The data will be embedded in a shapefile and stored with the help of various PHP scripts and system commands within the PostgreSQL/PostGIS database.
There is a direct link between Web GIS client and CMS. The user can easily switch from CMS to the client and from the client to the CMS. Due to direct linkages to the map material, changes in attribute data, such as an object category (e.g. a display symbol) have a direct impact on the associated map. It is also possible to open a Google Maps application from the Web GIS client, which provides additional help for orientation and navigation.

3. VRML-RBIS

The combination of a visualization component and a CMS is currently also being developed for the 3D sector. Within the scope of the project „Automated development of 3D city models“,for example, an attribute data link to three-dimensional university buildings has been implemented (see also Michel and Bockmuehl 2006) The application consists of a main window, showing a virtual reality scene, and an information window for written building information together with 2D photos, all managed by the Room Allocation Information System RBIS (fig. 2). Individual buildings can be selected in the 3D world via ”viewpoints” or from a list of buildings inside the information window. The location of the observer changes according to the selected object. At the same time the associated information is being displayed within the information window.

Figure 2: 3D world and CMS combined

4. SYSTEM STRUCTURE

It is possible to virtually walk into the buildings. This can be done in the information window by selecting relevant rooms after choosing the floor of interest. The displayed data contain information about room allocation, phone and internet connection, as well as WLAN access (fig. 3).

Figure 3: Content Management System

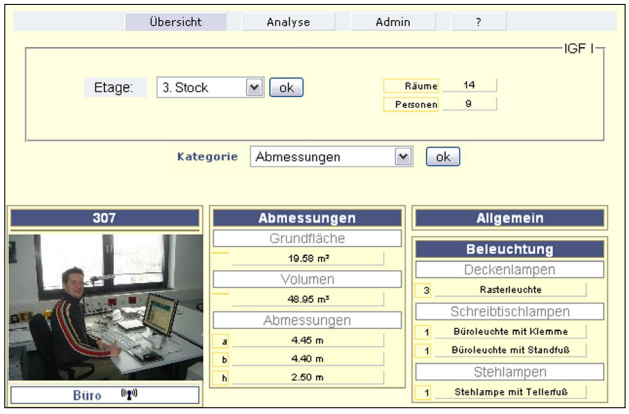

The opening of relevant doors allows the user to catch a glimpse of the room’s interior in the 3D world (fig. 4).
In general, every object of the virtual world can be linked to the database. However, time and effort of programming, modelling and maintenance increase accordingly. For this reason, many details, such as the display of current room schedules on virtual doorplates, have not been implemented yet.

Figure 4: Virtual computer room and room information

The database RBIS (2D and 3D visualization excluded) is able to run on Pocket PCs if they are connected to the internet via University WLAN (fig. 5). In this way certain information about the rooms, for example, the number of power supplies, can be collected and retrieved very easily. Data updates take place directly at the server. Thus, additional data input or synchronisation with pre-existing data can be avoided. Drawbacks are mainly that it is only possible to use special “PDA software” and that the small display results in limitations for example regarding the handling of the devices. The use of a mobile web server is still not possible, which means that some functions such as the possibility to work with PHP are not an option yet. Ultra Mobile PCs represent a promising alternative regarding memory intensive applications in particular.

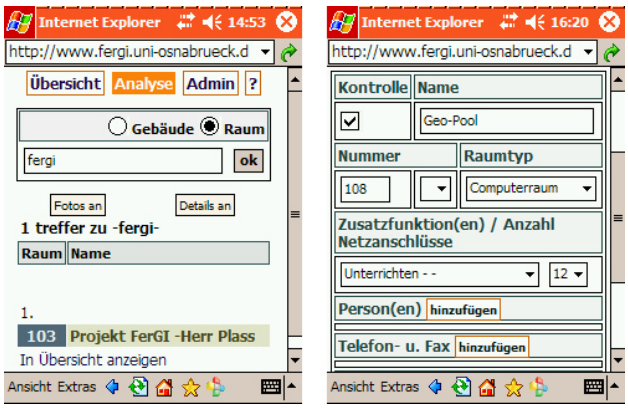

Figure 5: The Room Allocation Information System running on a PDA

For the realization of project ideas and implementation of basic possibilities an ASUS (R2H) UMPC was used. ASUS has shown to be a leading provider of new technology for mobile computers with the development of up-to-date digital devices based on Intel platforms and Microsoft software solutions.
UMPCs were designed for the growing demand of business users, who want to work efficiently with one single well-appointed device when out of the office, without having to make compromises in connectivity and security. Given its considerably more powerful performance and its larger display (800 x 480 pixel), the UMPC excels PDAs. Features like these offer many new fields of application. One of them is, for example, the on-site collection of complex structures via on-screen digitalization. In this way it is possible to capture geo objects which either are not visible on air photos or were still non-existing at the time of image acquisition. These are, for instance, green spaces at the university site, which where built after the digitation created the basis for a more accurate green space management.
The ASUS R2H is equipped with WLAN and a GPS receiver. It allows the use of conventional desktop (GIS) software and disc-space-intensive geodata through a CPU performance of 900 MHz, 786 MB memory and a 60 GB hard-drive.
Apache web server, PHP, an internet browser (Mozilla Firefox) and the GPS program “u-center” have been installed on the UMPC (fig. 6).

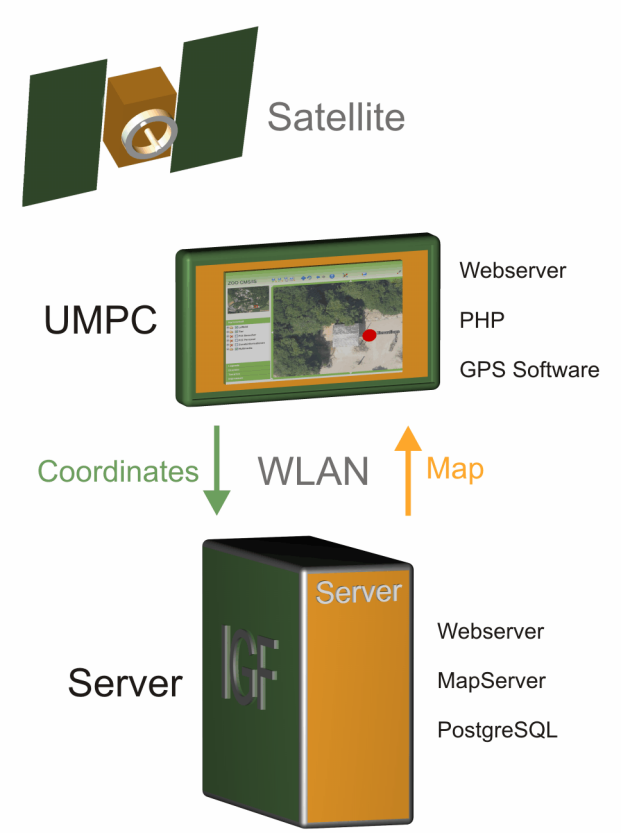

Figure 6: Schema of a GPS-supported system consisting of UMPC and Open Source software or Freeware respectively

The received GPS coordinates are read out at runtime of the NMEA-String of the u-center log file via a PHP script and subsequently transformed to Gauss-Krueger coordinates. These are then sent to a server via WLAN and stored in a PostgreSQL/PostGIS database.
The application launches itself every 30 seconds via JavaScript. Every time it launches an algorithm checks which data was added since the last launch. Newly received coordinates are then written into the database, which consequently is continuously completed. On the server the UMN Mapserver retrieves the GPS coordinates and displays them as layers. In theory, the user can then see his/her current location on a map in the internet browser, when he/she accesses an active WLAN (fig. 7).

Figure 7: Possible GPS-supported web-based navigation via an ASUS UMPC

5. OUTLOOK

The integration of a Location Based Service (LBS) will be created next. As aforementioned, the system “GeoPLP” is applicable to many different areas, including the CMS.
A web GIS application listing all the restaurants of the City of Osnabrueck is intended to be partly accessible by PDAs. Besides, a visualization component, users will receive information about offers or special events at places of interest while walking through the city.

A routing application will be also integrated in the web GIS client. For this purpose the free routing tool “pgRouting“ is being extended and integrated into the application. Due to the Mapbender object model this is a difficult and tedious process. It is intended to modularize the integrated routing function, which means, that it will be available to the general public in future Mapbender versions.

6. REFERENCES

Michel, U. und T. Bockmühl, 2006. GIS and Remote Sensing for 3D Urban Modelling by means of VRML Technology. Proceedings, SPIE Conference, Stockholm, Sweden, Vol. 6366.

Michel et al, 2007a. Virtuell über den ganzen Campus. GIS-Business 5/2007.

Michel et al, 2007b. WebGIS kostenlos. GIS-Business 1/2 - 2007.

ZOO OSNABRUECK CHANGES INTO A NEW SUITE - POTENTIAL OF A MODERN PRESENTATION OF ANIMAL AND ENVIRONMENTAL DATA

Ulrich Michel, Christian Plass & Constanze Tschritter

Institute for Geoinformatics and Remote Sensing (IGF), University of Osnabrueck, Seminarstrasse 19a/b, D-49069 Osnabrueck
umichel@igf.uni-osnabrueck.de

KEYWORDS: Mobile Database, Pocket PC, Remote Sensing, GIS, Content Management System

ABSTRACT:

The use of modern electronic media offers new ways of (environmental) knowledge transfer. All kind of information can be made quickly available as well as queryable and can be processed individually. The Institute for Geoinformatics and Remote Sensing (IGF) in collaboration with the Osnabrueck Zoo, is developing a zoo information system, especially for new media (e.g. mobile devices), which provides information about the animals living there, their natural habitat and endangerment status. Thereby multimedia information is being offered to the zoo visitors. The implementation of the 2D/3D components is realized by modern database and Mapserver technologies. Among other technologies, the VRML (Virtual Reality Modeling Language) standard is used for the realization of the 3D visualization so that it can be viewed in every conventional web browser. Also, a mobile information system for Pocket PCs, Smartphones and Ultra Mobile PCs (UMPC) is being developed. All contents, including the coordinates, are stored in a PostgreSQL database. The data input, the processing and other administrative operations are executed by a content management system (CMS).

1. INTRODUCTION

The use of modern electronic media offers new ways of (environmental) knowledge transfer. The possibility of user interaction makes the exploration of certain topic more attractive. The internet, nowadays one of the most important tools for information delivery, is utilized by all major institutions and business companies to reach a wide audience in the most efficient, attractive and clear way. Unfortunately, websites are often limited to a preset of information. The content of these websites is presented normally as texts or pictures, with little or no topicality. As a result, these websites show a lack of interactive elements. Furthermore, even “simple” options for systematic enquiries, such as text-based search are deficiently implemented. Three-dimensional content is virtually non existent in web presentations.

This paper describes a new project of the Institute for Geoinformatics and Remote Sensing at the University of Osnabrueck, funded by the DBU (Deutsche Bundesstiftung Umwelt, www.dbu.de).

One goal of this project is to develop a mobile zoo information system for Pocket PCs and Smart phones. Visitors of the zoo will be able to use their own mobile devices or borrow Pocket PCs from the zoo. The zoo information system will provide additional multimedia-based information such as audio material, animal video clips and maps of their natural habitat. To this end, we are currently collecting a large amount of information, such as, species facts and characteristics and any additional background information. Once the information is incorporated users will have access to the project at the zoo via wireless local area network or by downloading the necessary files using, for example, their internet connection at home.

In contrast to the standard information often provided at the zoos by information boards or brochures, in our project the visitor will be able to obtain a very comprehensive set of information (texts, maps and multimedia elements such as photos, audio and video streams) about the zoo’s specimens, which will significantly contribute to environmental education.

Our software environment mainly consists of non-proprietary software solutions, which will be used to develop a capable, reliable and flexible application. Within the system we will develop a 2D/3D zoo information system, available online, by means of modern mapserver technology and 3D visualization procedures such as VRML (Virtual Reality Modeling Language). Furthermore, we will use a consistent database and a content management system (CMS) for data entry, processing and other data management operations.

All contents (including coordinates) are stored within the object-relational database PostgreSQL, which supports geographic objects through the database extension PostGIS. The objects and their attributes can be easily administered online by the CMS and are displayed as well within an adapted Mapbender application. The combination of WebGIS and CMS is a very innovative and effective method for the project’s purposes. The interactive mapping application comprises fundamental necessary GIS functions and allows the digitalization of geo-objects that can be administered immediately by the CMS. It is no longer necessary to edit attribute tables of geo-objects laboriously. The (geo)-data can be updated at any time even by non-experts. All information about selected (geo)-objects can be generated dynamically so that they are always up to date.

A three-dimensional zoo information system is a modern and innovative way of external representation. Its technical implementation is only one aspect of this. The key factor is ultimately determined by the intention of institutions and companies to represent themselves as open-minded, modern and resourceful and in this context to let people partake in occurring events and happenings. A virtual reality zoo provides an information platform for all interested visitors. Users have access to current information and high-quality multimedia material. Web presentations with virtual reality content are still very uncommon. This is particularly based on the fact that the creation of 3D worlds requires a great effort if not done automatically.

access to current information and high-quality multimedia material. Web presentations with virtual reality content are still very uncommon. This is particularly based on the fact that the creation of 3D worlds requires a great effort if not done automatically.
The project is ideally suited to enable zoo visitors to achieve an understanding of duties and responsibilities of zoological gardens and to create public awareness and interest in environmental issues.

2. AREA OF INVESTIGATION

Our area of investigation is the zoo of the city of Osnabrueck in Lower Saxony, Germany (fig. 1). Osnabrueck is the third largest city in Lower Saxony with 164,000 inhabitants. It is the only German city situated in a national park – the 'UNESCO Geo park TERRA.vita', which includes the Teutoburg Forest and the 'Wiehengebirge'.
Osnabrueck is a university and a diocesan town. The German Foundation for the Environment and the German Foundation for Peace Research are also based here. Osnabrueck is the cultural centre of the western part of Lower Saxony and the vital centre of an economic region with around 780,000 inhabitants, which includes not only Lower Saxony but also parts of North Rhine-Westphalia. Its geographical location is 8° 3' 2" Longitude east and 52° 16' 28" Latitude north.

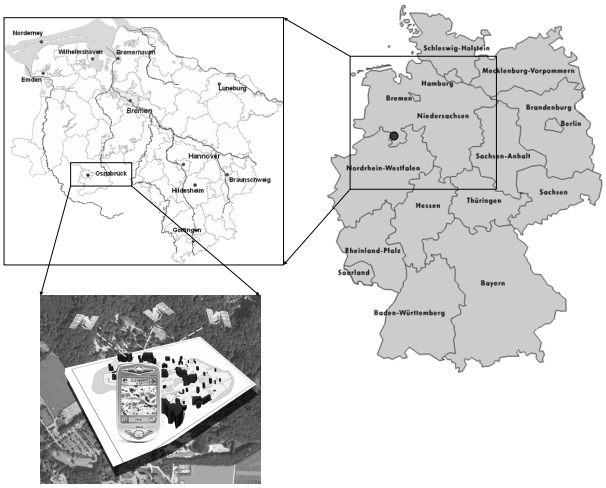

Figure 1: Area of Investigation

3. GOALS

The project goal is to test and apply new media for environmental education. In collaboration with the Osnabrueck Zoo information about the zoo animals, their natural habitat and endangerment status are to be presented clearly. For that purpose two popular media types are used. On the one hand information is presented in advance via a three-dimensional web-based tour to the zoo. On the other hand it is available via a mobile electronic zoo guide during the visit.
The information to be offered to the zoo visitor will go beyond the already existing information boards attached to the animal cages. The visitor will be able to access for example a map displaying the natural distribution area of the animal, to see pictures of this area, short video clips showing the animal in action and/or in his natural environment, hear animal sounds, or listen to interviews with zoo keepers or veterinarians.

4. SYSTEM STRUCTURE

Figure 2 shows the general structure of the zoo information systems and its components.

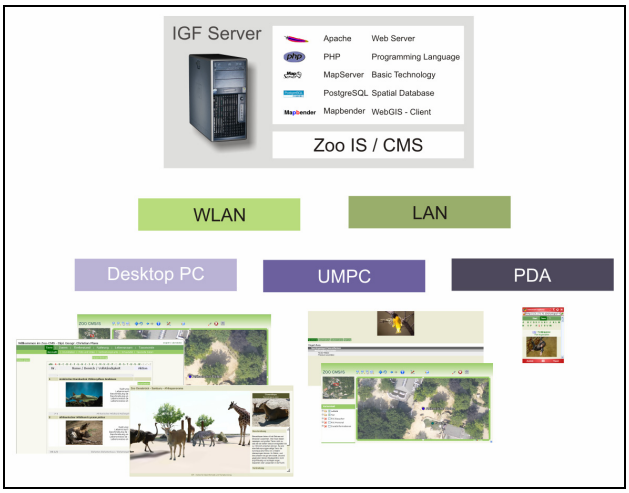

Figure 2: System Components

The core of the system is the content management system and its database underneath (see section 5). For accessing the system environment a conventional web browser could be used. This works not only on desktop PCs but also on mobile devices like Pocket PCs, Smartphone's and Ultra Mobile PCs (UMPC), which could be connected by LAN or wireless via WLAN or UMTS. Our software environment mainly consists of non-proprietary software solutions, which will be used to develop a capable, reliable and flexible application. We will develop within the system a 2D/3D zoo information system available online by means of modern mapserver technology and 3D visualization procedures such as VRML (Virtual Reality Modeling Language). Furthermore, we will use a consistent database and a content management system (CMS) for data entry, processing and other data management operations.

5. CMS – CONTENT MANAGEMENT SYSTEM

The in-house developed bilingual CMS for the administration of the animal data (fig. 3) is the central part of the Zoo Information System. It is already installed on a server and in use. The PHP-based CMS allows the access and manipulation of the data stored in the spatial database PostgreSQL/PostGIS.

Figure 3: Content Management System

6. PRESENTATION

6.1 Mobile Application

The mobile zoo guide for PDAs and a UMPC version for disabled people are currently in the set-up phase. Additionally, the existing map application is converted into an equivalent UMPC version for data acquisition purposes.

6.2 3D Visualization

Google SketchUp is an efficient, intuitively-operated program to create complex 3D models. The basic version is free of charge. What makes SketchUp so special is its ability to integrate three-dimensional objects directly into Google Earth. A previously selected image part in Google Earth can be imported to SketchUp in one step. In this process all spatial references are retained. In this way the 3D buildings - which are to be constructed - or any other three-dimensional objects can be placed according to the air photo. The 3D models can be integrated into Google Earth directly after their construction. The following figure (fig. 4) shows the generation of the zoo main building with SketchUp.

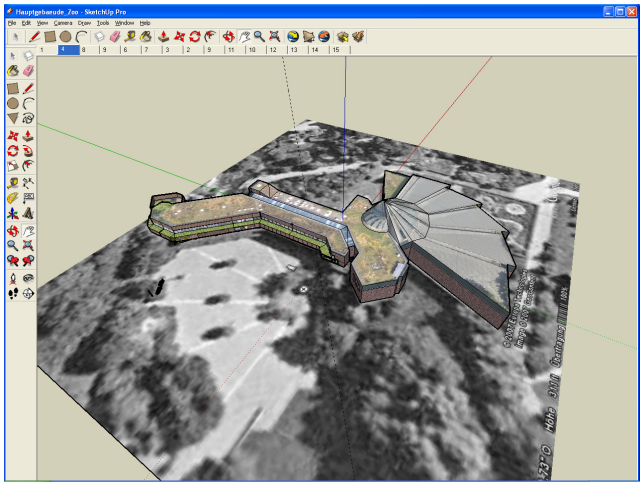

Figure 4: Modelling the main building with Google SketchUp

Up to now only the main building in the entrance area of the Osnabrueck Zoo has been modelled with SketchUp for testing and presentation purposes. The ground plan of this complex building was extracted from a Google Earth air photo. An especially authentic look of the model was achieved by placing real photo textures on all surfaces of the main building. Additionally, the roof textures were extracted from a high resolution air photo, whereas the textures for walls, doors and windows were generated from pictures taken especially for this purpose. For some areas of the building no realistic texturing could be achieved, because the respective outside facades were inaccessible or covered by vegetation.
The following figure (fig. 5) shows the final model of the zoo main building in Google Earth.

Figure 5: The model within Google Earth

In the future other buildings of the Osnabrueck Zoo, e.g. the aquarium, will be modelled this way. SketchUp offers many possibilities for this, for example, for the design of interior rooms.

6.2.1 VRML with connection to the database

At present, a first 3D test scene was developed in VRML, which, among other things, will help to better estimate future requirements regarding file sizes, resolutions, accuracies and efforts. At the same time, this first scene is used for presentation purposes, because it provides a preview, which already demonstrates one important concept of the zoo information system: the connection of a 3D object with the database.
The VRML scene shows the so-called „Africa panorama“ with the impalas, Masai ostriches, common Eland, Grevy’s zebras, giraffes and crested guinea fowl. In addition, a few trees and some shrubs were integrated into the 3D scene as inventory. The user, who can move around the scene freely, can access associated information in the database by simply clicking on the animals. The following screenshot (fig. 6) shows the 3D scene in the left main window and the dynamically generated animal information in the right window. In this example the common Eland is selected.

Figure 6: VRML linked to the database

One important goal in the design of interactive 3D worlds is to find the best compromise between performance and visual quality. Another aim is a semi-automated generation of the VRML code, where the dimensions of the displayed objects, among other things, play a major role.
The current 3D scene, whose underground consists of an air photo, is already true to scale, i.e. the animals are in proportion to each other and to the air photo. In this regard, there will be considerations concerning which objects are to be modelled and which not. For example there is an observation deck with tables and chairs, which belongs to the Africa panorama. Although the integration of such models increases the visual quality of the 3D scene, their realization is time-consuming and they provide

virtually no information content related to the project. The following figure (fig. 7) shows the first version of the Africa panorama from bird's eye view. The non-textured grey item is a test object, whose position corresponds to a part of observation deck.

Figure 7: The Africa panorama from birds view

6.2.2 Embedded panoramic graphics

The techniques of typical panoramic videos were used (fig. 8) also for orientation and visualisation purposes. We use this technology not stand alone but embedded in our mapserver application. From there the user will be able to access the panoramic videos by clicking on a given panoramic symbol.
With this technique we are able to implement changes to the zoo's environment very quickly. For example the zoo will have also an underground zoo next year, which could be represented by panoramic views.


Figure 8: panoramic view of the rhino enclosure

6.3 2D Visualization

6.3.1 Geotagging

The term *geotagging* (geocoding) is used, for instance, when photos are 'tagged' with coordinates. This can happen directly, when the photos are taken with a GPS camera or as a second step, when a GPS track is recorded in addition to photos taken with a common digital camera (fig. 9).

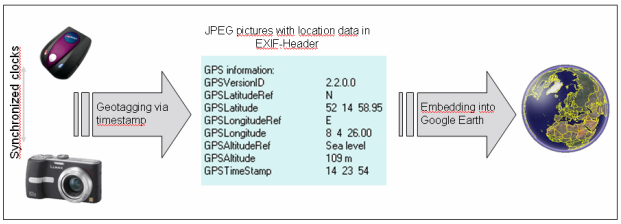

Figure 9: Geotagging operation mode

The digital photograph, containing information about its time of origin can only incorporate coordinates if the time stamps of camera and the GPS track match (fig. 9). In this case the image file can simply be extended to include the corresponding coordinates. For that purpose various software programs exist, often accessible free of charge. Geocoded photos can be embedded in Google Earth as a data layer in the form of symbols, whereas the corresponding pictures are displayed after clicking the symbol. To realize this in Google Earth a folder with these photos, as well as a KML file is necessary. In this context, it is probably possible to implement a KML export from the database because the KML file is a kind of text file. For that, all objects and pictures have to be geocoded. Geocoded photos from objects of varying categories *(waste bin, bench, information board, miscellaneous, art / culture and animal…),* were previously generated to test possible fields of application. Fig.10 shows different embedded data layers in Google Earth (left side), the associated symbols in the background of the main window, and a linked photo, which opens after one of the symbols was clicked.

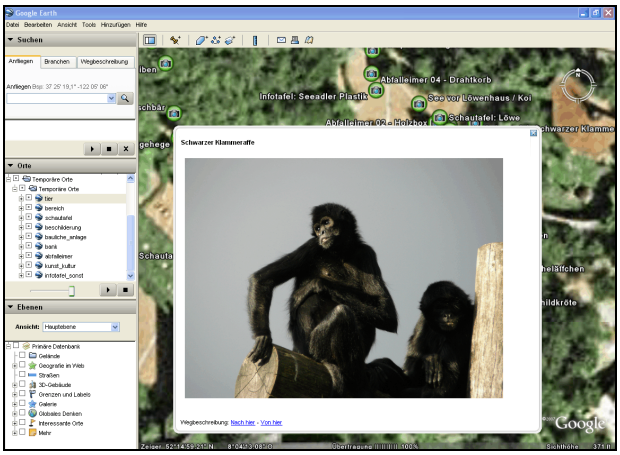

Figure 10: geotagged objects and visualisation in Google Earth

6.4 Web-Mapping

A major part of the project is dedicated to the 2D mapping application. The visualization principle of georeferenced data is similar to that introduced in the previous section, but more complex. The data layers are displayed within an interactive environment on the basis of an aerial or a satellite photo. The mapping application, which is based on the Open Source product Mapbender (www.Mapbender.org), goes far beyond the possibilities of Google Earth (Michel et al, 2007a). This includes the use of a high resolution air photo, which contains more detail than the corresponding Google Earth image. In addition the displayed objects (species) are linked to a database and the application allows the recording of locations. Currently the map application can be launched from the CMS. Up to now, 48 species are geocoded, i.e. they have assigned coordinates,

which are transferred when the map application is invoked. Thus, the animal location can be displayed immediately. As soon as the project is finished, we will have approximate 300 species geocoded. The following screenshot (fig. 11) shows the map application directly after it was launched by the CMS.

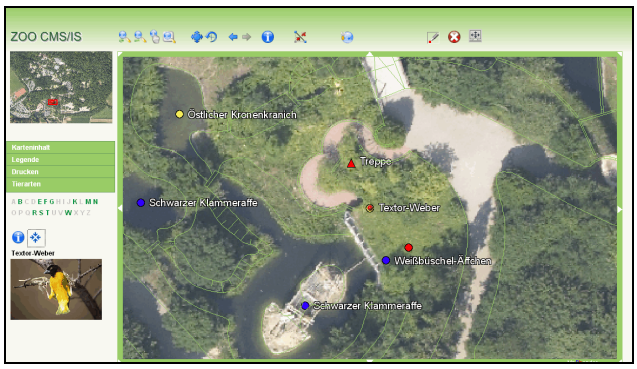

Figure 11: 2D Web-Mapping

7. CONCLUSION

The new project of the Institute for Geoinformatics and Remote Sensing at the University of Osnabrueck, was funded by the DBU (Deutsche Bundesstiftung Umwelt, www.dbu.de).

The information provided by our system to the zoo visitor is intended to represent a major step forward respect to the typical information available in zoos, which up to now consists mainly of boards attached to the animal cages and brochures. By accessing interactive maps displaying the location of the animals in the zoo; and by, for example, watching short video clips showing the animals in action and/or in their natural environment, or listen to animal sounds, or to interviews with zoo keepers and veterinarians, the visitor is able to come into closer contact with the animals and achieve a deeper and broader knowledge of their biology.

Our software environment mainly consists of non-proprietary software solutions, which will be used to develop a capable, reliable and flexible application (Michel et al, 2007b). We develop a 2D/3D zoo information system available online by means of modern mapserver- and 3D-technology. We also used a spatial database and a content management system (CMS) for data entry, processing and other data management operations.

In future developments we will have additional applications for different purposes and specific user groups, such a as zoo staff members, handicapped people (by means of ultra mobile PCs, UMPC), and teachers or students.

The project will be finished in April 2009 and its results and applications will be openly available for their use.

8. REFERENCES

Michel, U. und T. Bockmühl, 2006. GIS and Remote Sensing for 3D Urban Modelling by means of VRML Technology. Proceedings, SPIE Conference, Stockholm, Sweden, Vol. 6366.

Michel et al, 2007a. Virtuell über den ganzen Campus. *GIS-Business* 5/2007, pp. 20-23.

Michel et al, 2007b. WebGIS kostenlos. *GIS-Business 1/2* 2007, pp. 30-32.

Michel, U., 2007. MoZis – Mobile Zoo Information System- A case study for the city of Osnabrueck. Proceedings, SPIE Conference, Firenze, Italy, Vol. 6749.

SUSTAINABLE AND ECOLOGICAL URBAN DEVELOPMENT - CASE STUDY FOR THE BURENKAMP AREA, OSNABRUECK

M. S. Moeller

OEAW, GIScience, Schillerstrasse 30, A 5020 Salzburg, Austria – matthias.moeller@oeaw.ac.at

KEY WORDS: urban planning, commercial site construction, ecological, sustainable, airborne, HRSC, TM, ETM

ABSTRACT:

Urban planning for many cities is a special challenge keeping the balance between new commercial sites on the one hand and conserving nature for a healthy urban environment on the other hand. The City of Osnabrueck in the mid 1980ies was trying to link both ideas, planning a sustainable commercial and industrial site. This article follows the development of the area over a 19 years time span. The development phases and the impact were reconstructed based on digital aerial and spaceborne image data sets. Finally a critical discussion about the initial goals and the actual state of the remodelled site is given from a remote sensors and a Geographers perspective.

1. URBAN CHALLENGES

Urbanized areas are those regions, where people come together and specialize in individual abilities, trade and exchange their products. Cities in general follow the economic principle of our post-industrial society: they have to grow permanent to keep the pace with competitors. The City of Osnabrueck is located in Lower Saxony, Northern Germany and it is growing in terms of inhabitants, space for commercial sale is increasing permanently and industrial production of consumer goods raise as well. As a consequence, the city administration has to provide enough space for the permanent growth. However, space is limited inside the administrative boundaries of the city and it has to be used efficiently. The surrounding communities with a rural tradition may provide more space at cheaper rates for future development, e.g. a potential economic growth. Under certain aspects rural communities function like competitors in terms of local sales tax, employment rate and might somehow retract attractiveness from the major city. Osnabrueck with more than 160.000 people functions like a major city and is in fact the central market for surrounding villages. In an operating distance of 25-150 km, the catchment limits for Osnabrueck, it is the central place for many potential customers.

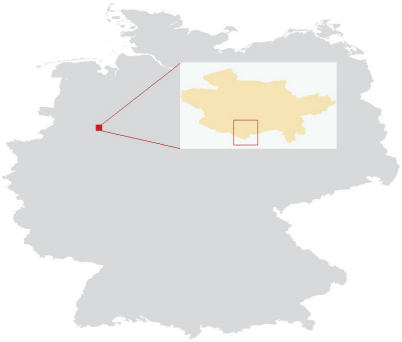

Figure 1. Germany; city of Osnabrueck located in the northwest; Burenkamp located almost south of the city

The boundaries of the catchment, measuring half the distance to neighboring major cities, are roughly defined with Bremen, 100 km north, Muenster, 50 km south, Enschede in the Netherlands, 100 km west and Hannover, 100 km east. The city administration of Osnabrueck of course would like to have so many potential customers as possible inside the city limits, buying their goods in Osnabrueck, not in surrounding commercial rural centers.

In the suburban regions of the administrative area of the city of Osnabrueck, within a distance of about 3-5 km to the city center, only little space with an appropriate minimum size and compact shape was left for potential commercial development in the mid 1980ies. One of those areas was the "Burenkamp" site, south of the city center. This paper will try to comprehend the remodeling and reconstruction of the commercial site "Burenkamp", originally declared as a 'sustainable and ecological balanced commercial and industrial site', where some of the traditional land use land cover (LULC) should still be kept to conserve its former value for the future. The planning phase and first developments of the construction has been described in detail by Moeller (1995) in an unpublished diploma thesis. The author used remote sensing image data (high spatial resolution airborne and moderate resolution space borne Landsat TM) and auxiliary cadastral geo-data from the digital ALK and the ATKIS data sets (ALK – Automated Cadastral Map; ATKIS – Automated Topographical Cartographical Information System). The combination of GIS data sources, both raster- and vector data, has been proposed by Ehlers 1991 for an efficient analysis of remote sensing image.

2. PLANNING ACTIVITIES FOR "BURENKAMP" SITE

2.1 Commercial vs. Ecological Interests

The Burenkamp area ("bur" is the ancient German expression for farmer, "kamp" means a compact agricultural area) with it's about 29 ha size was found appropriate for the construction of a commercial site with some small industrial companies as well. Although this area had a long farmland tradition for many

centuries with extensive agricultural usage, the pro-arguments for a further development under commercial aspects prevailed in the mid 1980, when planning activities started. Those are:

- short distance and good connection to German Interstates (exit in less than 100 m distance),
- located at a big entrance/exit route to the city center,
- local public transportation and logistic network already existent,
- close to urban infrastructure (phone-lines, energy, water, waste-water).

The main contra-arguments against the construction of a commercial site are those:

- positive climatologically function on local urban climate will be disturbed due to the decrease of vegetated areas (fresh cool air, Luekenga 1986),
- very old and valuable irregular fruit tree meadows (Streuobstwiesen), mainly apple trees, also pears and plums will mainly disappear,
- high diversity of plant species and small animals will decrease: insects, rodents (Lieth and Mindrup 1989),
- open soil, important for the permanent renewal of the groundwater regime will be paved with buildings and parking lots,
- the sites function as recreational area for citizens will be reduced.

2.2 Burenkamp Climatic Function

The Burenkamp site is embedded in a region with a long tradition of agricultural usage (fig. 2; burenkamp test site with hatched pattern). Due to the agricultural usage, dominant LULC was vegetation, mainly crop field and meadows and some trees in small groups. The area is located south of the city center and it consists mainly of a moderate slope with smooth incident angles, most directions face towards the densely populated residential areas of the city. Aspect, slope and contour lines have been derived from the Digital Elevation Model (DEM) provided by LGN, the cadastral and surveying authority of Lower Saxony. Dark colors in the aspect image (fig. 2 (a)) indicate a favorite exposition to north, northeast, west and northwest. Those directions are most important for the flow direction of fresh, cool air produced in that densely vegetated area (compare to Luekenga 1986). In the northern parts of Fig. 2 urban settlement areas are located, dominated by single family buildings and benefiting form the fresh air stream especially in warm summer nights. From the shape of the contour lines in conjunction with the aspect image, morphological relief pattern can be detected.

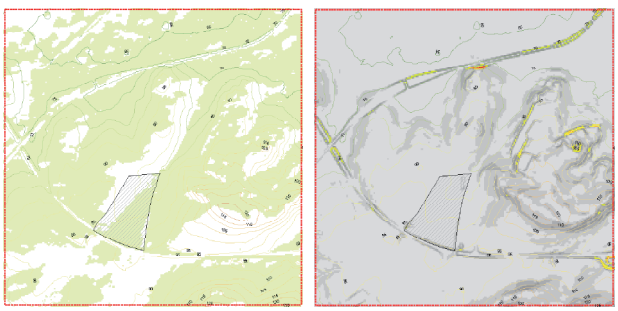

Figure 2. (a) Aspect image, darker colors indicate an aspect direction with a positive effect to urban climate; (b) Slope image; light tones indicate slope values useful for a climate effect. Extends of the subsets: 3 x 3 km

3. DEVELOPING PHASES

3.1 The Idea and its Realization

The planning and reconstructing of the Burenkamp site was not a single action; after an initial first cautious and restrictive planning with positive intentions to conserve somehow the character of the area and to develop a sustainable and ecological balanced commercial and industrial site, two additional planning processes were accomplished to improve economy by providing more sale and office space. These planning took only little time compared to that time, usual urban planning processes need, because the city administration was under increasing pressure to designate new space for future economic growth. Consequently the overall development process of the Burenkamp can be differentiated into these three clearly identifiable phases:

1. 1989-1999 build up of the southern and the north-west part,
2. 1999-2002 build up of parts in the center,
3. since 2003 build up of parts north of the center.

3.2 First Phase: Development between 1989 – 1999

Remote sensing image data with a very high spatial resolution is a reliable source to get the most realistic impression of LULC (Albertz 2007). Digitized aerial images acquired in 1989 represent the undeveloped state of the Burenkamp area (fig. 3 (a)). The photo was also basis for a regular study of the environmental condition of the site (Umweltverträglichkeitsuntersuchung, UVU), conducted by Lieth and Mindrup (1989). One outcome of the study was a land use map, transferred later in a GIS environment (fig. 3 (b)). This study was also presented to the cities planning authority as one criterion for future development. Finally plans for future development of the Burenkamp site became available for a public discussion process, a legal action. After that discussion the senate of the city decided to change the dominant usage from prior agriculture to a commercial and industrial use.

However, public discussion lead to these restrictive constrains for such a development: the overall character of the area should be kept in general, a certain percentage of impervious surface should not exceeded, a compact area within the Burenkamp site should be remodeled and upgraded in terms of biological quality and diversity. Major action for this upgrading was the construction of wetland meadows, swamp areas and small ponds, also used for water retention sites in case of heavy precipitation. These actions were planed for the northern part of Burenkamp site. Wetlands were thought to provide new habitats especially for endangered species (e.g. dragonfly, water beetle, etc.). Due to the paving of surfaces in the Burenkamp area, the groundwater level was expected to lower significantly and the foster of wetlands was thought as an action to absorb this negative effect. Figure 3 (c) represents the result of the planning as it has officially passed the city's senate. Burenkamp has been sub-divided into five separated zones, each with individual planning restrictions, compare to table 1.

The detailed planning and build-up map (Bebauungsplan 464) also defines the compensation activities outside the five construction zones. It contains the exact locations for new trees to be planted; it maps existing trees and bushes under protection and future traffic limitations for the roads. This detailed planning and build-up map was the legal basis for the upcoming development and it was meant as a conclusive fact.

zone	size (ha)	building	height (m)	compen-sation
1	0.75	2 stories, exception: 3 stories offices only	12	10% for ecol. dev.
2	2.3	2 stories, exception: 3 stories offices only	12	15% for ecol. dev.
3	4.3	1 story, exception: 3 stories offices only	8 . 5 (12)	10% for ecol. dev.
4 (a)	3.5	2 stories, exception: 3 stories offices only	12	10% for ecol. dev.
4 (b)	4.15	2 stories, exception: 3 stories offices only	12	10% for ecol. dev.

Table 1. Developing Zones of the Burenkamp Site

Activities started in the early 1990ies, when streets have been established to make the area accessible fur further construction action. First construction took place in zones 1, 3 and 4 a&b, where we can detect 12 new buildings in the 1999 aerial scanner image (fig. 4 (a)); however, big parts of zone 2 have been left unchanged so far. Most parts of the new construction zones have been paved and they are used as fabrics, commercial resale stores, offices and for car parking in 1999 (compare to the hatched signature in fig.4 (b)).
The land use land cover statistics have been changed significantly; almost 35% of the Burenkamp is under artificial/commercial usage in 1999 (table 2). This may result in a loss of the important climatic function of the Burenkamp (Luekenga 1986), because huge amounts parts of the natural vegetation was already diminished in 1999.

3.3 Excurse: HRSC-A Line Scanner Image Data

The Burenkamp aerial scanner image in fig. 4 (a) has been acquired with an experimental digital airborne scanner, the High Resolution Stereo Camera – Airborne in April 1999. The flight campaign was conducted by the German Aerospace Center (DLR) and it was supervised by the remote sensing and geoinformatics research group, University of Vechta. Manfred Ehlers formed this group and he was head and leading scientist for this digital flight campaign carried out for an entire city area for the very first time. HRSC-A consists of a DGPS - IMU (differential global positioning system) inertial measurement unit and the image data is acquired parallel with the recording of the 3D positioning coordinate and the rotation angles of the platform. This allows for a direct georeferencing of the image data and it results in a highly accurate all digital ortho-photo processing line. The HRSC-A spectral bands are sensitive for the blue, green, near infrared and mid infrared portion; the red spectral information has been calculated from the original infrared band. At the time of image acquisition, HRSC-A was designed for experimental purposes and for overall system optimization. Due to the small acquisition angle of only 17°, a huge overlap of neighboring image strips has to be assured. Sometimes the overlap failed for some spectral bands resulting in data gaps after mosaiking of the image data (fig. 4(a), ll corner). HRSC-A image data, geometric and spectral quality and application development for an urban usage has been scientifically investigated and published as Doctoral thesis by Moeller (2003). Manfred Ehlers was supervisor and assessor of this innovative research.

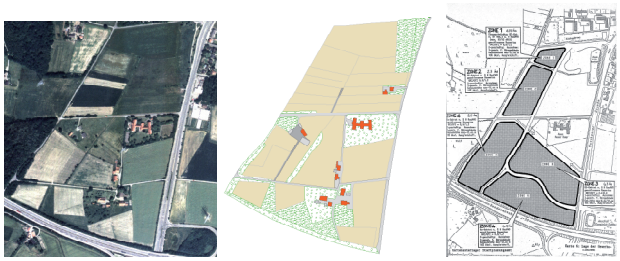

Figure 3. Burenkamp in 1989: (a) Aerial Image, (b) Burenkamp LULC, (c) Planning map from Lith and Mindrup 1989

3.4 Second Phase: Development between 1999 – 2002

Second development phase took place between 1999 and 2002, when new buildings were established in zone two and in parts of the Burenkamp area, which did not belong to the original legal planning map of 1989. Therefore changes have been made to the old sketch and a new planning and build-up map finally passed the senate of the city. However, this new construction leads to even more paved, impervious surfaces in the center of the area. The former children's home located in the center of the Burenkamp site has been brought down. Instead two car branches build their sale stores and offices at this location. Commercial car selling is a business with huge space consumption; those have to be presented in a clean, representative and open space atmosphere to customers. Total impervious area increased up to 47.06% from the original Burenkamp site (compare to tab. 2). However, until 2002 only small amounts of those areas originally under protection and defined as compensation space with an increased ecological function, have been remodeled. In the original planning and build-up map from 1989, the center of the Burenkamp was declared to become managed grassland with irregular fruit tree meadows, a habitat pretty similar to the traditional rural use. After the construction of the two car reseller stores and their surrounding facilities, the Burenkamp center appears with an almost entirely impervious surface.

3.5 Third Phase: Development between 2002 – 2005

A last significant change in the Burenkamp area took place between 2002 and 2005, when parts north of the center have been re-planned again by the cities planning authority. This third planning was started on special request of a construction enterprise for their new headquarter and some parking lots for construction equipment, e.g. heavy trucks, diggers etc. The delicate aspect is the fact, that this enterprise has significant economical impact on the City of Osnabrueck. After the final construction was finished, about 30% of that space, formerly under special protection for endangered species as wetland and wet-meadow, was remodeled. This area was meant to provide new habitat for protected and endangered species (both fauna and flora).

This construction of a central building and parking lots for machines and cars lead to an additional 15.000 m² of impervious area. Consequently, in 2007 more than 52% of the Burenkamp site has been remodeled and is now impervious (tab. 2).

Figure 4. Burenkamp in 1999: (a) the HRSC-A scanner image, (b) hatched signature indicates paved surfaces in 1999

4. QUANTITATIVE AND QUALITATIVE CONSEQUENCES OF THE DEVELOPMENT

4.1 Impervious Surfaces

Comparing the two aerial remote sensing images acquired before construction (fig. (1)) and after construction has finished (fig. 5 (a)), the huge shift in LULC becomes quite obvious. The subjective impression of an area with lots of man made construction and many paved surfaces prevails. However, an increased number of trees with bigger sizes can be detected. The compensatory measures and their consequences can be observed in the north-east corner; this part definitely reflects a more natural appearance in recent years. But more than 50% of the former agricultural Burenkamp site is under commercial usage in 2007, represented with the hatched signatures in Fig. 5 (b). When comparing the quantitative statistics of land conversion based on cadastral measures, we can clearly identify the three development phases. Table 2 gives a quantitative overview of the construction phases.

total Burenkamp area (m²)	289438
build up area 1999 (m²)	103156
% of build up from 1989	34.64
build up area 2002 (m²)	103156+33050=136206
% of build up from 1989	47.06
build up area 2005 (m²)	136206+14995=151201
% of build up from 1989	52.24

Table 2. Build up Area for the three Phases

Figure 5. Burenkamp in 2007: aerial image (a) and impervious, build up areas (b) with hatched signatures for three construction phases overlaid on the 1989 LULC; legend (b): dense hatched pattern: construction between 2002-2005, medium hatched pattern: construction between 1999-2002, wide hatched pattern: construction between 1989-1999

4.2 Burenkamp Changes as seen from Space

The rapid decrease of natural vegetation can be observed and mapped from true color aerial images; however, the loss can also be derived from satellite image data sets acquired by Landsat Thematic Mapper (197/23, May, 13 1988) and Enhanced Thematic Mapper (196/24, May 15 2000) respectively. Due to the almost same day/month of image acquisition, temporal variations in vegetation pattern can be excluded. However, there are some differences, because agricultural fields with various crop species may appear with different spectral values. The NDVI (Normalized Difference Vegetation Index) is a reliable measure for vegetation activity and serves as an indicator for healthy trees, shrubs and meadow. NDVI values have been calculated for both Landsat image data sets (fig. 6a&b), resulting NDVI values range from -1 - 1, indicating pixels with absolutely no vegetation (-1) and full vegetation (1) respectively.

The NDVI changes for both dates become quite obvious in Fig. 6, where the major LULC changes are overlaid. The 1988 Landsat image subset of the area is dominated by healthy vegetation, indicated by light gray to white colors. NDVI values for the 1988 image range from 0.2 through 0.7, a permanent increase of NDVI values can be observed in the corresponding chart (fig. 7). The situation has entirely changed in 2000, the NDVI image appears much darker, indicating less vegetation (fig. 6 (b)). NDVI values for 2000 range between -0.5 and 0.7 with a different distribution pattern compared to the 1988 NDVI. The sorted values represent a pattern similar to an equal distribution for the year 2000.

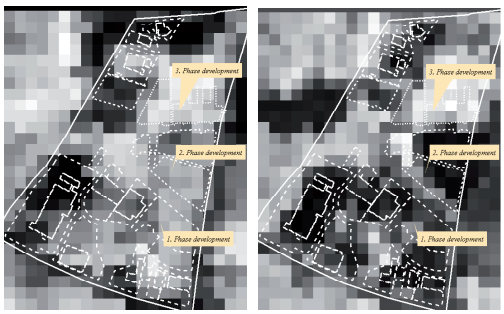

Figure 6. NDVI Charts, values derived from TM 1988 (a) and ETM 2000 (b)

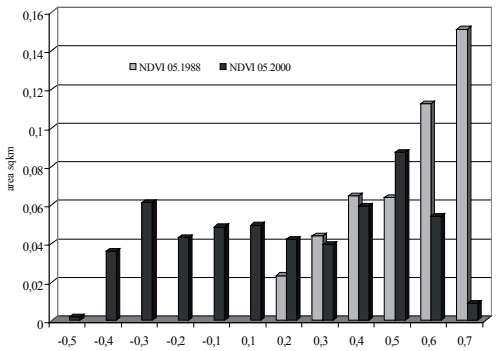

Figure 7. NDVI values: TM 1988 (light gray bars) and ETM 2000 (dark bars)

Fig. 7 also indicates the areas with the most active vegetation (NDVI value 0.7) in 1988 have been converted radically. For 1988 we can observe about 0.15 sqkm with very active vegetation, for 2000 it has become 0.01 sqkm, an overall reduction of 93%. The NDVI value 0.6 reflects a reduction of about 50%.
Active vegetation is the most important factor for clean fresh air production. Due to the plant assimilation processes, latent energy is reduced and the air temperature decreases. However, the changed NDVI values indicate a turn to worse conditions in 2000 compared to the state of 1988; the impact on surrounding settlement areas has to be verified by field temperature measures following the schema introduced by Luekenga (1986).

4.3 Economy versus Ecology

Finally a very important question has to be answered: What is still left from the initial idea of a sustainable and ecological balanced commercial and industrial site? The first remodeling phase was characterized by cautious planning intentions, conserving partly the original heritage and traditional land use of the Burenkamp area. This is of course a delicate task, bridging two absolutely contrary kinds of usage. To resolve this contradiction, the original plan was designed to upgrade parts of the area and to increase bio-diversity by planting trees and conserving parts of the traditional usage. Especially the ancient fruit tree meadows were under special protection and those should be conserved as trees beside the streets. However, the original plan has been extended twice and the idea of a sustainable and ecological balanced commercial and industrial site was reduced in each of the following planning phases. As a consequence, the overall current state of the site is far away from this noble goal. Instead we can observe a huge shift in land use to an industrial usage for most parts with all of its consequences. However, the remaining wetland and recreational area in the north-east corner has been improved in terms of natural appearance and as habitat for endangered plant and animal species. We can also still find an ancient farm with a surrounding fruit tree meadow conserved in the south of the Burenkamp area. But the overall planning goal has failed from an ecological and sustainable point of view.

Having this negative statement in mind, as Geographers we also have to look at the economic side of the medal. And under this perspective we can observe lots of positive developments. Many new jobs have been created in the Burenkamp area and due to the high end consumer products sold in the area, local sales taxes are very high. Those are true benefits for the City of Osnabrueck

4.4 Remote Sensing

From a remote sensors perspective, we must be really satisfied with the results of the interpretation of images acquired by the most important sensors for environmental mapping. Those are aerial photos (digitized), digital airborne sensor image data and the “work horse” of remote sensing, the Landsat sensor series. In combination, these three image data lead to reliable results when observing the change in LULC on a medium up to a large scale. Following the “paved highway of geoinformatics” into the future and thinking one generation ahead, we can still foresee a huge demand of those basic remote sensing products for scientific earth observation.

5. ACKNOWLEDGEMENTS

The author thanks Mr. Gert Heit from the cartography and geoinformation department of the City of Osnabrueck for providing the aerial image of 2007 as digital copy. Thanks to Prof. Walter Luekenga for the input and discussions about the climatic function of the Burenkamp site. Special thanks are directed to Prof. Manfred Ehlers, who supervised the diploma thesis (Moeller 1995) and who provided valuable thoughts for the monitoring of this special, sensitive urban area.

Actually, Manfred Ehlers guided the author right on the “geoinformatics highway” when he started his lectures about remote sensing and geoinformatics in the early 1990 at the University of Vechta. Manfred is not only a great international remote sensor and geoinformatics scientist, but he is also a friend and reliable partner for the discussion of themes and issues outside these sciences.

6. REFERENCES

Albertz, J., 2007. *Einführung in die Fernerkundung. Grundlagen und Interpretation von Luft- und Satellitenbilder*. Wissenschaftliche Buchgesellschaft, 3. Edt.

Ehlers, M., 1991. Data Types and Data Structures for Integrated Geographic Information Systems. In: *Proceedings of a special session held at the Baltimore 1991 ACSM-ASPRS Annual Convention: The Integration of Remote Sensing and Geographic Information Systems*, pp. 51-73.

Lieth, H., Mindrup, K., 1989. Ökologisches Gutachten für das Gebiet zwischen Sutthauser Straße/Burenkamp und nördlich der Autobahn A-30.

Luekenga, W., 1986. Untersuchungen zum Stadtkima von Osnabrück. Stadt Osnabrück.

Moeller, M., 1995. GIS - gestützte Analyse der Veränderung von ausgewählten Einflußfaktoren des Stadtklimas mit Hilfe multitemporaler Satellitenbilddaten am Beispiel der Stadt Osnabrück. Diploma thesis, Osnabrueck, not published.

Moeller, M., 2003. *Urbanes Umweltmonitoring mit digitalen Flugzeugscannerdaten*. Book with CDROM, Wichmann, Karlsruhe.

MULTI-DIRECTIONAL DECOMPOSITION BASED REMOTE SENSING IMAGE FUSION

Yan Na, Jie Meng & Hongmin Lu

School of Electronic Engineering, Xidian University, P.O.Box 140, 710071 Xi'an, China
yna@mail.xidian.edu.cn

KEY WORDS: remote sensing images fusion, multi-spectral image, panchromatic image, multi-directional transform

ABSTRACT:

In order to obtain high spatial resolution multi-spectral image, a multi-directional decomposition based remote sensing images fusion method is presented. Based on the imaging properties of Panchromatic image and multi-spectral images, the fusion procedure is ,first, multi-directional transform of Panchromatic and multi-spectral images, so more high frequency components of both images can be obtained. And then, the combination of multi-directional high frequency components of Panchromatic image with low frequency components of multi-spectral images, so more spatial and spectral information will be preserved. Finally, a high spatial resolution multi-spectral image can be obtained after inverse multi-directional transform. Preliminary experiment results show that the fused multi-spectral image has very good spatial resolution and spectral characteristic.

1. INTRODUCTION

High spatial resolution panchromatic images can provide detail geometric information and lower spatial resolution multi-spectral images can provide detail spectral information. High spatial resolution multi-spectral images can be obtained with images fusion methods.

Many images fusion methods have been presented in recent years, such as wavelet transform based fusion method, IHS transform based fusion method and PCA transform based fusion method. The disadvantage of IHS transform is that it can not decompose an image into different scale, so this transform can not be used to enhance image details. PCA transform based fusion method can not well maintain spectral information. Both IHS transform based fusion results and PCA transform based fusion results have serious spectral distortion. Wavelet transform can decompose image into different scale, but wavelet transform can only provide three different directions high frequency components of image.

In order to obtain high spatial resolution multi-spectral image, a multi-directional decomposition based remote sensing images fusion method is introduced in this paper. The fusion steps are: first, multi-directional transform of Panchromatic image and multi-spectral images, so more high frequency components of both images can be obtained. And then, the combination of multi-directional high frequency components of Panchromatic image with low frequency components of multi-spectral images, so more spatial and spectral information will be preserved. Finally, a fused multi-spectral image can be obtained after inverse multi-directional transform. Preliminary experiment results show that the fused multi-spectral image has very good spatial resolution and spectral characteristic.

This paper is organized as follows: Section 2 is the principle of multi-directional transform. Section 3 is multi-directional decomposition based remote sensing images fusion scheme. Section 4 is experiment results and analysis. Finally, in section 5 the conclusion is given.

2. THE PRINCIPLE OF MULTI-DIRECTIONAL TRANSFORM [1-3]

Wavelet transform has been widely used in images analysis and processing. But it can only be used to express high frequency components of images in three different directions, That is horizontal, vertical and diagonal.

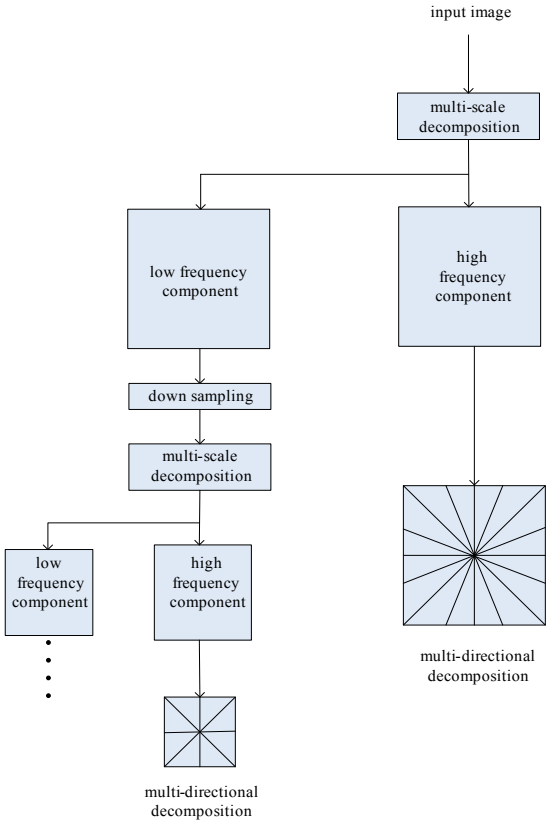

Fig.1 The process of multi-directional transform

Multi-directional transform was presented by Do and Vetterli based on Curvelet in the year 2002 and it is the development of wavelet transform. Multi-directional Contourlet is multi-scale and multi-directional. That means it can be used to analyze images in many different scale and directions. So multi-directional transform can be used to well descript texture and detail information of images.

Multi-directional transform is composed of Laplacian Pyramid Decomposition and Directional Filter Banks. Low frequency subband and high subband are obtained after Laplacian Pyramid Decomposition. 2^{l_j} different directional subband are obtained after Directional Filter Banks Decomposition. For different resolution j, l_j can choose different value. Multi-resolution and multi-directional decomposition will be obtained after above operation repeatedly.

Fig.1 shows the process of multi-directional transform.

Following are the results of multi-directional transform of black and white rings demo image. The principle of multi-directional transform will be explained in more detail with this example.

Fig.2 shows the demo image.

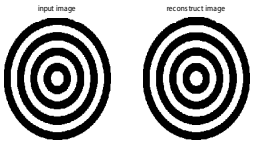

Fig.2 demo image

Fig.3 shows the level 1-4 multi-directional transform results of demo image.

Fig.3 level 1-4 multi-directional transform results of demo image

In fig.3 we can see multi-directional transform can provide high frequency information of an image in more directions than wavelet transform.

3. MULTI-DIRECTIONAL DECOMPOSITION BASED REMOTE SENSING IMAGES FUSION SCHEME [4-8]

The diagram of fusion scheme is in Fig. 4.

Registration of Panchromatic image with multi-spectral images need to be implemented before the fusion process.

The steps of fusion process are:

(1) Multi-directional transform of Panchromatic image and multi-spectral images.

(2) Combination of high frequency components of Panchromatic image with low frequency components of multi-spectral images.

(3) A high spatial resolution multi-spectral image will be obtained after inverse multi-directional transform.

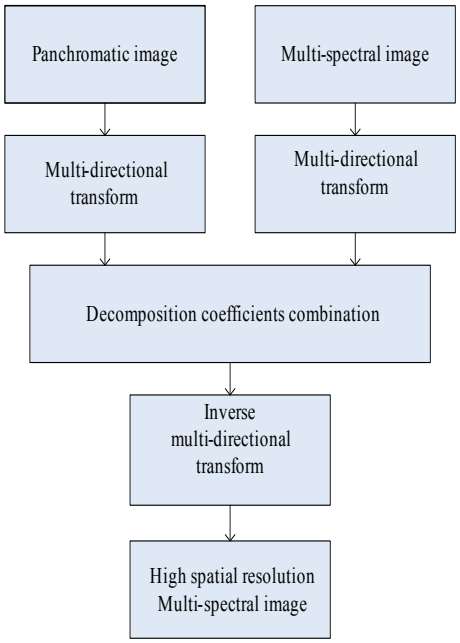

Fig.4 Multi-directional decomposition based remote sensing images fusion scheme

4. EXPERIMENT RESULTS AND ANALYSIS

SPOT Panchromatic image and Landsat multi-spectral image band 1,4,7 are used in the experiment.

Fig. 5 shows SPOT image and Landsat image used in this paper.

(a) SPOT Panchromatic image

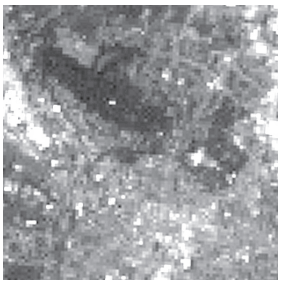

(b) Landsat band 1 image

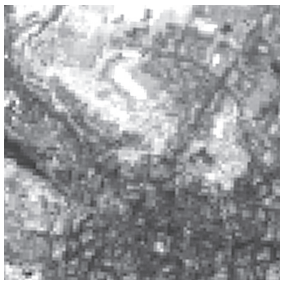

(c) Landsat band 4 image

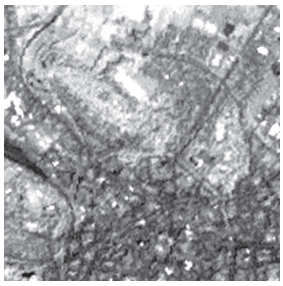

(d) Landsat band 7 image

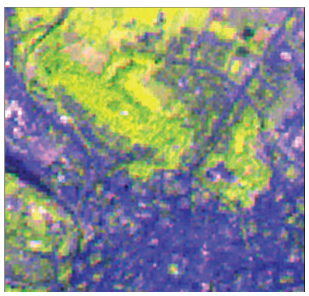

(e) Landsat band147 image

Fig. 5 SPOT image and Landsat image

(a) Fused Landsat band 1 image

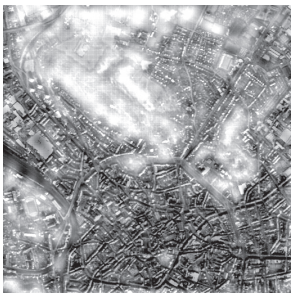

(b) Fused Landsat band 4 image

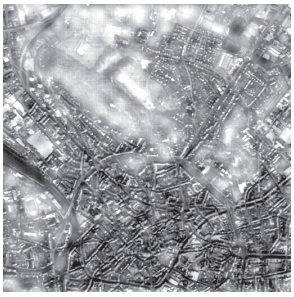

(c) Fused Landsat band 7 image

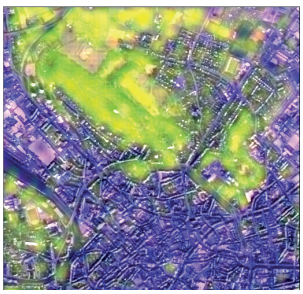

(d) Fused Landsat band147 image

Fig. 6 Fused images

		Farmland	Grove	Irrigation canal
	Farmland	81.8%	4.9%	53.7%
	Grove	18.2%	95.1%	46.3%
	Irrigation canal	0.0%	0.0%	0.0%

Producer's Accuracy	**User's Accuracy**
Farmland = 81.8%	Farmland = 96.5%
Grove = 95.1%	Grove = 49.4%
Irrigation canal = 0.0%	Irrigation canal = 0.0%
Overall accuracy = 81.6%	K-HAT = 21.3 %

Table 4: Error matrix for ISODATA results, two clusters

		Farmland	Grove	Irrigation canal
	Farmland	41.9%	5.3%	79.9%
	Grove	43.5%	91%	13%
	Irrigation canal	14.7%	3.7 %	7.2%

Producer's Accuracy	**User's Accuracy**
Farmland = 41.9%	Farmland = 91.2%
Grove = 91%	Grove = 29.7%
Irrigation canal = 7.2%	Irrigation canal = 1.7%
Overall accuracy = 48.9%	K-HAT = 10.8 %

Table 5. Error matrix for ISODATA results, three clusters

results for a number of cases. The XBI turned out to be the most accurate and by far the most robust index. The overall accuracy was consistently above 80 %, with the best values reaching 90 %. The DBI is much more sensitive to parameter tuning, and the KMI seems to be unsuitable for the use in unsupervised classification. The GA results are similar to those obtained with the ISODATA algorithm, if results with the same number of clusters are compared. However, whereas GA determines this number automatically, it nneds to pre-defined for ISODATA. Thus, GA algorithms seem to be more flexible and therefore advantageous to more traditional unsupervised classification techniques.
In the future we plan to extend our study to process more and larger scenes in order to confirm the results found so far. We are also interested to experiment with different termination

conditions such as an absolute fitness level which needs to be reached and to study under which conditions our approach reaches the best solution. Finally, we want to integrate indices based on fuzzy theory into the investigations.

9. ACKNOWLEDGEMENTS

We would like to thank the Ordnance Survey of United Kingdom to offer the IKONOS image data within the OEEPE test. Part of this research was made possible by a grant of the National Science Council (NSC) of Taiwan, Taipeh to the first author. We gratefully acknowledge this support.

10. REFERENCES

Bandyopadhyay, S., and U., Maulik, 2002. Genetic clustering for automatic evolution of clusters and application to image classification, *IEEE Pattern Recognition*, 35:1197-1208.

Bezdak, J.C., and N.R., Pal, 1998. Some new indexes of cluster validity, *IEEE Transactions on systems, man, and cybernetic*s, part B, 28(3):301-315.

Coley, A.D., 1999. *An Introduction to Genetic Algorithms for Scientists and Engineers*, World Scientific, Singapore, 185p.

Groenen, P.J.F., and K., Jajuga, 2001. Fuzzy clustering with squared Minkowski distances, *Fuzzy Sets and Systems*, 120:227 237.

Holland, J., 1975. Adaptation in Natural and Artificial Systems, University of Michigan Press, Ann Arbor.

Lillesand, T.M., and R. Kiefer, 2000. *Remote Sensing and Image Interpretation*, 4th edition, Wiley & Sons, New York, 721p.

Martini, H., and A., Schöbel, 2001. Median and center hyperplanes in Minkowski spaces -- a unified approach,*Discrete Mathematics*, 241(1):407-426.

Pham, D.T., and D., Karaboga, 2000. *Intelligent Optimisation Techniques*, Springer, London, Great Britain, 337p.

Rothlauf, F., 2006. *Representations for Genetic andEvolutionary Algorithms*, Springer, Netherlands, 314p.

Ross, T.J., 1995. *Fuzzy logic with engineering applications*, Mc Graw-Hill, Singapore, 486p.

Swanepoel, K.J., 1999. Cardinalities of k-distance sets in Minkowski spaces, *Discrete Mathematics*, 197(198):759-767.

Xie, X.L., and G., Beni, 1991. A Validity Measure for Fuzzy Clustering, *IEEE Transaction on Pattern Analysis and Machine Inteligence*, 13(8):841-847,

Yang, M.S., and K.L., Wu, 2001. A new validity index for fuzzy clustering, *IEEE International Fuzzy Systems Conference*, pp. 89-92.

SERIAL IMAGES FROM AIRBORNE DIGITAL FRAME CAMERA SYSTEMS FOR MONITORING OF TRAFFIC DYNAMICS

Peter Reinartz

Remote Sensing Technology Institute, German Aerospace Center
PB 1116, D-82230 Wessling
peter.reinartz@dlr.de

KEY WORDS: Aerial image series, traffic monitoring, velocity estimation, road database, applications

ABSTRACT:

Traffic monitoring with wide angle serial images from digital cameras on airborne platforms is a very new research field in remote sensing. The classical means to measure traffic density and velocity depend on local measurements from induction loops and other on site instruments. This information does not give the whole picture of the traffic situation. In order to obtain precise knowledge about the traffic flow of a large area, only airborne cameras or cameras positioned at very high locations (towers, etc.) can provide an up-to-date image of all roads covered. Especially for the near real-time monitoring of areas where a large disaster has happened, this technology will provide timely and accurate information of the state of infrastructure (streets, bridges) and the traffic situation. The paper aims at showing the potential of using image time series from airborne camera systems to derive traffic parameters on the basis of single car measurements. To be able to determine precise velocities and other parameters from an image time series, exact geocoding is one of the first requirements for the acquired image data. The methods presented here for determining several traffic parameters for single vehicles and vehicle groups involve recording and evaluating a number of digital aerial images from high altitude and with a large total field of view. Visual and automatic methods for the interpretation of images are compared. It turns out that the recording frequency of the individual images should be at least 3 Hz or more especially for automatic vehicle tracking. The accuracy and possibilities of the methods are analyzed and presented, as well as the usage of a digital road database for improving the tracking algorithm and for integrating the results for further traffic applications. Shortcomings of the methods are given as well as possible improvements regarding methodology and sensor platform.

1. INTRODUCTION

1.1 Traffic research

To derive information about traffic dynamics, statistics and behavior, the empirical studies, measurements, modeling attempts and simulation programs are numerous and diverse. The challenge is to develop robust methods for predicting, visualizing and modeling complex traffic events (Brockfeld et al., 2004). Only on the basis of reliable data, the simulation, control and planning of traffic systems can be optimized and thereby contribute to the efficient use of existing infrastructure, reducing emissions, and increasing safety.

Merely equipping the streets with conventional stationary measurement systems such as induction loops, radar sensors or cameras does not provide an adequate supply of suitable data for many possible applications. The challenge is to develop innovative solutions which augment the information from existing individual measurement sites, thereby closing the gaps in the traffic picture. Traffic research counts on so-called large area data collection to achieve a considerably improved data basis. New approaches currently under investigation include the recording of data by means of mobile measurement units in vehicles which flow with the traffic (floating car data, FCD, (Brockfeld et al., 2007)). The big advantage of the remote sensing techniques presented here is that the measurements can be applied everywhere and do not depend on any third party infrastructure.

Especially in areas beyond city and town limits it is difficult to obtain a complete picture of the traffic for a large area. On German freeways and national roads, for instance, numerous accident-prone sites have been identified for which the precise cause of accidents is not well known or adequately documented. It is also important to know how traffic congestion develops and how vehicle velocity reduces at the tail end of a jam or in response to speed limits; travel time in these dense traffic situations is also a matter of interest. Stationary camera systems relatively near the ground are not useful for rigorous observation, since detailed analysis of the traffic situation is only possible within a small area. For larger areas, relevant parameters such as travel time, distance between vehicles and velocities cannot be recorded because of significant shadowing effects.

1.2 Remote sensing approach

The advantage of satellite and aircraft observations is that with the view from high altitude a very large area can be recorded. However, continuous observation is impossible with satellites, since geostationary earth orbits cannot be used because of their high altitude of 36,000 km. Satellites in a low earth orbit (which is required for high resolution earth observation) have a high rotational speed (~7km/s) and can only supply snapshots of a momentary traffic scene, or several within a few minutes (Toth et al. 2003). The typical revisit time is in the order of a couple of days. Therefore, single satellites cannot replace airborne observations for traffic observation. Furthermore, optical sensor data from high altitudes are dependent on good weather conditions. But if traffic is to be analyzed with the help of satellites it is necessary to record the situation on typical days and times regardless of the weather. This is possible with radar equipment as, e.g., mounted on the German TerraSAR-X satellite. With this system traffic situations can be monitored worldwide and independently of weather and daylight (Runge et al. 2007). However, severe

problems are expected in inner city areas due to the inherent side-looking geometry of radar.
A technology, which combines the advantages of satellites and aircrafts for traffic monitoring, is provided by autonomous unmanned aircrafts permanently positioned in the stratosphere. These High Altitude Long Endurance (HALE) platforms are more flexible than satellites and allow permanent observation of large areas on a regional scale.

1.3 Airborne optical data

The usefulness of aircraft optical data from the visible (Stilla et al. 2004, Toth & Greijner-Brzezinska 2004) and thermal infrared (Ernst et al. 2003, Hinz & Stilla 2006) wavelength ranges for vehicle detection has been studied using many different approaches. However, there are not many investigations on optical time series recorded by satellite, aircraft or from very high positions and with a large field of view (Toth et al. 2003, Pötzsch 2005). Image Sequences of large areas taken at intervals of seconds or less are however easy to acquire with airborne sensors. Parameters relevant for traffic such as individual vehicle and vehicle group velocities, vehicle type, distance, traffic density and travel times can be derived from such data.
With an image time series it is possible to record the entire traffic dynamics for a given area and to analyze, for example, overtaking maneuvers, merge and exit behavior, as well as traffic jams for a certain time span. Such results are highly relevant input data for traffic modeling and simulation programs, for testing the efficacy of traffic control measures and for the input into GIS systems for traffic monitoring (Ernst et al. 2005). First results on the topic have been shown in (Reinartz et al. 2006).
The paper shows some improved methods for the automatic evaluation of serial image data using single vehicle tracking and describes comparisons and error estimations in combination with other methods for measuring the velocity of vehicles. The influence of image frequency is shown as well as the usefulness of digital vector data of the road network. Automatic vehicle tracking is compared with results of visual interpretation. Finally, an outlook is given on possible applications for large area traffic monitoring. The main scope is to show the potential of airborne serial image data, mainly from commercial non-calibrated frame cameras for monitoring traffic situations.

2. AERIAL IMAGE DATA AND GROUND REFERENCE

2.1 Canon serial data

The data acquisition of serial images for these investigations was performed using a Canon Camera EOS 1D Mark II 8 MPixel and the 3 camera system (3K) consisting of 3 Canon EOS 1Ds Mark II 16 MPixel digital cameras (image frequency 3 Hz) mounted on a DLR aircraft at flight altitudes from 1,000 m to 3,500 m above ground (with 50 mm and 100 mm lenses), leading to pixel sizes from 0.14 m to 0.75 m. The areas covered are the A96 freeway west of Munich, the A8 freeway south of Munich and a freeway in Austria. The image acquisition frequency is exactly 3 Hz. For operational work, automatic georeferencing with knowledge about exterior and interior orientation is necessary and has to reach sub-pixel registration accuracy for the consecutive images.

2.2 Street data base

In order to use the derived traffic parameters in a larger context, e.g., for simulations or traffic control, the data have to be stored in a traffic database. For this reason there is a need for automatic integration of the values to a common base of street lines. One of these road databases has been produced by the NAVTEQ Company (NAVTEQ 2006). The roads are given by polygons which consist of piecewise linear “edges,” grouped as “lines” if the attributes of connected edges are identical. With this data set it is possible to calculate mean traffic density or velocity per edge/line for a certain time span.
With a simple algorithm that uses the perpendicular distance of the vehicle coordinates to the single edges, more than 95% of the cars can be assigned correctly. Only in the case of street crossings (including bridges) and freeway exits some errors appear due to wrong street assignment, which can be eliminated to a high extent using algorithms that incorporate the direction of vehicle motion. Through this assignment, a database can be established which can be used for traffic simulation studies or traffic flow investigations.

3. AUTOMATIC DETECTION AND TRACKING OF VEHICLES

3.1 Method

The method for automatic detection of cars works on differences between two subsequent images (Lachaise 2005). The data sets used are described in section 2.1. Since the image difference is sensitive to noise and parallax changes, processing is restricted to the roads which are marked by using the NAVTEQ database with the correctly georeferenced data.
The procedure is shown for a set of two images (Fig. 1a shows part of one image.) A normalized difference image of two exactly co-registered images is calculated followed by a range threshold (too low and too high values are excluded) which creates a map of changes between the two images (Fig. 1b). These changes depict disappearing as well as appearing objects in one of the images.

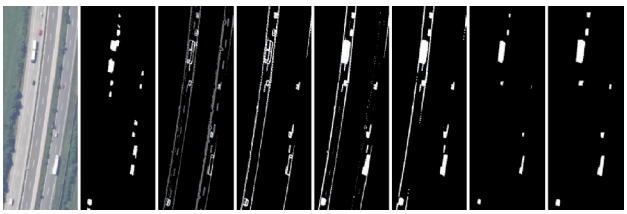

Figure 1. Detection of cars: (a) original image, (b) normalized difference image after double thresholding, (c) detected edges, (d) recovery of the whole vehicle, (e) filled, (f) suppression of small details, (g) 7x7 erosion, (h) 7x7 dilation = detected cars

To be able to differentiate between these two events, a technique was developed to decide if a car is leaving or arriving at the detected position. This is done by detecting edges with the Sobel operator on roads in both images, as shown in Fig. 1c. In the next steps the map of changes is used to recover entirely closed objects (Fig. 1d). If an object coincides with a marked area in the difference image, it is assumed that it belongs to the current image and it will be marked as a moving object. These objects are filled (Fig. 1e) and filtered (Fig. 1f) to separate them from road edges. By using erosion (Fig. 1g) and dilation (Fig. 1h) operators most of the residual noise can be eliminated.
As can be seen in Fig. 1b in the upper left corner, a large moving object (a truck) can overlap in the two following images. In this case the overlapping area is marked as “no change” in the difference image and this moving object is represented by two

objects of a wrong size. Using edges which coincide with the map of changes and processing the above depicted object extraction marks the whole object in the first image as well as in the second image (Fig. 1h).
As vehicles may have moved only a few pixels between the two images, the area in which the corresponding vehicle is searched for in the following image must start at the rear end of the vehicle in the first image. Hence, for each vehicle, the rear corners are selected by testing the vehicles bounding box against the road and driving direction, respectively. The corresponding vehicle is then searched only in a small area in driving direction of the current vehicle (see Fig. 2).

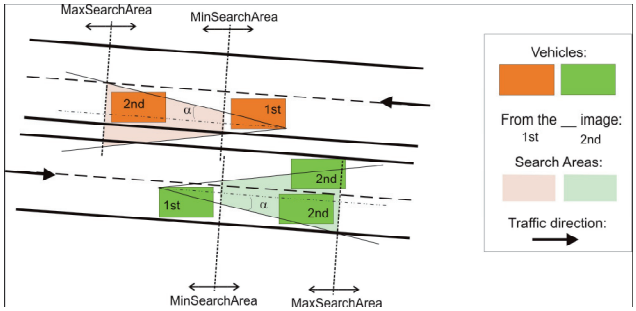

Figure 2. Aspect of search area

Three parameters (MinSearchArea, MaxSearchArea and α; see specification in Fig. 5), which have to be set by the user, determine the size of the possible corresponding area for the moving object. MinSearchArea can be zero and MaxSearchArea has to be larger than MinSearchArea. According to the used data (3 Hz), typical values are MinSearchArea = 10 pixels; MaxSearchArea = 50 to 60 pixels and α = 5º.
All moving objects of one image detected with this method are correlated with moving objects of the subsequent image by calculating a sum of absolute differences (SAD), as given in Eq. (1)

$$\mathrm{SAD} = \sum_{i,j} |I_1(u+i, v+j) - I_2(u+i, v+j)| \quad (1)$$

where I_1, I_2 are the two images, (u,v) is the starting coordinate of the object, and (i,j) is the index running from 0 to the size of the object in the first image. The use of some a priori knowledge such as traffic direction, typical velocity and angular ranges reduces the amount of possible corresponding objects and thus eliminates unlikely matches. Taking the best SAD correspondence value and using a threshold for a vehicle pair gives the corresponding vehicles. Finally, the velocity can be calculated based on the georeferenced images and the recording time of the images.

3.2 Results

The automatic car detection and tracking algorithm has been applied to several image series with different spatial resolutions and frame rates in the series (Schmeer 2005). The results show that the accuracy depends strongly on these parameters. The lowest spatial resolution for reasonable results is a pixel size of 0.5 m (with sufficient behaviour of the modulation transfer function (MTF), although the method is relatively robust with regard to image quality) and the frequency of the image series should be at least 3 Hz. For these values, the algorithm detects about 75 to 90 % of the manually measured cars correctly with a RMSE in velocity values of 1.2 km/h in comparison to the manual/visual measurements. For image series with frequencies of 1.5 Hz (taking every second image in the series) or less, the detection rate drops down to about 50 to 65 %. Therefore a good trade-off between the amount of data and the detection rate seems to be an frame rates of about 3Hz, a spatial ground resolution of about 0.5 m.

4. APPLICATIONS

The methodology described above should show the potential of measuring automatically the velocities of single cars for a large region. With a commercial off-the-shelf camera system consisting of three 16 MPix cameras, an area of about 7 km x 2 km can be covered with a single "shot," and by using a navigation system and camera calibration parameters, the geocoding can be done much faster. Actually a system with these parameters is now available at DLR. With such a system, operated on an aircraft, the possible derivable parameters and applications are as follows:

- Tracking and velocity estimation for single cars for a time span of about 100 sec
  - Vehicle distance
  - Time-to-collision
  - Track changing dynamics
  - Overtaking maneuvers
  - Driveway dynamics
- Mean velocity per section of road
  - Traffic congestion development
  - Dense traffic dynamics
  - Travel times
- Traffic density
- Controlling of on site instruments
- Input for simulations and traffic modeling and validation of traffic flow equations
- Fusion with other traffic monitoring data

As an example, one result for the calculation of travel time is shown here. This is in particular helpful since – when approaching a traffic jam – it would be in a car driver's interest to know how much time delay a congestion will cause rather than to know how long the congestion is, as he is usually told in traffic messages. When knowing the time delay he could decide if a detour is worthwhile or not, or whether he should simply give up the planned trip.
The motorway A8 south of Munich is one of the busiest parts of the German motorway network with an average load of around 100,000 vehicles per day. Figure 3 shows the *16 km* motorway section between motorway junctions "Hofolding" and "Weyarn", which was selected as test site on 2nd Sep. 2006. At this time, heavy traffic at this section was caused by homebound travellers.
The estimating of travel times are compared with vehicles on ground and with estimations from ground instrumentation which are available at this part of the motorway.

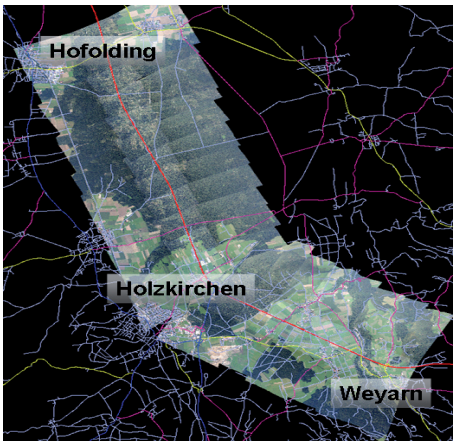

Figure 3. 16km motorway strip (A8) south of Munich as imaged by 3K camera system

As ground truth for travel times, two runs with a GPS equipped vehicle (ADAC) in northbound direction and one run in southbound direction was conducted. Table 1 lists the links between reference vehicle runs to 3K data takes. It should be mentioned, that a direct comparison between travel times from reference vehicle and 3K data takes contain systematic errors, as the northbound runs take around half an hour and the 3K data set represent a time span of ten minutes.

ID	Date	Strip	Travel-time	Data take	
R1	02-Sep-2006 14:02-14:36	16km	35 min	3K-Ia	North-bound
R2	02-Sep-2006 14:38-14:47	16km	9 min	3K-Ib	South-bound
R3	02-Sep-2006 14:48-15:18	16km	31 min	3K-Ic	North-bound

Table 1. Data from reference vehicle at A8 south of Munich

The results in table 2 now shows the comparison to the on-ground instrumentation (detector data).

ID	Ref	Travel time 3K		Detector data	
		Left lane	Right lane		
Ia	35’	39’48”	39’57”	34’	S-N
Ib	X	38’36”	40’42”	28’	S-N
Ib	9’	08’04”	x	x	N-S
Ic	31’	37’06”	37’27”	26’	S-N

Table 2. Comparison of travel times derived from 3K images with reference travel times

Instantaneous travel times derived from detector data do not completely comply with the reference measurements. That is because only speeds at certain stations are used that are more or less a set of random observations of the complete freeway stretch. Also, instantaneous speeds do not reflect the dynamics of traffic, as they do not consider the time a vehicle actually needs to pass the different stations. The calculated travel times from 3K-camera data are a little overestimated in comparison to the other values, but lie in the same range. More detailed results are shown in Kurz et al. 2007.

This experiment gives rise to further investigate the subject and to improve the traffic flow models included to arrive at optimized travel time estimations for traffic congestions.

Another important application for the methodology is the monitoring of large events like the Oktoberfest in Munich, or local disaster situations, since these events often induce heavy traffic problems and authorities therefore need simulated or better real-time data for controlling such situations and/or guiding relief actions. For this purpose the data have to be available in near real-time and new concepts for fast data geocoding and transmission are being developed to date.

5. CONCLUSIONS

The investigations show that it is possible to derive high quality traffic data from image series recorded by airborne cameras. With an easy to use visual interpretation tool nearly 100 % of the vehicles can be detected. These data can be used for verification of standard instrumentation, for validation of traffic flow equations, and for input into traffic models and simulations.

The automatic vehicle tracking method leads to reduced car detection accuracies, but the number of tracked vehicles is still high enough (75-90%, for open areas and normal traffic) to derive traffic parameters like density, mean velocity and travel times. These results were achieved by using the knowledge of the direction of the car movement through road databases. The automatic interpretation needs an image repetition frequency of 3 Hz or more. A lower frame rate results in a much lower automatic detection rate. In any case, very good geocoding and therefore co-registration of the subsequent images is a necessary prerequisite for high quality analysis. This geocoding has to be done automatically by using camera calibration values and navigation instrumentation for operational applications. Comparison of the derived velocities using automatic or visual interpretation methods shows an agreement in the order of 1 km/h. Constraints of this method are given in the case of occlusions through trees, houses or bridges and through the effective spatial resolution of the images. The minimum effective resolution should be in the order of 0.5 m. The pixel size alone does not guarantee this, e.g. if high image blurring appears through camera movement or other effects.

Further improvements of the method are envisaged by using other means of tracking the cars after their first detection, this will include phase correlation techniques in the Fourier domain and propagation of measured cars and their velocities to further images in the series. The latter will be probably able to reduce false alarms. Also the detection of not moving vehicles will be included in the process.

Actually, aircraft are not the ideal platform for collecting such data since due to their high speed the same area can be recorded only for a short time span (with the 48 MPixel camera system of DLR the time is about 100 sec, for longer observations many U-turns are necessary). To improve this, new platforms (e.g. UAV, helicopter, blimp or HALE) will be included in the investigations in future work. With these data sets a large area evaluation will be possible to demonstrate the capabilities and usefulness of image series for traffic monitoring for more applications.

6. REFERENCES

Brockfeld, E., Kühne, R. D., Wagner, P., 2004. Calibration and Validation of Microscopic Traffic Flow Models, Transportation Research Board Annual Meeting: Transportation Research Record, Volume 1876, 2004, Washington, DC (USA), p. 62-70.

Brockfeld, E., Wagner, P., Lorkowski, S., Mieth, P. 2007. Benefits and Limits of Recent Floating Car Data Technology – An Evaluation Study, In: CDROM-WCTR2007, S. C2-830, 11th World Conference on Transport Research, University of California, Berkeley, USA, June 2007

Ernst, I., Sujew, S., Thiessenhusen, K.-U., Hetscher, M., Raßmann, S., Ruhé, M., 2003. LUMOS - Airborne Traffic Monitoring System, In: Proceedings of 6th IEEE International Conference on Intelligent Transportation Systems, 12-15 October 2003, Shanghai, China

Ernst, I., Hetscher, M., Lehmann, S., Lippok, A., Ruhé, M., 2005. Use of GIS Methodology for Online Urban Traffic Monitoring, Proceedings of 3rd International Symposium Remote Sensing and Data Fusion over Urban Areas (URBAN 2005), Tempe Arizona, USA, March 2005, on CD-ROM.

Hinz, S., Stilla, U., 2006. Car Detection in Aerial Thermal Images by Local and Global Evidence Accumulation. In: Pattern Recognition Letters, 27: 308-315

Kurz, F., Charmette, B., Suri, S., Rosenbaum, D., Spangler, M., Leonhardt, A., Bachleitner, M., Stätter, R., Reinartz, P., 2007. Automatic traffic monitoring with an airborne wide-angle digital camera system for estimation of travel times, Proceedings of PIA 2007, Munich, Sept. 2007

Lachaise, M. 2005. Automatic detection of vehicles and velocities in aerial digital image series, Diploma thesis, Ecole Superieure de Chimie Physique Electronique de Lyon, CPE- Lyon, 76p.

NAVTEQ, 2006. http://www.navteq.com

Pötzsch, M., 2005. Messung von Fahrzeugpositionen und –geschwindigkeiten in Luftbildsequenzen und Zuordnung zu Straßendatenbanken, Diploma Thesis, Technical University of Dresden and DLR Remote Sensing Technology Institute, 97p.

Runge, H., Suchandt, S., Kotenkov, A., Breit, H., Vonavka, M., Balss, U. 2007. Space Borne SAR Traffic Monitoring. In: Proceedings of International Radar Symposium 2007, DGON Bonn, Germany, IRS 2007, Cologne, Germany, Sept. 2007

Reinartz, P., Lachaise, M. Schmeer, E., Krauss, T., Runge, H., 2006. Traffic Monitoring with Serial Images from Airborne Cameras, ISPRS Journal of Photogrammetry and Remote Sensing, 61 (2006), pp. 149-158.

Schmeer, E. 2005. Untersuchungen zur Orientierung und Auswertung digitaler optischer Luftbildserienaufnahmen für ein automatisiertes Verkehrsmonitoring, Diploma Thesis, Hochschule Karlsruhe and DLR Remote Sensing Technology Institute, 110p.

Stilla, U., Michaelsen, E. Soergel, U. Hinz, S. Ender, J., 2004. Airborne monitoring of vehicle activity in urban areas. ISPRS Congress, Istanbul, Turkey, International Archives of Photogrammetry Remote Sensing and Spatial Information Sciences, Vol. 35-3, 973-979.

Toth, C.K., Grejner-Brzezinska D., Merry, C., 2003. Supporting Traffic Flow Management with High-Definition Imagery. Proceedings of ISPRS Workshop High Resolution Mapping from Space, Hannover, Germany, 6p., on CD-ROM.

Toth, C.K., Grejner-Brzezinska, D., 2004. Traffic Management with state-of-the-art airborne imaging sensors. International Archives of Photogrammetry, Remote Sensing and Spatial Information Sciences, Vol. 35-2, 848-853.

7. AKNOWLEDGEMENT

I would like to thank Marie Lachaise, Franz Kurz and Elisabeth Schmeer for their contributions to the work as well as the DLR flight operations for their support in all campaigns

PAVING THE HIGHWAY TO A DIGITAL EARTH BY INTEGRATING GIS, REMOTE SENSING AND IMAGE PROCESSING

J. Schiewe

HafenCity University Hamburg, Hebebrandstraße 1, 22297 Hamburg, Germany
jochen.schiewe@hcu-hamburg.de

KEY WORDS: integration, GIS, remote sensing, image processing, visual interpretation, uncertainty

ABSTRACT:

The common focus on all major research projects that Prof. Manfred Ehlers has been conducted within the last decade was the idea of integrating data and methods from GIS, remote sensing and image processing. This contribution tries to outline Manfred Ehlers' overall vision of an integration framework, and concentrates on two specific aspects, namely on the integration of processing methods and on an integrated uncertainty assessment.

1. INTRODUCTION

- "GIS data are available - why don't you use them for your automated scene interpretation?"
- "Color imagery is available nowadays – why do you use only black-and-white images in your algorithm?"
- "Road databases are nearly complete everywhere – why do you develop an algorithm for their detection from satellite imagery?"

These are typical questions that everybody should be aware who gives a presentation with Manfred Ehlers being in the audience. These questions also give a perfect insight into his overall philosophy of thinking and working (at least during the last decade when the author was in luck to work together with him): He follows a very pragmatic approach for producing, processing and presenting geo data by integrating methods and techniques from Geographical Information Systems, remote sensing and image processing.

This paper will try to outline Manfred Ehlers' overall vision of a framework for an integration of GIS, remote sensing and image processing in more detail (section 2). In the following the focus will be laid upon two important aspects, namely on the integration of processing methods (section 3) and on an integrated uncertainty assessment (section 4), whereby the latter will be in the focus of a just granted joint project of Prof. Ehlers and the author.

2. CONCEPTUAL INTEGRATION FRAMEWORK

Remotely sensed scenes have a huge and continuously increasing importance for modeling and simulating structures and processes for topics like environment, planning, transport, or forest. Due to timeliness, small degree of generalization, and huge area performance, those data can be seen as an important source for generating and updating spatial databases. The development and usage of new digital remote sensing system – either spaceborne (like Ikonos, OrbView or QuickBird), or airborne (like HRSC, ADS 40, DMC) – has answered user demands concerning improved spatial, spectral and radiometric resolutions. Along with that a variety of new thematic applications, in general for generating and updating GIS databases at large scales, becomes possible. In return, GIS information can be used to support and automate the object extraction process. Figure 1 summarizes this general view on modeling the real world by integrating GIS and remotely sensed data.

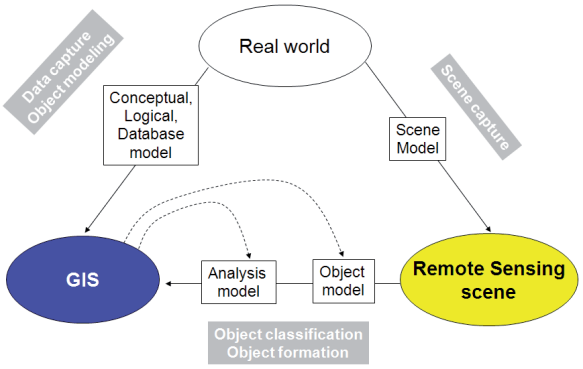

Figure 1. General integrated modeling framework

Within this conceptual framework several unique integration aspects have to be considered:

- Obviously there is no single sensor that can serve for all applications. With the complexity of specific applications also the need for **integrating data of different sensors or resolutions** increases. In this context Manfred Ehlers' work on a signal based and spectral characteristic preserving fusion (known as "Ehlers Fusion") should be pointed out. This approach is described in detail by Klonus & Rosso (2008; this volume).

This contribution is a revised and extended extract of the paper by Schiewe & Ehlers (2007).

- The above outlined conceptual framework suggests the existence of a more or less **integrated processing system for remote sensing and GIS**. The conceivable options, the actual status and some future directions for an integrated analysis will be discussed in section 3.
- Finally, it is also obvious that such a framework has to cover the topic of an **integrated uncertainty assessment** – relevant aspects will be dealt with in section 4.

3. ANALYSIS INTEGRATION

3.1 Concepts for low-level operations

The above outlined conceptual framework for an integration of GIS and remote sensing suggests the existence of an integrated processing system for remote sensing and GIS. Ehlers et al. (1989) presented a concept for a totally integrated system for remote sensing and GIS. They differentiated between three integration levels: (a) two separate systems with a data interface; (b) two principally separate systems with a common user interface; and (c) a totally integrated system.

Most of today's GISs offer hybrid processing, i.e. the analysis of raster and vector data. They also have image display capabilities or image analysis add-ons which offer some level (b) functionality (Bill, 1999; Ehlers, 2000). However, geospatial information is usually processed in either raster or vector form and has to be converted into the desired processing or output format. A truly integrated processing option (without prior conversion) does not really exist and GIS and remote sensing information is usually processed independently from each other.

What is needed for a truly integrated processing is an analysis of the necessary processing components. First attempts of a system and geo data model independent view could be seen by Tomlin's Cartographic Modeling (Map Algebra) approach which is still the basis for many raster GIS's (Tomlin, 1990). Another approach for raster and vector based systems was presented by Albrecht who proposed a set of system and data structure independent GIS operators (Albrecht, 1996). Based on these, Ehlers (2000) proposed four groups with 17 image processing functions which should be added.

It has to be noted, however, that these low-level operators are not sufficient to define and describe the complete functionality of integrated GIS. Still required is a thorough analysis of hybrid processing capabilities, i.e. functions that allow a joint analysis of remote sensing and GIS information. It has to be investigated how polymorphic techniques can be used to extend the capacities of the universal high level GIS/image processing functions. The operator *Overlay*, for example, should be able to process image-image, GIS-image, and GIS-GIS overlays without a different name for every function option. First results of such polymorphisms were investigated, for example, by Jung (2004). Additional functions have to be developed, on the other hand, that extend the capabilities of integrated GIS beyond the sum of the single components.

3.2 Concepts for high-level operations

Based on the statements above it is obvious that also concepts and implementations for integrated *high-level* operations cannot fulfill the demands yet. This problem is clearly evident for the task of thematic interpretation of remotely sensed data which has to be characterized as the bottleneck within the overall data flow (Nichol et al. 2007). The reasons for unsatisfying results are originating from the complex information space that remote sensing systems represent. This complexity is due to the variance of the topographical objects under consideration, to the variance of data acquisition configurations and conditions, and finally to the multi-dimensionality of input data. This all puts high demands on – integrated - methods and techniques for scene interpretation.

From a general point of view we can model the inherent interpretation process as outlined in figure 2. In analogy to cognitive perception it can be seen as a hybrid process, i.e. it contains procedures in both directions, top-down (or model driven) and bottom-up (or data driven), showing application dependent different sequences and weights. Furthermore, it is not simply a linear process, but it also includes feedback mechanisms at various stages.

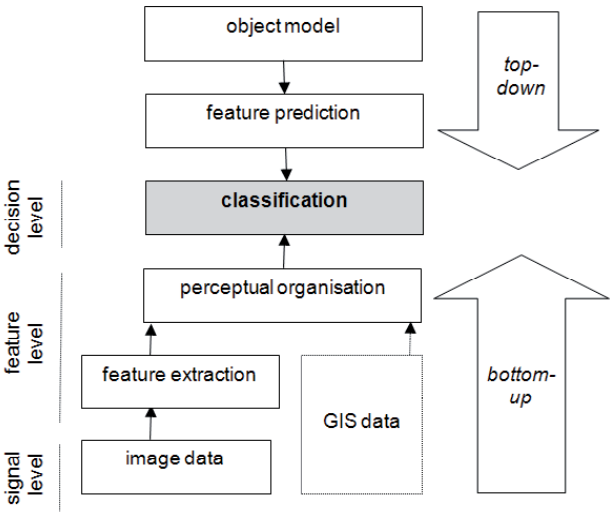

Figure 2. Generalized workflow for the interpretation of image data in an optional combination with GIS data

Applying a **visual interpretation,** structures and processes can be detected rather easily, i.e. feature extraction and organization yields reasonable results. On the other hand, visual methods often lack objectivity (e.g., between different interpreters) due to the fact that the process (which is not even fully understood by experts; refer to Goldstein, 2002) is intuitively rather than rule-based. Furthermore, visual interpretation is a rather time consuming – and with that a rather costly – process.

To overcome this problem huge efforts have been put into the development of **automatic interpretation methods** in the last two or three decades. However, reliable, transferable and

operational methods could not be developed so far which is again mainly due the complexity of the underlying data and information space. In particular, there is still a big and application dependent gap between the extracted scene features (like single edges) and the actual object characteristics as described in a knowledge (or memory) representation. The necessary bridging process of perceptual organization (like grouping of lines or areas into meaningful structures) has been neglected too much in the past or could not be modeled effectively so that in general unsatisfying classification results have been achieved (Schenk, 2003). Furthermore, present automatic techniques – like their visual counterparts – show problems with the increasing multi-dimensionality of input data, i.e. with a fusion of the numerous derived features and decisions and a follow-up multi-criteria analysis in a systematic manner (Ehlers, 2007; Schiewe, 1999). Summarizing the state of art Nichol et al. (2007) conclude: "…, the development of 'black box' algorithms, implying complete automation, is probably neither possible nor desirable and researchers are encouraged to work with end users to develop realistic local solutions".

Following the hypothesis, that neither visual nor automatic method alone will offer effective and efficient solutions for thematic interpretation within the next decade, it is – in analogy to the case of low-level operators – also necessary to develop a comprehensive and systematic taxonomy of high-level operations for scene interpretation processes.

Based on this in a first step it will be possible to go back to the classical visual approach and to improve it with methods and tools of geovisualization that allow for a user defined selection and combination of underlying representation types, the choice of efficient interactive elements for iterative interpretation operations, and a near real time performance of these operations. In a second step, the integration of visual and automatic operations should be envisaged.

Concentrating on the first step, we developed a concept for an assistant for change detection and analysis based on remotely sensed and classified scenes. This concept applies the principle of the basic questions related to spatio-temporal phenomena ("where", "when" and "what") from which two parts form the input and the remaining one the output of an operation (Schiewe, 2007).

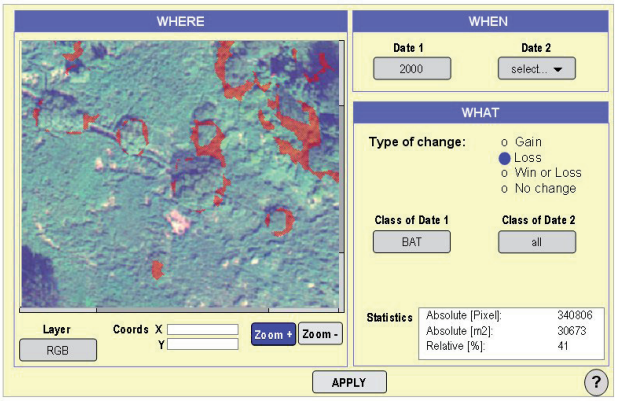

Figure 3. Screenshot of change detection assistant – detected changes are marked in transparent red.

A simple example (see figure 3) already showed that important additional information about patterns and neighborhood could be derived with this visual approach. In particular, the differentiation between existential changes (i.e. the appearance or disappearance of entire objects) and property changes of still existing objects (e.g., changes in size) leads to a more precise explanation of actual landscape variations.

4. INTEGRATED UNCERTAINTY ASSESSMENT

4.1 Uncertainty chain

It is evident that the issue of accuracy and errors within an integration process is of great importance. In this context Gahegan & Ehlers (2000) formulated a framework for modelling uncertainty in an integrated remote sensing environment. A typical path taken by data captured by satellite, then abstracted into a suitable form for GIS is shown in Figure 4, and involves four such models. Continuously varying fields are quantized by the remote sensing device into image form, then classified and finally transformed into discrete mapping objects. The overall object extraction process is sometimes referred to as semantic abstraction due to the increasing semantic content of the data as it is manipulated into forms that are easier for people to work with.

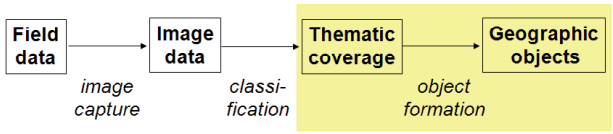

Figure 4. Continuum of Abstraction from Field Model to Object Model (after Gahegan & Ehlers, 2000)

However, in practice a strict quantitative error propagation modeling along this uncertainty chain is hardly to achieve. Hence, aggregated thematic uncertainty is determined after the classification process by comparing reference data ("ground truth") and the classification result from which error matrices and related measures like overall, producer's and user's accuracy or Kappa coefficient can be derived.

In this context generally the problems of indeterminate boundaries in both reference and classification results are neglected, which occur between mostly natural objects or are due to blurred or overlapping definitions of classes or related attributes in a given classification scheme. These problems are even amplified with the use of remotely sensed data showing high spatial resolution as given with the new digital airborne or spaceborne systems.

4.2 Integrated and fuzzy uncertainty measure

Motivated by the above outlined problems our goal was (and still is) to develop a profound integrated and fuzzy methodology for determining the a posteriori classification accuracy for high resolution data considering uncertainty in reference data as well as indeterminate boundaries in the reference and the classification result (Schiewe & Ehlers, 2007).

In order to focus on the above mentioned aspects, our approach starts with the – theoretical and ideal – assumptions that the classification schemes between reference and classification are identical and that no discrepancies occur due to different pixel sizes or temporal changes. Furthermore, we assume that an appropriate sampling procedure has been taken into account.

In order to model the inherent fuzziness, **transition zones** are now introduced. Those are defined a posteriori using a buffering zone along a given boundary between two topographical objects. Based on the investigations by Edwards and Lowell (1996) the width of this zone depends on the combination of objects (e.g., the transition zone between forest and meadow is obviously larger than those between building and road) as well as on the size of the object areas (figure 5). Within these zones a *membership function* (in our case simply a linear function) is applied perpendicular to the boundary for each class *c*. This procedure is performed for both, the classification result (leading to membership values $\mu_{CLASS}(c))$ and the reference data ($\mu_{REF}(c)$).

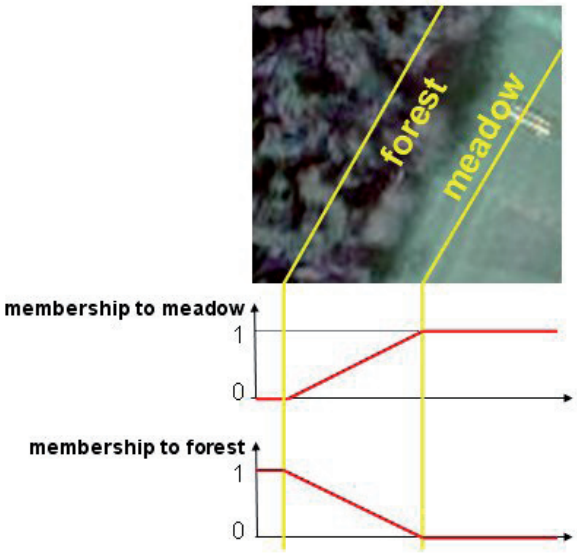

Figure 5. Principle of building transition zones and applying membership functions to a pair of topographical objects.

Figure 6 demonstrates the important additional value of the fuzzy approach: While a crisp method would have evaluated the classification result as clearly wrong, now the realistic chance of a correct categorization is no longer neglected.

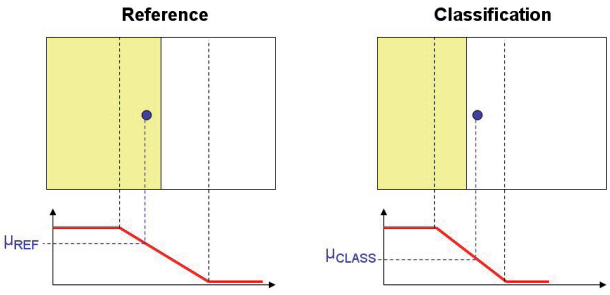

Figure 6. Principle of deriving Fuzzy Certainty Measure FCM: Building transition zones (dashed lines) in reference (left) and classification result (right), determining membership values of a selected location to shaded class in reference (μ_{REF}) and classification (μ_{CLASS}).

In order to derive one or more characteristic values, our approach consults the respective membership values for the same spatial elements (i.e., pixels or regions) in the reference as well as in the classification result. Those are compared separately for each topographical class and for those elements for which a possibility of existence (or membership values larger than 0, respectively) is present in reference and classification. The resulting **Fuzzy Certainty Measure FCM(c) per class c** is determined as follows:

$$FCM(c) = 1 - \frac{1}{n}\sum_{i=1}^{n} | \mu_{i,REF}(c) - \mu_{i,CLASS}(c) |$$

$$\forall i \,|\, \mu_{i,REF} > 0 \wedge \mu_{i,CLASS} > 0$$

where:

$\mu_{REF}(c)$: membership value of a pixel or region for class c in reference data

$\mu_{CLASS}(c)$: membership value of a pixel or region for class c in classification result

n: number of pixels or regions under consideration

The FCM(c) values vary between 0 and 1 – the larger the coincidence between reference and classification is, the larger the FCM(c) value becomes.

It can be expected that further developing and applying these methods a more complete and thorough modeling of uncertainty can be accomplished. Our future work is concerned with a sensitivity analysis of the parameters (in particular with the width of transition zones based on object class combination and area sizes). Furthermore, empirical investigations will be performed for the combination of fuzzy with additional probabilistic measures. Finally, the extension towards a change analysis will be taken into consideration by introducing thresholds for FCM values for the classifications of different time stamps. All these aspects will be dealt with in the next two years in a joint project between Prof. Ehlers and the author. This project – called CLAIM (CLassification Assessment using an Integrated Method) is funded by the German Research Foundation (DFG).

5. CONCLUSIONS

There is no doubt about the need for a general framework that describes the integration of multi-source data and methods for answering the various spatio-temporal questions.

But the two aspects that have been highlighted before, namely the integration of processing methods and an integrated uncertainty assessment, have also demonstrated the increasing complexity that comes with such integration. This supports the hypothesis that complete automation "is probably neither possible nor desirable" (Nichol et al., 2007). Hence, we favor a systematic and analytic approach that firstly decomposes the related processes into single operations. Prof. Manfred Ehlers has already given significant input on respective taxonomies for hybrid operators. This work has definitively to be elaborated. For instance, additional operators have to added (e.g., for uncertainty determination), a set of optimal methods for the operations has to be given, and interfaces for their linkage have to be defined.

Based on that also questions must be allowed whether all operations must be done in an automatic manner, or perhaps an enhanced manual or visual approach will lead to more effective and efficient results.

6. REFERENCES

Albrecht, J., 1996, Universal Analytical GIS Operations. Ph.D. Thesis, ISPA-Mitteilungen 23, Vechta., Germany.

Bill, R., 1999, GIS-Produkte am Markt – Stand und Entwicklungstendenzen. *Zeitschrift für Vermessungswesen* 6: 195-199.

Edwards, G. and Lowell, K.E., 1996: Modeling Uncertainty in Photointerpreted Boundaries. *Photogrammetric Engineering & Remote Sensing.* 62(4): 337-391.

Ehlers, M., 2000. Integrated GIS – From Data Integration to Integrated Analysis*, Surveying World*, 9: 30-33.

Ehlers, M., 2007. Neue Sensoren in der Fernerkundung. GIS Business, (12): 29-32.

Ehlers, M., Edwards, G., & Bédard, Y., 1989. Integration of Remote Sensing with GIS: A Necessary Evolution, *Photogrammetric Engineering and Remote Sensing* 55: 1619-1627.

Gahegan, M. & M. Ehlers, 2000. A Framework for Modeling of Uncertainty in an Integrated Geographic Information System, *ISPRS Journal of Photogrammetry and Remote Sensing*, 55, pp. 176-188.

Goldstein, E.B., 2002. Wahrnehmungspsychologie. 2nd edition. Spektrum Akademischer Verlag, Berlin, Heidelberg.

Jung, S., 2004. HYBRIS: Hybride räumliche Analyse Methoden als Grundlage für ein integriertes GIS, Ph.D. Thesis, University of Vechta, Germany (CD Publication).

Klonus, S. & Rosso, P., 2008. The development of the Ehlers Fusion. In: Schiewe, J. (Ed.): Paving the highway to digital earth. gi-reports@igf (this volume).

Nichol, J., King, B., Quattrochi, D., Dowman, I., Ehlers, M., & Ding, X., 2007. Earth Observation for Urban Planning and Management – state of the art and recommendations for application of earth observation in urban planning. Photogrammetric Engineering & Remote Sensing, 73(9): 973-979.

Schenk, T., 2003. From Data to Information and Knowledge. In: Schiewe et al. (Eds.): Challenges in Geospatial Analysis, Integration and Visualization II. Proceedings of Joint ISPRS Workshop, Stuttgart (CD-ROM): 105-110.

Schiewe, J., 1999. An advanced technique for pixel-based multi-sensor data integration. Schriftenreihe des Instituts für Photogrammetrie und Ingenieurvermessungen der Universität Hannover (ISPRS-Workshop "Sensors and Mapping from space"), auf CD-ROM

Schiewe, J. , 2007. Conceptual development of an assistant for change detection and analysis based on remotely sensed scenes. International Archives of Photogrammetry, Remote Sensing and Spatial Information Sciences, (XXXVI – 4/W45; Joint ISPRS/ICA/DGfK-Workshop "Visualization and Exploration of Geospatial Data"), CD-ROM.

Schiewe, J. & Ehlers, M., 2007. Fuzzy models for handling uncertainty in the integration of high resolution remotely sensed data and GIS. In: Morris, A. & Kokhan, S. (Eds.): Geographic Uncertainty in Environmental Security (NATO-Workshop), Springer: 89-106.

Tomlin, D., 1990. GIS and Cartographic Modeling, Prentice-Hall, Englewood Cliffs, NJ.

THE RELEVANCE OF SPATIAL RESOLUTION AND STEREO CAPABILITY FOR THE INTERPRETATION OF REMOTE SENSING IMAGERY

Manfred Schroeder

DLR – Remote Sensing Technology Institute
manfred.schroeder@dlr.de

KEY WORDS: Spatial resolution, Stereo capability, Detection efficiency, Satellite imagery

ABSTRACT:

Images of different resolution levels between 2 m and 0.25 m were analysed by several test persons in mono and stereo presentation with the aim to detect certain predefined objects. It could be shown that a clear functional relation between the average detection efficiency and the logarithm of the amount of data contained in the analysed images exists, independently of the interpretation mode (mono/stereo), i.e. the same interpretation results can be obtained from a stereo mage pair or from a mono image with a resolution increased by the factor √2. If only the ground resolution is considered as parameter then the interpretation results for stereo are superior to those of mono (at the same ground resolution).

FOREWORD:

It is a great pleasure for me to dedicate this article on the interpretability of satellite images to Prof. Dr. Manfred Ehlers on the occasion of celebrating his 60th birthday. Manfred Ehlers and I started our research activities in the field of remote sensing jointly in the "German geo-scientific airborne remote sensing program" in the year 1974. Since that time we always stayed in touch, exchanged ideas and experiences through which a friendly relationship developed over the years. I am glad to honour the personality of Manfred Ehlers who is an international accepted expert in the fields of remote sensing and geo-informatics. At the same time I thank Manfred for the valuable support he gave me and my work in the last decades and combine this with the hope for many opportunities to meet, discuss and work with him.

1. OBJECTIVE

The objective of the investigations presented in this paper was to find out, how the results of visual image interpretation depend on ground resolution and stereo capability of the images to be analysed. This research study was made in the view of use and development of future remote sensing satellite systems. A special objective was to see whether and how stereo images can improve the interpretability of satellite images.

2. METHOD

For this study black/white images with ground resolutions of 2m, 1m, 0.5m and 0.25m were analysed by eight test persons acting as image interpreters.

The images with different ground resolution levels were generated by digitizing stereo aerial photographs. The original aerial photographs had a ground resolution of 6–8 cm. For digitizing a pixel size corresponding to 3 cm ground resolution was applied. The different resolution levels were generated by summing up the corresponding amount of pixels. For image analysis a digital stereo workstation with liquid-crystal-shutter glasses was utilized. The images were presented to the interpreters successively in mono and stereo. In all resolution levels the images had the same scale, i.e. they contained the same amount of pixels. During the image interpretation process the observer could select an image scale on the monitor that seemed most suitable to him for the actual interpretation task. The scale could be varied in five steps between 1:1840 and 1:115.

The scenes covered an area of 575m x 575m each and contained parts of an airfield, industrial plants, administrative- and residential buildings, infrastructure facilities, different vegetation types and vehicles. The objects in the scenes could be categorized in the object classes shown in Table1.

Extended Plane Objects	**Traffic Routes**	**Buildings**	**Vehicles**	**Linear and Point Shaped**
Parking Sites	Runways	Halls	Aircrafts	Chimneys
Trees, Tree-Groups/ Forest	Multi-Lane Roadway	Office/ Residential Buildings	Trucks	Towers
Other Green Space	Single-Lane Roadway	Residential Houses	Vans	Parabolic Antennas
	Field Paths	Huts / Containers	Helicopters	Fences
	Foot Paths	Understories	Passenger Cars	Flagpole Antennas
	Railway Tracks	Fuel Pump	Bushes	
		Power Supply		

Table1: Object classes grouped according to their outside structure characteristics: Length-, width-, height ratio and so far as possible to their size.

The task of the image interpreters was to find the objects listed in Table 1. An object was considered "found", when it was described at least by one of the terms "detected", "recognized" or "identified" during the interpretation process. (This qualitative description of found objectives was not further used and evaluated in this study.)

For the assessment of the interpretation results the term "detection efficiency (DE)" was introduced which was defined as follows:

Number of the actual found objects (sum of Yes-answers of all test persons) related to the number of maximum possible objects to be found (sum of all possible Yes-answers of all test persons).

Three scenes, each in mono and stereo display, in all four resolution levels were analysed by the test persons. The "detection efficiency (DE)" was determined for each person and each scene in each resolution level, differentiated according to object class (see Table 1) and to mono and stereo.

3. RESULTS

It can be assumed that the DE increases proportional to the spatial resolution. The increase of spatial resolution is related to a corresponding growth of the provided amount of data. In the stereo imaging mode the amount of data is increased by the factor 2 with respect to the mono mode at the same resolution. By doubling the ground resolution in the mono mode the amount of data is even raised by the factor 4. Therefore it was anticipated that the DE increases proportional to the offered data volume. As furthermore, the interpretation activity is a psychological-physical process, it was presumed that the DE increases proportional to the logarithm of the amount of data. For establishing a functional relation a "relative data rate" was derived from the ground resolution value and the imaging mode (mono/stereo). For this purpose the relative data rate for 2m ground resolution was set to 1. With this normalisation the relative data rates and their logarithms can be computed (see Table 2).

Resolution/Modus	relative data rate	Log (relative data rate)
2 m / Mono	1	0
2 m / Stereo	2	0.3
1 m / Mono	4	0.6
1 m / Stereo	8	0.9
0.5 m / Mono	16	1.2
0.5 m / Stereo	32	1.51
0.25 m / Mono	64	1.81
0.25 m / Stereo	128	2.11

Table 2: Relative data rate and their logarithm computed from the amount of data offered to the interpreter per scene

It could be shown that a clear functional relation between the average DE and the logarithm of the relative data rate exists. The average DE is represented by the average of the interpretation results over all object classes, all scenes and all test persons (see Figure 1).

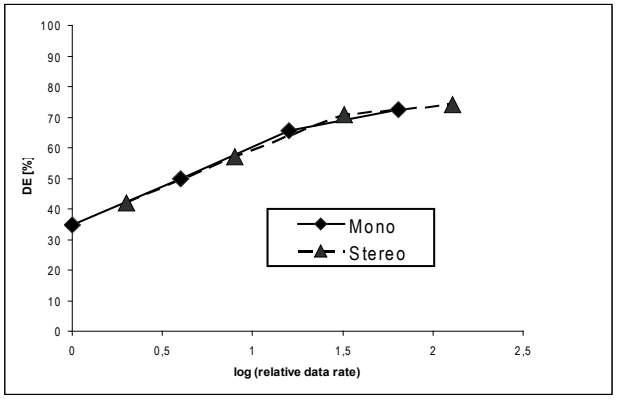

Figure 1: Detection efficiency (DE) in dependence of the relative data rate, averaged over all object classes, all scenes and all test persons

The DE increases initially linear (up to 0.5m) with the logarithm of the relative data rate and approaches with higher resolution asymptotical a saturation value. The resolution at which the saturation occurs however depends on the size and structure of the object to be discovered. The diagram (Figure 1) shows furthermore that under the aspect of data rate the interpretation of stereo images has neither advantage nor disadvantage over mono image interpretation, i.e. the same increase of DE can be achieved by using stereo images or by increasing the spatial resolution by the factor $\sqrt{2}$ for mono images.

The results shown in Figure 1 can also presented with the parameter "ground resolution" (Figure 2). In Figure 2 the logarithmic presentation on the x-axis is maintained. In this presentation the stereo interpretation proves clearly as more effective, i.e. the DE is initially (at 2 m resolution) by approx. 21% higher than for mono interpretation. With increasing resolution this difference reduces asymptotical to approx. 2.1% (at 0.25 m resolution).

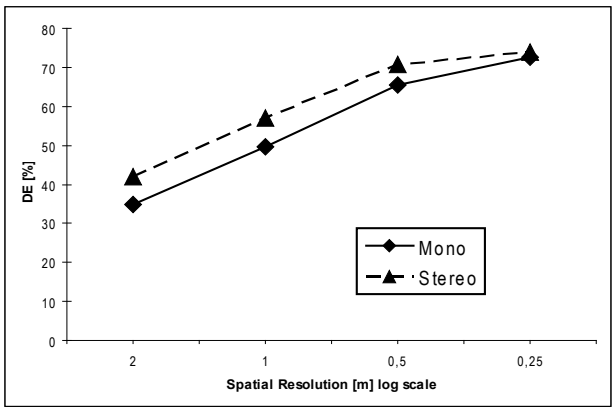

Figure 2: Detection efficiency (DE) in dependence of the ground resolution

This difference between mono and stereo diminishes with higher resolution because the DE generally increases with higher resolution for both imaging modes (mono/stereo) and converges asymptotical to the same limiting value. The limiting values in Figure 1 and Figure 2 stay even at the highest resolution level below 100% because the DE value is an average value over different object classes.

4. CONCLUSION

- It exists a clear functional relation between the average detection efficiency and the logarithm of the amount of data contained in the analysed images, independently of the interpretation mode (mono/stereo), i.e. the same interpretation results are obtained from stereo image pairs or from a mono image with a resolution increased by the factor √2.
- If only the ground resolution is considered as parameter then the interpretation results for stereo are superior to those of mono (at the same ground resolution).
- Objects with nearly no vertical structure are found in mono and stereo observation with the same effectiveness. Objects with a distinct vertical structure can be found in the stereo mode with significantly higher effectiveness for all resolution levels.

THE CHALLENGE OF PROCESS AND MANAGEMENT OPTIMIZATION FOR PHOTOGRAMMETRIC MAPPING PROJECTS

R. W. Schroth

Hansa Luftbild German Air Surveys, Elbestr. 5, 48145 Muenster, Germany - schroth@hansaluftbild.de

KEY WORDS: Photogrammetry, work flow, automation, project management

ABSTRACT:

The photogrammetric mapping process has reached a high level of efficiency and productivity. This is based mainly on the permanent technical development from analog to digital imagery during the last decades as well as on the consequent introduction of new managerial tools in the photogrammetric project work flow.

In general the photogrammetric mapping process is project oriented as a stand alone project or integrated into an other project such as construction, planning or general GIS project. Therefore project management is an essential part of the organization, in particular for the execution of several projects running parallel in a photogrammetric production environment.
For this reason this paper will focus on technical and managerial aspects. Photogrammetric products like Digital Terrain Models, 3-dimensional vector data or Digital Orthophotos, which are the results out of the project processes, are highly influenced by the used production processes and the degree of automation in the different production steps. Thus the single production steps are highlighted in respect of the most efficient techniques which are proven in quality and best price performance ratio. On the other hand project management tools are shown which are equivalent to the technical aspects in regard to the success of a photogrammetric mapping project.

ZUSAMMENFASSUNG:

Der photogrammetrische Prozeß zur Datengewinnung hat einen hohen Standard in bezug Effizienz und Produktivität erreicht. Dies basiert im wesentlichen auf der kontinuierlichen technischen Weiterentwicklung von analoger zu digitaler Bildbearbeitung in den letzten Jahrzehnten, aber auch auf der konsequenten Einführung neuer Managementtechniken im photogrammetrischen Produktionsprozeß.
Grundsätzlich ist der photogrammetrische Produktionsablauf projektorientiert, entweder als eigenständiges Projekt oder in andere Ingenieurprojekte wie bei Baumaßnahmen, Planungsaufgaben oder in allgemeine GIS-Projekte integriert. Deshalb stellt das Projektmanagement einen wesentlichen Teil in der Ablauforganisation dar, vor allem wenn mehrere Projekte parallel in der photogrammetrischen Produktionsumgebung bearbeitet werden müssen.
Aus diesen Grund werden die folgenden Darlegungen sich sowohl auf technische wie auf organisatorische Aspekte konzentrieren. Photogrammetrische Produkte wie Digitale Geländemodelle, 3-dimensionale Vektorkartierungen oder Digitale Orthophotos, welche die Ergebnisse der Projekte sind, werden stark durch den Produktionsprozeß und dessen Automationsgrad bei den einzelnen Produktionsschritten beeinflußt. Deshalb werden die einzelnen Produktionsschritte in Bezug auf hocheffiziente technische Ansätze, welche nachweisliche Qualität und das beste Preis-Leistungsverhältnis liefern, erläutert. Andererseits werden Werkzeuge des Projektmanagements aufgezeigt, welche gleichwertig zu den technischen Aspekten in Bezug auf den Erfolg eines photogrammetrischen Projektes zu betrachten sind.

1. INTRODUCTION

In July 1980 the jubilee and the author met for the first time during the Congress of the International Society for Photogrammetry (ISP) in Hamburg, where they both were involved in the hard "donkey" work of the operational handling of the conference under the leadership of their Professors Gottfried Konecny (Congress Director) and Fritz Ackermann (President of the German Association for Photogrammetry).
Already at those days Manfred's research activities were focusing on automation procedures which paved the way for modern techniques and software as we are nowadays using in the photogrammetric and remote sensing production processes (Ehlers, 1983).
The photogrammetric process in general is part of an engineering project like the construction of infrastructure, e.g. railways, highways, etc. Also for data acquisition and updating of GIS information photogrammetry plays a major role (see Figures 1 and 2). The superimposition of the vector data on the orthophotos is getting more and more a standard. That means a high quality digital terrain model with break lines is necessary. To get this information the latest technologies used in a production environment will be shown, starting from the aerial survey flight till the final photogrammetric product. The respective workflow can be seen in Figure 3.
But it is not only the technical aspect which makes a photogrammetric project or sub-project as part of a large engineering project successful. The management of the different process steps and especially the non-sequential and overlapping steps of different projects running parallel are quite challenging for any organization. Therefore different organizational structures for project management will be discussed too.

Figure 1. Highway, superimposition of orthophoto and vector data

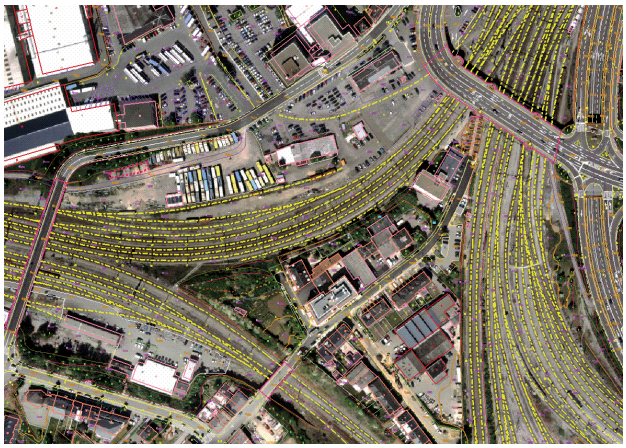

Figure 2. Railway, superimposition of orthophoto and vector data

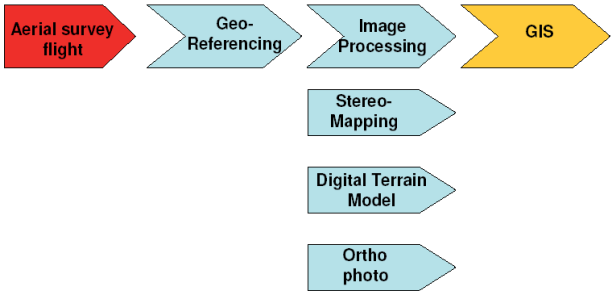

Figure 3. The total photogrammetric workflow

2. THE PHOTOGRAMMETRIC PROCESS

2.1 Aerial Survey Flight

Aerial survey flights with sensors like metric cameras, digital frame cameras or digital line scanners, airborne laser scanners (ALS, LiDAR), thermal scanners, hyper spectral scanners, etc. are still done like years before with fixed wing planes. These planes with piston engines or turbo-prop engines have an average age of 30 years. This is caused by economical reasons of the strong competition in the market but also on the non-availability of suitable planes by the manufacturers.

Besides the fixed wing planes, helicopters are more and more in use for the aerial survey flights for corridor mapping with medium format digital cameras and integrated LiDAR systems.

A new development is the use of unmanned airborne systems (UAS) with small and light sensors on board and working autonomously. The field of application is quite limited, mainly for small areas to be covered or reconnaissance.

The flight management and the flight planning for aerial survey flights is strongly computer assisted. 3D flight planning with the use of existing digital terrain models will be soon a standard. The navigation with GPS and related pin point photography is since more than 15 years a strong improvement in the flight process, the former navigator changed nowadays to a sensor operator responsible for the sophisticated combined sensors as GPS receivers, inertial measurement units, analogue or digital cameras and airborne laser systems.

The whole sub-process of the aerial survey flight is shown in Figure 4. The digitalisation of the process and the miniaturisation of the onboard sensors will end up in the near future with a one man crew, namely the pilot (Schroth, 2007b).

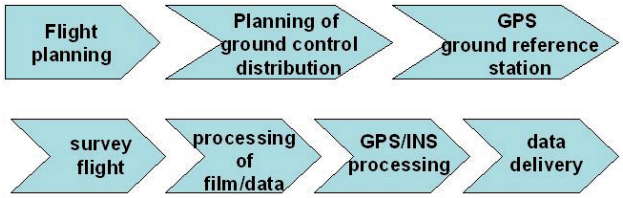

Figure 4. The sub-process of the aerial survey flight

2.2 Geo-Referencing

Today the geo-referencing of the sensor data depends on the type of sensor, the type of terrain to be documented and the requested accuracies. A short overview will be given. Figure 5 shows the principles for a camera sensor.

2.2.1 Direct Geo-Referencing: The direct geo-referencing is based on the information out of the differential GPS (dGPS) with ground reference stations and the inertial measurement unit (IMU) or inertial navigation system (INS) to determine the parameters of the exterior orientation of a sensor. This method is independent from any ground control information besides some GPS ground reference stations. The achieved quality and accuracy strongly depends on the system calibration and the design of the ground reference stations. There is no direct relation to the local geodetic network system and singular disturbances of the network cannot be covered.

Alternatives to the ground reference stations inside the area of interest are

- Virtual reference stations
- OmniStar HP by FUGRO
- Precise point processing (PPP)

These alternatives are not delivering the same precisions but can be sufficient depending on the requested accuracies. In general for all of them, empirical tests and experiences for aerial survey are still missing.

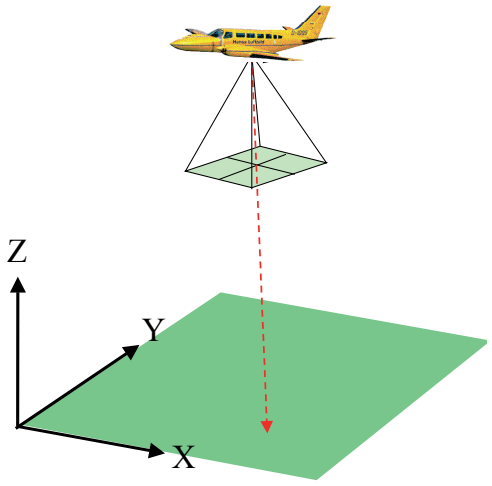

Figure 5. Principle of the exterior orientation of aerial sensor (analogue camera)

2.2.2 Indirect Geo-Referencing: The indirect geo-referencing, also called aerial triangulation in photogrammetry, has developed strongly from a highly interactive work with many manual measurements to a quasi fully automated process. Matching procedures substituted the manual tie and pass point measurements, only the measurements of the ground control points have to be done manually. The increase of efficiency can be easily seen by the decrease of the pricing of the geo-referencing per image which went down by a factor 20 in the last 15 years. Other cost savings were the reduced number of ground control points by the use of dGPS and the estimation of strip wise drift parameters during the determination of the projection centres out of the dGPS data which reduced the radius of the curves during the changing of the flight lines.
Some details of the achievable accuracies with the new large format digital camera sensors can be seen in Schroth, 2007a.

Integrated Sensor Orientation: The integrated sensor orientation (ISO) combines the advantages of the direct and the indirect geo-referencing. An aerial triangulation with auxiliary data from dGPS and the IMU is determined. This method will be used for high accuracies, over difficult terrain like water or big forest areas or desserts, etc. Also for special sensors like line scanners or platforms like the UAS.

2.3 Image Processing

In the field of photogrammetry the image processing is concentrating on stereo mapping / restitution, generation of digital terrain models (DTM) and differential rectification of aerial images to digital orthophotos (see figure 3).

2.3.1 Stereo Mapping: The feature based vector mapping by stereo restitution was the most common application of photogrammetry. The evolution from the 2.5D data capturing to fully 3D and the integration in GIS like Geographics (Bentley) or Geomedia (Intergraph) shows the latest developments in this field. It is still in all practical applications a highly interactive work. Automated procedures like feature recognition or extraction are still under development or not delivering the necessary quality. Also the overwhelming demand for raster data has brought the stereo mapping somehow out of the focus of further research.
Figures 6a and 6b are showing the typical result of stereo capturing and figure 7 shows the 3D feature extraction of typical 3D city modelling. In figure 8 the integration in a Geographical Information System can be seen.

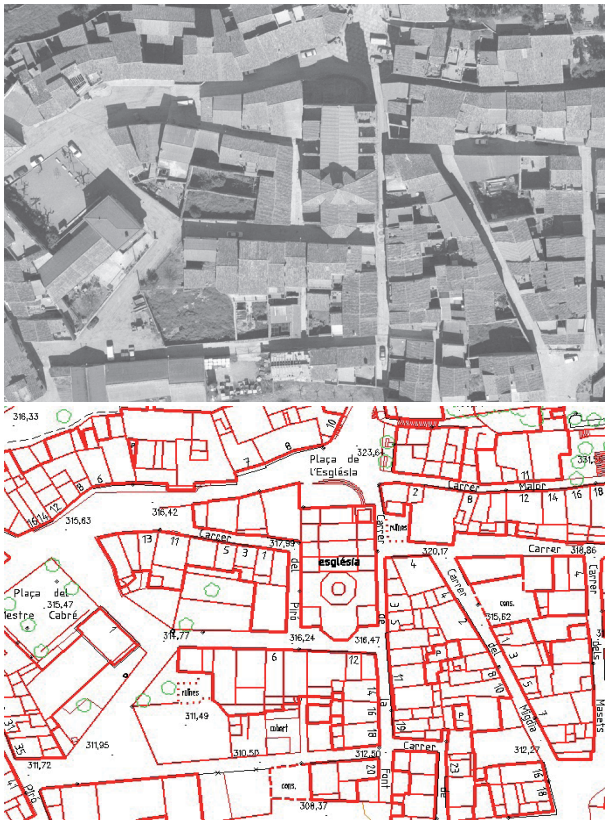

Figure 6a and 6b. Vector data generated by image stereo-mapping

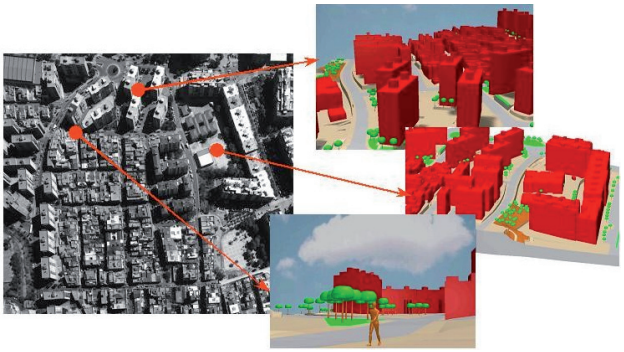

Figure 7. 3D image stereo-mapping

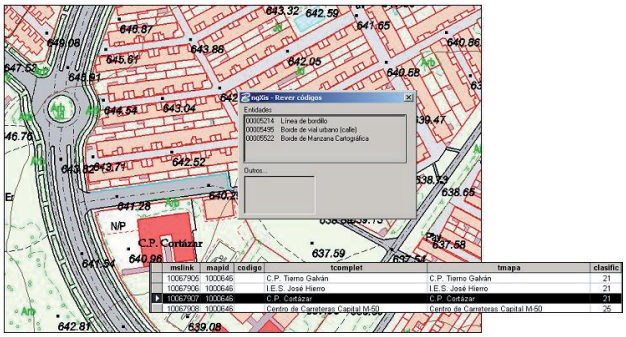

Figure 8. GIS integrated stereo mapping

Digital Terrain Model: As the DTM in the former days was mainly used to derive contour lines automatically it is now a stand alone product in photogrammetry. The increasing demand for digital orthophotos with high resolution also asks for a high quality DTM with accuracies better than 0.20 m and break lines to model linear features. Two different methods for DTM data capturing are common: airborne laser scanning (ALS) and automated image matching procedures. A comparison between them is given in Schroth, 2007b.

The principle of the ALS is shown in figure 9 where a laser beam is scanning the terrain. Figure 10 represents a digital surface model as the result of the first pulse reflection of the laser beam. Multi-pulse information and filtering techniques generating the DTM. An interactive data verification is highly recommended.

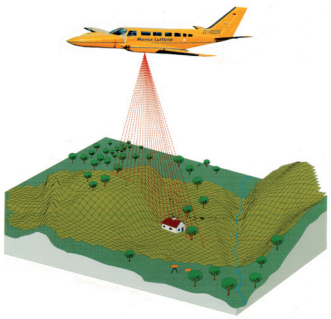

Figure 9. Principle of airborne laser scanning

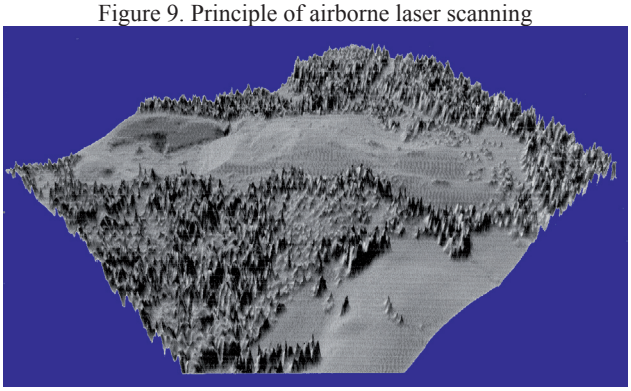

Figure 10. Digital surface model generated by ALS

Automated image matching has been developed in the last years to a very high standard and is achieving similar accuracies as the ALS principle. Multi-image matching (see figure 11) in combination with filter techniques and efficient data editing tools, already developed for ALS data editing, and stereo restitution for the break lines are generating a high quality DTM (see figure 12).

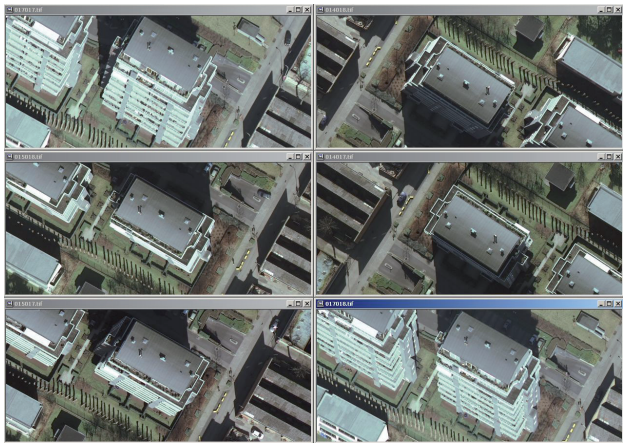

Figure 11. Multi-image matching with high overlapping photos

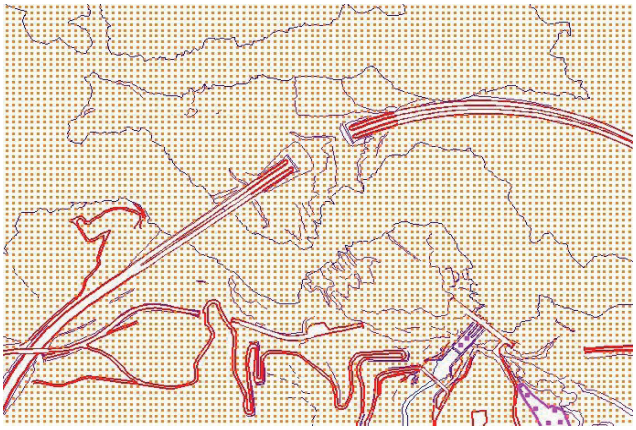

Figure 12. DTM with break lines

Figure 13. Digital orthophoto with DTM from figure 12

2.3.3 Digital Orthophoto: Out of the geo-referenced images and the DTM, digital orthophotos can be determined by differential rectification (see figures 12 and 13). The combination of several orthophotos as a mosaic under the assistance of radiometric adjustments and balancing is a standard product today (see figure 14). The total process is highly automated, the human interaction is minimized (quality checks). Only the process handling and its understanding needs however very well trained and educated engineers.

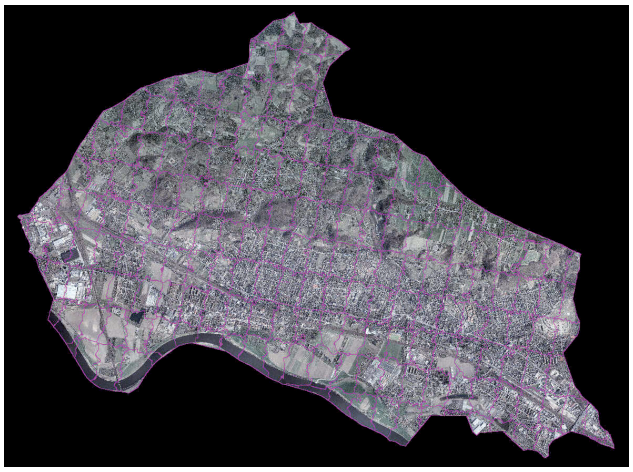

Figure 14. Digital orthophoto mosaic with seam lines

3. PROJECT MANAGEMENT

Photogrammetry services are strongly project oriented and less product oriented. And each project has its own individual characteristics. The different production steps as shown in chapter 2 are not really standardized. Some national standards are existing, but the fast technical and economical developments and changes make it difficult to keep these standards up-to-date. Thus an efficient project management and sufficient engineering know-how is essential.

In a photogrammetric production environment several projects are running parallel and their project volume varies between some thousands and several millions of Euros. Mass production like stereo mapping or DTM editing is quite often outsourced to low cost production zones. Therefore industrial organisation structures are no more applicable. Hierarchical organisation structure (see figure 15 as an example) are very often not covering the demands for multi-project handling and flexible behaviour. Also the complexity of the projects with different focuses like GIS integration, 3D-modelling, automation techniques etc require a project management with specialized knowledge.

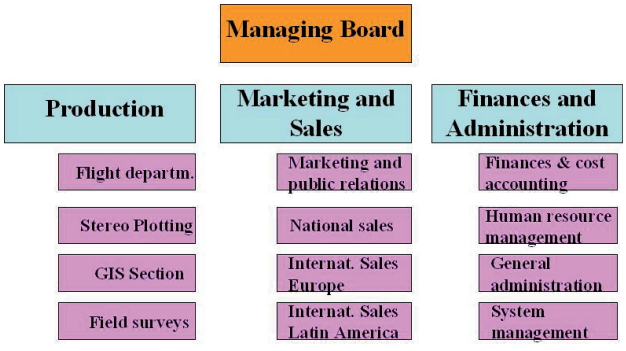

Figure 15. Org chart for hierarchical structure organisation

Under these conditions a matrix organisation as shown in figure 16 can be an alternative. Project management, responsible from the sales till the final delivery and invoicing of the project, is the key function of this concept. The management of the available human resources and the production environment needs of course coordination and some staff sections like for administrations are assisting the organisation.

	Sales & customer relations	Project prepa-rations	Survey flight	Film scannin g & AT	Digital ortho-photo	Stereo plotting	GIS process .
Project manager 1	X	X	X	X	X		
Project manager 2	X	X	X	X		X	
Project manager n	X	X					X
						Service departments	

Figure 16. Org chart for a matrix organisation

The concept is highly flexible and adoptable to varying project sizes and delivery schedules. The responsibility of the project manager also for the client leads to higher customer satisfaction and better project/product quality.

4. CONCLUSIONS

Photogrammetric mapping projects, their organization and their technical workflow are under the influence of short notice demands for data, global pricing, high efficiency and quality more and more optimized and automated. Their integration in GIS and spatial data infrastructure Manfred Ehlers already showed in 1998 (Ehlers, 1998). Under the influence and the impression of internet providers like Google Earth or Microsoft Virtual Earth and the consequentially following programmes for updating of these data in very short cycles with high resolution by national geographic administrations, the whole photogrammetric community is experiencing a challenging future. Especially with all these new demands, there should not be forgotten all the major scientific and practical achievements of the last decades in our discipline and they should be used and adopted to the latest trends and technologies in a sophisticated way.

5. REFERENCES

Ehlers, M., 1983. Untersuchung von digitalen Korrelationsverfahren zur Entzerrung von Fernerkundungsaufnahmen. Wissenschaftliche Arbeiten der Fachrichtung Vermessungswesen der Universität Hannover, Nr. 121, Hannover, Germany

Ehlers, M., 1998. Geo-Informationssysteme und deren Einsatz in der Planung. 75th Anniversary of Hansa Luftbild, Münster, Germany

Schroth, R., 2007a. The Digital Mapping Camera DMC and its Application Potential. ISPRS Hannover Workshop "High-Resolution Earth Imaging for Geospatial Information", *IntArchPhRS XXXVI-1/W51*, Hanover, Germany

Schroth, R., 2007b. Efficient Processing and Management of Multiple Large Photogrammetric Mapping Projects. In: *Proceedings of Trimble Dimensions 2007*, Las Vegas, NV, USA

PROGRESS IN UNICERTAINTY MODELING AND DATA QUALITY CONTROL IN GEOGRAPHIC INFORMATION SCIENCE

Wenzhong Shi

Advanced Research Centre for Spatial Information Technology, Dept. of Land Surveying and Geo-Informatics, The Hong Kong Polytechnic University, Hong Kong
lswzshi@polyu.edu.hk

KEY WORDS: Uncertainty modeling, quality control, spatial data, spatial analysis, GIS

ABSTRACT:

Uncertainty modeling and quality control for spatial data and spatial analyses are key issues in geographic information science together with space and time in geography, as well as spatial analysis. In the past two decades, a lot of efforts have been made on discovering the uncertainty nature in spatial data and analyses, and furthermore to control the quality of spatial data and information. This paper summarizes the progresses we made in these research areas as the follows: from determinedness- to uncertainty-based representation of geographic objects in GIS; (b) from uncertainty modeling for static data to dynamic spatial analyses; from modeling uncertainty for spatial data to models; and from error descriptions to quality control for spatial data.

1. INTRODUCTION

In the past three decades, GIS has been developed from Geographic Information *System* to Geographic Information *Science*. As a science, GIS needs to be supported by its fundamental principles. GIS is composed of, at least, the following three principles: (a) space and time in GIS, (b) uncertainty and data quality, and (c) spatial analysis (Longley, Goodchild, Maguire and Rhind, 1999). In fact, uncertainty modeling covers all these three areas, besides the most obvious one – data quality. Space and time modeling in GIS should not only be for the determined spatial objects, but also cover the uncertain spatial objects. In fact, these are two fundamental types of spatial objects in the real world, which should be modeled in GIS, although most of the existing GIS mainly handle the determined spatial objects at this stage. Spatial analyses in GIS are the major functions for the spatial related decision making. Such spatial analyses are not error free. Uncertainty in the source data and limitations of the spatial analysis models may propagate and further introduce uncertainties in spatial analysis processes.

Spatial objects in the real world can be represented in the object-based model or field-based model. In either of these two types of spatial data, there exist the following uncertainties: positional uncertainty, attribute uncertainty, temporal uncertainty and logic inconsistency, and incompleteness.

A framework for modeling uncertainty in spatial data and spatial analyses has been formed (Shi, 2005). The framework is built based on a systematic study on uncertainty modeling and quality control for spatial data and spatial analysis. Among the development, a number of major theoretical breakthroughs have been made. This paper outlines four of them, namely (a) advances in spatial objects representation -- from *determinedness*- to *uncertainty*-based representation of geographic objects in GIS; (b) from uncertainty modeling for *static* spatial data to *dynamic* spatial analyses; (c) from uncertainty modeling for spatial *data* to spatial *models*; and (d) from error *description* of spatial data to spatial data quality *control*. In fact, there are a large number of achievements made by other international peers in the four areas, but they will not be introduced due to the limitation of paper length, and I will focus on the progresses made by us.

2. FROM DETERMINEDNESS – TO UNCERTAINTY-BASED REPRESENTATION OF SPATIAL OBJECTS IN SPACE

One of the fundamental issues in geographic information science is the representation of space and time. Euclidean space is regarded as one of the applicable spaces for representing geographic entities and phenomena, where the basic elements are points, lines, areas and volumes of the space.

In fact, geographic phenomena can be classified into two categories: determined and uncertain ones. According to the nature of uncertainties in geographic lines, Shi (Shi, 1994) classified the geographic lines into the following two types: Type I line and Type II line. The fundamental difference between the two types of lines is that there are

"real points" in the real world which construct a Type I line, while there is no real world point for a Type II line. Thus we have to determine or interpret these points for a Type II line by ourselves. An example of a Type I line is a building boundary, while a boundary between a forest and grassland is an example of a Type II line. In principle, we should use a determinedness-based representation for a Type I line; on the other hand, we should apply an uncertainty-based representation for a Type II line. Unfortunately, we only have the determinedness-based representation model for most of the current GIS. Therefore, there is room to further develop uncertainty-based spatial representations for uncertain geographic objects.

In our development, the uncertainty-based spatial representations of the geographic entities and phenomena cover points, line segments/ straight lines, curve lines and polygons.

2.1 Uncertainty-based Representation of Points

Instead of a determined point represented by its coordinates (x, y), a point with uncertainty can be represented by its confidence region, error ellipse, or error distribution of the point.

(a) Confidence Region Model for a Point

The confidence region of a point gives a region around the measured point, which contains the true location of the point with the probability that is larger than a predefined confidence level.

(b) Error Ellipses and Distribution

If the errors in the coordinates of a point are assumed to be normally distributed, their two-dimensional probability density function can be formed, and the error of the point coordinates is indicated by the standard ellipses. The probability that the point is inside the error ellipse is estimated by the volume of the two-dimensional error curved surface over the error ellipse. This probability increases with the size of the error ellipse.

2.2 Uncertainty-based Representation of Lines

(a) Confidence Region Model for a Two-dimensional Line Segment

A confidence region for a two-dimensional line segment is defined as a region containing the true location of the line segment with a predefined confidence level (Shi 1994). This confidence region J_2 is the union of the confidence regions J_{2r} for all points Q_{2r} on the line segment for $r \in [0, 1]$, so that the true locations $\varnothing_{2r}$ of all points on the line segment are contained within J_2 with the probability larger than a predefined confidence level:

$$P(\varnothing_{2r} \in J_{2r} \text{ for all } r \in [0, 1]) > \alpha \quad (1)$$

The confidence region J_{2r} is a set of points $(x_1, x_2)^T$ with x_1 and x_2 satisfying

$$X_{1r} - c_{21} \le x_1 \le X_{1r} + c_{21} \quad (2)$$

$$X_{2r} - c_{22} \le x_2 \le X_{2r} + c_{22} \quad (3)$$

where $c_{21} = [k((1-r)^2 + r^2)]^{1/2}\sigma_1$
$c_{22} = [k((1-r)^2 + r^2)]^{1/2}\sigma_2$
$k = \chi^2_{2;(1+\alpha)/2}$

Based on the confidence region model for a line segment, the confidence region for a two-dimensional polyline, or a polygon, was also built. Furthermore, the confidence region model was also extended to a generic one for *N*-dimensional lines (Shi, 1998).

(b) Probability Distribution Model for a Line Segment

The probability analysis can be applied to depicting the error distribution of that line. Based on the probability analysis, positional error on any straight line is modeled from a joint probability function of those points on the straight line. This joint probability function gives the probability distribution for the line in a particular region. The probability of the line falling inside the corresponding region is defined as the volume of the line's error curved surface formed by integrating the error curved surfaces of individual points on the line.

(c) The G-band Error Model

The G-band error model provides the quantities and characteristics of the error of the points on the line segment. The concentric band which is cut by the plane passing through the error ellipses of the endpoints of the line segment is defined as the generic error band, known as the G-band (Shi and Liu, 2000). The model describes the error of an arbitrary point on the line segment, given the error of the two end points are either correlated or independent. The model also gives the analytical relationships between the band shape and size with the error at the two endpoints and the relationships between them.

2.3 Uncertainty-based Representation of Curves

The positional uncertainty of a curve feature is described by two error indicators: ε_σ to measure the error in any point on the curve in the direction of the curve normal, and ε_m to describe the maximum error at the point to the curve. Both of them can assess positional error on a curve feature. The two error indicators are applied to describing uncertainty of both a regular curve (such as a circular curve) and an irregular curve (such as a third-order spline curve) (Shi, Tong and Liu, 2000).

2.4 Uncertainty-based Representation of Polygons

Positional error for a polygon in GIS is caused by the positional error in its boundary, mainly from the component vertices of the polygon. Two approaches on positional error modeling for a polygon are given: one is based on the error of the component vertices of the polygon, and the other is based on the error of the component line segments through their error bands [2].

Error Modeling Based on Its Component Vertices: A polygon is composed of its component vertices. Error of a polygon is thus determined by the error of its vertices. Error of the polygon is quantified according to the error of its vertices based on the error

propagation law in statistics. A polygon is also described by its parameters, such as its area, perimeter, gravity point, etc. Therefore, uncertainty of a polygon is described by these parameters.

Error Modeling Based on Its Component Line Segment: In fact, the area of a polygon is also a function of length of the component line segments of the polygon. This implies that positional error for the area of the polygon is subject to the positional error in these line segments. The relationship of the positional error in the line segment and the error in the area of the polygon are quantified, and uncertainty of the polygon can thus be estimated based on the error of the component line segments.

3. FROM MODELING UNCERTAINTY IN STATIC DATA TO DYNAMIC SPATIAL ANALYSES

Spatial analysis refers to the spatial analyses in GIS, such as overlay analysis, buffer analysis, line simplification, projection, *etc*. In fact, each of these spatial analyses is a transformation based on one or more original spatial data set(s). Uncertainty inherited in the original data sources will be further propagated or even amplified through such a spatial analysis. Sometimes, new uncertainties will be generated through such a spatial analysis. Therefore, besides modeling uncertainty in static spatial data, a step further is to model uncertainty in spatial analysis.

3.1 Modeling Uncertainty in Overlay Spatial Analysis

Modeling uncertainties in overlay spatial analysis provides an estimation of the uncertainty propagated through the analysis.

Two methods are proposed to estimate the propagation of errors in vector-based overlay spatial analysis: an analytical error model which is derived by the error propagation law, and a simulation error model (Shi, Cheung and Tong, 2004). For each of the two error models, it is proposed that the positional error in the original or derived polygons be assessed by three measures of error: (a) the variance-covariance matrices of the polygon vertices, (b) the radial error interval for all vertices of the original or derived polygons, and (c) the variance of the perimeter and that of the area of the original or derived polygons. The variance-covariance matrix of the vertices of an original or derived polygon is a relatively comprehensive description of error. The radial positional error interval is proposed and it is more effective for describing the error at the vertices of a polygon.

The experimental results demonstrated that the number of vertices and the error at the vertices of a polygon are two major factors that affect the accuracy of parameters of the polygon such as perimeter and area. Increasing (or decreasing) both the number and the error of the vertices of a polygon will similarly influence the error of these polygon parameters.

3.2 Modeling Uncertainty in Buffer Spatial Analysis

Modeling uncertainty in buffer spatial analysis provides a solution of quantifying uncertainty propagation through a buffer spatial analysis. A method of modeling the propagation of errors in a buffer spatial analysis for a vector-based GIS has been developed (Shi, Cheung and Zhu, 2003). Here, the buffer analysis error is defined as the difference between the expected and measured locations of a buffer. The buffer can be, for example, a point, line-segment, linear, or area features. The sources of errors in a buffer analysis include errors of the composed nodes of points or linear features, as well as errors of buffer width. These errors are characterized by their probability density function.

Four indicators of error and their corresponding mathematical models, in multiple integrals, have been proposed for describing the propagated errors in a buffer spatial analysis, including the error of commission, error of omission, discrepant area, and normalized discrepant area. Both the error of commission and the error of omission are suitable for describing a situation where the expected and measured buffers overlap. The discrepant area indicator has been defined, taking into consideration the possibility that the expected and measured buffers might not overlap with each other. This error indicator in fact provides a more generic solution for the cases, where the measured and expected buffers either overlap with each other or do not. Furthermore, the normalized discrepant area has been proposed, considering the mathematical rigors of the definition – to meet the conditions of the definition of distance in algebra.

3.3 Modeling Uncertainty in Line Simplification

Modeling uncertainty in line simplification provides a solution on uncertainty estimation for a line simplification or generalization process. The error sources of a line simplification are the uncertainty in an initial line, and the uncertainty due to the deviation between the initial and simplified lines. We classified the uncertainties in a line simplification process as a combination of the propagated uncertainty, the modeling uncertainty, and the overall processing uncertainty (see Figure 1) (Cheung and Shi, 2004). The propagated uncertainty is used to identify the uncertainty effect of the initial line, and the modeling uncertainty represents the uncertainty arising from the line simplification process. The overall uncertainty in the simplified line is modeled by the overall processing uncertainty that integrates both the propagated and the modeling uncertainties in the line simplification process.

Three uncertainty indices and corresponding mathematical solutions were proposed for each type of uncertainty by measuring its mean, median, and maximum values. For the propagation uncertainty, we proposed the mean discrepancy, the median discrepancy, and the maximum discrepancy; for the modeling uncertainty, we proposed the mean distortion, the median distortion, and the maximum

distortion; and for the overall processing uncertainty, we proposed the mean deviation, the median deviation, and the maximum deviation.

The distributions of all the types of uncertainty are positively skewed. The mean uncertainty index provides the general value of the type of uncertainty. The relation between the mean uncertainty index for the overall processing uncertainty and the threshold distance in the DP line simplification was studied. It was found that the mean uncertainty index is a monotonic increasing function of the threshold distance. Also, this function is used to determine the threshold distance such that an uncertain simplified line is close to the "true" initial line to a predefined acceptable level of accuracy.

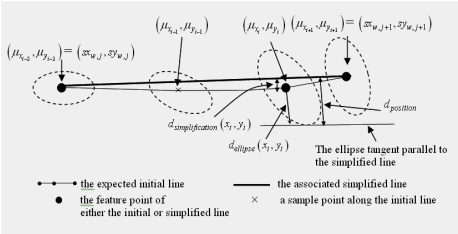

Figure 1: A comparison between the original

4. FROM MODELING UNCERTAINTY FOR SPATIAL DATA TO SPATIAL MODELS

In stead of describing real world objects by data, real world objects can also be described by spatial models. For example, digital terrains can be represented by digital elevation models. The models can be either a regular one, such as regular tessellation like a square, or an irregular one, such as Triangulated Irregular Network (TIN). Therefore, it is a natural evolution of uncertainty modeling to go: from spatial data to spatial models.

The difference between what in the real world and what represented by the models in GIS is referred to as model uncertainty. Here in this paper, uncertainty modeling of DEM model is taken as an example of model uncertainty estimation in GIS. One of the achievements has been made is a formula to estimate the average model accuracy of a TIN, as illustrated in Figure 2.

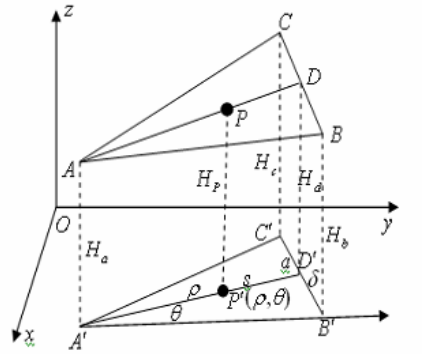

Figure 2: Estimation of average accuracy of TIN model

TIN is a widely used model for the representation of digital terrain by irregular triangles due to its higher accuracy of terrain representation and with the considerations of feature lines in the model. However, this does not mean that there is no error in a TIN model. The mean error of the DEM is identified and is estimated by the following mathematical formula (Zhu, Shi, Li, et al., 2005):

$$\sigma_H^2 = \frac{1}{2}\sigma_{node}^2 \,. \tag{4}$$

As an estimator of overall accuracy, the mean error of TIN is invariant to both the shape and spatial locations of triangles. From the formula, it can be determined that the mean elevation accuracy in a triangle is dependent on the error σ_{node}^2 of the original data but is independent of the shape and size of the triangle.

5. FROM UNCERTAINTY DESCRIPTION TO SPATIAL DATA QUALITY CONTROL

Most of the early studies mainly focused on describing uncertainties, including the uncertainties in spatial data, in a spatial analysis, or in a spatial model. From the point of view of an uncertainty handling, description is a necessary first step; a further step is to control or even reduce the uncertainties in the spatial data, analyses or models, if we are able to do so. Therefore, another progress made in handling uncertainties in spatial data and spatial analysis is from uncertainty description to quality control of spatial data and analyses. In this regard, the quality control for the following three data and models are given in this paper:

- Quality control for object-based spatial data – to control overall geometric quality of vector spatial data by the least square adjustment methods;
- Quality control for field-based spatial data – to geometrically rectify high resolution satellite imageries by point- and line-based transformation models; and
- Quality control for digital elevation models – to improve DEM accuracy by newly proposed hybrid interpolation model.

5.1 Quality Control for Object-based Spatial Data

This section briefs the principles of quality control for object-based spatial data, taking the vector cadastral data as an example (Tong, Shi and Liu, 2005). The statistical method for the spatial data quality control is the least square adjustment. The least squares method is adopted to solve the inconsistencies between the areas of digitized and registered land parcels, which has been proposed for adjusting the boundaries of the land parcels.

In this regard, the land parcel is the target to be adjusted in the data quality control process. A systematic strategy has been proposed for the cadastral data quality control by the least square adjustment, including: (a) to let the registered area in a land parcel as a true value and a digitized point with coordinates as the observations for the establishment

of the adjustment conditional equations; (b) to let both the registered area and the digitized point with coordinates as the observations, the weights of the two types of observation are estimated based on the variance components; and (c) to add the scale factor of the land parcel in the adjustment model and to estimate the weight of the observations based on the variance component from conditional adjustment with parameters. The adjustment for the land parcels is then realized. Furthermore, a hierarchical approach for spatial data quality control is proposed and illustrated in Figure 3. The control is from a smaller scale level (the upper figure), to middle scale level (the middle figure) and finally to the lower scale level (the lower figure).

For example, in method (a), the size of the registered area of a land parcel is taken as its true value and we adjust the geometric position of the boundaries of the digitized parcel. An area adjustment model is derived by incorporating the following two categories of constraints: a) attribute constraints: the size of the true area of the parcel, and b) geometric constraints: such as straight lines, right angles, and certain distances. Second, the method is then used to adjust the areas of the parcels.

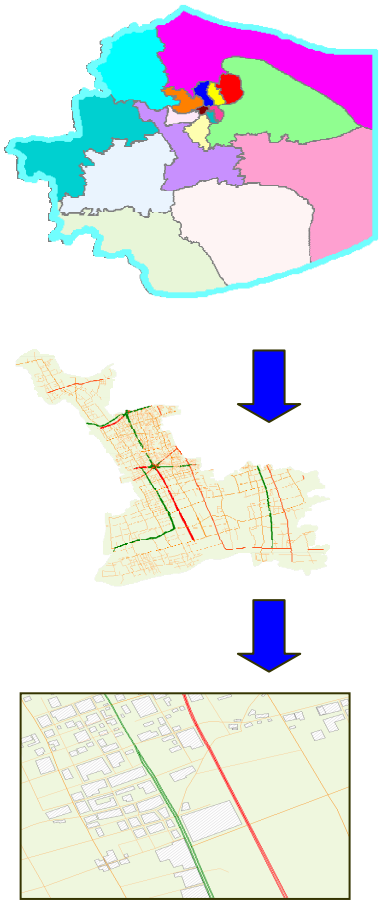

Figure 3: A quality control strategy based on multiple scale data

The quality control method (b) is further developed due to the considerations that both digitized coordinates of a land parcel and the registered area of the land may contain errors, although the quantity may be different. Now, the problem becomes how to solve the inconsistencies between the digitized and registered areas of land parcels under the condition that both of them are treated as observations with errors. Here, the key issue is to determine the weights of the two types of observations. The least squares adjustment, based on the Helmert method, is proposed for estimating the weights between the two types of observations. The insistency between the registered area and digitized area of the parcel is then adjusted through the least squares adjustment.

It is demonstrated, via several applications of the solution, that the proposed approaches are able to solve the problem of data inconsistency between the digitized area value and registered area value of the land parcels. This method has, in fact, solved one of the most critical problems in a vector GIS – data inconsistency in the databases.

5.2 Quality Control for Field-based Spatial Data

Satellite imagery is a kind of field-based spatial data. Due to the terrain effects, projection of imaging, and image scanning, as well as positioning error of the satellites during image capture, the geometry of an originally obtained satellite image contains positional errors. To control the quality and improve the positional accuracy of the obtained images, a geometric rectification process needs to be applied to the images. Instead of the traditional, point-based approach, line-based transformation model is proposed as a further development (Shi and Shaker, 2006).

(a) Point-based Geometric Rectification
In the point-based geometric rectification methods for improving the quality of the satellite image, the ground control points (GCPs) are used to build transformation models – a relationship between satellite imaging coordinate system and the ground coordinate system. Here, GCPs are obtained either through ground surveying by GPS, or by using those control points from maps. The transformation models can be, for example, polynomials, affine transformation model, or other mathematical models. These models with known parameters are then used to rectify the original satellite images – to control their quality by improving the positional accuracy.

A transformation model (non-rigorous models) from a 2D satellite image coordinate system to ground 3D object space is studied (Shi and Shaker, 2003; Shi and Barakat, 2005), and the transformation model is applied to the geo-positioning of IKONOS imagery. In particular, the following two factors that affect the data quality control are investigated: a) change in terrain heights, and b) the number of GCPs with 3D ground coordinates.

It is found that for the 2D transformation models, the rectification accuracy can be improved if the ground point coordinates are corrected by projecting them into a compensation plane before the 2D IKONOS imagery is geometrically rectified. It is also found that

the second order polynomial model presented the best positional accuracy results with a modest number of GCPs required.
The results of the affine model showed that one-meter 3D ground point determination accuracy is achievable for stereo images without any need to obtain further information about the satellite sensor model and ephemeris data. Furthermore, increasing the number of GCPs significantly improves the accuracy of the results when the affine model is applied to an area with different types of terrain, such as in the Hong Kong study area with its flat, hilly, and mountainous types of terrain.

(b) Line-based Transformation Model
In many cases, the precise GCPs are not available, but lines are available from maps, for example. The line-based rectification method, the Line-Based Transformation Model (LBTM) for image-to-image registration, and image to 3D ground space transformation, has been proposed [15]. This new model builds the relationship between image coordinate systems and ground coordinates systems using unit vector components of the line segments of line features. The LBTM is in two forms: 2D affine LBTM, and 2D conformal LBTM.

Several experiments showed that both forms of the LBTM are applicable for the image-to-image registration of high-resolution satellite imagery. In particular, the results revealed that an accuracy of better than two pixels can be achieved using a moderate number of GCLs and the LBTM.

5.3 Quality control for DEM data

Quality of a DEM is determined by the model used to represent the terrain. Therefore, the quality of a DEM can be controlled or improved by a better designed interpolation model. A hybrid interpolation method by integrating conventionally used linear and non-linear interpolation models has been proposed to improve interpolation accuracy (Shi and Tian, 2006) with the following mathematical expression:

$$I = \rho A + (1 - \rho) B, (0 \le \rho \le 1) \quad (6)$$

The hybrid parameter (ρ) adjusts both the linear and non-linear components in the hybrid model. Here, A and B represent the linear (such as a bilinear) function and non-linear (such as bi-cubic) function respectively. The value of the hybrid parameter is related to the complexity level of a terrain. This model was proposed based on an understanding of both the low- and high-frequency components contained in the surface of real world terrains.

The experiments showed that the hybrid model can generate more accurate DEM than that from the bilinear and bi-cubic methods in terms of RMSE. The proposed hybrid interpolation method provides an alternative solution to the existing DEM interpolation methods, combining the advantages of both linear and nonlinear interpolation models.

6. THE FUTURE

Within the framework of uncertainty modeling and quality control for spatial data and analyses, this paper presents four progresses we developed so far: from determinedness- to uncertainty-based spatial representation geographic entities in space; from uncertainty modeling for static data to dynamic analyses; from uncertainty modeling for simple data to comprehensive models; and from passive uncertainty description to active quality control for spatial data. With these developments, our understanding on the nature of uncertainty in spatial data analyses, and the solutions to control quality in spatial data and information has been advanced significantly.

In the future, I think the following issues should be further investigated and developed within the framework of modeling uncertainty in spatial data and spatial analysis. (a) To study the effects of uncertainties in spatial data on the results of spatial decision making. One of the objectives of having spatial data and information is to support spatial analysis and decision making. In fact, quality of the original spatial data will significantly affect the results of spatial decision making. The functional and quantitative relations between the quality of the original spatial data and model with the results of decision making need to be further studied. (b) Spatial data quality control. It is the final target of uncertainty study to control and improve the quality of spatial data and information. Our solutions for controlling the quality of spatial data, especially for complex error problems in spatial data, are still very preliminary, and therefore need to be further improved. (c) To implement the theoretical development in commercial GIS and other software. In the past decades, we have accumulated quite a number of developed methods for modeling uncertainties and controlling spatial data. However, we do not have much software in the application domain which can be used to solve the practical data quality problem. This gap can be filled in by implementing the developed theoretical solutions into the commercial GIS software. (c) To introduce the newly developed methods for assessing spatial data quality in national and international standards.

ACKNOWLEDGEMENTS

Supported by the National Natural Science Foundation of China (Grant No. 40629001) and the Hong Kong Polytechnic University (Grant No. G-YF24)

REFERENCES

Longley, P.A., M.F. Goodchild, D.J. Maguire and D.W. Rhind, 1999. Geographical Information Systems, *Principles and Technical Issues* (Volume 1). John Wiley & Sons, Inc., New York, Chichester, Weinheim, Brishane, Sigapore and Toronto.

Shi, W.Z., 2005. Principle of modeling uncertainties in *spatial data and analysis*. Science Press, Beijing, ISBN: 7-03-015602-1, 408 pages.

Shi, W.Z., 1994. Modeling Positional and Thematic Uncertainties in Integration of Remote Sensing and Geographic Information Systems. *ITC: Publication* No.22, Enschede, ISBN 90 6164 099 7, 147 pages.

Shi, W.Z., 1998. A generic statistical approach for modeling error of geometric features in GIS. *International Journal of Geographic Information Science*, Vol. 12, pp: 131-143.

Shi, W.Z. and Liu, W.B., 2000. A stochastic process-based model for the positional error of line segments in GIS. *International Journal of Geographic Information Science*, Vol. 14, pp: 51-66.

Shi, W.Z., Tong, X.H. and Liu, D.J., 2000. An approach for modeling error of generic curve features in GIS. *Acta Geodaetica et Cartographica Sinica*, Vol. 29, pp: 52-58 (in Chinese).

Shi, W.Z., C.K. Cheung and X.H. Tong, 2004. Modeling error propagation in vector-based overlay spatial analysis. *ISPRS J Photogrammetry and Remote Sensing*, Vol. 59, Issues 1-2, pp: 47-59.

Shi, W.Z., C.K. Cheung and C.Q. Zhu, 2003. Modeling error propagation in vector-based buffer analysis. *International Journal of Geographic Information Science* Vol. 17, No. 3, pp: 251-271.

Cheung, C.K, W.Z. Shi, 2004. Estimation of the positional uncertainty in line simplification in GIS. *The Cartography Journal*, Vol. 41, No.1, pp: 37-45.

Zhang, J.X., and M. Goodchild, 2002, *Uncertainty in Geographic Information*, Taylor and Francis.

Tong, X.H., Shi, W.Z. and Liu, D.J., 2005. A least squares-based method for adjusting the boundaries of area objects. *Photogrammetric Engineering and Remote Sensing*, Vol. 71 No.2, pp: 189-195.

Shi, W.Z., A. Shaker, 2006. The Line-Based Transformation Model (LBTM) for image to image registration of high-resolution satellite image data. *International Journal of Remote Sensing*, Vol. 27, No. 14, pp: 3001-3012.

Shi, W.Z., A. Shaker, 2003. Analysis of terrain evaluation effects on IKONOS imagery rectification accuracy by using non-rigorous models. *Photogrammetric Engineering and Remote Sensing*, Vol. 69, Number 12, pp: 1359-1366.

Shaker, A., W.Z. Shi and H. Barakat, 2005. Assessment of the rectification accuracy of Ikonos imagery based on two-dimensional models. *International Journal of Geographic Information Science*, Vol. 26, No.4, pp: 719-731.

Shi, W.Z., Y. Tian, 2006. A hybrid interpolation method for the refinement of regular grid digital elevation model. *International Journal of Geographic Information Science*, Vol. 20, No. 1. pp: 53-67.

DIGITAL EARTH BRAINWARE.
A FRAMEWORK FOR EDUCATION AND QUALIFICATION REQUIREMENTS

Josef Strobl

Centre for Geoinformatics, University of Salzburg, Hellbrunnerstraße 34, 5020 Salzburg, Austria *and*
GIScience Research Unit, Austrian Academy of Sciences, Schillerstraße 30, 5020 Salzburg
josef.strobl@sbg.ac.at

KEY WORDS: Digital Earth, virtual globes, e-learning, geospatial education, spatial awareness, spatial thinking

ABSTRACT:

This paper argues that in order to succeed with the emerging implementations of Digital Earth at this vision's tenth anniversary it is critically important to focus on the 'brainware component'. Powerful virtual globes and online map interfaces today facilitate access to global information by everybody with Internet access. Qualifications of users, though, still have not been completely transferred from traditional map reading skills towards the navigation on virtual globes. Beyond that, the author proposes a broad framework of educational levels from citizens ('everybody') communicating spatially to the professionals providing the spatial information infrastructure behind Digital Earth and analysts serving as experts for methodologies and application domains.

1. THE DIGITAL EARTH VISION

Starting with a speech given by then US vice president Al Gore in 1998, the vision of a 'Digital Earth' (DE) as a virtual representation of the Earth on the Internet that is spatially referenced and interconnected with the world's digital information and knowledge archives has become a powerful concept. In late 1999 the International Society for Digital Earth (ISDE) was conceived in Beijing, recognized primarily through its series of 'International Symposia on Digital Earth'.

Mr. Gore had suggested '*a digital future where a young girl could sit before a computer generated 3-dimensional spinning Earth and access information from around the planet with vast amounts of scientific, natural, and cultural information to describe, entertain, and understand the Earth and its human activities. This vision states that any citizen of the planet, linked through the Internet, should be able to access vast amounts of free information in this virtual world …*' (quoted after Anon, 2006).

As we have now arrived at the tenth anniversary of this seminal Digital Earth speech, we recgonize that the vision of 'any citizen of the planet' having access to the Internet and 3D spinning globes has probably moved ahead faster than most people would have imagined in 1998. Due to the emergence of several 'globe viewers' in recent years (Strobl, 2006) driven by the local search and 'yellow pages' markets the share of citizens regularly using DE technologies has at least arrived in the several hundred millions, if we are to believe the frequently quoted numbers of downloads and unique server accesses.

While we have to acknowledge that most users might only occasionally look up a holiday destination, use a route finder function or explore a hotel environment, we notice an increasing fascination with DE tools in the general public far beyond geospatiial professionals. Much beyond the wildest dreams of the geospatial industry trying to reach out to the general public with 'GIS browsers' and other GIS tools, only virtual globes envisioned through DE and driven by the local search market have actually managed to transcend the 'professional barrier' and reach the mainstream of personal desktops.

Many educators have been fascinated by the learning opportunities offered through this development, and by the curiosity and motivation shown by students. Today virtual globe and online map environments are used in innumerable formal and informal settings for learning, slowly moving Al Gore's original vision towards reality. To support this process, educators need to consider how the required skills, cognitive patterns and knowledge frameworks can be developed. In short, how we can establish the 'brainware component' of Digital Earth covering the entire range between general public and professional users.

A set of concepts and technologies known as Spatial Data Infrastructures (SDI) has become the enabling backdrop for the DE vision (Masser, 2005; Masser 2007). Technologies and software cannot be considered sufficient to facilitate DE, though:

2. CITIZEN AND PROFESSIONAL BRAINS

While the original Digital Earth vision is clearly focussed on the general public, DE is increasingly becoming relevant, and in many cases indispensable for many professional activities. Actually, it won't even work well trying to separate everyday personal 'spatial awareness'-driven actions from using DE technologies to support mundane professional tasks and from jobs typically ascribed to geospatial professionals.

As a general foundation, though, educators need to think about how to structure learning processes towards learning objectives important for Digital Earth citizens in all their roles from everyday activities to (for some of them) tasks in geospatial professions. One early attempt at categorising different levels of individuals was the GIS-centric distinction of professional creators of geospatial data ('doers') from 'users' working on an applications level, analyzing data and generating information from data within their respective contexts, and end users or map 'viewers' who

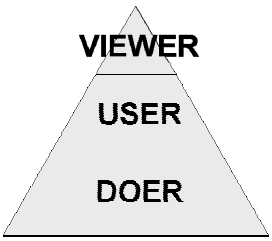

would be consumers of geospatial information. Clearly this model had been established before the days of Web 2.0, as it does not really expect end users to have an interactive role and to participate in the creation of data.

In terms of numbers of users, this pyramid could just as well be turned around, as of course the number of people in these categories increases from 'Doers' towards 'Viewers', with Roosaare et al. (2002) suggesting a full order of magnitude (1:10:100) difference in numbers. Still, this view does certainly not yet account for the impact of 'general public' or 'citizen' level involvement as envisioned by Digital Earth.

Another, more workflow-oriented concept is the *author > serve > use* paradigm. Again, this might help with assigning particular qualifications and skills to groups of users or professionals involved with digital geospatial activities, but does not provide a complete framework useful for defining educational requirements and qualification objectives.

From a current view of Digital Earth as a well connected and coordinated framework providing an explicitly geospatial angle on the Internet – leveraging the concept of Spatial Data Infrastructures and OpenGIS technologies – it is suggested to define three distinct roles with clear 'brainware' requirements:

(C) Spatial Communication: based on a solid foundation of spatial awareness / orientation and fundamental spatial thinking capabilities, this is a role each and every citizen should accept. In order to fully participate in society a spatially literate and cognizant person is able to communicate via maps and other spatially referenced visuals, understands community-related maps (zoning, environment, development), can express location-specific opinions and is aware of spatial processes and interdependencies.

(A) Spatial Analysis: analysis as a process deriving information from data starts from a problem framed into a question: this can be as simple as a best route or closest facility, or much more complex as land use suitability or scenarios for climate change impact. Spatial analysis always requires an application logic context, in simple cases coded into application functions for standard questions like 'best route', but in more complex cases requires deep conceptual, methodological and technical understanding.

(S) Spatial Systems: in order to follow SDI concepts, to avoid redundancies and aiming for efficiency the groundwork for client-side functionality like viewing, browsing, query or analysis is increasingly being built and maintained as an interconnected web of distributed servers. Communication follows the 'service' paradigm requiring the standards developed through OpenGIS and prescribed e.g. in ISO. Establishing systems and services components for geospatial infrastructures requires a high level of conceptual and technical knowledge.

This **C – A – S** framework of course can be linked to the viewers/citizens-to-geospatial-professionals gradient, with some of the spatial analysis section certainly allocated to questions citizens frequently ask in their daily lives. The main focus of discussion, though, is how to structure educational objectives and requirements using this framework. The above identified roles are important to understand educational needs, and ultimately to design curricula, learning processes and learning media for everybody involved on all levels of education.

3. THE C-A-S FRAMEWORK

As briefly outlined above, the main roles of Communication, Analysis and Systems implementation are considered as defining the participants' roles in Digital Earth. These roles clearly are interdependent, and individuals can act in different roles. Roles not only define what actors do, but how they interact and what services they provide for each other:

- **C**itizens participate in society, make it work and contribute to livable spaces, sustainable economies and clean environments.
- **A**nalysts frequently are domain experts understanding WHAT needs to be done, as well as the HOW to do it, providing critical subject matter and methodological knowledge.
- **S**ystems experts supply a working infrastructure; essentially geo-enabling the information society through a spatial data/information infrastructure.

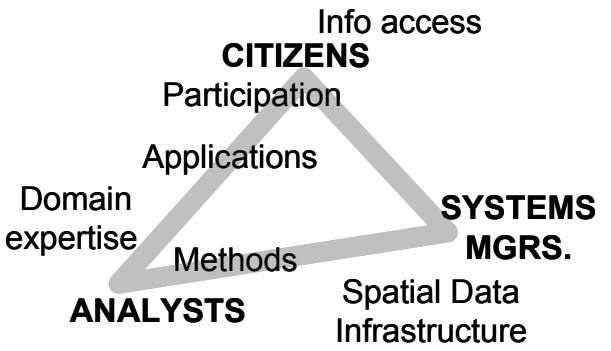

When this general framework of roles is used to define target groups for education and to assess qualifications, a more detailed perspective is needed in order to design learning objectives and curricula. One aim of this initiative is the definition of a general framework for levels and directions of education, another targets the general understanding of how to spatially enable our information society and economy.

3.1 Spatial Communication

Interaction between individuals about places and spaces is a fundamental requirement for a working society, and likely goes back to the early days of humankind. Petroglyphs detailing hunting grounds, oral traditions guiding Polynesian navigators, or attempts to measure the globe and to document property all were essential in their respective societies. Technologies have changed, but not so much the problems and questions addressed.

In 'Learning to Think Spatially' (NRC, 2006) it is argued that *everybody* (thus a focus on K-12 education!) needs to acquire spatial thinking as a universal and distinctive form of thinking. It is based on the concepts of space, tools of representation, and processes of reasoning. Only by understanding the meaning of space we can use its properties (like dimensionality, continuity, proximity etc.), express spatial relationships (distance, scale, adjacency) and thus structure spatial problems for finding answers and identifying solutions.

Spatial awareness and spatial thinking are generally understood as being independent from technologies and tools. Practical application, though, requires skills which do depend on the available tools. As Digital Earth attemps to leverage the Internet to access information about our planet and our neighbourhoods, it is mandatory to build skill sets relating spatial concepts to the tools we are using.

As recently discussed (e.g. in Strobl and Lindner-Fally, 2007 and Strobl, 2006) 'map reading skills' as traditionally taught need to be revisited and adjusted to online maps and particularly virtual 'spinning' globes. Skills like general directional and topographic orientation, moving across scales, controlling perspectives and swapping themes can easily be acquired in a playful manner, but are essential for actively *participating* in any geospatial discourse, and therefore in society.

For the 'general public' and 'citizenry' target groups of 'C' three progressively advancing levels of qualification are suggested:

C1 – 'Consumer' – map reading, orientation and navigation, finding one's place and identifying a destination.

C2 – 'Prosumer' – ability to participate by labelling a feature, mark up ('redlining') and rate a place or feature of interest and comment on alternative spatial scenarios, like a zoning proposal.

C3 – 'Producer' – contribute one's own data like a GPS-recorded hiking track, a geocoded photograph and perhaps even a draft proposal map for a conservation measure.

Moving from C1 to C3 we clearly advance from the Web 1.0 understanding of the original Digital Earth vision of 'accessing global information' towards a Web 2.0, or Geoweb 2.0 concept of 'participating as global citizens'. This general evolution of geospatial interaction and participation is reflected in the recently discussed concept of 'volunteered geographic information' (Goodchild, 2007).

Clearly, C1 to C3 are qualifications intended for the general public, learned in general education whether in schools or alternative environments. From a business perspective, 'C' identifies customer skills in a marketplace, from a societal viewpoint 'C' aims at educated citizens.

3.2 Spatial Analysis

As indicated above, spatial analysis is a set of concepts, methods and techniques for the extraction of new information (and ultimately knowledge) from data. Spatial analysis creates value added information by applying spatial concepts to data within a given application domain. Questions can only be answered and problems solved if a problem is properly stated in an application context.

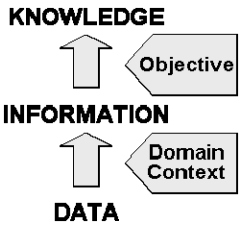

Many questions and problems can be related to generic problems, like 'best route through a network' (whatever kind of network this might be) or 'estimate a continuous surface from sample points'. While parameters for any such method depend on the application context, a generic method ('Dijkstra', 'IDW-interpolation') can be identified. The knowledge and skills required to apply an established method using an existing software tool is designated as level A1.

Many, maybe most spatial problems cannot be solved by applying just a single method. It rather is frequently necessary to find a solution to 'best location for service *X*' by aggregating and transforming multiple input themes, perform some kind of weighted overlay, then apply a distance decay scaling operation and finally compare and rank a number of location scenarios. Designing such a kind of analytical process requires not only knowledge regarding the entire toolbox of analytical operations, but design skills based on experiential knowledge.

When the above qualification is identified as A2, an advanced level of A3 aims at the conceptual development and implementation of new methods, the ability of finding new solutions to new or existing problems.

Summarizing, spatial analysis qualifications are ranked as:

A1 – 'Applying tools' by competently using existing functionality to answer simple questions and fulfil single-step tasks.

A2 – 'Design analytical workflows' by creatively using established methods and existing functionality to solve complex problems requiring multiple transformations and operations.

A3 – 'Develop methods' for new problems or conceptualise new solutions or complex workflows, and implement them for general use.

While A1 will in a few cases be relevant for the general public (e.g. when using a best route tool in a web-based travel planning portal), we will typically identify A1 to A3 as progressively advanced stages in (academic) education for geospatial professionals. 'GIS courses' in application disciplines will aim at A1 and struggle with some A2, while more technically oriented programmes will at least target the development skills needed for A3, but will rarely have the opportunity to build the experience needed for full mastery of the subject.

3.3 Spatial Systems

From the perspective of distributed 'Spatial Data Infrastructures', even when limiting ourselves to 'Enterprise GIS' or a workgroup geodatabase, it will be clear that the 'C' and 'A' jobs require the establishment and operation of a server side infrastructure in order to function well.

Traditional 'stovepipe architectures' as well as 'do-everything-yourselves' desktop GIS wizardry is increasingly giving way to well defined professional roles distinguishing client ('C', 'A') from server side tasks. While quite some common conceptual understanding is needed most service architectures allow for a clear distinction. Server: provides data catalog service and metadata profile - client: searches for and/or documents data sets; server: provides web processing service – client: makes an application workflow or analytical procedure available as WPS.

Designing, building and maintaining SDI components comes in different levels of complexity as well, which again are distinguished into three levels:

S1 – 'System setup' and maintenance for out-of-the-box installation of well-documented system components.

S2 – 'Architecture design' – competence to orchestrate multiple components, set up complex interfaces and profiles and link to external services.

S3 – 'Server / service development' – implement specifications and design and develop new services.

Clearly, this set of qualifications is primarily oriented towards ICT and computer science skills, will not necessarily be emphasized in typical Geoinformatics study programmes, but due to the increasing importance of SDI a subset of S1 and S2 will certainly be required by all-round GIS professionals

3.4 Complementary Qualifications

When applying this C-A-S framework to the entire set of skills, competences and qualifications needed in mainstream GIS operations, even more so in a well-structured Digital Earth environment where geospatial data are being acquired, organised, analyzed and visually communicated in order to solve spatial problems of all kinds, it will emerge that some types of needed activities and qualifications are missing from this schema.

By analyzing workflows and interdepencies across geospatial use cases and applications, these 'missing pieces' are identified in three domains of knowledge:

G/R – Competence in establishing, using and transforming Spatial Reference Systems (SRS), 'measuring space' and advanced geocoding. This geodetic / surveying engineering qualification is an essential prerequisite for setting up DE frameworks and to guarantee high quality operations.

T/A – Technician qualification mostly for data acquisition and data conversion. As a profession this can be implemented from a vocational angle, or in other cases from a technologist or sensor specialist viewpoint.

P/M – Project management and organisation is a generic skill and frequently implemented as a standalone (e.g. consulting) career path, critically important to cover business perspectives and for managing complex projects and implementations.

Altogether, the Digital Earth 'brainware framework' suggested above can be rendered into this simple matrix schema:

Levels

C	*C1*	*C2*	*C3*	*G/R*
A	*A1*	*A2*	*A3*	*T/A*
S	*S1*	*S2*	*S3*	*P/M*

This table presents all key areas of qualifications needed for using Digital Earth, as well as for the different roles in the geospatial industry, the driving technology and business forces behind the implementation of the Digital Earth vision and concept.

Some topics which might be expected in this kind of high level overview have not been included on purpose. Perhaps most prominently the area of (application) software skills which certainly are needed from a practical point of view, but not necessarily from a wider educational perspective (this would ultimately lead to the training vs. education debate).

The different demands of various GIScience application domains have not been discussed here either, although the suggested schema would be applicable to courses in these disciplines as well. Similarly, the connections between spatial thinking, cognition, skills development and knowledge acquisition in individuals (Golledge, 2002) have been relegated to the teaching perspective. Finally, the connection between Digital Earth as 'popular GIS' or 'spatially aware Internet' and the domain traditionally referred to as 'GIS' is not necessarily compelling, but is considered helpful in order to integrate these two different views at least from an educational perspective.

4. BENCHMARKING QUALIFICATIONS

A clear and simple conceptual framework like the one suggested above is useful when assessing and comparing the strategic orientation of qualifications, like academic study programmes. While a detailed analysis and certainly formal accreditation always will have to involve the curriculum and programme implementation levels, comparing the general orientation of (a) a programme of study and/ or (b) an individual's qualifications would likely get bogged down in syllabic and curricular details.

As an example, the postgraduate University of Salzburg UNIGIS distance learning programme (Molendijk and Scholten, 2005; Car, 2007) offering core GIScience and Geoinformatics qualifications to students from various application domains can be tentatively characterised like this (three different shading levels according to intensity of exposure to topics in the respective area, including prerequisites):

UNIGIS MSc profile

C	*C1*	*C2*	*C3*	*G/R*
A	*A1*	*A2*	*A3*	*T/A*
S	*S1*	*S2*	*S3*	*P/M*

In contrast, a graduate from a Geomatics program with a development / technical focus might bring different qualifications to his job:

Tech programme

C	*C1*	*C2*	*C3*	*G/R*
A	*A1*	*A2*	*A3*	*T/A*
S	*S1*	*S2*	*S3*	*P/M*

A much more general, Digital Earth 'good citizen' qualification hopefully acquired by graduating from high school could show a profile like this:

DE citizen

C	*C1*	*C2*	*C3*	*G/R*
A	*A1*	*A2*	*A3*	*T/A*
S	*S1*	*S2*	*S3*	*P/M*

From a range of different backgrounds it has frequently been suggested (Kemp, 2003) to establish certification frameworks for GIS professionals, and some formal certifications are currently being offered (e.g. GIS Certification Institute, www.gisci.org). By inspecting the high-level C-A-S framework of qualifications it becomes clear that any benchmarking of qualifications can only be reasonably proposed for comparable profiles, otherwise it would be an apples-vs-oranges approach. A 'broadband' GIS certification will therefore hardly be able to capture and benchmark qualifications as required in specific professional roles.

5. CONCLUSIONS

The vision of Digital Earth, as well as the academic and professional domains of geospatial technologies ultimately depend on users' skills and knowledge. It is therefore mandatory to reflect the demands on education in schools curricula (for everybody as a 'Digital Earth citizen' and in academic programmes for the scientific and professional enablers of the complex architectures behind DE as well as for the experts creating DE content.

The qualifications needed to **C**ommunicate spatially, **A**nalyze spatial information and manage geospatial **S**ystems can be clearly identified and described from the roles of all involved stakeholders and actors. Sets of qualifications can be combined to profiles, assigned to and required for successfully acting in one or more of the identified roles.

Traditionally, a lot of work has been invested in the development of curricula and syllabic catalogs like most recently the GIS&T Body of Knowledge (DiBiase et al, 2007), but a higher level and simpler view driven by actor's roles has been missing. The suggested C-A-S framework is intended as such a reference helping with the characterisation of study programmes as well as the assessment of individuals' qualifications.

6. REFERENCES:

Albert, W. S., and Golledge, R. (1999). The use of Spatial Cognitive Abilities in Geographical Information Systems: The Map Overlay Operation. Transactions in GIS, 3(1), 7-21.

Anon. (2006). ISDE5 – Digital Earth History. http://www.isde5.org/history.htm (accessed Feb. 24, 2008).

Bednarz, S. W. (2004). Geographic Information Systems: A Tool to Support Geography and Environmental Education. GeoJournal, 60(2), 191-199.

Car, A. (2007). UNIGIS@Salzburg: Successful Career Development for Professionals Through Online Distance Learning. INTERGEO EAST: Proceedings of the 4th International Conference for Landmanagement, Geoinformation, Building Industry, Environment, Sofia, Bulgaria.

DiBiase, D., M. DeMers, A. Johnson, K. Kemp, A. Taylor Luck, B. Plewe and E. Wentz (2007): Geographic Information Science and Technology Body of Knowledge. UCGIS-AAG.

Golledge, R. (2002). The Nature of Geographic Knowledge. Annals of the Association of American Geographers, 92(1), 1-14.

Golledge, R., Battersby, S., and Marsh, M. (2006). Minimal GIS to support Geospatial Concept Education through K-12 Curriculum. Paper presented at the 2006 Meeting of the AAG, Chicago.

Goodchild, M. (2007). Citizens as sensors: the world of volunteered geography. GeoJournal (DOI 10.1007/s10708-007-9111-y).

Kemp, K. K. 2003. Guest Editorial: Why GIS Professional Certification Matters to Us All. Transactions in GIS 7(2): 159-163.

Masser, I. (2005). GIS Worlds: Creating Spatial Data Infrastructures. ESRI Press

Masser, I. (2007). Building European Spatial Data Infrastructures ESRI Press.

Molendijk, M. and H. J. Scholten. (2005). From Local Heroes towards Global Communicators: The experiences of the UNIGIS network in educating GIS professionals worldwide. Nuffic Expert Meeting "A Changing Landscape". The Hague. 24-25 May 2005. http://www.nuffic.nl/pdf/os/em/molendij.pdf

NRC., 2006. Learning to Think Spatially: GIS as a Support System in the K-12 Curriculum. Washington, DC: National Academics Press.

Roosaare, J.; Liiber, Ü.; Oja, T. (2002). GIS in eLearning - maintaining the proportions of user's pyramid. Third European GIS Education Seminar (EUGISES) = http://www.geo.ut.ee/roosaare/EUGISES_2002.pdf

Strobl, J. und M.Lindner-Fally (2007): Global Learning - Pedagogical Concepts involving Virtual Globes. In: Donert K. (ed.), Teaching Geography in Europe using GIS, ESRI Inc. with HERODOT, ISSN 1752-4208 (CD-ROM).

Strobl, J. (2007): Geographic Learning in Social Web Environments. In: Changing Geographies: Innovative Curricula (eds. S. Catling and L. Taylor), pp.327-332. IGU Commission for Geographical Education and Oxford Brookes University, Oxford.

Strobl, J. (2006): Der Globus ist des Atlas Tod. In: Jekel, T., A.Koller und J.Strobl (Hrsg.): Lernen mit Geoinformation. Wichmann, Heidelberg.

NUTZERBASIERTE ADAPTION DES FAHRRADROUTENPLANUNGSPROZESSES IM INTERNET - KONZEPTION VON FUNKTIONALITÄTEN AUF BASIS EINER EMPIRISCHEN UNTERSUCHUNG –

Katrin Stroemer

Steria Mummert Consulting AG, Hans-Henny-Jahnn-Weg 29, 22085 Hamburg

katrin.stroemer@steria-mummert.de

KEY WORDS: Fahrradroutenplanung, Geoinformatik, Navigation, Routenplaner, Routenberechnung

KURZFASSUNG:

Dieser Artikel beschreibt die Konzeption eines Fahrradroutenplaners im Internet, dessen Funktionalitäten an die Bedürfnisse und Wünsche der Anwender angepasst sind. Um diese Bedürfnisse zu erfassen, wurde zunächst eine Nutzerbefragung im Internet durchgeführt. Basierend auf den Ergebnissen ist ein Funktionsumfang erstellt und in einem letzten Schritt ein Konzept erarbeitet worden, wie diese vom Anwender gewünschten Funktionalitäten realisiert werden können. Besonders die Loslösung der Routenberechnung von der Eingabe von Haltepunkten stellte eine Herausforderung dar. Der Anwender erhält dadurch die Möglichkeit lediglich durch die Auswahl eines Startpunkts sowie die Eingabe einer zu fahrenden Distanz eine Route zu berechnen, ohne weitere anzufahrende Punkte auswählen zu müssen. Das Konzept und die Entwicklung des Fahrradroutenplaners erfolgte am Institut für Geoinformatik und Fernerkundung (IGF) der Universität Osnabrück, wo bereits seit etlichen Jahren im Bereich der Fahrradroutenplanung im Internet gearbeitet wird.

ABSTRACT:

This paper describes the conceptual design of an internet based bicycle routing system, which functions are adapted to the needs and interests of the potential users. To capture the users needs an internet based survey was implemented at first. Based on the survey results a set of functions was developed and a concept was worked out, how to realise the implementation of the functionalities desired by the users. Especially the route planning without selecting stops was a challenge. In this way the user gets the opportunity to receive an individual route just based on a selected starting point and a distance to drive (e.g. 20 km). He doesn't have to select any other stops for the route calculation. Design and implementation of the internet based bicycle routing system was done by the Institute for Geoinformatics and Remote Sensing (IGF) at the University of Osnabrück. The IGF is working on bicycle routing systems since many years now.

1. FAHRRADROUTENPLANUNG IM INTERNET

Für den motorisierten Individualverkehr existiert im Internet bereits eine Vielzahl an Systemen, die dem Anwender eine Route zwischen zwei oder mehreren Orten berechnen. Weniger berücksichtigt waren bisher die Fahrradfahrer, die sich mit Hilfe eines Routenplaners eine Strecke für berufliche oder Freizeit-Zwecke planen möchten. Mittlerweile gibt es eine Reihe statischer Fahrradroutenplaner, die dem Nutzer zwar Tourenvorschläge bieten, jedoch nicht die Option beinhalten, individuelle Touren zu planen. Erst wenige Systeme beschäftigen sich mit der interaktiven, internetgestützten Berechnung einer Fahrradtour (z.B. Fahrradies, Radroutenplaner NRW, Ruhrtal a la Carte).

Grundlegend fehlen Konzepte, um die Radroutenplanung an die Wünsche der Anwender anzupassen. Zudem ist nicht klar, welche Interessen und Wünsche die Anwender in Bezug auf Fahrradroutenplanung im Internet besitzen. Für die Ermittlung der Nachfrage ist es notwendig, die Vorstellungen zu erfassen, die von einem Anwender an einen Fahrradroutenplaner, der im Internet zur Verfügung steht, gestellt werden. Interessant ist z.B., welche Funktionalitäten ein Fahrradroutenplaner bereitstellen sollte. Zusätzlich ist es sinnvoll, die Gewohnheiten bei der Planung einer Route sowie die Akzeptanz neuer Medien für die Ausgabe einer Fahrradkarte z.B. auf einem PDA abzufragen. Zur Beantwortung dieser Fragestellungen anhand einer empirischen Studie wurde im Rahmen dieser Arbeit eine Online-Befragung durchgeführt, um ein Routingkonzept zu entwickeln, welches flexibel auf die Wünsche der Anwender reagieren kann.

2. ERMITTLUNG DER NACHFRAGE

Die Befragung richtete sich an die Personen, die in ihrer Freizeit Fahrradtouren durchführen. Bei der Auswertung einer Online-Befragung muss berücksichtigt werden, dass nicht alle Menschen via Internet zu erreichen sind. Laut Tns Infratest et al. (2005) verfügt zwar mehr als jeder zweite Deutsche über einen Internetzugang (55,1% im Jahr 2005), 38,6% der Deutschen werden allerdings immer noch als Offliner bezeichnet. Da es nicht realisierbar ist, alle Freizeitradler im deutschsprachigen Raum zu erfassen, konnte für die Befragung nur ein bewusstes Auswahlverfahren in Betracht gezogen werden. Zum einen wurde die Befragung im Internet zur Verfügung gestellt, zum anderen wurden der ADFC sowie ca. 320 Radvereine aus ganz Deutschland angeschrieben. Zusätzlich wurden weitere Portale rund um das Thema Fahrrad gebeten, die Befragungsseiten dort zu verlinken.

Die Befragung wurde ab Februar 2005 mit einer Laufzeit von 12 Monaten durchgeführt. Insgesamt haben sich ca. 800 Personen an der Befragung beteiligt. Wichtig erschien unter anderem eine große räumliche Verteilung der Rückläufe. Durch die Abfrage des Wohnortes mit Postleitzahl konnte eine Übersicht über die räumliche Verteilung der Befragten erarbeitet werden (s. Abb. 1).

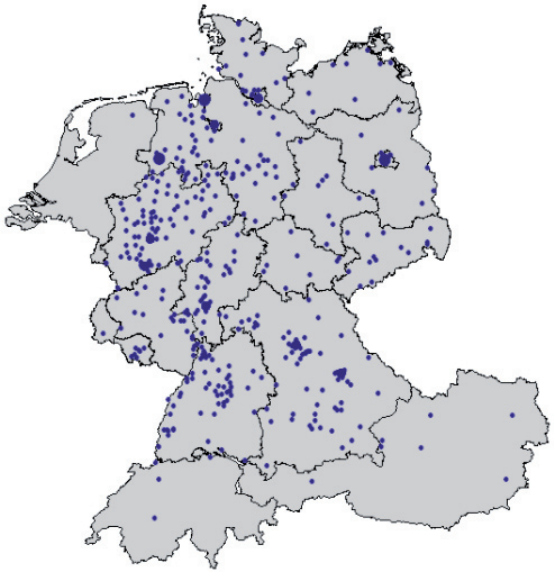

Abb. 1. Räumliche Verteilung der Befragungsrückläufe.

Mehr als ein Drittel der Befragten (42,5% = 328 Nennungen) nutzt für die Planung einer Route weiterhin die herkömmliche analoge Fahrradkarte. Nur 10,1% (78 Nennungen) planen ihre Route ausschließlich digital. Davon nutzen nur 39,8% (35 Nennungen) der digitalen Planer das Internet, 60,2% (53 Nennungen) bevorzugen die CD ROM als Medium. Immerhin 29,8% aller Befragten (230 Nennungen) nehmen sowohl die analoge Karte als auch digitale Medien für die Planung einer Route zur Hilfe. Beachtlich ist die Tatsache, dass sogar 17,5% (135 Nennungen) die Route im Vorfeld überhaupt nicht planen.

Besonders interessant gestaltet sich die Antwort auf die Frage, ob die Befragten bereits einen Fahrradroutenplaner im Internet genutzt haben. 87,4% (674 Nennungen) verneinen dies. Nur 12,6% (97 Nennungen) geben an, bereits Erfahrungen mit Fahrradroutenplanern im Internet gemacht zu haben. Dabei steht an erster Stelle der Fahrradroutenplaner NRW mit 37 Nennungen. 8 der Befragten geben an, Map24 als Routenplaner für eine Fahrradtour zu nutzen. Da es sich bei Map24 ausschließlich um einen Planer für den motorisierten Individualverkehr handelt, ist nicht davon auszugehen, dass er für die Planung von Fahrradtouren aufgrund von fehlenden Radwegen oder Nebenstrecken geeignet ist. Immerhin noch 6 der 97 Personen haben bereits das Fahrradies (vgl. Ehlers et al., 2004) getestet. Das Portal Geolife der Landesvermessung und Geobasisinformation Niedersachsen (LGN) nutzten 5 Befragte.

Es hat sich gezeigt, dass ca. drei Viertel der Befragten (76 %) es vorziehen, eine individuelle Route zu planen, anstatt sich eine Tour aus bereits fertigen Routenvorschlägen auszuwählen. Dabei wird vor allem die Berechnung einer Rundtour sowie einer Tour zwischen zwei Orten gewünscht, wobei die Optionen Beschaffenheit des Radwegs und die Steigung miteinbezogen werden sollten. Die Berechnung einer Route nach einer bestimmten Distanzeingabe wird von ca. 50 % aller Befragten nachgefragt (vgl. Abb. 2).

Für die Ausgabe der Route zur Mitnahme ins Gelände geben 73,7% aller Befragten (568 Nennungen) an, sich vorstellen zu können, einen Computerausdruck mit auf die Tour zu nehmen. Dieses Ergebnis zeigt, dass Akzeptanz für die Planung einer Fahrradroute am PC vorhanden ist. Allerdings schwören 53,2% aller Befragten (410 Nennungen) weiterhin auf die Mitnahme der analogen Fahrradkarte. Lediglich 19,6% (151 Nennungen) könnten es sich vorstellen, eine Trackliste aus dem Internet auf ein GPS-Gerät zu laden, 15,2% (117 Nennungen) würden ein PDA im Gelände nutzen. Dieses Ergebnis macht deutlich, dass die digitalen Medien im Fahrradtourismus noch wenig Beachtung finden.

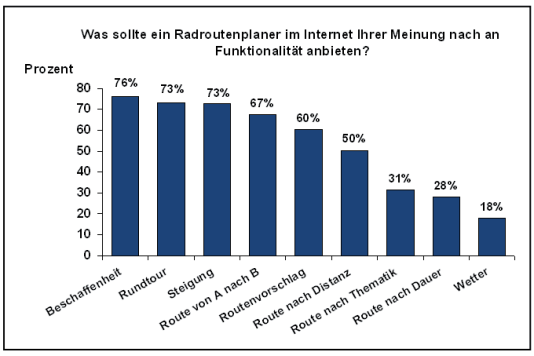

Abb. 2. Gewünschte Funktionalität für einen Fahrradroutenplaner im Internet (Mehrfachnennungen möglich).

Allerdings hat die Befragung auch gezeigt, dass ein erhöhtes Interesse an der Unterstützung zur Planung einer Fahrradtour im Internet besteht. Die Befragungsergebnisse sollen in die Konzeption eines adaptierten Fahrradroutenplaners einfließen, wobei versucht wird, bei der Realisierung so viele gewünschte Aspekte wie möglich mit einzubeziehen. So soll ein Routenplaner entwickelt werden, der neben der standardmäßigen Berechnung einer Rundtour sowie einer Route zwischen zwei Orten die Optionen Steigung und Beschaffenheit in die Routenberechnung einbindet sowie eine Route lediglich auf Basis einer Distanzeingabe erstellt.

3. ENTWICKLUNG ADAPTIERTER ROUTINGFUNKTIONALITÄTEN

Zur Umsetzung einer adaptierten Routenberechnung wurde zunächst ein Algorithmus entwickelt, der grundlegend eine Route zwischen zwei Orten sowie eine Rundtour ohne die Eingabe von weiteren Optionen erstellt. Für die Berechnung einer Route zwischen zwei Orten wurde das Konzept des A-Stern-Algorithmus zugrunde gelegt. Der A-Stern-Algorithmus ist ein Derivat des Dijkstra-Algorithmus und ermittelt den kostengünstigsten Pfad zwischen einem Start- und einem Zielpunkt innerhalb eines Suchbaums, wobei während der Suche eine Schätzfunktion verwendet wird, die für jeden Knoten eine untere Schranke für den noch zu erwartenden Abstand zum Zielknoten, also die noch zu erwartende Pfadlänge, liefert (Michalewicz und Fogel, 2000). Dadurch ergibt sich eine zielgerichtete Suche auf den Endknoten. Tests an der Universität Bonn, die auf dem Wegnetzgraphen von Bonn (ca. 30.000 Knoten und 60.000 Kanten) durchgeführt wurden, wiesen dem A-Stern- gegenüber dem Dijkstra-Algorithmus eine fünf- bis sechsfach bessere Performanz nach (Plümer et al., 2004).

Für die Berechnung einer Rundtour wurde nach dem Prinzip des Ameisenalgorithmus vorgegangen. Dieser Algorithmus macht

es sich zu nutze, dass Ameisen fast immer auf direktem Weg zwischen Ameisenhaufen und Futterquelle ihre Ameisenstraßen errichten. Ameisen besitzen eine Drüse am Hinterleib, über die sie einen chemischen Lockstoff (Pheromon) auf ihrem Weg hinterlassen können. Nachfolgende Ameisen orientieren sich am Pheromon ihrer Vorgänger und wählen mit höherer Wahrscheinlichkeit den am stärksten markierten Weg (Boysen, 2004). Zwar können Ameisen als Heuristik zur Lösung eines Traveling Salesman Problems im Gegensatz zu exakten Verfahren wie z.B. Branch and Bound (Korte und Vygen, 2006) nicht garantieren, dass ihr Ergebnis eine optimale Lösung für das Problem ermittelt. Trotzdem erzielt dieser Algorithmus bei einer Tour-Berechnung für viele Städte, die exakte Verfahren nicht in angemessener Zeit lösen können, einen guten Kompromiss zwischen Lösungsgüte und Laufzeit. Eine Tour mit 20 Städten z.B. löst der Ameisenalgorithmus mit einer Laufzeit von unter einer Sekunde. Die in Java implementierten Algorithmen wurden in eine Architektur eingebettet, die auf dem Konzept freier Software (OpenSource) basiert. Zur Visualisierung der Routenberechnungsergebnisse dient der lizenzkostenfreie UMN MapServer.

3.1 Einbinden von Optionen in die Routenberechnung

Neben der Berechnung einer Rundtour und einer Route zwischen zwei Orten werden die Optionen Steigung und Beschaffenheit bei der Routenberechnung berücksichtigt. Der Anwender erhält so die Möglichkeit, diese Optionen für die Routenberechnung wahlweise ein- oder auszuschalten. Gerade im Bereich der Navigation von Rollstuhlfahrern werden diese Optionen bereits eingesetzt (Frasch 2006). Aber auch im Radverkehr sind Steigung und Beschaffenheit vor allem bei Mountainbike- und Rennradfahrern sowie Familien mit Kindern von großem Interesse. Um die Optionen in den Routingalgorithmus einzubinden, muss zunächst ein Kostenmodell erarbeitet werden, welches die verschiedenen Optionen bewertet und den einzelnen Linienabschnitten, für die diese Kosten berechnet werden, je nach Ausprägung einen Kostenanteil zuweist. Hierfür erhält jeder Linienabschnitt des Netzwerks ein weiteres Kostenfeld pro Option. Werden Optionen bei der Routenberechnung angegeben, so sind die Kosten, die für jede Linie gespeichert sind, ausschlaggebend für die Bewertung dieser Option. Zu beachten ist jedoch, dass die Kosten zu jeder Zeit auch in Beziehung zu der Länge eines jeden Linienabschnitts gesehen werden, da ansonsten ein verzerrtes Kostenbild entsteht. Das bedeutet, dass die akkumulierten Kosten, die durch die Optionen verursacht werden, als Koeffizient der Länge eines jeden Linienabschnittes dienen.

3.2 Routenberechung auf Basis einer Distanzeingabe

Neben der Einbindung von Optionen soll die Routenberechnung von dem Anfahren bestimmter Haltepunkte losgelöst werden. Der Anwender erhält damit die Möglichkeit, mit wenigen Eingabeparametern (z.B. einer Startpunkt- und Distanzeingabe) einen Routenvorschlag zu erhalten. Erste Ergebnisse in diese Richtung gibt es bereits im Bereich von personalisierten, mobilen GI-Services für die Fußgängernavigation (Zipf et al., 2005). Hier erhält der Anwender einen Routenvorschlag auf Grundlage einer gewünschten Routendauer und Angabe von Points of Interest (POI) oder Interessensbereichen. Diese Entwicklungen sind stark auf die Einbindung von POI ausgerichtet. Gerade bei der Navigation in der Stadt liegt es nahe, den Besucher durch die Stadt zu führen, indem POI nach Interessen angesteuert werden. Im Bereich des Fahrradtourismus außerhalb von Städten mit einer geringen Dichte von POI ist dieser Ansatz nicht immer sinnvoll. Um dem Anwender in einem Gebiet mit wenig bis hin zu gar keinen POI trotzdem einen sinnvollen Routenvorschlag zu präsentieren, soll die Routenberechnung allein auf der Geometrie der Linienabschnitte des zugrunde liegenden Routennetzes durchgeführt werden.

Im Rahmen der entwickelten Methode für eine Routenberechnung auf Grundlage einer Distanzeingabe wird zunächst ein kreisförmiger Bereich erzeugt, dessen Umfang der gewünschten Routenlänge entspricht. Um eine möglichst kompakte Routenform zu erzielen, wird der kreisförmige Bereich so platziert, dass der Startpunkt auf dem Rand und nicht im Zentrum des Puffers liegt. Die Ausrichtung des Pufferbereichs kann zum einen durch die Eingabe einer Himmelsrichtung durch den Nutzer vorgenommen werden. Da der Nutzer aber so wenig Angaben wie möglich machen soll, wird der Pufferbereich zunächst nach einem vom Startpunkt abgehenden Linienabschnitt, der zufällig ausgewählt wird, ausgerichtet. Im weiteren Verlauf werden alle Linienabschnitte, die sich innerhalb des Pufferbereiches befinden, selektiert und ihre Endkoordinaten ermittelt. Die so gewonnene Punktemenge wird durch die Berechnung der konvexen Hülle minimiert. Die Punkte der konvexen Hülle zusammen mit dem Startpunkt bilden die Grundlage für die Routenberechnung (s. Abb. 3).

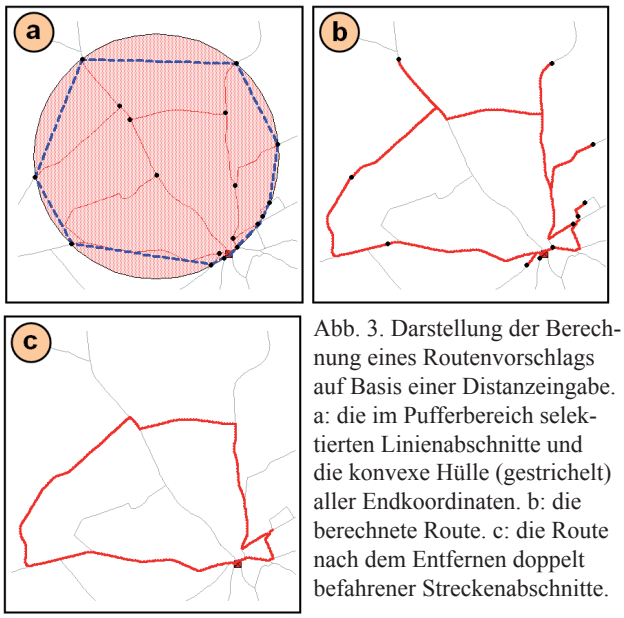

Abb. 3. Darstellung der Berechnung eines Routenvorschlags auf Basis einer Distanzeingabe. a: die im Pufferbereich selektierten Linienabschnitte und die konvexe Hülle (gestrichelt) aller Endkoordinaten. b: die berechnete Route. c: die Route nach dem Entfernen doppelt befahrener Streckenabschnitte.

Erste Ergebnisse dieses Vorgehens waren sehr positiv, zeigten aber auch, dass die Route gerade in Bereichen, in denen ein dichtes Liniennetz vorherrscht, die Längenvorgaben des Nutzers häufig überschreitet. Zur Reduzierung der Routenlänge wurde zunächst die anzufahrende Punktemenge durch Herausnehmen einzelner Punkte verringert. Zusätzlich stellte sich in zahlreichen Tests heraus, dass durch den Umfang der konvexen Hülle die Länge der zu erzeugenden Route abgeschätzt werden kann. Beträgt der Umfang der konvexen Hülle ca. 70-80% der gewünschten Routenlänge, so wird in den meisten aller durchgeführten Fallbeispiele ein zufrieden stellendes Ergebnis erzielt. Ist der Umfang der konvexen Hülle nicht entsprechend lang, muss solange ein Punkt aus der Menge herausgenommen oder hinzugefügt werden, bis der erforderliche Wert erreicht ist (s. Abb. 4). Ein Vorteil dieses Vorgehens ist, dass eine Route auf diese Weise selten mehrfach berechnet werden muss und so kostbare Rechenzeit eingespart werden kann.

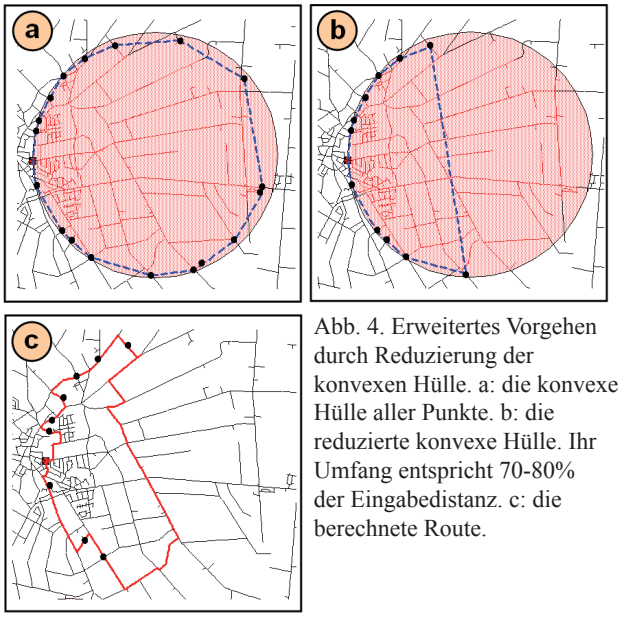

Abb. 4. Erweitertes Vorgehen durch Reduzierung der konvexen Hülle. a: die konvexe Hülle aller Punkte. b: die reduzierte konvexe Hülle. Ihr Umfang entspricht 70-80% der Eingabedistanz. c: die berechnete Route.

Nach der Routenberechnung wird die Ergebnisroute durch die Entfernung doppelt befahrener Streckenabschnitte optimiert. Hierfür gibt es zwei mögliche Vorgehensweisen. Zum einen werden die Strecken, die direkt hintereinander zweimal befahren werden, entfernt. Zum anderen werden ganze Routenverästelungen gelöscht. Letztere Methode ist zwar für die Form der Route von Vorteil, allerdings kann sich die Länge der Route sehr stark verändern. Als Ergebnis erhält der Anwender die bestmögliche Route für seine Anfrage. Denkbar ist es, ihm wahlweise auch weitere Routen zur Auswahl anzubieten, die sich z.B. in andere Richtungen orientieren.

Die hier beschriebene Vorgehensweise zur Berechnung einer Route auf Basis einer Distanzeingabe soll im Folgenden um die Möglichkeit erweitert werden, konkrete POI oder themenbezogene Kategorien in die Routenberechnung mit einzubinden. Dadurch kann die Route noch stärker auf die Nutzerwünsche angepasst werden.

3.2.1 Einbinden konkreter POI

Gibt der Anwender zusätzlich zu der zu fahrenden Distanz einen konkreten anzufahrenden POI ein, muss zunächst geprüft werden, ob der POI sich in einer angemessenen Distanz zum Startpunkt befindet. Die euklidische Distanz zwischen Startpunkt und POI darf den doppelten Pufferradius 2r nicht übersteigen, damit der POI sich noch in dem zu erstellenden Puffer befindet (s. Abb. 5).

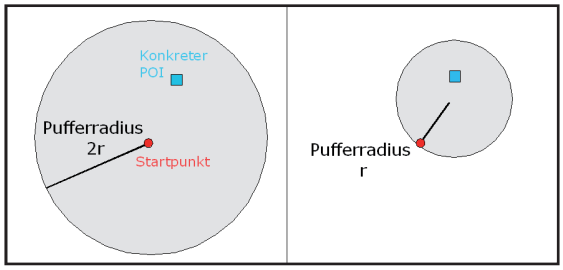

Abb. 5. Links: Puffer mit Radius 2r und darin befindlicher, vom Nutzer ausgewählter POI. Rechts: Der Puffer mit dem Radius r wird nach dem POI ausgerichtet.

r ist dabei der Radius, der sich durch die Berechnung des Umfangs, welcher der vom Nutzer gewünschten Distanz entspricht, ergibt. Befindet sich der gewählte POI in der entsprechenden Distanz zum Startpunkt, kann der Puffer mir dem Radius r erzeugt werden. Die Ausrichtung des Puffers erfolgt diesmal nicht durch einen vom Startpunkt abgehenden Linienabschnitt sondern in Richtung des POI.

Nach der Bildung der konvexen Hülle aller Start- und Endpunkte der im Pufferbereich selektierten Linienabschnitte wird der POI zu der Punktemenge der konvexen Hülle hinzugefügt. Jetzt kann die Längenprüfung gestartet werden. Ist der Umfang der konvexen Hülle zu groß, muss der Punkt mit der größten räumlichen Distanz zum Startpunkt aus der Punktemenge gelöscht werden. Wichtig ist, dass der POI nicht entfernt wird. Entspricht der Umfang ca. 70-80% der gewünschten Distanzeingabe, kann die Route berechnet werden. Abbildung 6 zeigt ein mögliches Ergebnis bei einer Distanzeingabe von 15 km und einem POI (Dreieckssymbol) im ländlichen Raum. Auch hier zeigt sich, dass die Längenabschätzung über die konvexe Hülle sehr hilfreich ist.

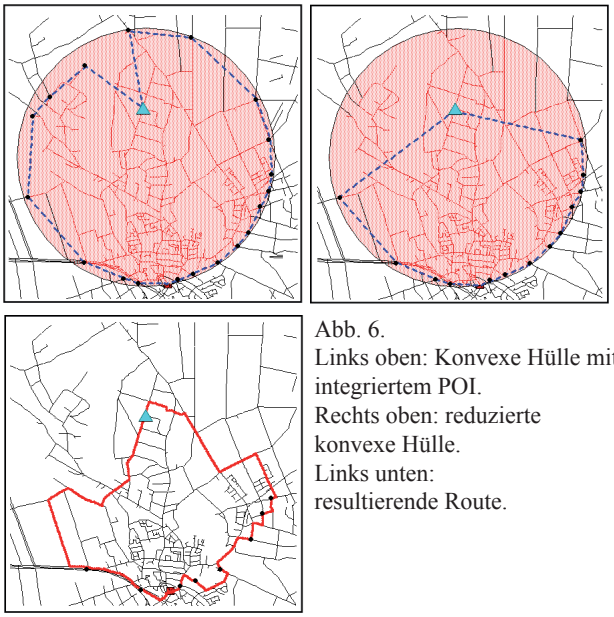

Abb. 6.
Links oben: Konvexe Hülle mit integriertem POI.
Rechts oben: reduzierte konvexe Hülle.
Links unten: resultierende Route.

3.2.2 Einbinden von Kategorien

Zusätzlich ist es möglich auch themenbezogene Kategorien in die Berechnung zu integrieren. Dabei kann zwischen POI-basierten (Cafè, Schwimmbad, etc.) und flächenbasierten Kategorien (Wald, See) unterschieden werden. Die Einbindung von Kategorien erfolgt nach dem gleichen Prinzip wie die oben vorgestellte Einbindung von konkreten POI. In einem ersten Schritt müssen die Kategorien ermittelt werden, die sich in erreichbarer Distanz zum Startpunkt befinden (s. Abb. 7).

Bei einer Kombination mehrerer Kategorien muss zusätzlich geprüft werden, ob auch die Kategorien untereinander in einer angemessenen Distanz zueinander liegen, um innerhalb der gewünschten Fahrdistanz angesteuert werden zu können. Erst wenn dies zutrifft, kann eine Route berechnet werden, die den Nutzeranforderungen entspricht.

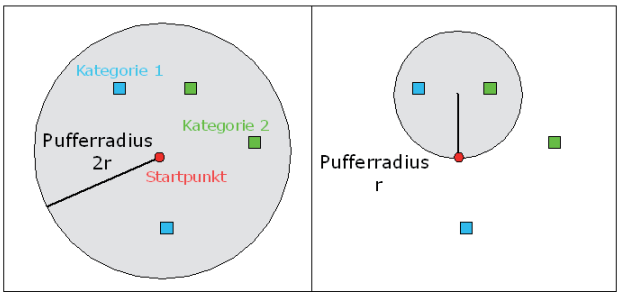

Abb. 7. Links: Der Puffer mit Radius 2r ermittelt alle innerhalb der gewünschten Distanz erreichbaren Kategorien. Rechts: Der Puffer mit Radius r wird nach den anzufahrenden Kategorien ausgerichtet.

4. AUSGABE DER INDIVIDUELL ERZEUGTEN ROUTE

Abgesehen von der Möglichkeit, sich die Route in Form einer analogen Karte als Übersicht auszudrucken, erhält der Anwender für seinen individuellen Routenvorschlag auf Wunsch eine Trackliste zum Download auf ein GPS-Gerät. Wie die Befragung gezeigt ist, wird diese Art der digitalen Routenausgabe zunehmend genutzt.

Zusätzlich wurde am IGF ein mobiler Viewer entwickelt, der dem Anwender auf einem PDA basierend auf Windows Mobile 2003 die Route im Vektorformat in Kombination mit einer georeferenzierten Hintergrundkarte visualisiert. Durch den Einsatz von GPS ist es so möglich, die analoge Karte für die Navigation zu ersetzen. Die notwendigen Daten wie Route und Hintergrundkarte werden dynamisch für den individuellen Routenausschnitt generiert. So wird die Datenmenge auf den gewünschten Ausschnitt beschränkt. In Entwicklung ist auch die Erweiterung des Viewers um eine eigene Routingkomponente. Damit erhält der Anwender die Möglichkeit einen berechneten Routenvorschlag direkt auf der Tour zu erweitern oder abzuändern.

5. FAZIT

Neben der Adaption des Fahrradroutenplanungsprozesses durch das Einbinden von Optionen wie Steigung und Beschaffenheit, ist ein Konzept erstellt worden, die Routenplanung losgelöst von der Eingabe von Haltepunkten durchzuführen. Der Anwender muss lediglich einen Startpunkt und eine gewünschte Distanz für die Routenberechnung eingeben. Das Verfahren kann durch die Auswahl weiterer konkreter POI oder Kategorien wie z.B. Café, Wald, Schwimmbad, erweitert werden. Die Schwierigkeit bestand darin, eine Methode zu entwickeln, die zum einen auf bekannten Algorithmen zur Wegfindung basiert, zum anderen jedoch für die Berechnung der Route keine Haltepunkte erhält. Daher ist diese Methode auch in Regionen mit wenig oder gar keinen POI gut geeignet. Zusätzlich besteht die Möglichkeit, bei Bedarf konkrete POI oder Kategorien in die Routenberechnung einzubinden. Dadurch kann diese Methode sehr stark auf die Nutzerwünsche eingehen. Allerdings besteht auch die Gefahr, durch zu detaillierte Nutzereingaben möglicherweise kein passendes Ergebnis mehr erzielen zu können. Da die Methode lediglich ein Liniennetz als Basis für die Routenberechnung benötigt, ist es denkbar, sie neben den Radfahrern auch für andere Gruppen wie z.B. Wanderer oder Reiter einzusetzen. Durch den Download der berechneten Route auf ein GPS-Gerät oder PDA erhält der Anwender die Möglichkeit einer komfortablen Navigation im Gelände.

6. LITERATUR

Aho, A.; J. Ullman, 1996. *Informatik. Datenstrukturen und Konzepte der Abstraktion*. International Thomson Publishing, Bonn.

Boysen, N., 2004. "*Ameisenalgorithmen*" http://www.ameisenalgorithmus.de/downloads/ameisenalgorithmen.pdf (Stand Juli 2005)

Ehlers, M.; Stroemer, K., 2004. ‚Fahrradies': the GIS Based Bicycle Routing System for the World Wide Web (WWW) and Mobile Use. *GIS – Zeitschrift für Geo-Informationssysteme Ausgabe 3-2004*, S. 29-34.

Frasch, G., 2006. Routenplanung für barrierefreien Tourismus. *GIS – Zeitschrift für Geo-Informationssysteme Ausgabe 4-2006*, S. 22-25.

Korte, B.; Vygen, J., 2006. *Combinatorial Optimization. Theory and Algorithms.* Springer Verlag, Heidelberg.

Michalewicz, Z.; Fogel, D., 2000. *How to Solve It: Modern Heuristics.* Springer Verlag, Berlin.

Plümer, L.; Steinrücken, J.; Kolbe, T., 2002. Multimediale Visualisierung von Geoinformationen im Internet. *Tagungsband des Symposiums Praktische Kartographie 2002 in Königslutter*. Kirschbaum Verlag, Bonn.

Plümer, L; Schmittwilken, J.; Kolbe, T., 2004. Mobile GIS für die Orientierung von Fußgängern in städtischen Umgebungen. Universität Bonn. In: *Tagungsband zum Symposium Praktische Kartographie 2004, Königslutter, Kartographische Schriften, Band 9*, Kirschbaum Verlag.

Tns Infratest, Initiative D21 (Hrsg.) 2005. *„(N)ONLINER Atlas 2005. Eine Topographie des digitalen Grabens durch Deutschland."* http://www.nonliner-atlas.de/pdf/dl_NONLINER-Atlas2005.pdf (Stand 17. Oktober 2005)

Zipf, A.; Jöst, M., 2005. Implementing Adaptive Mobile GI Services based on Ontologies - Examples for pedestrian navigation support. In: *CEUS - Computers, Environment and Urban Systems - An International Journa*l. Special Issue on LBS and UbiGIS. Pegamon Press, Elsevier.

EARTH OBSERVATION AND DISASTER MANAGEMENT IN EUROPE

L. Tufte

PRO DV Software AG. Hauert 6, 44227 Dortmund, Germany – lars.tufte@prodv.de

KEY WORDS: Remote Sensing, Disaster Management, Emergency Response, GMES, Emergency Response Core Service

ABSTRACT:

Earth observation (EO) data can be utilised in many phases of the disaster management cycle. Currently several projects (e.g. RISK-EOS, PREVIEW, RESPOND) promote the use of EO data in disaster management. These projects deliver various services and products supporting disaster management actions for natural disasters, man made disasters and complex (political) emergencies. Products and services are, for instance, windstorm risk mapping, flood mapping and assets maps. The future GMES Emergency Response Core Service (ERCS) will provide a set of basic services based upon a common denominator to improve the capability of the users emergency response to face major emergencies either within Europe or outside Europe. The rapid mapping service of the ERCS will provide reference maps (e.g. geographic maps) and assessment maps (e.g. actual situation maps). This service should be fast, available (24/7) and reliable (known quality).

1. INTRODUCTION

Earth observation (EO) data can be utilised in many phases of the disaster management cycle (Figure 1).

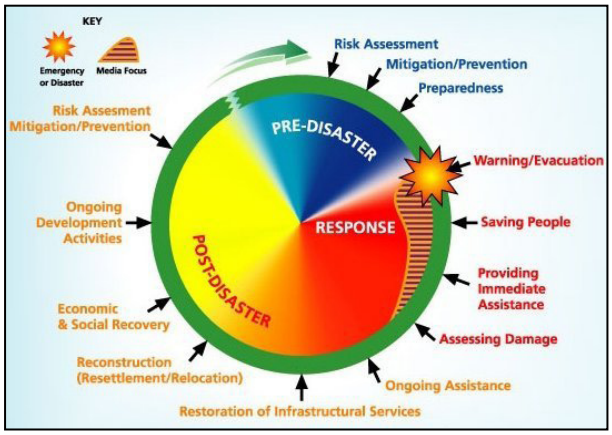

Figure 1. Disaster Management Cycle (Bernardinis, 2007a)

In the pre-disaster stage actions to assess the risk, mitigate and prevent damage (e.g. building a dam) and activities to ensure an effective and appropriate response to a disaster are taken (e.g. first responder training). In the response phase measures to respond to the disaster are taken (e.g. fire fighting). Rehabilitation and reconstruction activities are part of the post-disaster stage. Examples of measures taken in the different phases are given in Table 1.

The purpose of this paper is to briefly describe ongoing European activities utilising EO data in the field of disaster management. One of the main drivers is the Global Monitoring for Environment and Security (GMES) initiative. The future GMES Emergency Response Core Service (ERCS) is described in chapter 2. The European Union (EU) and the European Space Agency (ESA) are funding several projects, which promote the use of EO data in disaster management. An overview about these projects is given in chapter 3.

Table 1. Examples of measures in each disaster management cycle phase (Asian Disaster Reduction Center, 2005)

Disaster / Phase	Earthquake	Flood	Storm (cyclone, typhoon, hurricane)	Landslide
Prevention/ Mitigation	- Seismic design - Retrofitting of vulnerable buildings - Installation of seismic isolation/ seismic response control systems	- Construction of dike - Building of dam - Forestation - Construction of flood control basins/ reservoirs	- Construction of tide wall - Establishment of forests to protect against storms	- Construction of erosion control dams - Construction of retaining walls
Preparedness	- Construction and operation of earthquake observation systems	- Construction and operation of meteorological observation systems	- Construction of shelter - Construction and operation of meteorological observation systems	- Construction and operation of meteorological observation systems
Preparedness	- Preparation of hazard maps - Food & material stockpiling - Emergency drills - Construction of early warning systems - Preparation of emergency kits			
Response	- Rescue efforts - First aid treatment - Fire fighting - Monitoring of secondary disaster - Construction of temporary housing - Establishment of tent villages			
Rehabilitation/ Reconstruction	- Disaster resistant reconstruction - Appropriate land use planning - Livelihood support - Industrial rehabilitation planning			

2. GMES EMERCENCY RESPONSE CORE SERVICE (ERCS)

A workshop organised in Nov. 2005 identified user needs concerning a GMES emergency response service (Malingreau, 2006). In order to supervise and validate the implementation of the service an Implementation Group was established. The mandate of the Emergency Response Core Service (ERCS) Implementation Group is to, in open cooperation with the relevant user communities, supervise and validate the implementation of the service and to report on their progress to the GMES management structure (De Bernardinis, 2007d). For further information about the Implementation Group please refer to the Term of Reference (De Bernardinis, 2007d).

As stated in the Strategic Implementation Plan (De Bernardinis, 2007a) the purpose of the ERCS is *"…to make available and deliver a set of basic services based upon a common denominator to improve the capability of the users emergency response to face major emergencies at the national level (C), at the European level (D) and at the Global level (E) to face major emergencies either within Europe or outside Europe*.".
Unless otherwise indicated the information given in this chapter are taken from the Strategic Implementation Plan.
Three levels of ERCS service products are foreseen:

- Basic EO data (archived and new acquisition)
- Value added EO data (archived or new products, "general purpose" products)
- Final thematic maps

Value added products of the rapid mapping service are divided into Reference Maps and Assessment Maps. It is further necessary to distinguish between services that deliver common or general information and services delivering products directly related to the emergency event.

Reference Maps

Reference Maps can give an overview or provide tactical information. They are available before an event occurs (pre-existing data or pre-event simulation). The products should mainly be routinely delivered. However, they must be available whenever requested. Products are geographic maps, historical assets maps, historical situation maps, events reports log books, historical hazard maps and historical damage scenario maps.
Reference maps are expected to be available within 6 hours before actual observed information or products are available.

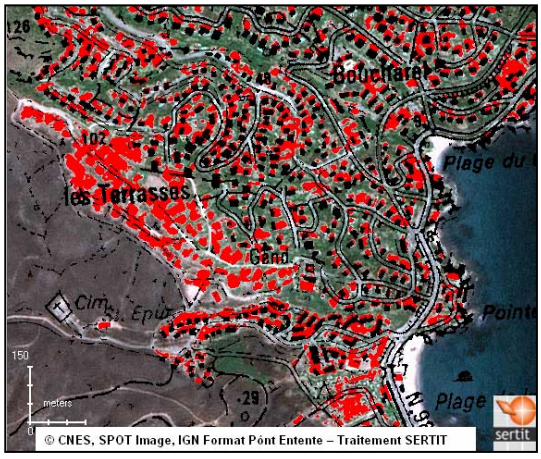

Figure 2. Example asset map: Urban areas (Very High Resolution) - AM 2 product (source: http://www.risk-eos.com/actus/pge/zoom.php?zoom=urbain_cartoamelioree.jpg)

Assessment Maps

Assessment Maps provide detailed information (scales 1:10 000 - 1:25 000) or an overview (scales 1:50 000 . 1:100 000) about the event timing, location, extent, level of hazard and damage. They should be delivered within 12-24 hours after an event occurred. Products are actual situation map, actual assets map, actual damage assessment map, event rapid map, actual hazard map, actual damage scenario map and situation maps.

The rapid mapping service should offer a very short delivery time (fast), should be available 24 hours 7 days a week (available) and should be providing products of known quality (reliable).
Further rapid mapping examples are given in De Bernardinis (2007c).

3. EUROPEAN PROJECTS

3.1 PREVIEW

PREVIEW (www.preview-risk.com) aims to develop new geo-information services for atmospheric, geophysical and man-made risk management on a European level. The integrated project is co-funded by the European Commission in the 6th Framework Programme. The Consortium consists of 58 partners from 15 countries. Project coordinator is Infoterra France.
The following risks are covered by the service portfolio: windstorms, floods, fires, landslides, earthquakes/volcanoes and man-made. In addition so called general services offers transverse services. An overview about the provided services is given in the following table.

Risk	Service
Windstorms	- Windstorm Risk Mapping - Windstorm forecasting
Floods	- Medium-range plain flood forecasting - Short-range plain flood forecasting - Very-short-range flood forecasting - Northern flood forecasting
Fires	- Fuel Parameters - Fire Danger indexes - Fire Meteo indices - Fires monitoring - Fire propagator - Fire damage assessment
Landslides	- Monitoring of slow-moving landslides - Prediction of shallow rapid slope movements
Earthquakes and volcanoes	- Earthquake monitoring and damage evaluation - Volcanic monitoring and damage evaluation
Man-made	- Dispersion forecasting of airborne Hazardous substances
General Services	- Assets Mapping - Damage and disaster intensity assessment - Damage Observation (Rapid Mapping)

Table 2. PREVIEW Services (source: www.preview-risk.com)

Some services are further subdivided into sub services and deliver different products.
An overview about the service utilisation and the need of EO data is given in the following table.

	EO data needs		
	PAN	**MS**	**SAR**
Fuel Parameters	Quickbird IKONOS ALOS (Prism) *PLEIADES*	TERRA (Aster) CBERS2 SPOT	-
Fire Propagator	SPOT 5	AQUA & TERRA (Modis) LANDSAT 7	-
Fire Danger Indexes	-	SPOT (VEG) AQUA & TERRA (Modis) TERRA (Aster)	-
Fire Monitoring	-	NOAA (AVHRR) AQUA & TERRA (Modis) MSG-2	-
Fire Damage Assessment	-	ENVISAT (Meris) AQUA & TERRA (Modis) LANDSAT 5 TERRA (Aster) EO1 (Hyperion) SPOT	-
Floods	-	LANDSAT 7ETM+ SPOT 4 (VEG)	TerraSAR-X
Slow Moving Landslides	QUICKBIRD IKONOS	LANDSAT TERRA (Aster)	ERS Radarsat ENVISAT ASAR
Rapid Slope Movements	QUICKBIRD IKONOS	NOAA (AVHRR) AQUA & TERRA (Modis) LANDSAT (TM, ETM+) TERRA (Aster)	-
Earthquakes	QUICKBIRD IKONOS	SPOT IRS EROS	ERS Radarsat ENVISAT ASAR
Volcanic	-	LANDSAT NOAA (AVHRR) TERRA (Aster) EROS	ERS ENVISAT ASAR
Assets Mapping	SPOT	SPOT	-
Damage Estimate	IKONOS	ENVISAT (Meris) SPOT	-
Rapid Mapping	Yes	Yes	Yes

Table 3. PREVIEW Services EO data needs (Source: http://www.space-risks.com/SpaceData/index.php?id_page=11)

The project provides a data web server (http://preview-risk.web.cern.ch/preview-risk/). The purpose of this web server is "*…to provide the scientific community with a space database acquired during the International Charter context with the objective to encourage and to allow this community to develop and validate new image processing methods in the area of Risk management…*" (Source: PREVIEW data web server).

3.2 RISK-EOS

The ESA GMES Service Element (GSE) RISK-EOS (www.risk-eos.com) is financially supported by the European Space Agency. It is an operational network of European service providers delivering geo-information services to support the disaster management of floods and fires. The project coordinator is Infoterra France. The consortium comprises 15 service providers.
In phase 3 (2008) of the project 28 Service Level Agreements with user organisation in Italy, Spain, Germany, France, Sweden, EC, Portugal and Luxembourg have been signed.
The following services are provided by RISK-EOS:

- Assets Mapping,
- Flood Risk Analysis,
- Flash Flood Early Warning,
- Flood Rapid Mapping,
- Fire Rapid Mapping,
- Regional Fire Monitoring,
- Burn Scar Mapping,
- Automatic Burn Scar Mapping,
- Flood Risk Analysis.

The services combine EO data with in-situ measurements and computer modelling techniques.

The Flood Rapid Mapping Service is taken as an example to demonstrate some of the RISK-EOS service capabilities. The main technical features of the products are depicted in the following table. A product example is shown in Figure 3.

Product	**Updating frequency**	**Accuracy / Localisation**	**Resolution**	**Format**
Near Real Time Flood Rapid Mapping - FLRM1	12h after image acquisition (2 to 3 days)	Depends on EO data	30 m	Raster
Non Real Time Flood Rapid Mapping - FLRM2	2 weeks	Depends on EO data	30 m	Raster / Vector
Non Real Time Maximum Flood Extent Mapping - FLRM3	2 weeks	Depends on EO data	30 m	Raster / Vector
Non Real Time Flood Damage assessment - FLRM4	2 weeks	Depends on EO data	30 m	Raster / Vector
Non Real Time Flood Duration per area - FLRM5	2 weeks	Depends on EO data	30 m	Vector

Table 4. Main technical features of the Flood Rapid Mapping products (Source: http://www.risk-eos.com/actus/pge/contenu.php?arbo=2&page=02portfolio_FlRM)

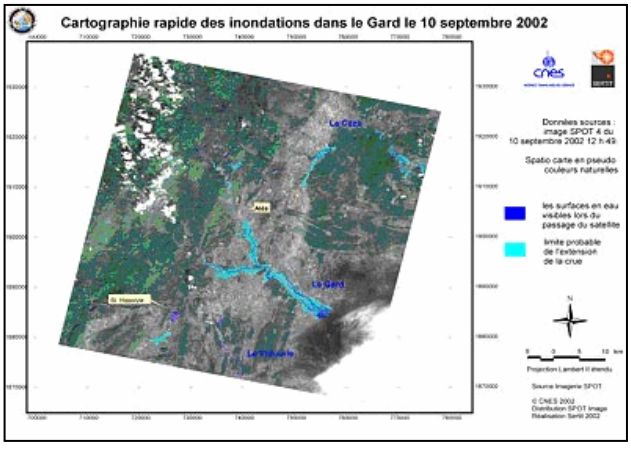

Figure 3. Example Non Real Time Maximum Flood Extent Mapping - FLRM3 product (Source: http://www.risk-eos.com/actus/pge/contenu.php?arbo=2&page=02portfolio_FlRM2)

3.3 RESPOND

The aim of the GSE RESPOND project (www.respond-int.org) is to improve access to maps, satellite imagery and geographic information to support humanitarian relief, disaster reduction and reconstruction. The prime contractor is Infoterra UK Ltd. The team comprise 19 partners.
The following product types are available:

Product Types	Typical Content Type
Basic Mapping (digital, paper, EO, non-EO)	Maps & Map archive to use for other themes
Crisis and Damage Mapping	Damage Maps
Situation Mapping	Maps and GIS
Refugee/IDP Support Mapping	Maps and GIS
Thematic maps for Prevention / Reconstruction Planning purposes	Thematic Maps
Health Maps	Thematic Maps
Environmental Impact Assessment Maps	Thematic Maps
Alert Services	Global Services
Communication / reporting resources	Ad-Hoc Mapping and graphics
Infield Mapping	Ad-Hoc Mapping and graphics

Table 5. RESPOND product types (source: http://www.respond-int.org/respondlive/public/html/products_and_services/availableProducts.html)

An example of a Crisis and Damage Mapping product is given in Figure 4.

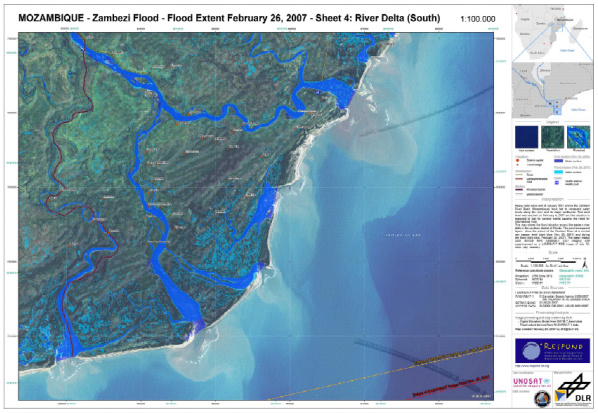

Figure 4. Example of Crisis and Damage Mapping product (source: RESPOND 2008)

The RESPOND product catalogue offers 4 main elements (Saull et al., 2006):

- A listing of the 20 most recently published products on the home page
- A search page known as “maps home”
- A simple map interface
- A map publishing and edit delete area

Additionally an RRS feed and a Google Earth version of the catalogue is provided.

4. CONCLUSION

Earth observation (EO) data can be utilized in many phases of the disaster management cycle. Currently GMES projects offer operational or pre-operational services and products supporting actions in various phases of the cycle. In the future the GMES Emergency Response Core Service will offer valuable services to face major disasters in Europe and outside Europe.

5. REFERENCES

Asian Disaster Reduction Center, 2005 (Ed.). Total Disaster Risk Management - Good Practices -. Japan.

De Bernardinis, B., 2007a. GMES Fast Track Emergency Response Core Service. Strategic Implementation Plan Final Version, 24/04/2007.

De Bernardinis, B., 2007b. GMES Fast Track Emergency Response Core Service. Strategic Implementation Plan Final Annex c – Rapid mapping services.

De Bernardinis, B., 2007c. GMES Fast Track Emergency Response Core Service. Strategic Implementation Plan Final Annex g – Rapid mapping examples.

De Bernardinis, B., 2007d. GMES Fast Track Emergency Response Core Service. Strategic Implementation Plan Final Annex a – Terms of Reference for the Implementation Groups of GMES “fast track” Services.

Malingreau, J.-P., 2006. Workshop on GMES INSCRIT GMES INSCRIT In Information formation Service in Response to Crises, Disasters & Emergencies Nov. 7-8.2005 Conclusion.

RESPOND, 2008. Crisis & Damage Mapping. http://www.respond-int.org/respondlive/public/images/products_and_services/Mapping Products/Crisis and Damage Mapping.pdf html (accessed 25 Feb. 2008)

Saull, R., Lakey, R., Downey, I., 2006. Respond Prototype Product Catalogue User Manual V1.0. http://www.respond-int.org/respondlive/partners/Respond Map Catalogue Manual.pdf (accessed 25 Feb. 2008)

HIGH PRECISION DIGITAL TERRAIN MODELS - INNOVATIVE TOOLS FOR REGIONAL PLANNING

M. Weisensee, H.-P. Ratzke & Th. Luhmann

Institute for Applied Photogrammetry and Geoinformatics
University of Applied Sciences, Ofener Str. 16, D-26121 Oldenburg, Germany
weisensee@fh-oow.de

KEY WORDS: Digital Elevation Model, Flood Risk Management, Regional Planning

ABSTRACT:

Digital methods are of increasing importance for regional planning processes. In contrast to traditional analogue planning utilities (maps, drawings etc.) digital tools can not only be used for the planning itself but provide efficient instruments for process simulation and visualisation of the planning results, both for specialists and the public – especially laypersons - as well. Planning costs can be reduced, planning duration can be shortened and planning results can be achieved much faster, if simulation, planning and visualisation are inter-operating optimally. Digital terrain models being used as a basis for digital planning are usually derived from topographic maps. Since this analogue map information is often generalised to a certain scale, derived digital terrain models also represent a generalised model of reality. This paper presents and discusses recent developments for the use of high precision digital terrain models that model the environment by a high level of detail.

1. DIGITAL TERRAIN MODELS

Digital terrain models (DTM) approximate the real surface (terrain heights and shapes) of an area in digital form by three-dimensional coordinates of a high number of surface points (anchor points), interpolation algorithms between these points, and additional information about the terrain structure such as edges, break lines, ridges and others (Kraus 2000, Fürst 2004).

In Germany the DGM5 based on the Deutsche Grundkarte (German Base Map, scale 1:5.000) is used as the standard product for a DTM provided by legal authorities. It is generated in a grid resolution of 12.5 m (distance between anchor points). For special applications (e.g. for flood simulations) DTMs of higher resolutions have been created and applied. There are a number of applications where the DTM can be used for region building in the sense of equal or similar properties, e.g. based on Operational Taxonomic Units (OTU) (Tiede & Strobl 2006).

2. HIGH PRECISION DIGITAL TERRAIN MODELS

Airborne laser scanning is the most effective way to generate high precision and high resolution digital terrain models. Data acquisition is provided by a multi-sensor system consisting of a GPS (Global Positioning System) receiver, an inertial navigation unit (INU), the laser scanning device and digital imaging sensors. The system is installed either in helicopters or aircrafts, hence larger terrain sections can be recorded in relatively short times.

Under optimal operational conditions a point density of up to 30 terrain points per m² can be achieved that provide an accuracy of ±10 cm in ground and height coordinates. A number of software packages is available that enables the processing of huge amount of data. In order to ease data handling, laser scanner data is often divided into rectangular sections (patches).

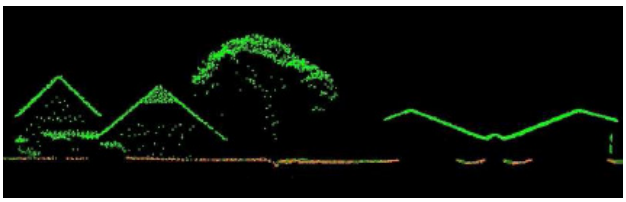

Figure 1. Cross profile of classified laser points

Laser scanning points are automatically classified into building, ground or vegetation points. According to the application either the complete point clouds (including a classification into low, medium and high vegetation) or selected points, e.g. ground points, can be processed.

Figure 2. Sub-section of an Orthophoto

The aerial images acquired during the laser scan can be used for texture mapping of the DTM. Hence the DTM information can be visualised in order to provide understandable results both for specialised users and/or laypersons.

3. CONVENTIONAL VS. HIGH PROCISION DTM

Due to larger grid resolutions of conventional DTMs, which are generated through existing maps, topographic surveying or photogrammetric processes, detailed surface structures often is not resolved. Particularly with regard to local applications and spatially limited effects, high resolution DTM data is of major importance. Applications in the area of environmental protection (flood control measures, noise protection, air purification) or infrastructural planning (e.g. design of hiking or biking tracks, line planning for supplying and disposal purposes) should be addressed in this context.

	grid	points/m²
conventional digital terrain model (DGM5) (Germany)	12.5 m x 12.5 m	1 / 156 m²
high precision digital terrain model	1 m x 1 m	4 / 1 m²

Tab. 1: DGM5 vs. high precision DTM based on airborne laser scanning

Figure 3 shows the significant benefit in precision of an identical terrain section, which is part of a project in the flat part of Northern Germany. The left model results from airborne laser scanning while the right model is a patch of the conventional DGM5.

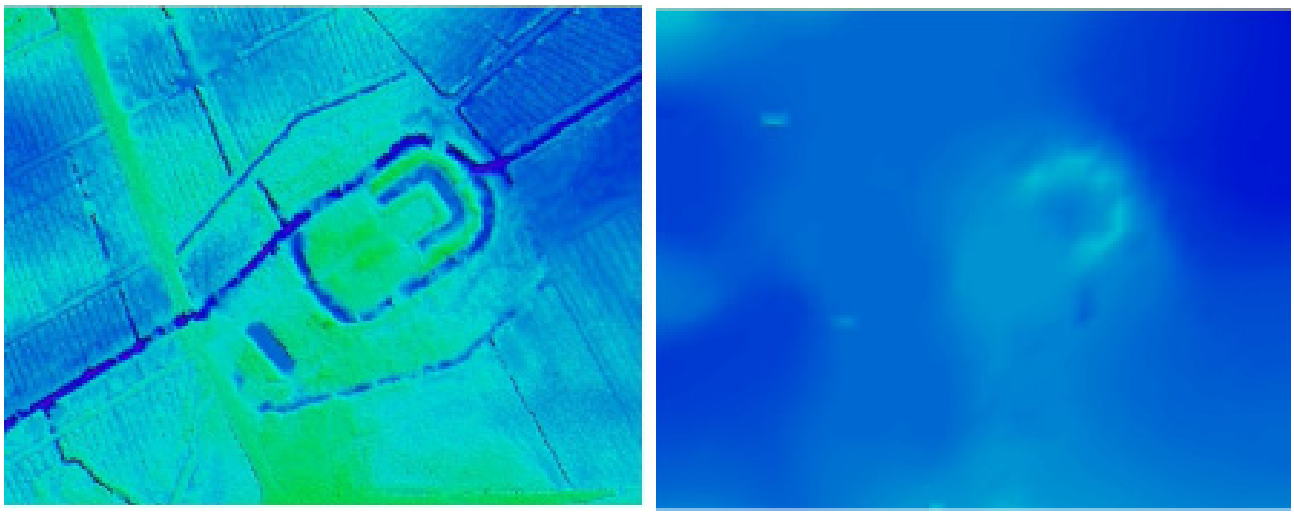

Figure 3. Comparison between a high precision DTM (left) and conventional DGM5 (right)

Many applications, especially hydrologic applications discussed in the following, often work with linear models using profiles (sections and cross-sections), which are either measured directly by topographic methods or can be derived from terrain models as well.

Figure 4 shows the position of the profile that is used for comparison between the conventional terrain model and the high precision terrain model in Figure 5.

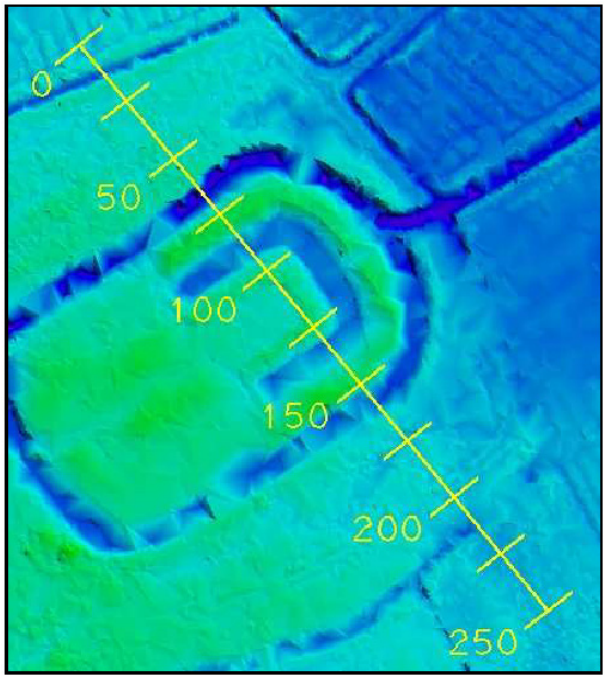

Figure 4. Position of profile for comparison between High Precision and Conventional Terrain Model

The profiles in Figure 5 clearly show that significant differences in any hydrologic simulation are to be expected when using both data sets as input in water storage calculation or even more in flood simulation.

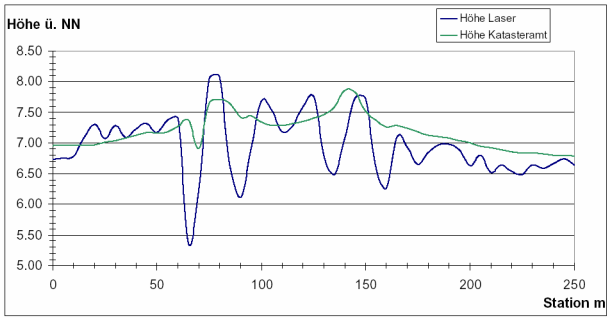

Figure 5. Comparison of profiles from High Precision Terrain Model and Conventional Terrain Model (with different scales on both axes)

4. APPLICATION EXAMPLE: FLOOD SIMULATION IN NORTH GERMAN LOWLANDS

According to the Directive 2007/60/EC of the European Parliament and of the Council on the assessment and management of flood risks (2007/60/EG), flood risk management systems have to be established for each river basin and partial catchments. In general this can be provided by maps and plans enhanced by additional regulations. However, with respect to increasing digitisation of environmental data and the existence of simulation programs for flood events, the development of digital flood risk management systems can be suggested. On the one hand such a digital system would provide straightforward data maintenance. On the other hand a simulation of preventing actions can already be performed in an early stage of planning. In addition, during urban land use planning the effects of ground sealing (e.g. as a result of road construction) to water management can be simulated, predicted and investigated. Hence compensatory measures can be derived, that suppress overwhelming delivery of surface water into on-site preflooders (Merz 2006, Kolf 2005).

In Lower Saxony flood areas and possible preventing actions against flooding is defined by counties (Landkreise). A partial river catchment in the North German lowlands is investigated in a research project on the investigation of 3D analysis mechanisms that is funded by the European Union (ESF/EFRE).

Particularly for plain areas even smallest terrain modulations (depressions and elevations) can have a significant effect on the maximum capacity of water within a region. Therefore two DTMs with different level of detail have been generated to being used for the prediction of a 100-year flood. For this investigation the official DGM5 is compared with a DTM established by airborne laser scanning.

As a result of the research we could prove that the simulation of the 100-year flood of the test area based on the DGM5 results in much earlier flooding of sensitive areas rather than a simulation based on airborne laser scanning DTM. Consequently, rescue and evacuation activities for threatened regions must be organised in earlier time schedules. In addition, preventing activities, optionally in conjunction with investment programs of local authorities, must be planned to a larger extend as it would actually be necessary.

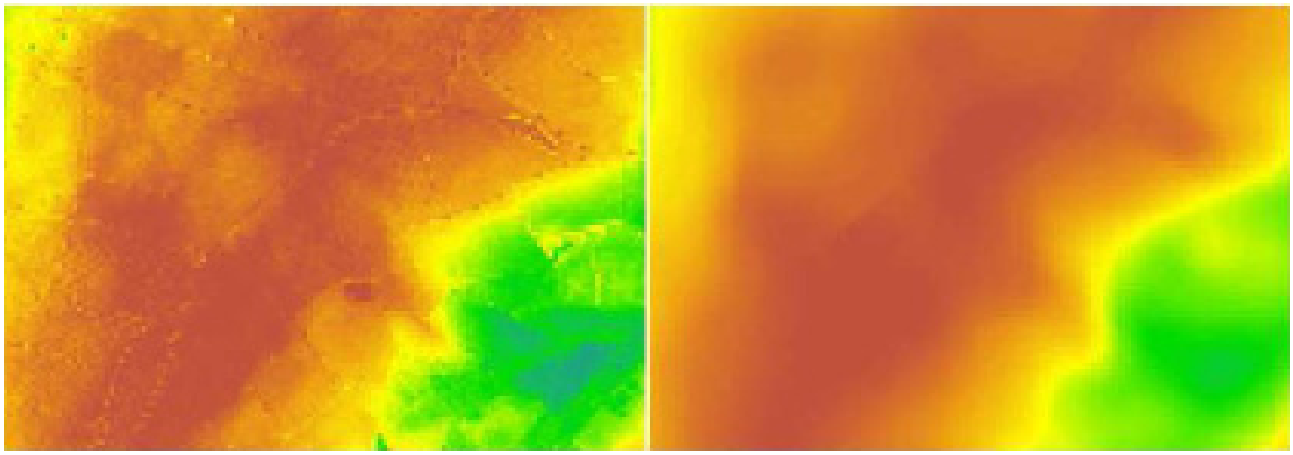

Figure 6. Colour coded DTM from airborne laser scanning (left) and conventional DGM5 (right)

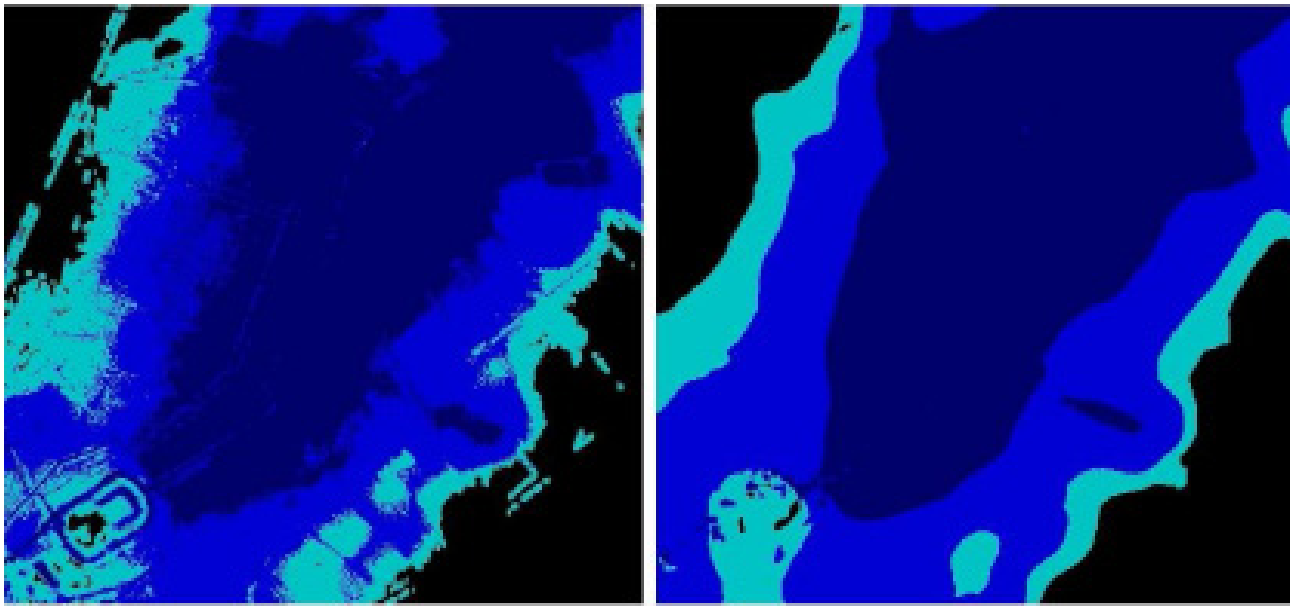

Figure 7. Flooding regions displayed as depth contours for laser scanning data (left) and conventional DGM5 (right)

A comparison of flood simulations based on differently precise DTMs yield a difference of about 134000 m² of less flooded area when laser scanner data is used. This corresponds to about 1.5% with respect to the complete test area of 8.5 km²; hence the effect is of minor importance in more or less rural areas. However, if projected on areas with private property real estates, high investments can be avoided since damages by a 100-year flood can be excluded from particular regions. The results of these researches are currently discussed with local authorities in order to be considered in future flood risk management systems.

The special benefit of visualisation techniques based on digital terrain models is primarily given by the order of Time Travel Options (modifications over time) and Viewing Options when users of interactive visualisation systems for planning purposes are investigated. Since these two options are first ranked (Schroth and Schmid, 2006), even ahead of photo-realistic illustrations of planning scenarios, it becomes clear that computer-based visualisations overcome the classical shortcomings of static maps for the presentation of time variant processes.

5. OUTLOOK

The establishment of needless flood preventing activities, hence the dispensable investment of public money, can be avoided if a high precision digital terrain model is used for comparative studies of flood risks.

However, the opposite case is also imaginable. Assuming an area with slightly different relief energy (corresponding to a higher amount of elevated areas) and single house development, it is possible that flooding happens in the above-mentioned amount. As a consequence, the following damages would appear if no preventing actions were taken:

flooded area (m²)	134 000
estate size (m²)	500
number of estates	268
average damage per real estate (€)	10 000
total damage (€)	**2 680 000**

Tab. 2: Extrapolation of potential damage values for invalid planning of flood protection activities in the test area

This simple calculation points out the enormous potential of damages that should be considered when high precision digital terrain models are used for the establishment of flood risk management systems. Besides the protection of buildings rescue routes or other protecting activities can be planned with higher precision and reliability

Precise digital terrain models can also be used for master plans in land use regulation, i.e. significant savings during planning processes and in later stages of activities can be achieved. The multi-functional use of high precision DTMs provides a valuable data and information pool if correctly generated and maintained, yielding new value added chains.

6. REFERENCES

2007/60/EG: Directive 2007/60/EC of the European Parliament and of the Council on the assessment and management of flood risks.

Fürst, J., 2004: *GIS in Hydrologie und Wasserwirtschaft*. 1. Aufl., Wichmann Verlag, Heidelberg,

Kolf, R., 2005: Flood Control in Germany. In: Nijland, H. and Menke, U.: *Flood Risk Management and Multifunctional Land Use in River Catchments*. Rijkswaterstaat, The Netherlands.

Kraus, K., 2000: Photogrammetrie, Topographische Informationssysteme Band 3. Dümmler, Köln.

Merz, B., 2006: *Hochwasserrisiken – Grenzen und Möglichkeiten der Risikoabschätzung*. Schweizerbart'sche Verlagsbuchhandlung, Stuttgart

Nebel, K., 2006: Aufbau eines Geoinformationssystems und Untersuchungen von digitalen Geländemodellen aus Laserscannerdaten für Hochwassersimulationen, Diploma Thesis, University of Applied Sciences Oldenburg/Ostfriesland/Wilhelmshaven.

Nebel, K., Ratzke, H.-P., Schmidt, K., Smit-Philipp, H., Weisensee, M., 2007: Hochwassersimulation im flachen Gelände – sind unsere Geobasisdaten ausreichend? In *Von der Medizintechnik bis zur Planetenforschung – Photogrammetrie und Fernerkundung für das 21. Jahrhundert*. DGPF-Tagungsband 16, Muttenz, Switzerland.

Schroth, O. und Schmid, W. A., 2006: How Much Interactivity does the Public Want? An Assessment of Interactive Features in Virtual Landscapes. In: Buhmann, Ervin, Jorgensen, Strobl (eds.): *Trends in Knowledge-Based Landscape Modeling*. Wichmann-Verlag, Heidelberg.

Tiede, D. und Strobl, J., 2006: Polygon-based Regionalisation in a GIS Environment. In: Buhmann, Ervin, Jorgensen, Strobl (eds.): *Trends in Knowledge-Based Landscape Modeling*. Wichmann-Verlag, Heidelberg.

GENETIC ALGORITHMS FOR MULTI-SPECTRAL IMAGE CLASSIFICATION[1*]

Yeh Fen Yang[1], Peter Lohmann[2] & Christian Heipke[2]

[1] Dept. of Civil Engineering, National Chung Hsing University, Taiwan
[2] Institut für Photogrammetrie und GeoInformation, Leibniz Universität Hannover

KEY WORDS: classification, unsupervised, genetic algorithms, experimental study

ABSTRACT:

In this paper we describe the application of genetic algorithms (GA) to unsupervised multi-spectral image classification. We shortly review the principles of GA and discuss its iterative nature. One of the main advantages of GA is that the number of relevant clusters is derived during the computations rather than having to be determined prior to the classification, as is e. g. the case in the well known ISODATA algorithm. So called fitness functions are introduced and serve as criteria for controlling the iterations. In particular, we study the Davies-Bouldin, the Xie-Beni, and the K-Means Index. We illustrate our work with the help of examples. A multi-spectral satellite image is classified into several classes using both, various versions of GA and – as a reference – the ISODATA algorithm. The results demonstrate the feasibility of using GA for multi-spectral classification.

1. INTRODUCTION

Multi-spectral image classification, including supervised and unsupervised classification, is a major analytical procedure in remote sensing. Supervised classification requires a human analyst to provide training areas in order to derive associated statistical descriptions. In comparison, unsupervised classification proceeds with only minimal input. An unsupervised classification divides all pixels within an image into a corresponding cluster pixel by pixel. Providing class labels to the clusters done by a human analyst in a separate step after clustering. Typically, the only input an unsupervised classification needs is the number of clusters of the scene. However, this value is usually not known a priori. Moreover, the spectral properties of specific classes within the images can change frequently and the relationships between the object classes and the spectral information are not always constant, and once defined for one image cannot necessarily be extended to others. Supervised and unsupervised classification suffers from these drawbacks.

Heuristic unsupervised classification works by establishing some mathematical model and then optimizing a predefined index to determine the number and centroids of the clusters in feature space automatically. Heuristic optimization processes, therefore, are seen as a repeatable, accurate, and time-effective method to classify remote sensing imagery automatically, which is the main objective of this research.

Genetic algorithms (GA) constitute one possibility for heuristic unsupervised classification. They are numerical optimization algorithms inspired by the nature evolution process and directed random search techniques and were introduced by John Holland in 1975 (Holland 1975). GA have been widely and successfully applied to optimization problems, such as the analysis of time series, water networks, work scheduling, and facial recognition (Coley, 1999; Rothlauf, 2006), which confirm the potential of GA to deliver high quality results especially when applied without any ground truth (Coley, 1999). Starting from multiple initial solutions selected randomly, GA preserve the appropriate solution based on a so called fitness function (evaluating index). In this way, GA can avoid problems associated with inhomogeneous data distributions and automatically select the best solution through employing its three standard building blocks: selection, crossover, and mutation.

The research described in this paper focuses mainly on integrating GA with different fitness functions and on comparing the different results. A software program was developed in MATLAB and the GA unsupervised classifier was tested on an IKONOS satellite image, using ground truth information derived from a topographic map for the estimation of classification accuracy. The error matrix (confusion matrix) and K-HAT (kappa) statistics were adopted together with visual inspection to evaluate the results. Finally, the obtained results were compared with those from the traditional ISODATA analysis.

2. METHODOLOGY

In our work we concentrate on using GA for unsupervised classification. In GA the number of clusters does not have to be determined a priori, but can be determined during an iterative computational scheme. So called indices or fitness functions are used to determine whether convergence has been reached.

It is known that the choice of the index has a major impact on the results. Previous research used different indices, such as cluster distance, separation index, Fuzzy C-Means, K-means (KMI), Davies-Bouldin Index (DBI), and Xie-Beni Index (XBI) (Ross, 1995; Bandyopadhyay and Maulik, 2002). In our work, the DBI, XBI, and KMI were adopted. All three of them assign a pixel to one cluster only rather then using the concept of fuzzy membership. In this sense they form a group of related indices, and we believe there is value in comparing them prior to possibly extending the study to other indices and/or to a fuzzy framework. We also used the ISODATA algorithm to validate the effect of GA.

The following sections describe genetic algorithms and the way they can be applied to unsupervised image classification.

3. GENETIC ALGORITHMS

3.1 Chromosome representation

In GA applications, the unknown parameters are encoded in the form of strings, so-called chromosomes. A chromosome is encoded with binary, integer or real numbers. Since multi-spectral image data are usually represented by positive integers,

- dedicated to Prof. Manfred Ehlers at the occasion of his 60th birthday
- Part of this research was carried out while Y.F. Yang was with the Institut für Photogrammetrie und GeoInformation, Leibniz Universität Hannover.

in this research a chromosome is encoded with units (tuples) of positive integer numbers. Each unit represents a combination of brightness values, one for each band, and thus a potential cluster centroid.
The length of the chromosome, K, is equivalent to the number of units and thus of potential clusters in the classification problem. K is selected from the range $[K_{min}, K_{max}]$, where K_{min} is usually assigned to 2 unless special cases are considered (Bandyopadhyay and Maulik, 2002), and K_{max} describes the maximum chromosome length, which means the maximum number of possible cluster centroids. K_{max} must be selected according to experience.
Without assigning the number of clusters in advance, a variable string length is used. Invalid (non-existing) clusters are represented with negative integer "-1". The values of the different chromosomes are then changed in an iterative process involving different rules (called crossover and mutation) to determine the correct number of clusters (the number of valid units in the chromosomes) and the cluster centroids for a given classification problem.

3.2 Chromosome representation

A population is the set of chromosomes. The typical population size can range from 20 to 1000 (Coley, 1999). The following example is given to explain the representation a the population: we assume to have a satellite image with three bands; K_{min} is set to 2 and K_{max} to 8. At the beginning, for each chromosome i ($i = 1, 2, \ldots, P$, where P is the size of population) all values are chosen randomly from the data space (universal data set; here: positive integers with the appropriate radiometric resolution). Such a chromosome belongs to the so-called parent generation. One (arbitrary) chromosome of the parent generation is given here (note that it contains only five valid centroids, since "-1" appears three times in this chromosome):

-1 (110,88,246) (150,78,226) -1 (11,104,8) (50,100,114) – 1 (227,250 192)

3.3 Selection and crossover

The purpose of selection and crossover (the latter is also called recombination) is to create two new individual chromosomes from two existing chromosomes selected randomly from the crossover pool. The crossover pool contains a percentage (the so called crossover percentage) of the current population, which constitutes the best chromosomes according to the chosen index (see below). Typical crossover operations are one-point crossover, two-point crossover, cycle crossover and uniform crossover. The following example illustrates a one-point crossover operation (the point for crossover is situated after the 4^{th} position):

Parent1:

-1 (110,88,246) (150,78,226) -1 (11,104,8) (50,100,114) – 1 (227,250 192)

Parent 2:

(210, 188, 127) (110,88,246) -1 -1 (122,98,45) -1 (98,174,222) (125,101,233)

Child 1:

-1 (110,88,246) (150,78,226) -1 (122,98,45) -1 (98,174,222) (125,101,233)

Child 2:

(210, 188, 127) (110,88,246) -1 -1 (11,104,8) (50,100,114) – 1 (227,250 192)

3.4 Mutation

Mutation follows crossover. During mutation, all the chromosomes in the population are checked unit by unit and according to a pre-defined probability all values of a specific unit may be randomly changed. An example explains this procedure; the bold-faced and italic units represent the result of the mutation.

Old string:

(210, 188, 127) (110,88,246) -1 -1 (122,98,45) -1 (98,174,222) (125,101,233)

New string:

(210, 188, 127) (97,22,143) -1 -1 (122,98,45) -1 (98,174,222) (125,101,233)

4. THE FITNESS FUNCTION (INDEX)

Based on crossover and mutation, the chromosomes, once initiated, iteratively evolve from one generation to the next. In each generation the fitness function (index) is used to measure the fitness or adaptability of each chromosome in the population. After calculating the index for each chromosome of a given population, the best chromosome is compared to the best one of the previous generation (iteration). The termination condition for the iterations is that the difference between these two values lies below a pre-defined threshold. In case this condition holds the best chromosome of the current generation is considered as the final result, it contains the number of clusters (number of units with values different from "-1") and the cluster centroids (the values of the valid units). If the termination condition is not met, the best chromosomes are selected into the crossover pool (see above, the number of selected chromosomes is given by the crossover percentage) and after mutation a new iteration is started. The population thus evolves over generations in the attempt to maximize or stabilize the index. The computations are also stopped once a maximum number of generations is reached.
The different indices used in this research are described in the following.

4.1 Davies-Bouldin Index (DBI)

The Davies-Bouldin index (DBI) is one possibility to represent the fitness of a chromosome (see Eq. (1)~(7)) (Xie and Beni, 1991; Bezdek and Pal, 1998; Swanepoel, 1999; Martini and Schöbel, 2001; Yang and Wu, 2001; Groenen and Jajuga, 2001). First, each pixel of the whole image is assigned to the nearest cluster centroid of the given chromosome by setting the corresponding membership value μ to 1; μ is set to 0 for all other clusters, see Eq. (1). Next, the average and the standard deviation for each cluster are computed (Eq. (2) and (3)), followed by determining the Euclidian distance between the clusters (Eq. (4)). Subsequently, the value R for each cluster is computed as shown in Eq. (5). Then, the average R for all clusters in the chromosome is computed. For a chromosome to survive this average should be as small as possible, thus the DBI is defined as the inverse of the average value for R, see Eq. (6), which is equivalent to the clustering with the smallest inner-cluster scatter (total variation) and the largest cluster separation.

$$\mu_{i,k} = \begin{cases} 1; & \|x_i - u_k\| \le \|x_i - u_j\|, \\ 0; & otherwise \end{cases} \qquad 1 \le k, j \le K \;;\; j \ne k \;;\; 1 \le i \le N \qquad (1)$$

$$v_k = \frac{\sum_{i=1}^{N} (\mu_{i,k}) x_i}{\sum_{i=1}^{N} (\mu_{i,k})} = \frac{\sum_{x_i \in X_k} x_i}{M_k} \qquad 1 \le k \le K \qquad (2)$$

$$S_k = \left(\frac{1}{M_k} \sum_{x_i \in X_k} \|x_i - v_k\|^2\right)^{1/2} \qquad 1 \le k \le K \qquad (3)$$

$$d_{kj} = \|v_k - v_j\| \qquad 1 \le k, j \le K \;;\; j \ne k \qquad (4)$$

$$R_k = \max_{j, j \ne k} \left\{ \frac{S_k + S_j}{d_{kj}} \right\} \qquad 1 \le k \le K \qquad (5)$$

$$DBI = 1 \,/\, \left(\frac{1}{K} \sum_{k=1}^{K} R_k\right) \qquad (6)$$

where

x_i = pixel i with grey values x (one for each band)
u_k = grey values of k^{th} cluster centroid
$\mu_{i,k}$ = membership function of each pixel x_i belonging to the k^{th} cluster
N = total number of pixels
K = total number of clusters
v_k = average value of k^{th} cluster in the current iteration
X_k = set of pixels assigned to cluster k
M_k = the number of pixels belonging to the k^{th} cluster
S_k = standard deviation of the pixels in the k^{th} cluster
d_{kj} = Euclidian distance between the k^{th} and j^{th} centroid

4.2 Xie-Beni's separation Index (XBI)

The XB separation index (XBI) was proposed by Xie and Beni in 1991 (Xie and Beni, 1991; Yang amd Wu, 2001). The XBI is computed similarly to the DBI. Again, each pixel is first assigned to the nearest cluster centroid of the given chromosome according to Eq. (1). Then, the minimum distance d_{min} of all distances d_{kj} between two clusters of the chromosome is calculated, see Eq. (7). Finally, the XBI which expresses the ratio between the total variation and N times the minimum separation of the clusters, is computed, the inverse of which is the XBI, see Eq. (8).

$$d_{\min} = \min_{\substack{k, j = 1 \ldots K \\ and \;\; k \ne j}} \{d_{kj}\} \qquad (7)$$

$$XBI = 1 \;/\; \left(\frac{\sum_{k=1}^{K} \sum_{i=1}^{N} \mu_{ik} \|x_i - v_k\|^2}{N * (d_{\min})^2}\right) \qquad (8)$$

4.3 K-Means Index (KMI)

K-Means is a simple and common clustering algorithm which can also be used in te GA framework (see e. g. Bandyopadhyay and Maulik, 2002). Compared to the XBI the minimum separation is omitted from the computations, the rest is identical. Thus, KMI represents the total variation disregarding the distance between different clusters. KMI is computed according the Eq. (9) as follows:

$$KMI = 1 \;/\; \left(\sum_{k=1}^{K} \sum_{i=1}^{N} \mu_{ik} \|x_i - v_k\|^2\right) \qquad (9)$$

5. GROUND TRUTH DATA

For our research we used a multi-spectral IKONOS image. The image depicts Chandlers Ford in the U.K. and was taken on 2000/08/25 with 4 meters pixel size and 11 bits per pixel (see Figure 1. (a), (b)). We selected a small test image with a total of about 15,000 pixels for our experiments. A higher resolution map served as a reference for obtaining ground truth information.

In the test image, there are three object classes. They are *farmland*, *grove*, and *irrigation canal*, respectively, see also Figure 1(c)-(e). It should be noted that the *farmland* area in the left part of the test image is significantly darker than the *farmland* in the other parts and is spectrally closer to *grove*. Thus, we expect some mixture between *farmland* and *grove* in this area. Also, the *irrigation canal* visually has a certain spectral similarity to *grove*; in addition it only covers a relatively small amount of the test image. It is for these aspects that we have selected the test image, as it presents a rather difficult case for classification.

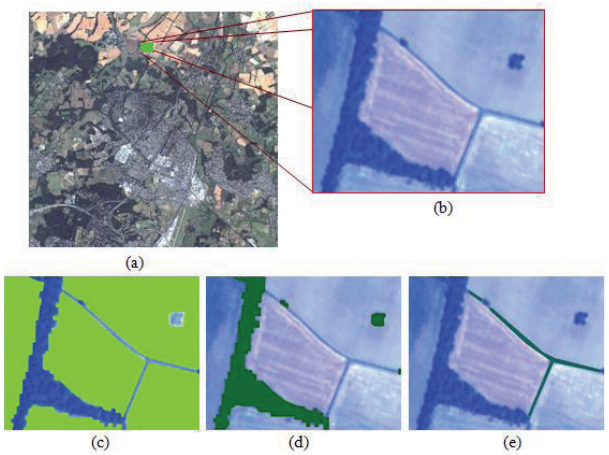

Figure 1. (a) The original IKONOS image; (b) The test image; (c)-(e) Masks for the three classes : (c) *farmland* (81% of the total amount of pixels in the subset image); (d) *grove* (16%); (e) *irrigation canal* (3%).

6. EXPERIMENTAL TESTS AND ANALYSIS OF RESULTS

6.1 Criteria of evaluation

In order to evaluate the different results we compared the ground truth data to the individual classification results. For this purpose we computed the error matrix (confusion matrix) and the well-known criteria *producer's accuracy* or completeness (the number of pixels that are correctly assigned to a certain class divided by the total number of pixels of that class in the reference data), *user's accuracy* or correctness (the number of pixels correctly assigned to a certain class divided by the total numbers of pixels automatically assigned to that class), the overall accuracy and the K-HAT statistics (see Lillesand and Kiefer, 2000 for a quantitative definition).

6.2 Test description

For GA algorithms used as classifiers there are basically seven parameters which influence the result. These are the maximum length of the chromosome, the way to encode the chromosome units (binary, real number and so on), the population size, the crossover type and probability, the mutation probability, and the employed fitness function (Pham and Karaboga, 2000).
In our research a maximum chromosome length of K_{max}=8 was chosen, which is well above the maximum number of clusters in the test image. As explained above, coding was done using positive integers. To simplify our investigations and in accordance with many of the investigations on GA, only one-point crossover operations were considered. The other four parameters were systematically varied in order to study their influence on the result. For selecting the actual parameter values we took advice from general GA references (e. g. Coley, 1999). More specifically, the population size was set to 30, 60, and 90 chromosomes, respectively, the crossover percentage was defined as 40%, 60%, and 80%, and for the mutation probability we selected values of 0.05, 0.25, and 0.5. One set of parameters, namely a population size of 90 with a crossover percentage of 80% and a mutation probability of 0.05 was considered as the baseline set, against which the other parameters were varied. Iterations were terminated as soon as the best chromosome (the one with the largest index) did not change any more from one iteration to the next. In this way, the three presented indices, DBI, XBI, and KIM were investigated, resulting in a total of nine results of each index.

7. RESULTS AND DISCUSSION

Figure 2 displays the visual results with respect to the variation of population size. The colors indicate the different classes: light green stands for *farmland*, dark green for *grove*, and bright for *irrigation canal*. The first row (Figure 2 (a)-(c)) contains the DBI results, the second one (Figure 2 (d)-(f)) the XBI results, and the third one (Figure 2 (g)-(i)) the KMI results. In the left column the results for a population size of 30 are presented, in the centre for a size of 60, and to the right for a size of 90. The Figures 3 and 4 contain similar results for the variation of crossover percentage (the chosen values are 40%, 60% and 80%) and mutation probability (0.05, 0.25 and 0.5).
Tables 1 to 3 are structured in the same way and contain the numerical results of the study. For each case, the producer's accuracy (PA), the user's accuracy (UA) for both, *farmland* and *grove*, the overall accuracy (OA) and the K-HAT value are given. The PA and UA values for *irrigation canal* are not recorded, since in all cases they are very small. The reason is that (as mentioned above) the canal is very narrow, and is spectrally rather similar to *grove*. While this fact can be considered a shortcoming of the present study it can also be interpreted as a rather difficult case for unsupervised multi-spectral classification. It should be noted that the right columns of Figures 2 and 3 and the left column of Figure 4 and the related Tables entries show results of the same experiments. They have been duplicated for reasons of clarity.

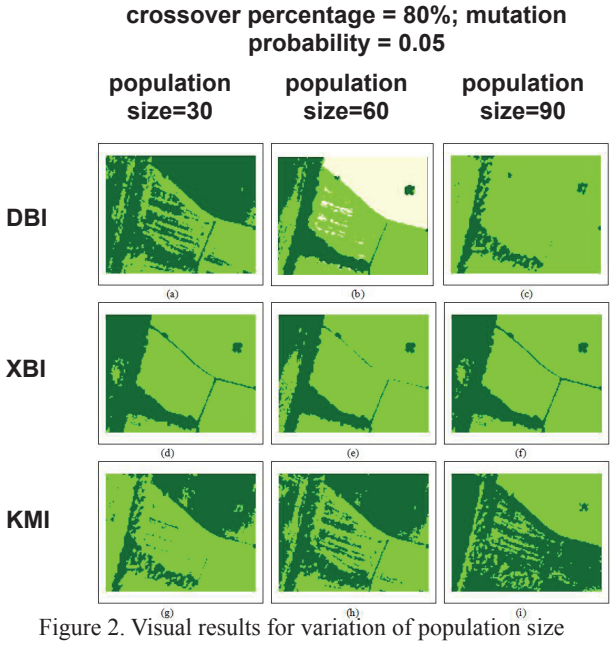

Figure 2. Visual results for variation of population size

From the provided results the following conclusions can be drawn:
- Most results only show two clusters, which can be associated with *farmland* and *grove*. The class *irrigation canal* is only visible in Figures 2(b), 3(a) and 4(b). The areas classified as *irrigation canal* in these cases are, however, wrong.

- As far as a comparison of the different indices is concerned, the XBI clearly performs best. This is true when comparing the visual results to the reference image (Figure 1), and also when studying the numerical results. For XBI the overall accuracy lies consistently above 80% and reaches up to 89.7 % in the best case. Also the producer's accuracy is very good; only the user's accuracy for *grove* is a little low, because part of the *farmland* in the left part of the test image is classified as *grove* (see also discussion about ground truth). Furthermore, XBI is rather insensitive to the variation of parameters, which is obviously an additional advantage.

- The DBI must be rated second. Acceptable results are obtained for the case depicted in Figure 2 (c), which is identical to the one shown in Figure 3(c) and the one shown in Figure 4(a), see above. For the other cases the quality of the results quickly degenerates. Thus, the DBI is much less robust than the XBI. Problems occur mainly for the user's accuracy for *grove*, but the other indicators are also effected in a number of cases.

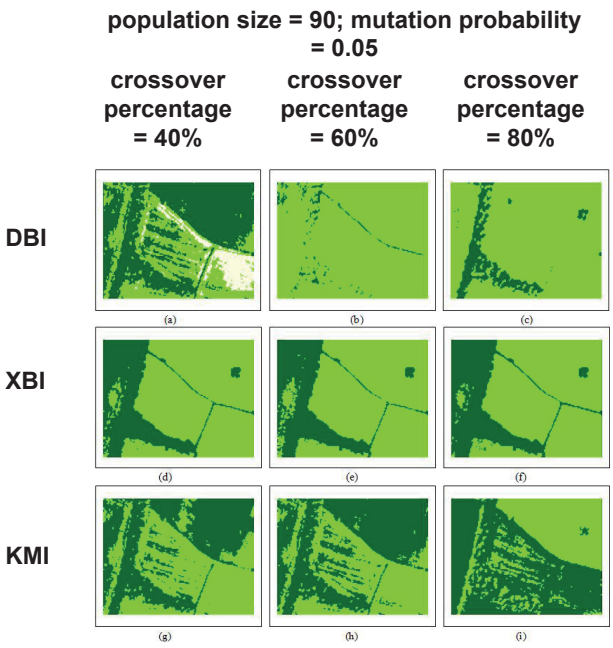

Figure 3. Visual results for variation of crossover percentage

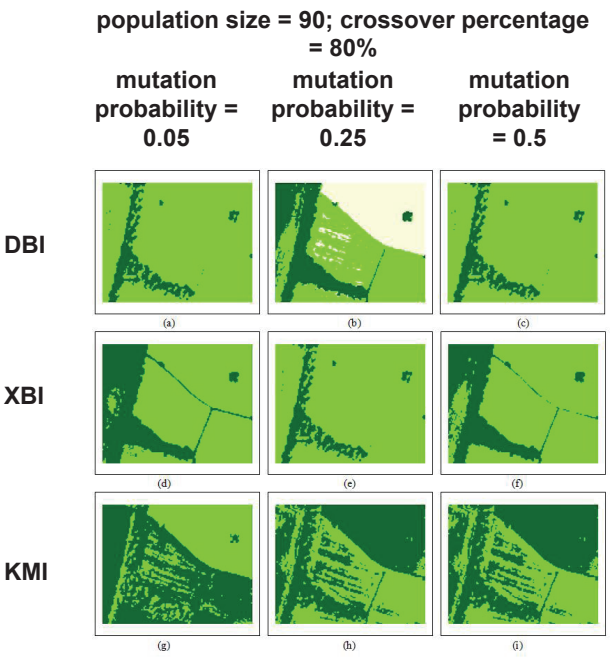

Figure 4. Visual results for variation of mutation probability

-KMI yields unacceptable results. For the best case, the overall accuracy reaches only 65.3 %. There seems to be very little possibility to distinguish between *farmland* and *grove*. The user's accuracy for *grove* is again the largest problem, but the other values are not much better.

- In terms of computational resources, XBI also possesses advantages over DBI, because it can be computed with fewer steps (see also the equations given above). While it is true that KMI is even faster to compute, the results indicate that it is not a suitable index for the given task.

- In all presented cases, also for the good XBI results, the K-HAT value is rather low. This indicates a number of errors of omission and commission, which can also be observed when investigating the full error matrices (due to space limitations, these matrices are not given in their complete form in this paper).

- The results do not consistently depend on the input parameters. For DBI a larger population size, a larger crossover percentage and a smaller mutation probability seems to be advantageous, XBI is rather robust with respect to changing the parameters, and for KMI no definite conclusions should be drawn, since the results are too poor.

In order to be able to better evaluate the overall quality of the results obtained with GA, we have also run the ISODATA algorithm to find clusters for our test image. We asked the

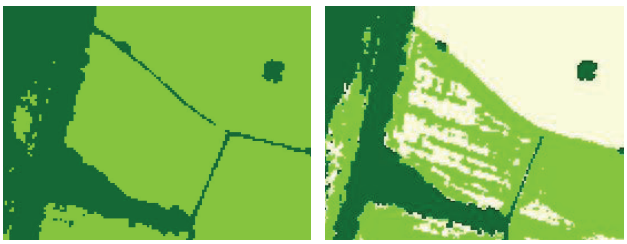

(a) (b)

Figure 5. Visual results for ISODATA algorithm: (a) with two clusters, (b) with three clusters.

	crossover percentage = 80%; mutation probability = 0.05								
	population size=30			**population size=60**			**population size=90**		
DBI		PA [%]	UA [%]		PA [%]	UA [%]		PA [%]	UA [%]
	Farmland	49.5	91.3	Farmland	54.0	91.9	Farmland	97.7	90.4
	Grove	90.1	26.3	Grove	89.7	61.6	Grove	67.1	85.3
	OA = 54.7 %	K-HAT = 10.2 %		OA = 58.4 %	K-HAT = 16.3 %		OA = 89.8%	K-HAT = 17.5 %	
	(a)			(b)			(c)		
XBI		PA [%]	UA [%]		PA [%]	UA [%]		PA [%]	UA [%]
	Farmland	81.4	96.7	Farmland	87.0	95.6	Farmland	81.6	96.6
	Grove	95.2	48.6	Grove	94.0	57.9	Grove	95.0	48.9
	OA = 81.2%	K-HAT = 21.2 %		OA = 85.6 %	K-HAT = 22.1 %		OA = 81.4 %	K-HAT = 21.3 %	
	(d)			(e)			(f)		
KMI		PA [%]	UA [%]		PA [%]	UA [%]		PA [%]	UA [%]
	Farmland	67.9	86.4	Farmland	49.3	89.8	Farmland	41.6	85.4
	Grove	64.6	28.9	Grove	86.8	25.5	Grove	35.7	17.8
	OA = 65.3 %	K-HAT = 8.2 %		OA = 54.0%	K-HAT = 9.2 %		OA = 44.3 %	K-HAT = 2.7 %	
	(g)			(h)			(i)		

Table 1: Num. results for variation of population size (PA: producer's accuracy, UA: user's accuracy, OA: for overall accuracy)

algorithm to find two or three clusters, respectively. The rationale for this selection is that the user would probably ask for three clusters based on the ground truth knowledge (there are three different object classes on the ground), while most GA results only reported two clusters. Thus ISODATA was also run with two clusters to enable a better comparison.

The results are shown in Figure 5(a) and (b) and in Tables 4 and 5. It can be seen that the ISODATA result with two clusters is very similar to the best XBI result, while the one with three clusters is far worse. In the latter case similar problems occur as in some of the GA cases (see Figures 2(b), 3(a) and 4(b)): in particular the *irrigation canal* poses a major obstacle to a correct classification, since much of the *farmland* in the upper right part of the test image is misclassified as *irrigation canal*. Also, the user' accuracy for *grove* is unacceptably low. Thus, while the results of both methods are similar, GA does not need the desired number of classes as additional input.

8. CONCLUSION

In this research we have described how to employ genetic algorithms (GA) for unsupervised multi-spectral classification. GA provides a possibility to compute the number of clusters present in a scene from the image data by using a particular fitness function (index). We have tested three different indices, namely the Davies-Bouldin Index (DBI), the Xie-Beni, Index (XBI) and the K-Means Index (KMI). Experimental data were obtained by classifying a part of a multi-spectral IKONOS scene depicting three different classes, namely *farmland*, *grove* and *irrigation canal* with the different indices while varying a number of parameters of the GA. We have also compared our results to those obtainable by employing the well known ISODATA algorithm. We have based our evaluation on visual inspection of the results, the error matrix and the K-HAT statistics, computed from independent reference data.

We could show that while all experiments somewhat suffer from the difficult test scene, the GA provides acceptable

	population size = 90; mutation probability = 0.05								
	crossover percentage = 40%			**crossover percentage = 60%**			**crossover percentage = 80%**		
DBI		PA [%]	UA [%]		PA [%]	UA [%]		PA [%]	UA [%]
	Farmland	38.3	88.5	Farmland	98.5	82.4	Farmland	97.7	90.4
	Grove	85.8	25.5	Grove	11.0	48.7	Grove	67.1	85.3
	OA = 45.6 %	K-HAT = 8.4 %		OA = 81.2 %	K-HAT = 3.0 %		OA = 89.8%	K-HAT = 17.5 %	
	(a)			(b)			(c)		
XBI		PA [%]	UA [%]		PA [%]	UA [%]		PA [%]	UA [%]
	Farmland	82.8	96.4	Farmland	84.1	96.3	Farmland	81.6	96.6
	Grove	94.8	50.6	Grove	94.8	52.6	Grove	95.0	48.9
	OA = 82.3%	K-HAT = 21.5 %		OA = 83.4 %	K-HAT = 21.8 %		OA = 81.4 %	K-HAT = 21.3 %	
	(d)			(e)			(f)		
KMI		PA [%]	UA [%]		PA [%]	UA [%]		PA [%]	UA [%]
	Farmland	56.9	91.5	Farmland	55.0	85.2	Farmland	41.6	85.4
	Grove	88.5	29.1	Grove	85.6	25.0	Grove	35.7	17.8
	OA = 60.4 %	K-HAT = 11.8 %		OA = 55.0%	K-HAT = 9.2 %		OA = 44.3 %	K-HAT = 2.7 %	
	(g)			(h)			(i)		

Table 2: Num. results for variation of crossover percentage (PA: producer's accuracy, UA: user's accuracy, OA: overall accuracy)

	population size = 90; crossover percentage = 80%								
	mutation probability = 0.05			**mutation probability = 0.25**			**mutation probability = 0.5**		
DBI		PA [%]	UA [%]		PA [%]	UA [%]		PA [%]	UA [%]
	Farmland	97.7	90.4	Farmland	53.6	92.0	Farmland	34.6	58.0
	Grove	67.1	85.3	Grove	90.1	61.0	Grove	54.0	12.6
	OA = 89.8 %	K-HAT = 17.5 %		OA = 58.1 %	K-HAT = 16.2 %		OA = 30.5%	K-HAT = 14.7 %	
	(a)			(b)			(c)		
XBI		PA [%]	UA [%]		PA [%]	UA [%]		PA [%]	UA [%]
	Farmland	81.6	96.6	Farmland	97.8	90.3	Farmland	86.3	95.9
	Grove	95.0	48.9	Grove	66.2	85.6	Grove	94.3	56.4
	OA = 81.4%	K-HAT = 21.3 %		OA = 89.7 %	K-HAT = 17.2 %		OA = 85.0 %	K-HAT = 22.1 %	
	(d)			(e)			(f)		
KMI		PA [%]	UA [%]		PA [%]	UA [%]		PA [%]	UA [%]
	Farmland	41.6	85.4	Farmland	46.2	89.0	Farmland	34.5	56.4
	Grove	35.7	17.8	Grove	53.8	24.3	Grove	53.6	13.6
	OA =44.3 %	K-HAT = 2.7 %		OA = 51.4%	K-HAT = 8.1 %		OA = 30.5 %	K-HAT = 5.7 %	
	(g)			(h)			(i)		

Table 3: Num. results for variation of mutation probability (PA: producer's accuracy, UA: user's accuracy, OA: overall accuracy)

		Farmland	Grove	Irrigation canal
	Farmland	81.8%	4.9%	53.7%
	Grove	18.2%	95.1%	46.3%
	Irrigation canal	0.0%	0.0%	0.0%

Producer's Accuracy	**User's Accuracy**
Farmland = 81.8%	Farmland = 96.5%
Grove = 95.1%	Grove = 49.4%
Irrigation canal = 0.0%	Irrigation canal = 0.0%
Overall accuracy = 81.6%	K-HAT = 21.3 %

Table 4: Error matrix for ISODATA results, two clusters

		Farmland	Grove	Irrigation canal
	Farmland	41.9%	5.3%	79.9%
	Grove	43.5%	91%	13%
	Irrigation canal	14.7%	3.7 %	7.2%

Producer's Accuracy	**User's Accuracy**
Farmland = 41.9%	Farmland = 91.2%
Grove = 91%	Grove = 29.7%
Irrigation canal = 7.2%	Irrigation canal = 1.7%
Overall accuracy = 48.9%	K-HAT = 10.8 %

Table 5. Error matrix for ISODATA results, three clusters

results for a number of cases. The XBI turned out to be the most accurate and by far the most robust index. The overall accuracy was consistently above 80 %, with the best values reaching 90 %. The DBI is much more sensitive to parameter tuning, and the KMI seems to be unsuitable for the use in unsupervised classification. The GA results are similar to those obtained with the ISODATA algorithm, if results with the same number of clusters are compared. However, whereas GA determines this number automatically, it nneds to pre-defined for ISODATA. Thus, GA algorithms seem to be more flexible and therefore advantageous to more traditional unsupervised classification techniques.
In the future we plan to extend our study to process more and larger scenes in order to confirm the results found so far. We are also interested to experiment with different termination

conditions such as an absolute fitness level which needs to be reached and to study under which conditions our approach reaches the best solution. Finally, we want to integrate indices based on fuzzy theory into the investigations.

9. ACKNOWLEDGEMENTS

We would like to thank the Ordnance Survey of United Kingdom to offer the IKONOS image data within the OEEPE test. Part of this research was made possible by a grant of the National Science Council (NSC) of Taiwan, Taipeh to the first author. We gratefully acknowledge this support.

10. REFERENCES

Bandyopadhyay, S., and U., Maulik, 2002. Genetic clustering for automatic evolution of clusters and application to image classification, *IEEE Pattern Recognition*, 35:1197-1208.

Bezdak, J.C., and N.R., Pal, 1998. Some new indexes of cluster validity, *IEEE Transactions on systems, man, and cybernetic*s, part B, 28(3):301-315.

Coley, A.D., 1999. *An Introduction to Genetic Algorithms for Scientists and Engineers*, World Scientific, Singapore, 185p.

Groenen, P.J.F., and K., Jajuga, 2001. Fuzzy clustering with squared Minkowski distances, *Fuzzy Sets and Systems*, 120:227 237.

Holland, J., 1975. Adaptation in Natural and Artificial Systems, University of Michigan Press, Ann Arbor.

Lillesand, T.M., and R. Kiefer, 2000. *Remote Sensing and Image Interpretation*, 4th edition, Wiley & Sons, New York, 721p.

Martini, H., and A., Schöbel, 2001. Median and center hyperplanes in Minkowski spaces -- a unified approach,*Discrete Mathematics*, 241(1):407-426.

Pham, D.T., and D., Karaboga, 2000. *Intelligent Optimisation Techniques*, Springer, London, Great Britain, 337p.

Rothlauf, F., 2006. *Representations for Genetic andEvolutionary Algorithms*, Springer, Netherlands, 314p.

Ross, T.J., 1995. *Fuzzy logic with engineering applications*, Mc Graw-Hill, Singapore, 486p.

Swanepoel, K.J., 1999. Cardinalities of k-distance sets in Minkowski spaces, *Discrete Mathematics*, 197(198):759-767.

Xie, X.L., and G., Beni, 1991. A Validity Measure for Fuzzy Clustering, *IEEE Transaction on Pattern Analysis and Machine Inteligence*, 13(8):841-847,

Yang, M.S., and K.L., Wu, 2001. A new validity index for fuzzy clustering, *IEEE International Fuzzy Systems Conference*, pp. 89-92.

SEAFLOOR CHARACTERIZATION DETECTION BY ACOUSTIC BACKSCATTER

D.Zheng [a,] *, H.Stoelinga [a,] & M.Hartog[a]
[a] RESON B.V., Stuttgartstraat 42-44 3047AS Rotterdam, The Netherlands
ding.zheng@reson.nl; hms@reson.nl; hartogm@reson.nl;

KEY WORDS: Ocean Remote Sensing, Seafloor, Multi beam sonar, Bathymetry, Backscatter

ABSTRACT:

In this paper we have investigated the potential for detecting characteristics of the seafloor by multi beam acoustic backscatter and bathymetry data. The proposed method is based on the combination of the angular response characteristics of the seafloor and the bottom backscatter model. The angular response characteristics are used to adjust the model parameters in which a set of characteristics of the seafloor can be estimated by running backscatter back model in an inverse way. The approach has been tested using a 369 kHz RESON 7125 multi beam sonar. The results show the potential of this method for a robust seafloor characterization.

1. INTRODUCTION

A traditional method of collecting information of the seafloor characterization is by taking samples of the sediment by divers or by survey vessels that procure grab samples and cores. These measurements are slow, expensive, time-consuming, and provide information at point positions only. As the products of acoustic methods, multi-beam sonar systems (MBSS) are rapidly developed over the last few decades, and are currently the most advanced and efficient tool for remote observations and characterization of the seafloor (Kenny, 2003). Such a tool has been applied in many marine activities such as marine geology, marine biology, and coastal engineering, etc. Among them, one of emerged applications is how efficiently replace traditional methods of seafloor sediments investigation to classify seafloor characterizations based on the rich data resulted from echo sounder. There are a variety of approaches for this goal by multi-beam backscatter and can be broadly categorized into one of four methodologies: textural analysis (Reed and Hussong, 1989, Imen et al., 2005); power spectral analysis of echo amplitudes (Tamsett, 1993); AR (angular response) method or AVO method (amplitude-versus offset) (Matsumoto et al, 1993, Hughes Clarke, 1994 and Fonseca 2007); echo peak probability density function analysis (Stewart, 1994). The most popular used methods are textural analysis and RA. In this study, we focus on the application of RA method with the RESON SeaBat 7125 multi beam data. The paper will give preliminary results and conclusions.

2. ACOUSTIC BACKSCATTER MEASUREMENT AND CORRECTION

Acoustic backscatter measurement is usually carried out by multi beam sonar or side scan sonar. In general two types of information are available from a multi beam echo sounder system. Bathymetry, or water depth, is common use and is computed from the two-way-travel time, depression angle, and azimuth of each beam of the system through the water column. Another type of information is the backscatter which is recorded in an average value or a time series array of each beam. The time series backscatter product is called a snippet image which is an option when multi beam system is in operation. A set of continues and contiguous beams is called one ping. The bottom area that is covered by the ping is called one swath. Instead of measuring the depth to the bottom, side scan sonar only collects data about time series backscatter strength per beam.

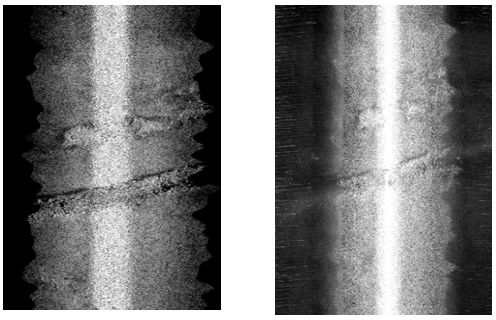

Figure 1. Uncorrected acoustic backscatter strength

Figure 1 shows the example of uncorrected multi beam snippet and side scan backscatter strength images within one survey line from the RESON 7125 sonar. In the images, the white lines are sonar nadir routes. Backscatter strength has the advantages reflecting characteristics of different bottom materials due to the different sound absorption and reflection. For example, volcanic rock is very efficient at reflecting acoustic pulses. Clay and silt do not reflect sound well. Strong reflectors create strong echoes, while weak reflectors create weaker echoes. These characteristics of bottom materials, acoustic backscatter data and multi beam depth information are of immense interest to geologists and geoscientists to infer physical properties of the sea bottom, such as impedance, roughness and volume inhomogeneity. Once knowing these characteristics, we can detect what material composition the bottom type is.

Before using collected backscatter strength to detect characteristics of the seafloor, an advance calibration of the backscatter value has to be done so that the data becomes more reliable and accurate as possible. This is because the received acoustic energy could be influenced by the water column, the seafloor slope, sediment angular and possibly other factors.

Such a calibration processing mainly includes two parts: radiometric correction and geometric correction. The radiometric correction reduces the influences on the backscatter strength by sonar transmit power, gain and beam pattern, while the geometric correction reduces the influences of the slant range and sonar attitude. Besides the corrections of backscatter strength value, another important processing is the geo position corrections based on GPS, vessel attitude and sonar mounting offsets. Figure 2 reveals an example of corrected side scan backscatter strength and its geo position in which X and Y axis are absolute UTM coordinates and right side is the legend of backscatter strength with the energy unit db. The contents of Figure 1 is located in the red box of Figure 2.

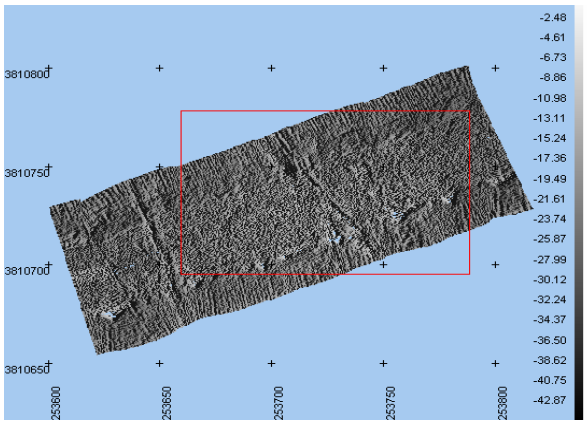

Figure 2. Corrected side scan acoustic backscatter

3. METHOD OF SEA FLOOR CHARACTERISTIC DETECTION BY ACOUSTIC BACKSCATTER

3.1 Angular response

As mentioned in section one, angular response is one of the most popular methods used in the seafloor characteristic detection. Angular response is the term normally used to designate the dependency of the bottom backscatter strength to the incidence angles (Hughes Clarke, 1997). The seabed backscatter strength can be regarded as a function of grazing angle (see eq.1).

$$BTS = 10\log(AE) + Ar \qquad (1)$$

Where BTS is the seabed backscatter strength (target backscatter strength); AE is the area of insonification and Ar is angular response.

For a given sonar power frequency, angular response represents an inherent property of the seafloor. So, the angular dependence of backscatter strength is an important characteristic that distinguishes different types of the seafloor type. Since it is difficult to define replicas of the angular dependence for every type of the seafloor and classify the bottom surface by searching for the best-fit replica for the measured backscatter data, the whole angular range is usually divided into a several specific domains according to the physical peculiarities of acoustic scattering at different angles. The boundaries of these domains are defined by a degree range and then calculating a set of comprehensive values such as mean backscatter strength, angular dependence slopes and so on for further analysis in the bottom backscattering model.

3.2 Bottom backscatter model

The bottom backscattering model was formulated by Jackson *et al* (1986). The start point of the backscatter model is that backscatter is a result from two different processes: interface scattering and volume scattering. The interface scattering occurs at the water sediment interface where the seafloor acts as a reflector and scatterer of the incident acoustic energy. A portion of the incident acoustic energy will also be transmitted into the seafloor, although the amount of penetration into the seafloor will be reduced with increasing frequency and thus attenuation. This transmitted energy will be scattered by heterogeneities in the sediment structure, which are the source of the volume scatter. The total cross section backscatter energy in per unit solid angle and per unit area is defined as:

$$\sigma_t(\theta) = \sigma_r(\theta) + \sigma_v(\theta) \qquad (2)$$

Where $\sigma_r(\theta)$ is the sediment interface backscatter and $\sigma_v(\theta)$ is the sediment volume backscatter per unit solid angle per unit area.

For interface backscatter, the calculation is a combination of the Kirchhoff solution for grazing angles near vertical incidence and the composite roughness solution for other angles.

$$\sigma_r(\theta) = F_r(\theta, f, \rho, v, \delta, \omega_2, \lambda) \qquad (3)$$

θ is the grazing angle, f is the frequency, ρ is the ratio of sediment mass density to water mass density, v is the ratio of sediment sound speed to water sound speed, δ is the loss parameter: ratio of imaginary to real wave number for the sediment, ω_2 is the spectral strength of bottom relief spectrum (cm^4) at wave number 1(cm^{-1}), and λ is the spectral exponent of bottom relief spectrum.

For volume backscatter, in areas predominantly covered with sediments, the volume scattering from sub bottom sediment layers or from discrete scatters within the upper sediment layers can contribute extensively to the total backscattering cross section intensity. The model for volume scattering includes refraction at the sediment interface and attenuation in the sediment itself. The total volume contribution is dependent on a free parameter σ_2, which is based on the ratio of the sediment volume scattering cross section to sediment attenuation coefficient.

$$\sigma_v(\theta) = F_v(\theta, f, \rho, v, \delta, \omega_2, \lambda, \sigma_2) \qquad (4)$$

F_r and F_v are very complex functions in which backscatter parameters have to be calculated by different functions called parameter functions. These parameter functions depend on some defined constant parameters and non constant parameters. The details can be found in Jackson (1986, 1992).

The bottom model defines the seafloor type based on five parameters that reflect sediment physical properties and seafloor roughness. (a) Two parameters for impedance: sound velocity ratio and density ratio, (b) one parameter for attenuation: loss parameter, and (c) two parameters for

roughness: the spectral strength and the spectral exponent of bottom relief.

3.3 Angular response and bottom backscatter model

In equation 2, the total cross section backscatter energy in per unit solid angle and per unit area can be calculated based on measured backscatter strength by the multi beam sonar. The parameters in equation 3 and 4 can be used to assume the characteristics of the seafloor such as roughness and impendence. However, how are these parameters determined? As the sediment of the seafloor can be taken as a homogeneous fluid characterized by its mass density and compressional wave speed (Jackson 1986), a fluid factor can be a function of parameters ρ and v. Therefore, the problem becomes if we find out fluid factor, how do we determine other non-constant parameters in equation 2 and 3? Fonseca (2007) applied a constrained iterative inversion of the bottom backscatter model, imposing constraints based on Hamilton relations for sediment physical properties (Hamilton, 1974). The inversion of the model is carried out by adjusting a set of parameters resulted from angular response to satisfy a constrain condition, and then obtain bottom backscatter parameters to compute sea floor characteristic such as roughness, impendence and fluid factor.

As discussed in section 3.1, backscatter angular range is usually divided into a several specific domains. In this research, first we define each time series of 30 pings as a patch in which two angular response analysis stacks: port and starboard are defined too. For each stack, there are three specific domains: Near, Far and Outer are separately defined as grazing angle ranged from 65° to 90°, 35° to 65° and 5° to 35°. Figure 3 shows the variation of backscatter in which a near angle is defined as 80° and a far angle is defined as 50°. The angular response parameters are results from the analysis on each stack.

- Stack interception. Near intercept and Far intercept are calculated from the mean backscatter at Near angle and Far angle within one patch.
- Stack slopes. Near slope and Far slope are calculated from the gradient at the points (“Near angle”, “Near mean”) and (“Far angle”, “Far mean”).
- Stack fluid factor. It is an orthogonal distance from the point (stack slope, stack intercept) to the general slope-intercept line. The stack slope and stack intercept are results from the stack backscatter trend line which is the line that goes through the points (“Near angle”, “Near mean”) and (“Far angle”, “Far mean”). The general slope-intercept line is a result from the regression by all stack backscatter trend lines.
- Stack Outer mean backscatter.

The calculated angular response parameters are treated as part of the parameters of bottom backscatter model. And the equation 2 is changed to

$$\sigma_t(\theta) = F(\theta, f, AR, \rho, v, \delta, \omega_2, \lambda, \sigma_2) \qquad (5)$$

Where *AR* is the parameters of angular response.

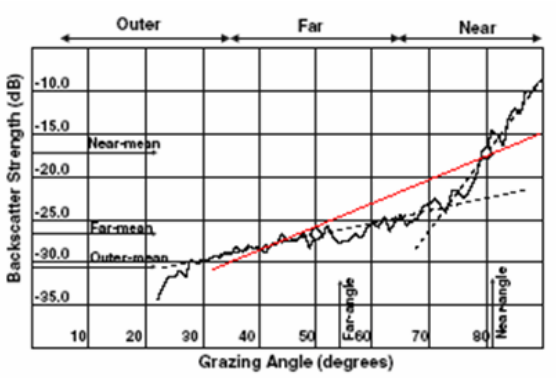

Figure 3. Backscatter angular response (Fonseca, 2007)

The inverse bottom backscatter model iterates equation 5 to meet a set constrain conditions as mentioned below and find the characteristics of the seafloor.

For each patch,

- The roughness parameters of the model are adjusted iteratively until the near-slope of the modelled angular response equals the near-slope of the measured backscatter patch.
- The sound speed ratio and the density ratio parameters of the model are adjusted iteratively until the near-intercept of the modelled angular response equals the near-intercept of the patch.
- The far-intercept of the model is adjusted to the far-intercept of the patch by changing the volume parameter, the sound speed ratio and the density ratio.

4. EXPERIMENT

The method is tested offshore close by Santa Barbara with a RESON 7125 multi beam sonar system. The system operates at a frequency of 369 kHz and forms 512 beams across the ship track in a 128° swath. The maximum ping (update) rate is 40 pings per second and the depth resolution is 5 mm. The whole area covers about 300 x 300 square meters. The time series backscatter strength data of side scan is used for this experiment. The experiment is implemented in PDS2000 (a hydrographical survey package built by RESON B.V.).

4.1 Normalization and mosaic of backscatter data

As discussed in section 2, a set of radio metric and geo metric corrections have to be done to collect test data in this area. Such a process is called normalization. In order to organize all the survey lines in the same image to represent the entire coverage of the seafloor a mosaic process is necessary. The process has to cope with overlapping data by some specific methods such as selecting highest backscatter strength value from all backscatter values within the same cell. The normalized backscatter mosaic is geographically representing the spatial variation with seabed backscatter strength.

Figure 4 shows the corrected backscatter image of this experimental area. There are two pipe lines that are easily distinguished from their surroundings. On the right side is a big pipe line visible and on the left side a small pipe line which is located in the red box. On the other hand, pipe lines have a

higher bottom backscatter strength value than their surroundings. For example, Figure 5 shows the small pipe line's backscatter strength in 3D.

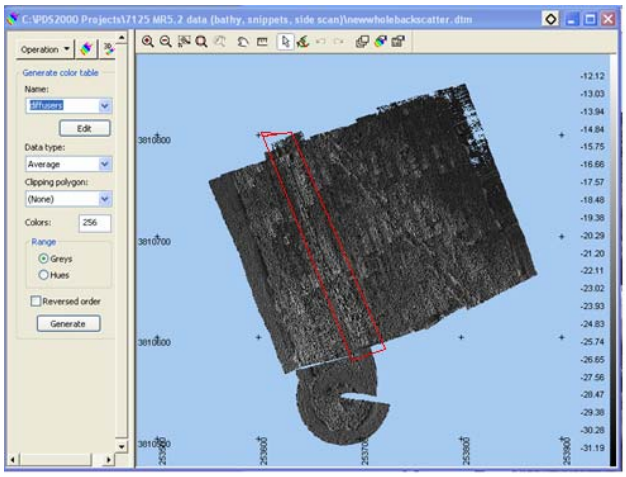

Figure 4. Normalized mosaic 2D backscatter of the experimental area

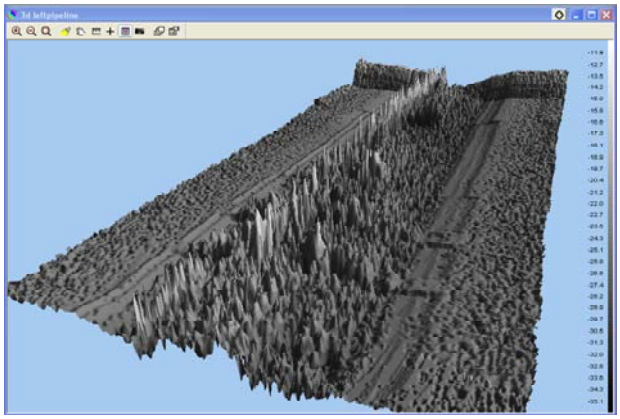

Figure 5. Backscatter 3D image of the small pipe line

4.2 Sea floor characteristics and type

As mentioned in previous sections, the analysis of angular response is based on each time series of 30 pings which are defined as patches. The inversion bottom backscatter model computes a set of parameters mentioned in equation 5 based on the results from angular response analysis. These parameters include the characteristic of the seafloor such as roughness, impendence, fluid factors and so on. Finally a general index is computed based on these parameters to classify a seafloor material type.

A previous knowledge for this area is that there are several kinds of sand materials types in this experimental area. Figure 6 presents the results of this experimental classification which consists of clay, clay sand, sand silt, mud sand, fine sand, coarse silt etc,. Most of the types are "sand" and "very fine sand". We extract the angular response results from 5 sites shown in the figure. The curve is reasonably presenting the characters of different material's having different backscatter angular response. In the response figure of the Figure 6, the red line presents the port's angular response while the green line presents starboard's angular response and the blue line presents the total backscatter. Another analysis is the variation of the seafloor type. From the depth profile figure in Figure 6 (the red line represents the direction of the depth profile), along with the increment of depth, the variation of the seafloor type is changed in the order: clay, clay sand, very fine sand, muddy sand, coarse silt, very file sand,…etc. Such a variation of the bottom needs to be verified in field investigation.

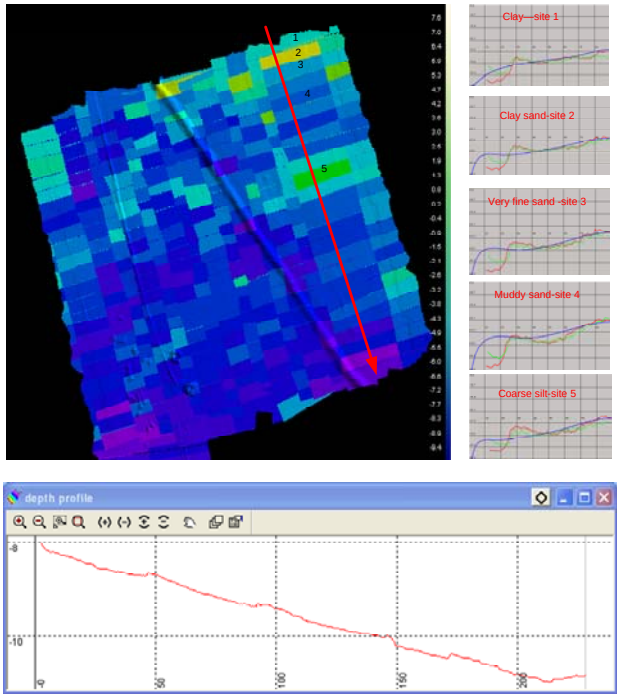

Figure 6. Sea floor type, angular response and depth profile

5. CONCLUSION

We have discussed multi beam backscatter strength, angular response of the seafloor and bottom backscatter model in this paper. As shown in the experimental results, multi beam backscatter is a useful information source for detecting the seafloor in which the corrected backscatter strength is a good presentation of the seafloor situation. For example, the presentation of the pipe line is shown in backscatter 3D view. On the other hand, the character of angular response of the seafloor materials also can be represented by backscatter strength. Such an inherent character of sea floor material is used in bottom backscatter model that estimates material's characteristics and type. The estimated seafloor type is basically matched with a realistic situation. As described in this paper, the approach has the potentials in a robust seafloor characterization. Since current bottom classification cell depends on the definition of multi beam patch size. In order to get accurate results the size is usually defined as 20 to 30 pings which lead to a low resolution in final classification presentation. The further research should be focus on improving classification resolution. The performance of backscatter mosaic is another topic to be studied to solve how extracting more accurate backscatter in overlap area of survey lines.

6. ACKNOWLEDGEMENTS

The research is support by RESON B.V. Data is provided by RESON INC. Bottom backscatter model source code is provided by L. Fonseca, Center for Coastal and Ocean Mapping, University of New Hampshire, USA

7. REFERENCES

Fonseca L, Mayer L, 2007. Remote estimation of surficial seafloor properties through the application Angular Range Analysis to multi beam sonar data. Mar Geophys Res. DOI 10.1007/s11001-007-9019-4

Hamilton, E. 1974. Prediction of deep-sea sediment properties: state-of-theart. In Deep-Sea Sediments, Physical and Mechanical Properties, Plenum Press, pp. 1-43.

Hughes-Clarke JE, 1994. Towards remote seafloor classification using the angular response of acoustic backscatter: a case study from multiple overlapping GLORIA Data. *IEEE Journal of Oceanic Engineering*, 19(1): 112-127.

Hughes Clarke, J.E., B.W. Danforth, and P. Valentine 1997, Areal seabed classification using backscatter angular response at 95KHz. *Proceedings of the* NATO SACLANT Conference CP-45, Lerici, Italy.

Imen, K., Fablet, R., Boucher, J.M. and Augustin, J.M., 2005. Statistical Discrimination of Seabed Textures in Sonar Images Using Co-Occurrence Statistics. *IEEE Oceans'2005Conference Proceedings*, vol. 1, p. 605-610, Brest, France.

Jackson DR, Winebrenner DP, Ishimaru A, 1986. Application of the composite roughness model to high frequency bottom backscattering. Journal of the Acoustical Society of America, 79(5): 1410-1422.

Jackson DR, Briggs KB, 1992. High-frequency bottom backscattering: roughness versus sediment volume scattering. Journal of the Acoustical Society of America 92(2):962–977

Kenny AJ, Cato I, Desprez M, Fader G, Schuttenhelm RTE, Side J, 2003. An overview of sea bed mapping technologies in the context of marine habitat classification. *ICES Journal of Marine Science*, 60(2): 411-418.

Lurton, X. 2002. An Introduction to Underwater Acoustics. Praxis Publishing, UK.

Matsumoto, H., Dziak, R.P. and Fox, C., 1993. Estimation of seafloor microtopographic roughness through modeling of acoustic backscatter data recorded by multibeam systems. *JASA*, v.94, p.2776-2787.

Reed TB, Hussong D, 1989. Digital image processing techniques for enhancement and classification of SeaMARC II side scan sonar imagery. *Journal of Geophysical Research*, 94(B6): 7469-7490.

Stewart WK, Chu D, Malik S, Lerner S, Singh H, 1994, Quantitative seafloor characterization using a bathymetric sidescan sonar. *IEEE Journal of Oceanic Engineering*, 19(4): 599-610.

Tamsett, D., 1993. Sea-Bed Characterization and Classification from the Power Spectra of Side-Scan Sonar Data. *Marine Geophysical Research*, v.15, p.43-64.